Ana Margarida Amaral Gomes

SYSTEMATIC MOLECULAR DISSECTION OF CHROMOSOME CONGRESSION IN HUMAN CELLS UNVEILS A NEW ROUTE FOR MICRONUCLEI FORMATION

Tese de Candidatura ao grau de Doutor em Biologia Molecular e Celular;
Programa Doutoral da Universidade do Porto (Instituto de Ciências Biomédicas de Abel Salazar e Faculdade de Ciências)
Porto, Portugal
2023

Orientador: Prof. Doutor Helder José Martins Maiato
Categoria: Investigador Coordenador
Afiliação: Instituto de Investigação e Inovação em Saúde (i3S), Universidade do Porto

Departamento de Biomedicina, Faculdade de Medicina, Universidade do Porto

Financial Support

This work was funded by National Funds though Fundação para a Ciência e Tecnologia (FCT) (PTDC/MED-ONC/3479/2020), by NORTE 2020 under PORTUGAL 2020 Partnership Agreement though the European Regional Development Fund (NORTE-01-0145-FEDER-000051), as well as by the European Research Council (ERC) consolidator grand CODECHECK, under the European Union´s Horizon 2020 research and innovation programme (grant agreement 681443) and a La Caixa Health Research Grant (LCF/PR/HR21/52410025). The author was supported by a PhD fellowship from FCT (SFRH\BD\130938\2017).

LIST OF ORIGINAL ARTICLES

The results and few sections of the introduction included in this thesis constitute research work of scientific articles published in international journals. In accordance with article 8º do Decreto-Lei nº 388/70, the author of this thesis declares that was involved in the conception and execution of the experimental work, in the interpretation of the results and in the redaction of the published manuscripts under the name of Gomes AM:

Gomes AM, Orr B, Novais-Cruz M, De Sousa F, Macário-Monteiro J, Lemos C, Ferrás C, Maiato H. Micronuclei from misaligned chromosomes that satisfy the spindle assembly checkpoint in cancer cells. Curr Biol. 2022 Oct 10; 32(19):4240-4254.e5. DOI: 10.1016/j.cub.2022.08.026.

Orr B, De Sousa F, **Gomes AM**, Afonso O, Ferreira LT, Figueiredo AC, Maiato H. An anaphase surveillance mechanism prevents micronuclei formation from frequent chromosome segregation errors. Cell Rep. 2021 Nov 9;37(6):109783. DOI: 10.1016/j.celrep.2021.109783.

Maiato H, **Gomes AM**, Sousa F, Barisic M. Mechanisms of Chromosome Congression during Mitosis. Biology (Basel). 2017 Feb 17;6(1):13. DOI: 10.3390/biology6010013.

Acknowledgements

Em primeiro lugar, gostaria de agradecer ao meu orientador Helder Maiato por me ter dado a oportunidade de realizar este trabalho. Acima de tudo, obrigada pela constante partilha de conhecimentos e pelas discussões científicas que em muito contribuíram para a minha evolução. Muito obrigada pelos conselhos e por me encorajares a fazer mais e melhor. A minha profunda gratidão e admiração!

A todos os membros do CID lab (Danica, Nina, Tozé, Ana Almeida, Margarida, Vanessa, Joana O., Joana L., Alexandre, Elias, Hugo, Ariana, Naoyuki, Sónia, Carolina, Jorge and Liam) por todas as discussões científicas (e não tão cientificas!) e por todo o apoio. Queria agradecer todos os momentos de alegria e boa disposição que tornaram esta jornada mais fácil. Um agradecimento especial ao Bernardo, Marco e Joana M. que muito contribuíram para a publicação do meu trabalho. À Luisa, Olga e Ana Figueiredo obrigada por fazerem a vida dentro e fora do laboratório mais interessante, por me fazerem sorrir e estarem sempre presentes quando precisei.

Quero também agradecer ao André Maia, Paula Sampaio e Maria Azevedo, membros das plataformas científicas do i3S por todo o apoio e por estarem sempre disponíveis para ajudar.

Aos meus amigos, os de sempre e os mais recentes, que são verdadeiros portos de abrigo.

Aos meus pais e sogros, por tudo o que fizeram e ainda fazem por mim. Por estarem sempre lá.

À minha irmã Gabriela por caminhar comigo, pela partilha de sonhos…

Ao Jota pelo incentivo constante e por me fazer acreditar. Obrigada por tornares os meus dias muito mais alegres! Sem ti teria sido muito difícil…

Por fim, queria agradecer à minha filha Matilde, por ser uma inspiração constante e por todos os dias fazer de mim uma pessoa melhor.

Abstract

Chromosome alignment to the spindle equator is a hallmark of mitosis thought to promote chromosome segregation fidelity in metazoans. Despite its key role in promoting mitotic fidelity, chromosome alignment is only indirectly supervised by the spindle assembly checkpoint (SAC), which monitors the establishment of end-on kinetochore-microtubule attachments required for chromosome bi-orientation and regulates the metaphase-anaphase transition. It is therefore widely assumed that cells only enter anaphase once all chromosomes align and bi-orient. However, chromosome alignment may occur independently of end-on kinetochore-microtubule attachments and chromosome bi-orientation, and conditions exist in which vertebrate cells enter anaphase in the presence of misaligned chromosomes. Thus, understanding how human cells respond to chromosome alignment defects and determining what happens to an enduring misaligned chromosome remain fundamental unanswered question with strong clinical implications. Here we investigated how human cells respond to chromosome alignment defects of distinct molecular nature by following the fate of live HeLa cells after RNAi-mediated depletion of 125 proteins previously implicated in chromosome alignment. This systematic analysis revealed that entering anaphase with misaligned chromosomes is a frequent outcome in cancer cells. Surprisingly, cells with misaligned chromosomes satisfy the SAC. Previous studies have shown that specific types of erroneous chromosome-microtubule attachments satisfy the SAC and result in lagging chromosomes during anaphase. This condition is potentially dangerous, since anaphase lagging chromosomes might result in micronuclei, recently implicated as key intermediates of massive genomic rearrangements that may drive rapid tumor evolution and account for acquired drug resistance and oncogene activation. In this study, we compared the relative contributions of lagging and misaligned chromosomes, as well as DNA bridges, to micronuclei formation during human cell division. In-depth analysis of specific molecular perturbations that prevent proper kinetochore-microtubule attachments revealed that misaligned chromosomes that missegregate frequently result in micronuclei. Higher-resolution live-cell imaging indicated that, contrary to most anaphase lagging chromosomes that correct and reintegrate the main nuclei, misaligned chromosomes are a strong predictor of micronuclei formation in a cancer cell model of chromosomal instability, but not in normal near-diploid cells. Complementary experiments suggest that intrinsic differences in kinetochore-microtubule attachment stability between cancer and non-cancer cells account for this distinct outcome. Thus, misaligned chromosomes that satisfy the SAC may represent a previously overlooked mechanism driving chromosomal/genomic instability during cancer cell division, and we unveil genetic conditions predisposing for these events. Overall, these new findings incite

for an in-depth characterization of the properties and fate of micronuclei of different origins, while evaluating their respective potential to drive and/or sustain cell transformation. Because micronuclei formation from misaligned chromosomes appears to be a specific outcome of cancer cells, it may represent a possible therapeutic opportunity in human cancers.

Resumo

O alinhamento cromossómico no equador do fuso é uma característica da divisão celular que promove a fidelidade da segregação cromossómica em metazoários. Apesar do seu papel crucial na promoção da fidelidade mitótica, o alinhamento cromossómico é supervisionado indiretamente pelo ponto de controlo ou checkpoint do fuso, que controla o estabelecimento da ligação entre cinetócoros e microtúbulos necessários para a biorientação cromossómica e regula a transição da metáfase para anáfase. Portanto, é amplamente assumido que as células só entram em anáfase quando todos os cromossomas se alinham e se biorientam. No entanto, o alinhamento dos cromossomas pode ocorrer independentemente das ligações terminais do cinetócoro e microtúbulos e da biorientação dos cromossomas, e existem condições nas quais as células dos vertebrados entram na anáfase na presença de cromossomas desalinhados. Deste modo, a compreensão de como as células humanas respondem a defeitos no alinhamento cromossómico e determinar o que acontece com um cromossoma desalinhado é uma questão fundamental que permanece por esclarecer e com fortes implicações clínicas. Neste estudo, investigamos como as células humanas respondem a problemas no alinhamento cromossómico de natureza molecular distinta, seguindo o destino de células HeLa depois da depleção mediada por RNAi de 125 proteínas previamente implicadas no alinhamento cromossómico. Esta análise sistemática revelou que a entrada em anáfase com cromossomas desalinhados é um resultado frequente em células cancerígenas. Surpreendentemente, as células com cromossomas desalinhados satisfazem o ponto de controlo ou checkpoint do fuso. Estudos anteriores mostraram que tipos específicos de erros nas ligações cromossomas-microtúbulos satisfazem este checkpoint e resultam em cromossomas atrasados que ficam para trás durante a anáfase. Esta condição é potencialmente perigosa, uma vez que cromossomas atrasados podem resultar em micronúcleos, recentemente implicados como intermediários chave em rearranjos genómicos que podem conduzir à rápida evolução do tumor e serem responsáveis pela resistência adquirida a terapias, assim como na ativação de oncogenes. Neste estudo, comparamos as contribuições relativas de cromossomas atrasados e desalinhados, bem como pontes de DNA, para a formação de micronúcleos durante a divisão celular humana. A análise aprofundada de perturbações moleculares específicas que impedem as ligações adequadas do cinetócoro aos microtúbulos revelou que os cromossomas desalinhados que se segregam incorretamente frequentemente resultam em micronúcleos. Microscopia de células vivas de alta resolução revelou que, ao contrário da maioria dos cromossomas atrasados durante a anáfase que se corrigem e reintegram no núcleo principal, os cromossomas desalinhados são indicadores mais fortes da formação de micronúcleos em

um modelo de células cancerígenas com instabilidade cromossómica, mas não em células normais quase diplóides. Experiências complementares sugerem que diferenças intrínsecas na estabilidade da ligação cinetócoro-microtúbulos entre células cancerígenas e não cancerígenas são responsáveis por este resultado distinto. Assim, cromossomas desalinhados crónicos que satisfazem o ponto de controlo ou checkpoint do fuso podem representar um mecanismo anteriormente negligenciado que conduz à instabilidade cromossómica/genética durante a divisão células de células cancerígenas, e revelamos condições genéticas que predispõem a esses eventos. No geral, esta nova descoberta incita a uma caracterização aprofundada das propriedades e do destino dos micronúcleos de diferentes origens, ao mesmo tempo em que se avalia o respetivo potencial para iniciar e/ou sustentar a transformação celular. Como a formação de micronúcleos a partir de cromossomas desalinhados parece ser um fenómeno específico de células cancerígenas, este pode representar uma possível oportunidade terapêutica em cancros humanos.

Table of Contents

LIST OF ABBREVIATIONS

ACA – Anti-centromere Antiserum
APC/C – Anaphase Promoting Complex/Cyclossome
ATM – Ataxia Telangiectasia Mutated
ATP – Adenosine triphosphate
CCAN – Constitutive Centromere Associated Protein Network
cDNA – complementary DNA
Cdks – Cyclin-dependent kinases
CENP – Centromere protein
CIN – Chromosomal Instability
CPC – Chromosomal Passenger Complex
CLASP – CLIP-Associated Protein
CLIP-170 – Cytoplasmic Linker Protein 170
DAPI – 4´,6-Diamidino-2´phenylindole dihydrochloride
DNA – Deoxyribonucleic Acid
DSBs - (Double-Stranded DNA breaks)
h - hour
KMN – KNL-1, Mis12 complex, and Ndc80 complex
KT-MT – Kinetochore-Microtubule
KT - Kinetochore
MAD1/2 – Mitotic Arrest Deficiency 1/2
MAPs – Microtubule Associated proteins
MCAK – Mitotic centromere-associated kinesin
MCC – Mitotic Checkpoint Complex
min – minute
MT - Microtubule
MTOCs – Microtubule Organizing Centers
NEBD – Nuclear Envelope Breakdown
NE – Nuclear Envelope
PCM – Pericentriolar Material
PEF – Polar Ejection Force
PP1 – Protein Phosphatase 1
PTMs – Post-translational modifications
RNA – Ribonucleic Acid
RNAi – RNA interference
RPE-1 – Retinal Pigment Epithelial-1

SAC – Spindle Assembly Checkpoint

Ska1 – Spindle and kinetochore associated 1

UFBs – DNA Ultrafine Bridges

β – Beta

α – Alpha

γ – Gamma

γH2AX – phosphorylation of the histone H2AX on serine 139

γ-TURC – γ-Tubulin Ring Complex

CHAPTER 1

General introduction

1.1. The cell cycle

The cell cycle is a coordinated sequence of periodic events that lead to formation of two daughter cells, each containing chromosomes identical to those in the parental cells. This sequence of events is characterized by its tight regulation that ensure the control of each stage to preserve the chromosome number of the progenitors. The eukaryotic cell cycle takes typically 24 hours to be completed and can be divided into two fundamental parts: the longest, called interphase, where cells grow and DNA is replicated, and a shorter stage, named mitosis (or M phase) where segregation of the replicated genetic material occurs. Interphase can be further subdivided into three distinct phases: two gap phases (G1 and G2) and S phase. DNA replication occurs in a specific part of the interphase called S phase (synthesis phase). S phase is preceded by a gap during which the cell grows in preparation for DNA replication (G1) and is followed by a gap during which the cell prepared for mitosis (G2). These gap phases allow cells to continue to grow and serve as important regulatory periods known as cell cycle transitions (reviewed in (Morgan, D. O., 2007).

1.1.1. Molecular control of the cell cycle

The organization of the cell cycle and its control system are highly conserved among eukaryotic organisms. Cell cycle progression is driven by the sequential activation, and subsequent inactivation, of two key classes of regulatory molecules, cyclins and cyclin-dependent kinases (Cdks). While Cdks are constitutively expressed throughout the cell cycle, cyclins are synthesized (and destroyed) in specific stages of the cell cycle, which is often dependent upon various signaling molecules (Darzynkiewicz et al., 1996). Once activated by cyclins, Cdks phosphorylate specific substrates that drive events of the cell cycle and cell division. Formation of specific Cdk-Cyclin complexes triggers the switch between the major phases of the cell cycle, namely, the commitment from G1 into S, the progression of G2 into M and the metaphase/anaphase transition during cell division (reviewed in (Morgan, D. O., 2007)). In metazoans, three Cdks that regulate interphase (Cdk2, Cdk4 and Cdk6), one mitotic Cdk (Cdk1) and a few Cyclins (Cyclins - A, - B, -C, - D and – E) have been identified and play critical role in the cell cycle (reviewed in (Martínez-

Alonso and Malumbres, 2020)). During G1 phase progression, Cyclin D promotes the activation of Cdk4 and Cdk6 in preparation for DNA replication (Sherr, 1994). The transition from G1 to S phase is determined by Cyclin E-dependent Cdk2 activation (Ohtsubo et al., 1995). An increase in Cyclin A levels and its association with Cdk2 allows the progression through G2 phase (Pagano et al., 1992). Higher levels of Cyclin A mediate the activation of the Cyclin B-Cdk1 complex, the major regulator of mitotic entry (reviewed in (Alvarez-Fernández and Malumbres, 2014)). After nuclear envelope breakdown (NEBD), Cyclin A starts to be degraded by the Anaphase-Promoting Complex/Cyclossome (APC/C), to facilitate the initial attachments between chromosomes and mitotic spindle, as cells progress though mitosis (den Elzen and Pines, 2001; Kabeche and Compton, 2013). The Cyclin B-Cdk1 complex directly regulates mitosis and its levels remain high until all chromosomes are attached to spindle microtubules. At this point, the APC/C targets Cyclin B for degradation, leading to Cdk1 inactivation and mitotic exit (reviewed in (Holder et al., 2019).

Proper progression through the cell cycle is ensured by the existence of multiple cell cycle checkpoints (reviewed in (Hartwell and Weinert, 1989)) (Figure 1.1). Cell-cycle checkpoints are responsible for ensuring that each earlier process has been completed before the cell moves on to the next phase of the cycle. In the presence of errors or stress stimuli, checkpoints induce a cell cycle delay in order to provide time for error correction (reviewed in (Morgan, D. O., 2007)). Different checkpoints have been described, namely the G1/S checkpoint (restriction/Start checkpoint), G2/M checkpoint (DNA damage checkpoint), spindle assembly checkpoint (M phase checkpoint), chromosome separation checkpoint and abscission checkpoint (reviewed in (Maiato et al., 2015; Matthews et al., 2022; Murray, 1994). The G1/S checkpoint is the point at which the cell commits to either enter the cell cycle or to stay in a quiescent state, known as G0, depending on internal and external conditions (reviewed in (Peeper et al., 1994)). The G2/M checkpoint prevents cells to undergo mitosis in the presence of damaged or unreplicated DNA. After nuclear envelope breakdown (NEBD), the spindle assembly checkpoint (SAC) controls the metaphase-anaphase transition by monitoring the attachment status between microtubules and a specialized structured at the chromosomes composed by more than one hundred proteins, called the kinetochore (reviewed in (Lara-Gonzalez et al., 2021; Musacchio, 2015)) (see section 1.4 for in-depth characterization). Recently, it was proposed the existence of an anaphase surveillance mechanism that monitors the efficiency of chromosome separation and promotes anaphase error correction during cell division. This “Chromosome Separation Checkpoint” is centered on a constitutive midzone-based Aurora-B phosphorylation gradient, which monitors and delays chromosome decondensation and nuclear envelope reformation until effective separation of sister chromatids during anaphase is achieved. This

decondensation and nuclear envelope reformation delay facilitate the incorporation of lagging chromosomes into the main nucleus, thereby preventing micronuclei formation from chromosome segregation errors (Afonso et al., 2014; Maiato et al., 2015; Orr et al., 2021; Sen et al., 2021). Finally, in cytokinesis, the abscission (NoCut) checkpoint, also dependent on Aurora B, delays abscission in the presence of chromosome bridges (Amaral et al., 2016; Nähse et al., 2017; Steigemann et al., 2009).

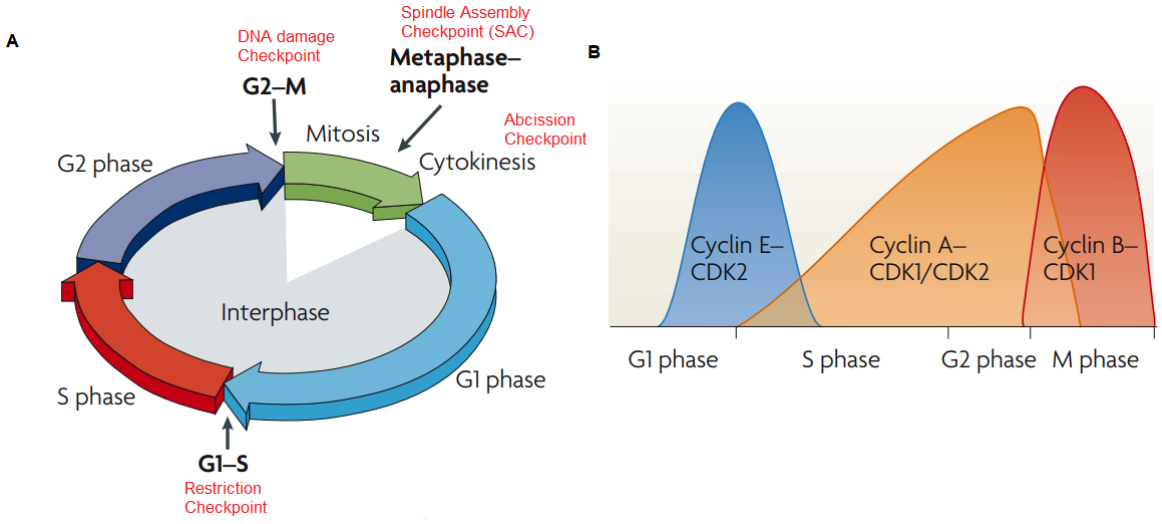

Figure 1.1: Overview of cell cycle checkpoints and the regulatory Cyclin-Cdk complexes. **A.** The cell cycle is divided in two main stages: mitosis and interphase, further sub-divided in G1, S and G2 phases. Several checkpoints operate during the cell cycle and control progression through the different stages: in interphase, entry in mitosis and DNA damage are regulated by the restriction checkpoint and DNA damage checkpoint, respectively. During mitosis, unattached kinetochores are monitored by the spindle assembly checkpoint, while the presence of incompletely segregated DNA is sensed by the abscission checkpoint. **B.** The oscillatory nature of the cyclins and the complex network between cyclins and Cdks throughout the cell cycle. Adapted from (Hochegger et al., 2008).

1.2. Mitosis

1.2.1. Overview of mitosis

Mitosis is a fascinating process that distributes equally the replicated genome into two daughter cells. In eukaryotic cells, mitosis is typically divided into five phases, based in the gross structural changes that take place: prophase, prometaphase, metaphase, anaphase and telophase (Figure 1.2). During prophase, the duplicated genetic material undergoes dramatic morphological changes. The DNA is progressively condensed and individual chromosomes become discernible. The centrosomes, which are replicated during S-phase and serve as microtubule-organizing centres in most animal cells, start to move apart to opposite sides of the nucleus. This process initiates the assembly of a dynamic

macromolecular machine: the mitotic spindle. At the start of prometaphase, the nuclear membrane breaks down, the interphase array of microtubules is reorganized, and microtubule dynamics drastically increase allowing the interactions between microtubules and kinetochores. Prometaphase continues until all chromosomes become properly attached and aligned at the spindle equator in a process known as chromosome congression. After all chromosomes have aligned at the spindle equator, the cell is said to be in metaphase, and is now ready to segregate the duplicated genome. The sudden separation of sister chromatids marks the beginning of anaphase, during which the chromosomes move to opposite poles of the spindle. By telophase, the chromosomes have reached the spindle pole regions, and the nuclear envelope is reformed around each set of decondensed chromosomes. Formation of the cleavage furrow ensures the physical separation of the cytoplasm, giving rise to two identical daughter cells (cytokinesis) (reviewed in (Morgan, D. O., 2007)).

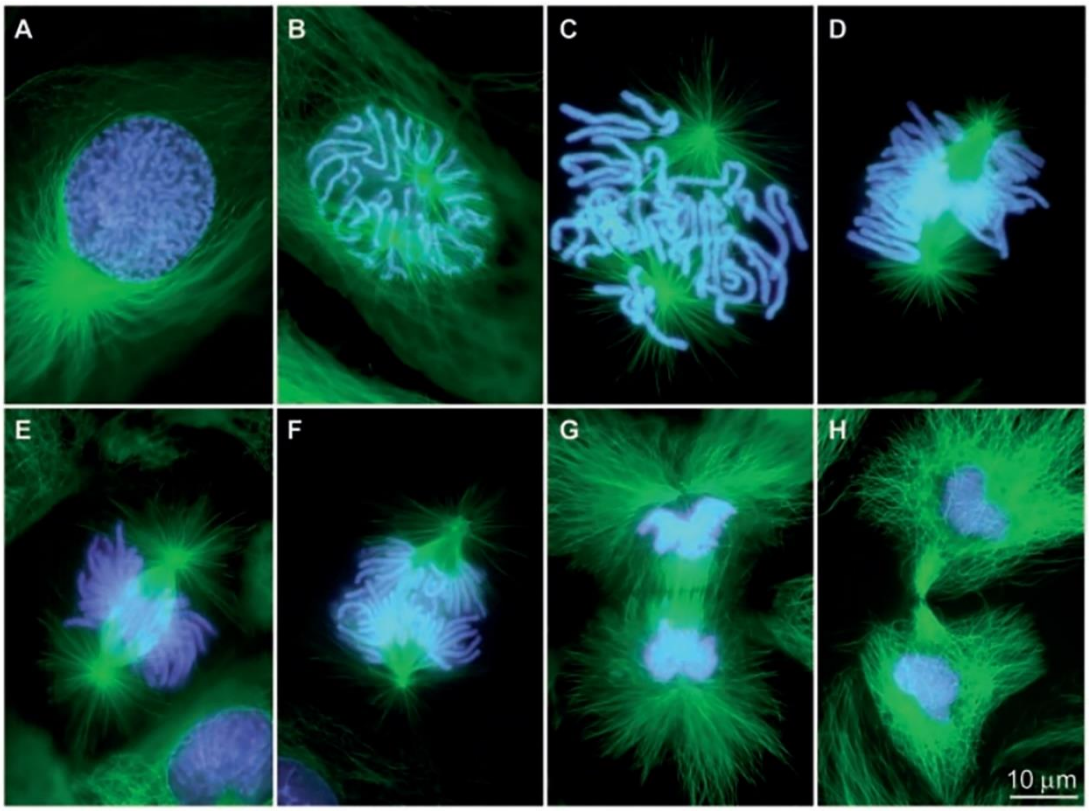

Figure 1.2: Mitotic phases. Fluorescence micrographs representing the different stages of mitosis in fixed newt lung cells. Microtubules are shown in green and chromosomes in blue. At prophase (A), the previously replicated genetic material condenses, and centrosomes start to migrate to opposite poles. After nuclear envelope breakdown (NEBD), the cell enters in prometaphase (B-D), spindle microtubules interact and attach to kinetochores. In metaphase (E), chromosomes are aligned on the spindle equator and all kinetochores are attached to microtubules. In anaphase (F-G), sister chromatids are separated and moved towards opposing centrosomes, together with spindle elongation. In telophase (H), the nuclear envelope begins to reform around the two daughter cells, and the DNA begins to decondense. Finally, the physically separation of the cytoplasm allows the segregation of the two daughter nuclei into individual cells (cytokinesis, not represented). Adapted from (Rieder and Khodjakov, 2003).

1.2.2. The Mitotic Apparatus

Experimental research carried over many years had shown that faithful chromosome segregation during cell division relies on the assembly and regulation of a highly complex molecular machine, the mitotic apparatus. This machine is composed of centrosomes, kinetochores, and a mitotic spindle (Figure 1.3).

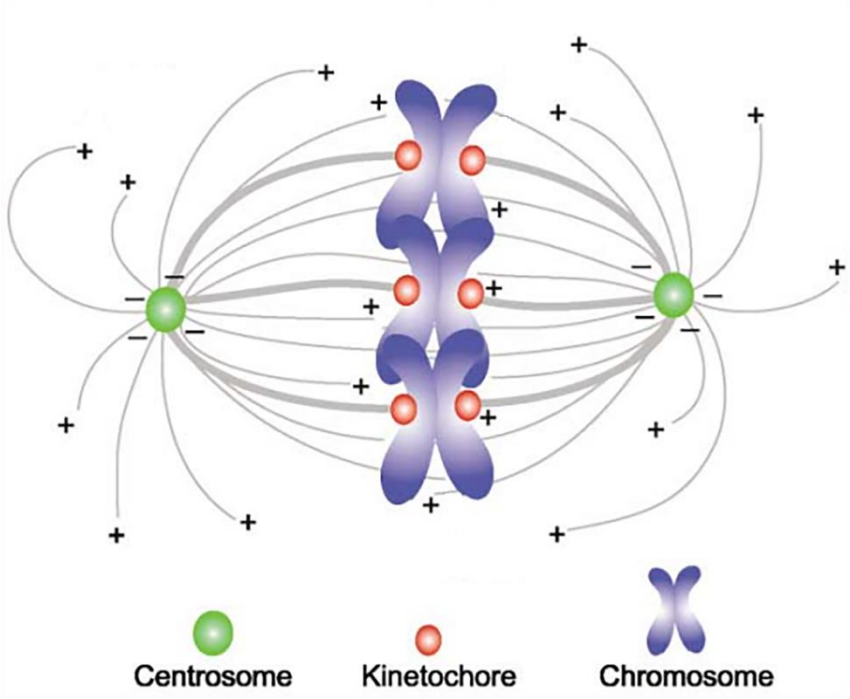

Figure 1.3: Schematic representation of the mitotic apparatus in somatic cells. Microtubules are shown in gray, centrosomes in green, kinetochores in red, and chromosomes in blue. Positions of microtubules minus (-) ends versus plus (+) ends are indicated. Adapted from (Kline-Smith and Walczak, 2004).

1.2.2.1. The centrosomes

The centrosome, which was first described in the late 19th century, is the major microtubule-organizing center (MTOC) in animal cells. This complex structure plays a critical role during mitosis and its duplication is tightly regulated throughout the cell cycle (reviewed in (Bettencourt-Dias and Glover, 2007; Nigg, 2007)). Centrosomes play a crucial role in the regulation of cell cycle transitions (G1-S, G2-M, and metaphase-anaphase), cell migration, polarity of cell, mitotic spindle formation, and mitotic spindle orientation (reviewed in (Bettencourt-Dias and Glover, 2007; Nigg and Raff, 2009)). Centrosomes are complex structures formed by two centrioles which are surrounded by a mass of proteins forming the pericentriolar material (PCM) (Figure 1.4a,b) (reviewed in (Conduit et al., 2015)). Each

centriole is composed of nine triplets of microtubules varying from 150 to 500 nm in length depending on cell type (reviewed in (Gönczy and Hatzopoulos, 2019)). One of the components of the pericentriolar material is a type of tubulin called γ-tubulin, which, together with several other proteins, makes up γ-tubulin ring complexes (γ-TURCs) (reviewed in (Bärenz et al., 2011)). γ-tubulin is highly conserved in all eukaryotes and is the main microtubule nucleation center at the microtubule minus-ends (Moritz et al., 2000, 1995; Moritz and Agard, 2001). Interestingly, the fact that spindle formation occurs in cellular systems that lack centrosomes, such as plant cells and female oocytes (Bonaccorsi et al., 1998; Megraw et al., 2001; Murata et al., 2005; Schuh and Ellenberg, 2007; Wadsworth and Khodjakov, 2004), or after experimental centrosome inactivation in animal somatic cells (Hinchcliffe, 2011; Hinchcliffe et al., 2001; Khodjakov et al., 2000), suggests the existence of redundant MTOCs that contribute to spindle assembly. In support of this theory, microtubules have been found to nucleate at non-centrosomal sites, even in cells containing centrosomes (De Brabander et al., 1981; Nicklas and Gordon, 1985; Witt et al., 1980).

In proliferating cells, centrosomes are duplicated in interphase and separated at the beginning of mitosis (Figure 1.4c). Centriole duplication begins at G1, when they also lose their orthogonal orientation and split slightly apart. Each old centriole – the mother centriole – provides a pre-existing template upon which a daughter centriole is build (procentriole). During S phase, daughter centrioles elongate and form a right angle to the old centrioles. When cells enter mitosis, the two centrosomes separate and migrate towards opposite poles of the cell. After mitosis, each daughter cell inherits one centrosome, with a pair of centrioles, which will be duplicated in the next cell cycle (reviewed in (Bettencourt-Dias and Glover, 2007)).

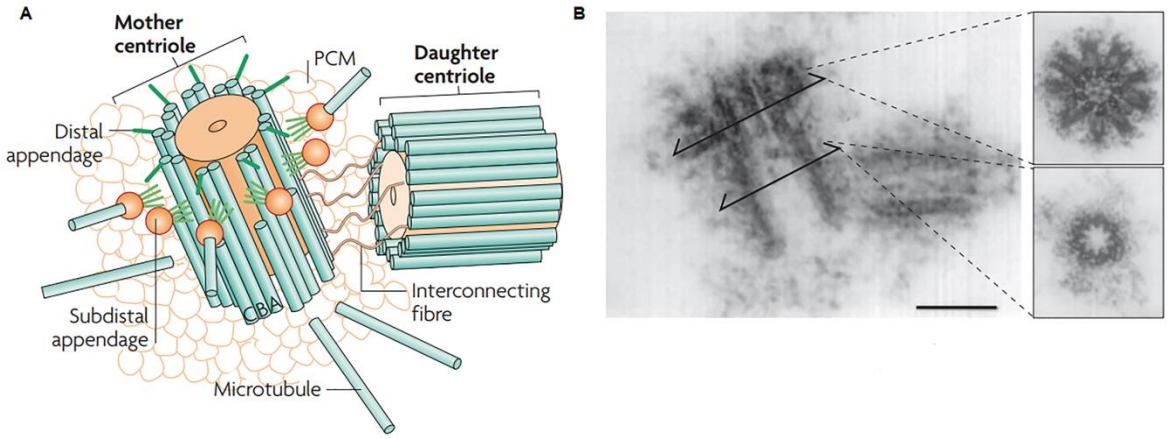

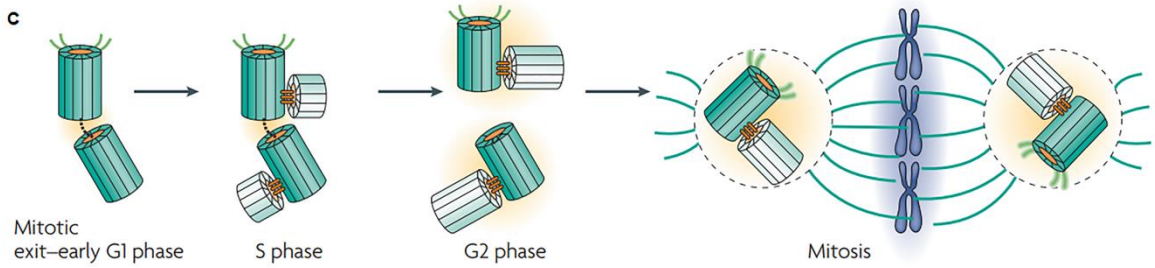

Figure 1.4: Schematic view of the centrosome and its replication cycle within animal cells. A. schematic organization of the centrosome. The centrosome is composed of a pair of orthogonally positioned centrioles. Each centriole consists of a structure made of nine microtubules triplets surrounded by the pericentriolar material (PCM). **B**. Electron micrograph of the centrosome. The top inset indicates a cross-section of subdistal appendages; the bottom inset indicates a cross-section of the proximal part of the centriole. Scale bar: 0.2µm. **C**. Diagram representing the centriole replication cycle. At mitotic exit-early G1 phase, the centriole disengage and lose the orthogonal configuration. In the next G1 to S phase the daughter centrioles start to originate from the mother centrioles, originating two pairs of procentrioles (light green). During G2, the linkage between centrosomes is disrupted and the maturation/elongation process initiates giving rise to two mature centrosomes. At G2-M transition, centrosomes further separate from each other, recruit the PCM and begins to act as the MTOC. Adapted from (Bettencourt-Dias and Glover, 2007).

Accurate control over centrosome number is crucial, as differences in centrosome numbers can cause severe errors in cell division, promoting chromosomal instability (CIN), a phenomenon often correlated with human cancer (reviewed in (Levine and Holland, 2018)). Centrosome number aberrations arise from failure in cytokinesis or cell cycle deregulation (reviewed in (Jusino et al., 2018)). Proper timing of centrosome separation has been also considered as a potential source of chromosome missegregation (Silkworth et al., 2012). Centrosome defects are frequently observed in many types of human tumors including ovaries, breast, lung, head and neck, prostate and liver cancer (reviewed in (Chan, 2011)). In addition, centrosome aberrations may be a promising therapeutic target for cancer suppression (reviewed in (Rivera-Rivera, 2016)).

1.2.2.2. The Kinetochores

At the onset of mitosis, each chromatid develops a large proteinaceous structure called kinetochore (from the Greek *kinetos*=movement and chore=place) at its centromeric region that forms the major interaction site for spindle microtubules (reviewed in (Cheeseman, 2014)). The improvement of biochemical and super resolution imaging techniques has been crucial for the mapping and resolution of kinetochore structure and composition. Kinetochores are very dynamic structures, as they have to assemble and disassemble every cell cycle. The simplest kinetochore is found in budding yeast and it attaches to only one microtubule (Winey et al., 1995). In human cells, kinetochores bind to approximately nine microtubules (Kiewisz et al., 2022) and are composed of more than 100 different

proteins (reviewed in (Cheeseman and Desai, 2008)). Based on the spatial localization and function of these proteins, the kinetochore is divided into three core parts: 1) a constitutive inner network that is involved in tethering the outer kinetochore to chromosomes, 2) a constitutive outer network that interacts with microtubules, and 3) a dynamic regulatory set of proteins that control the activities of the kinetochore (Figure 1.5) (reviewed in (Musacchio and Desai, 2017)). These dynamic components are principally focused on the KMN network (KNL-1, Mis12 complex and Ndc80 complex), which is responsible for regulating the kinetochores in two main functions: the physical attachment to microtubules and SAC activity.

The kinetochore is assembled on a specialized chromatin locus named the centromere, which is epigenetically defined by the localization of centromere protein CENP-A (CENtromere Protein-A), a histone H3 variant (reviewed in (Fukagawa and Earnshaw, 2014)). CENP-A is required for the recruitment of a constitutive centromere-associated protein network (CCAN). The CCAN makes up the core of the kinetochore and is responsible for the establishment of the outer kinetochore, which in turn constitutes the microtubule binding interface. CCAN is divided into 5 sub-complexes: CENP-C, the CENP-L, CENP-N and CENP-M sub-complex (CENP-LNM), the CENP-H, CENP-I and CENP-K sub-complex (CENP-HIK), the CENP-T, CENP-W, CENP-S, and CENP-X sub-complex (CENP-TWSX), and the CENP-O, CENP-P, CENP-Q, CENP-U, and CENP-R sub-complex (CENP-OPQUR) (reviewed in (Perpelescu and Fukagawa, 2011))(Figure 1.5). Moreover, CENP-A directly binds to CENP-C and the CENP-LNM complex (Weir et al., 2016), which interacts with the KMN network though the Mis12 complex at the outer kinetochore (Petrovic et al., 2016). Inner kinetochore proteins are constitutively present throughout the cell cycle. In contrast, outer kinetochore proteins are recruited to the kinetochore, via the CCAN, during mitosis (reviewed in (Cheeseman and Desai, 2008)). A key component of the outer kinetochore is the KMN-network, composed by the Mis12 complex (Mis12, Dsn1, Nnf1, and Nsl1), Knl1 and the Ndc80 complex (Ndc80 (Hec1), Nuf2, Spc24, and Spc25). The Ndc80 complex makes a direct contact with microtubules via Ndc80 and Nuf2, forming an interface between the kinetochore and microtubules (reviewed in (Cheeseman, 2014)). The Mis12 complex forms the central part of the KMN-network by establishing the interaction between the Ndc80 complex and Knl1 (Hara and Fukagawa, 2018; Petrovic et al., 2016). Knl1 is required for kinetochore recruitment of checkpoint components such as Bub1 and BubR1 and interacts stably with Zwint (reviewed in (Caldas and DeLuca, 2014)). Other regulatory complexes associate with the outer kinetochore, namely motor proteins and plus-end-tracking microtubule proteins (reviewed in (Cheeseman and Desai, 2008; Kops and Gassmann, 2020)).

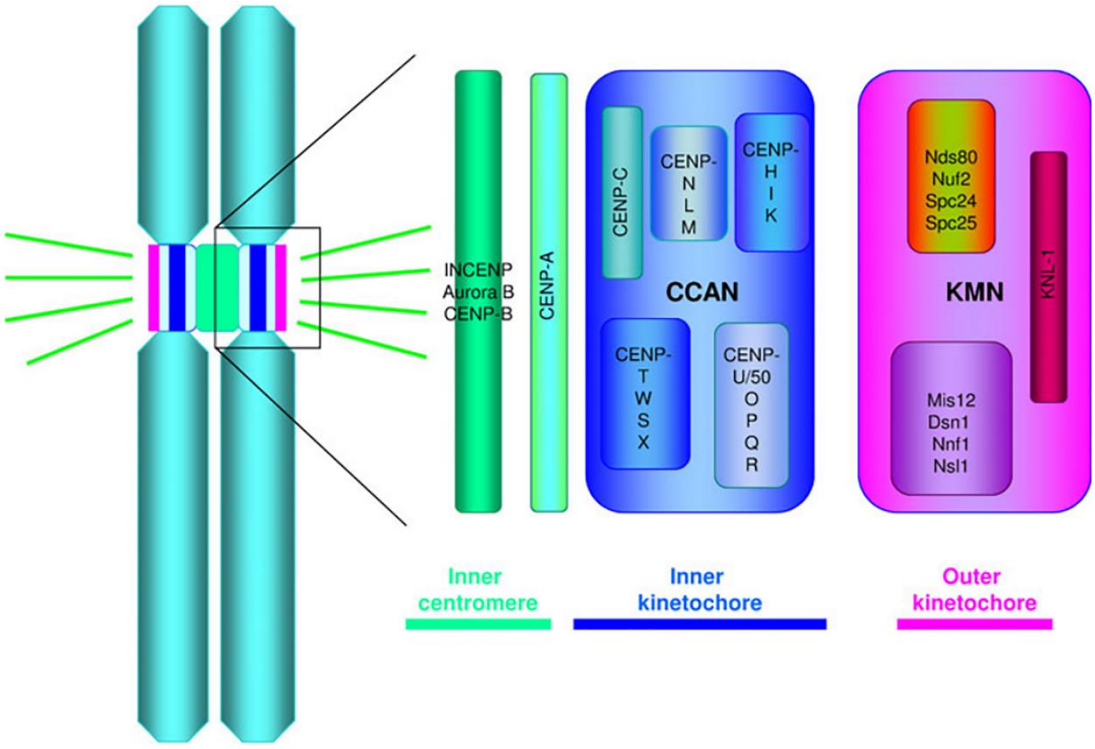

Figure 1.5: Schematic representation of the spatial distribution of centromeric and kinetochore proteins. The kinetochore is a proteinaceous structure that localizes at the centromeric region of chromosomes and mediated the interaction between chromosomes and spindle microtubules. Members of the CCAN complex constitute the inner kinetochore (in blue). The CCAN directs assembly of the KMN network comprising the KNL1, Mis12 and Ndc80 subcomplexes (in magenta). Adapted from (Perpelescu and Fukagawa, 2011).

1.2.2.3. Mitotic spindle

The mitotic spindle is essential for faithful chromosome segregation during mitosis. The most abundant component of the mitotic spindle are the microtubules, cytoskeleton straw-shaped structures organized in three different populations inside the cell, namely astral, interpolar and kinetochore microtubules. Astral microtubules are nucleated from centrosomes at the spindle poles towards the cortex and are involved in proper spindle positioning and centrosome separation during prophase (reviewed in (Rosenblatt, 2005)). Interpolar microtubules emanate from the spindle pole and extend towards the center of the spindle, thereby forming an antiparallel overlap at the spindle equator. They are important for spindle bipolarity and spindle elongation during anaphase (reviewed in (Dumont and Mitchison, 2009; Prosser and Pelletier, 2017)). Kinetochore microtubules organize into bundles that attach at the kinetochore region on each chromosome, forming kinetochore (k)-fibers. These structures are required to maintain chromosome position at the metaphase plate, as well as for operating the forces necessary for chromosome movement during anaphase (reviewed in (Godek et al., 2015; Prosser and Pelletier, 2017)).

Microtubules are dynamic, hollow cylindrical structures typically formed by thirteen laterally associated protofilaments of α-/β-tubulin heterodimers that interact head-to-tail (Nogales et al., 1999). Since the α-/β- tubulin heterodimer is intrinsically asymmetric, microtubules are polarized structures with β-tubulin exposed at one end (plus-end) and α-tubulin at the other end (minus-end) (reviewed in (Desai and Mitchison, 1997)). In addition to their role in the spindle, microtubules are involved in a number of cellular processes, including cell shape, cell motility, differentiation and intracellular transport. Microtubules in living mitotic spindles were initially visualized using polarized light microscopy, which demonstrated the polymerization/depolymerization dynamics of spindle microtubules. The development of imaging techniques combined with the use of fluorescently-tagged tubulin further revealed the dynamics of microtubules in live spindles (Mitchison, 1989; Waterman-Storer et al., 1999; Waterman-Storer, 1998). Microtubules are dynamic filaments that undergo successive cycles of growth (rescue) and shrinkage (catrastrophe), behavior known as dynamic instability (Mitchison and Kirschner, 1984) (Figure 1.6). In interphase, microtubules are typically long and rarely undergo catastrophe. During mitosis, microtubules are much more dynamic, with the less dynamic minus ends near the spindle poles while the fast growing plus-ends extend to the spindle equator and the cortex of the cell. Dynamic instability results from GTP hydrolysis within the β-tubulin subunit that occurs upon assembly and destabilizes the lattice by promoting a conformational change (reviewed in (Desai and Mitchison, 1997)). Under conditions that favor polymerization, a cap of GTP-tubulin subunits is maintained at the growing end that holds the microtubule together (Drechsel and Kirschner, 1994; Schek et al., 2007). However, if GTP hydrolysis catches up with subunit addition and the terminal subunits are converted to GDP-tubulin, the microtubule depolymerizes (Nogales et al., 1999).

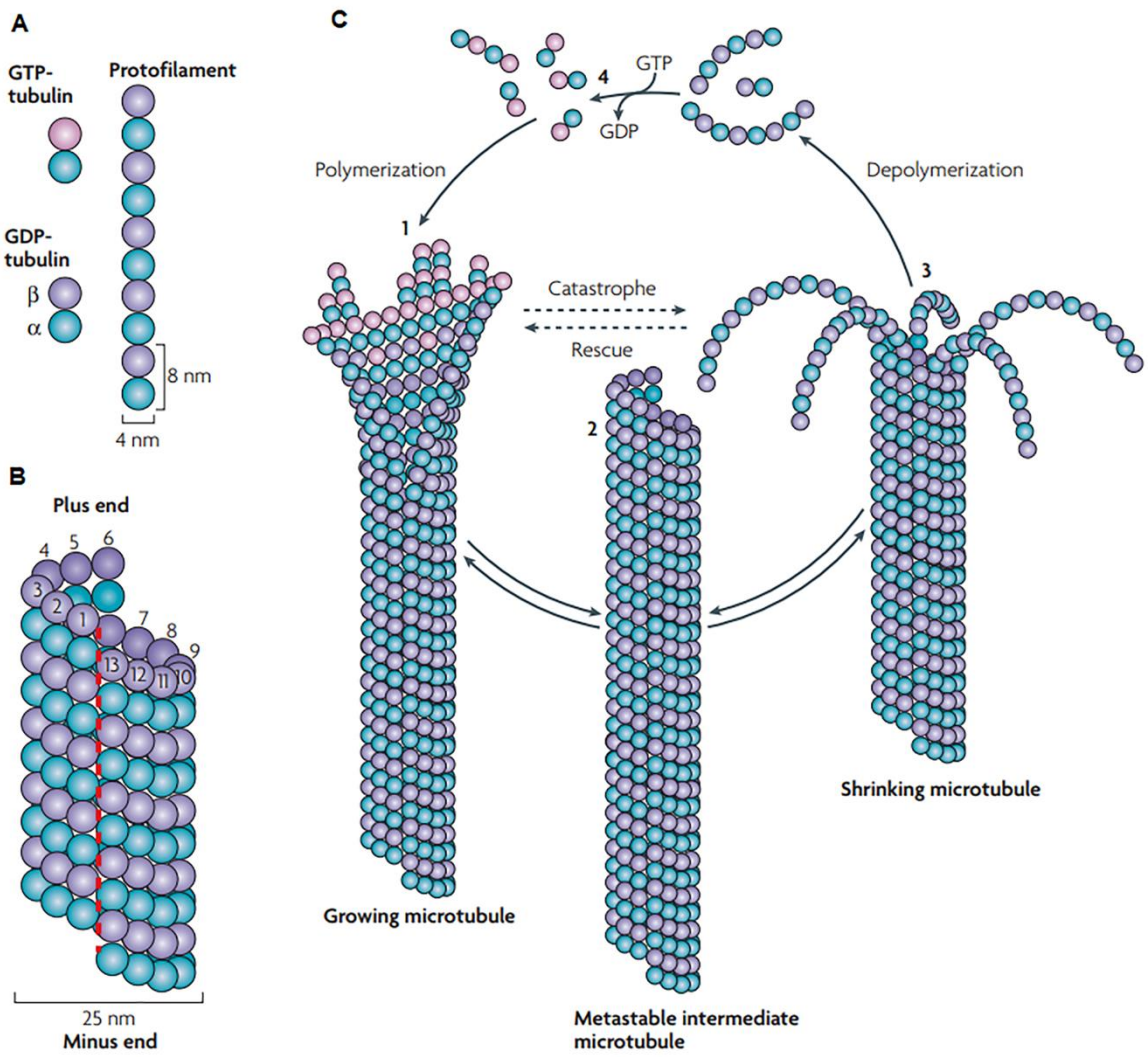

Figure 1.6: Microtubule dynamic instability. A. Microtubules consist of polymers of α-/β tubulin that are aligned in a head-to-tail fashion to form protofilaments. **B**. Microtubules are hollow tubes (25nm diameter) typically composed of 13 protofilaments. **C**. Mechanism of assembly (polymerization) and disassembly (depolymerization) of microtubules is driven by the binding, hydrolysis and exchange of a GTP on the β-tubulin monomer. Polymerization is initiated by a pool of GTP-loaded tubulin subunits (C1). The GTP-cap on growing microtubules stabilizes the subunits in straight tubulin conformation within the microtubule lattice. Intermediate metastable blunt-ended microtubule (C2) may pause, undergo further growth or switch to the depolymerization phase. GTP hydrolysis changes the conformation of a protofilament from a slightly curved tubulin-GTP to a curved tubulin-GDP structure and microtubule depolymerization occurs by the outward peeling of protofilaments (C3). The polymerization-depolymerization cycle is completed by exchanging GDP of the disassembly products with GTP (C4). Adapted from (Akhmanova and Steinmetz, 2008).

Although microtubules are highly conserved cytoskeleton filaments, many α-tubulin and β-tubulin isotypes encoded by several different genes have been identified in almost all organisms (reviewed in (Ludueña, 2013)). The different tubulin isotypes show specific cellular localization (reviewed in (Janke, 2014)). In addition, α- and β-tubulin isotypes may undergo multiple post-translational modifications (PTMs), such as phosphorylation, acetylation, detyrosination, polyglycylation and polyglutamylation. The combination of

different tubulin isotypes with PTMs generate microtubule diversity or a “tubulin code”, that controls properties and functions of microtubules in diverse cellular processes (Barisic and Maiato, 2016; Janke, 2014; Janke and Bulinski, 2011; Janke and Magiera, 2020; Roll-Mecak, 2020; Yu et al., 2015). In mitosis, spindle microtubules are mostly tyrosinated (α-tubulin with a tyrosine residue at the C-terminal tail) with high dynamics. The establishment of end-on kinetochore-microtubule attachments promote the gradual stabilization of spindle microtubules and they become increasingly detyrosinated (enzymatic removal of the last tyrosine residue from the α-tubulin C-terminal tail by tubulin carboxypeptidases (TCPs), including the recently identified Vasohibin 1 (VASH1) and Vasohibin 2 (VASH2) complexes with their associated Small Vasohibin-Binding Protein (SVBP)) (Janke and Magiera, 2020; Landskron et al., 2022; Roll-Mecak, 2020). It has been shown that motor proteins have different affinities to spindle microtubules depending on tubulin PTMs. Importantly, previous works in neurons revealed that the Kinesin-1 motor protein has a preference for microtubules with particular tubulin PTMs, namely detyrosination and acetylation (Konishi and Setou, 2009; Reed et al., 2006). Moreover, the microtubule plus-end-directed motor CENP-E/kinesin-7 shows higher affinity towards the detyrosinated microtubules, whereas the minus-end-directed motor dynein/dynactin preferentially binds to tyrosinated microtubules. Thus, detyrosinated/tyrosinated α-tubulin regulates the activity of opposing kinetochore motors and functions as a navigation system for chromosome congression to the spindle equator (Barisic et al., 2015, 2014; Barisic and Maiato, 2016; Lopes and Maiato, 2020) (see section 1.3.3 for in-depth characterization). Additionally, tubulin PTMs are also involved in spindle orientation/positioning, through tyrosinated astral microtubules and dynein at the cell cortex (Barbosa et al., 2017; Kotak et al., 2012; Liao et al., 2019). Recently, it was proposed that the levels of tyrosinated and detyrosinated α-tubulin regulate mitotic error correction by modulating mitotic centromere-associated kinesin (MCAK) activity at centromeres/kinetochores (Ferreira et al., 2020). Moreover, several works have reported an emerging link between alterations of tubulin PTMs and/or associated modifying enzymes with certain cancers (reviewed in (Lopes and Maiato, 2020)).

1.2.3. Microtubule associated proteins (MAPs) and motor proteins

The establishment of a proper bipolar spindle and chromosome segregation depends on microtubule-associated proteins (MAPs) and motor proteins. While MAPs directly influence microtubule dynamics and stability through the interaction with the microtubule lattice and/or ends, motor proteins use adenosine triphosphate (ATP) hydrolysis to generate forces and motion (reviewed in (Bodakuntla et al., 2019; Glotzer, 2009)). Among these, microtubule

plus-end-tracking proteins (+TIPs) are of special interest due to their specific accumulation at the plus-ends of microtubules (reviewed in (Akhmanova and Steinmetz, 2010, 2008; Schuyler and Pellman, 2001)) where they promote microtubule growth by catalyzing the addition of tubulin subunits to microtubule plus-ends (Brouhard et al., 2008), by inducing rescue (Komarova et al., 2002), or by stabilizing microtubules (Akhmanova et al., 2001; Mimori-Kiyosue et al., 2005). CLIP-170 was the first +TIP reported (Perez et al., 1999) and was initially associated with microtubule rescue (Komarova et al., 2002). Functional inhibition of CLIP-170 during mitosis results in chromosome alignment defects, possibly associated with defective kinetochore-microtubule attachments (Dujardin et al., 1998; Tanenbaum et al., 2006). However, CLIP-170 inhibition does not seem to affect kinetochore microtubule dynamics or stability, possibly because it is stripped from the kinetochore by Dynein upon the establishment of end-on kinetochore-microtubule attachments (Dujardin et al., 1998; Tanenbaum et al., 2006). Moreover, phosphorylation of CLIP-170 at S312 by Plk1 regulates its binding to microtubules and is crucial for chromosome alignment (Kakeno et al., 2014). CLIP-170 appears to promote kinetochore-microtubule attachments and chromosome congression by counteracting Dynein/Dynactin (Amin et al., 2015). The XMAP215/Ch-TOG and CLASP families of +TIPs have also been implicated in spindle assembly and maintenance. The XMAP215/Ch-TOG proteins act as microtubule polymerases at microtubule plus-ends and promote microtubule assembly (Bonfils et al., 2007; Brouhard et al., 2008; Gard and Kirschner, 1987), whereas CLASPs promote microtubule rescue and suppress catastrophe (Al-Bassam et al., 2010; Al-Bassam and Chang, 2011). Depletion of proteins from the XMAP215/Ch-TOG family results in the presence of unattached kinetochores and chromosome alignment defects (Gandhi et al., 2011; Gergely et al., 2003; Kitamura et al., 2010; Miller et al., 2016). Moreover, XMAP215/Ch-TOG contributes to chromosome oscillations (Cassimeris et al., 2009). Recruitment of CLASPs to microtubule plus-ends requires interactions with CLIP-170 and EB1 (Akhmanova et al., 2001; Mimori-Kiyosue et al., 2005). Importantly, CLASPs also localize to kinetochores in a microtubule-independent manner and remain at kinetochores upon microtubule attachment (Maiato et al., 2003; Pereira et al., 2006). This localization at the kinetochore-microtubule interface favors a role of CLASPs in the regulation of microtubule dynamics at the kinetochore (Maffini et al., 2009; Maiato et al., 2005), thereby contributing to chromosome congression (Maiato et al., 2003). Surprisingly, perturbation of either CLASPs or XMAP215/Ch-TOG increases the stability of kinetochore-microtubule attachments (Cassimeris et al., 2009; Maffini et al., 2009). One possibility might be that during mitosis the activity of these proteins is regulated by phosphorylation and/or binding to other proteins that promote microtubule depolymerization (Maia et al., 2012; Manning et al., 2010). Further stabilization of kinetochore-microtubule attachments is thought to be

mediated by the activity of HURP, which decorates the kinetochore-proximal end of k-fibers in a Ran (Ras-related nuclear protein)-GTP dependent manner (Silljé et al., 2006) and promotes chromatin-induced microtubule assembly (Casanova et al., 2008). HURP depletion impairs k-fiber stability and leads to chromosome congression defects, whereas its overexpression increases microtubule stability (Silljé et al., 2006; Wong and Fang, 2006).

The members of the Kinesin-13 family Kif2a, Kif2b and Kif2c/MCAK are important regulators of microtubule dynamics, including at kinetochores (reviewed in (Walczak et al., 2013)). Kinesin-13 proteins are non-motile but use the energy from ATP hydrolysis to promote microtubule depolymerization by binding both the plus- and the minus-ends of microtubules and inducing a conformational change that leads to a catastrophe event (Desai et al., 1999; Manning et al., 2007; Walczak, 2003). In the context of the mitotic spindle, Kinesin-13 proteins associate with both spindle poles and kinetochores where they play distinct roles (Ganem and Compton, 2004; Manning et al., 2007). Kif2b and MCAK regulate microtubule plus-end dynamics at the kinetochore where they play an important role in the correction of erroneous microtubule attachments (Bakhoum et al., 2009b; Kline-Smith and Walczak, 2002; Manning et al., 2007; Walczak et al., 1996; Wordeman et al., 2007), while Kif2a appears to have a preference for microtubule minus-ends where it plays an important role in the regulation of spindle microtubule flux (Gaetz and Kapoor, 2004; Ganem et al., 2005).

Chromokinesins are kinesin-like motor proteins that have DNA-binding properties and associate with chromosomes during mitosis (Vernos et al., 1995; Wang and Adler, 1995). The best characterized mammalian chromokinesins are Kif4a and Kid, which belong to two distinct families: Kinesin-4 and Kinesin-10, respectively (reviewed in (Almeida and Maiato, 2018; Vanneste et al., 2011)). Functional analysis revealed a combined role for Kinesin-4 and Kinesin-10 in chromosome congression, arm-orientation and normal chromosome oscillations, consistent with an active role of Kinesin-4 and Kinesin-10 in the generation of polar ejection forces (PEFs) (Antonio et al., 2000; Barisic et al., 2014; Funabiki and Murray, 2000; Goshima and Vale, 2003; Levesque and Compton, 2001; Magidson et al., 2011; Mazumdar et al., 2004; Theurkauf and Hawley, 1992; Vernos et al., 1995; Wandke et al., 2012; Zhu et al., 2005).

The microtubule minus-end-directed motor dynein plays a variety of mitotic functions (reviewed in (Mountain and Compton, 2000)). Dynein was shown to localize at the kinetochores (Pfarr et al., 1990), cell cortex (Fink et al., 2006) and along spindle microtubules (Varma et al., 2008). Dynein at kinetochores controls SAC silencing by removing SAC proteins from kinetochores (Gassmann et al., 2010; Wojcik et al., 2001). Cortical dynein with dynactin is involved in spindle positioning by pulling forces exerted on astral microtubules (Barbosa et al., 2017; Kotak et al., 2012). Dynein, together with

HSET/kinesin-14 (minus end directed motor protein), slides anti-parallel microtubules, generating an inward force required for spindle pole focusing (Ferenz et al., 2009; Hepperla et al., 2014; Tanenbaum et al., 2013). Moreover, dynein is also involved in the poleward movement of chromosomes early in mitosis (Barisic et al., 2014; Maiato et al., 2004).

Different kinesins were shown to be involved in spindle assembly and chromosome movement. Members of the Kinesin-5 family, such as Eg5, are responsible for the generation of poleward forces that can drive microtubule sliding and promote pole-to-pole separation (Gatlin and Bloom, 2010). Kinesin-14 family (HSET in human) are minus-end directed motors that cross-link microtubules and play key roles during spindle assembly (Cai et al., 2009). The microtubule plus-end-directed motor CENP-E, a member of the kinesin-7 protein family, localizes at kinetochores and is essential for chromosome congression (Kapoor et al., 2006).

The widely conserved Kinesin-8 family has been proposed to function both as plus-end-directed motors and as microtubule depolymerases (Gupta et al., 2006; Mayr et al., 2007; Varga et al., 2009, 2006). However, the depolymerase activity of human Kif18A remains controversial. Although Kif18A was initially proposed as a microtubule depolymerase (Mayr et al., 2007), further studies suggested that Kif18A suppresses microtubule growth by capping the microtubule plus-ends (Du et al., 2010; Stumpff et al., 2011). This would be consistent with the emerging role of Kinesin-8 motors as negative regulators of microtubule length, since loss of Kinesin-8 activity generally leads to longer cellular microtubules (Gandhi et al., 2004; Goshima et al., 2005; Mayr et al., 2007; Rischitor et al., 2004; Straight et al., 1998). Importantly, genetic and siRNA-based studies demonstrate that Kinesin-8 motors are necessary for proper chromosome alignment by suppressing chromosome oscillations on bi-oriented chromosomes (Gandhi et al., 2004; Goshima and Vale, 2003; Mayr et al., 2007; Stumpff et al., 2008; West et al., 2002; Zhu et al., 2005). Accordingly, in the absence of functional Kif18A, kinetochores exhibit an increase in the oscillation amplitude leading to a deregulation of metaphase plate organization (Stumpff et al., 2008). Furthermore, loss of Kif18A leads to a modest increase in spindle size and longer microtubules (Mayr et al., 2007; Stumpff et al., 2008). In agreement, overexpression of Kif18A decreases chromosome oscillations, favoring chromosome alignment at the metaphase plate (Jaqaman et al., 2010; Stumpff et al., 2008).

1.3. Chromosome congression and bi-orientation

1.3.1. What is chromosome congression?

In preparation for cell division, two poles and an equator start to be defined by the mitotic spindle axis. Precisely at the onset of mitosis, when chromosomes start condensing and the nuclear envelope breaks down, dispersed chromosomes initiate directed movements that culminate with their position at the spindle equator before migrating to the poles after sister chromatid separation. This stochastic motion towards the equator coincides with the beginning of prometaphase and is known as “chromosome congression” (from the English “to come together”; terminology first introduced by Darlington (Darlington, C.D., 1937)). Chromosome congression truly represents the first challenge of mitosis and culminates with the formation of a metaphase plate, a hallmark of mitosis in metazoans, and occurs in tight spatiotemporal coordination with the assembly of the mitotic spindle that mediates the microtubule-chromosome interactions required for chromosome movement.

1.3.2. Why do chromosome congress?

At first glance, it may seem counterintuitive that before chromosomes segregate to the poles (during anaphase), they first meet at the equator. This likely reflects millions of years of evolution aiming to improve chromosome segregation fidelity. For instance, if one imagines a mitotic cell in which chromosomes do not congress, the risk of chromosome missegregation after sister chromatid separation at anaphase would be too high, unless all chromatids are extensively moved apart, like in the budding yeast *S. cerevisiae*, in which the anaphase spindle elongates about 5-fold relative to the metaphase spindle length (Straight et al., 1997). In contrast, metazoan spindles only elongate less than 2-fold the metaphase spindle length (reviewed in (Goshima and Scholey, 2010)) and thus must rely on different strategies to ensure faithful chromosome segregation during anaphase. One of these strategies is precisely the formation of a metaphase plate, forcing all chromosomes to start subsequent poleward motion from the same position relative to the spindle axis, i.e., from the equator. The other is to trigger an abrupt cleavage of cohesin by separase-mediated degradation of securin, leading to the synchronous separation and movement of sister chromatids towards the pole. This anaphase synchrony has been shown to depend on the uniform distribution of spindle forces acting on all chromosomes prior to anaphase (Matos et al., 2009). Aligning chromosomes at the equator also maximizes the chances of kinetochore capture by microtubules emanating from both spindle poles leading to

chromosome bi-orientation, which is required to satisfy the spindle assembly checkpoint (SAC) (reviewed in (Joglekar, 2016)). Finally, chromosome congression is important to prevent unstable/erroneous kinetochore-microtubule attachments because the proximity to the poles promotes microtubule destabilization at kinetochores due to high Aurora A kinase activity that leads to phosphorylation of Ndc80 (among others), thereby reducing its affinity for microtubules (Barisic et al., 2014; Chmátal et al., 2015; Ye et al., 2015). In addition, tension generated by opposing pulling forces on aligned bi-oriented chromosomes is required and sufficient to stabilize correct attachments (King and Nicklas, 2000).

1.3.3. An integrated model of chromosome congression

In mammalian cells, chromosome congression can be explained by two main mechanisms that operate in parallel (Figure 1.7), meaning that not all chromosomes relie on the same mechanism to complete congression (reviewed in (Maiato et al., 2017)). A key aspect that determines which mechanism is used depends essentially on whether chromosomes establish lateral or end-on attachments at their kinetochores on their way towards the equator. This is influenced by the position of chromosomes relative to the spindle poles at NEBD. Those chromosomes that are able to bi-orient soon after NEBD would use a “direct congression” mechanism in which opposite kinetochore-pulling forces, resulting from the tight regulation of microtubule dynamics and length at the kinetochores, in coordination with PEFs along chromosome arms, drive chromosome oscillations until net force is zero near the equator (Auckland and McAinsh, 2015). A corollary from this model is that the establishment of stable end-on attachments inhibits the other congression mechanism relying on lateral interactions between microtubules and kinetochores. The second mechanism, called “peripheral congression”, would take advantage of the high processivity of the Dynein/Dynactin motor localized on unattached kinetochores to capture peripheral chromosomes, which are unable to bi-orient at NEBD and establish stable end-on kinetochore microtubule attachments (Barisic et al., 2014). The minus-end directed motion of Dynein/Dynactin along tyrosinated astral microtubules transports peripheral chromosomes close to one of the spindle poles, where Aurora A activity is highest and prevents the stabilization of end-on kinetochore-microtubule attachments. This configuration also imposes a dominance of kinetochore Dynein/Dynactin over the action of Chromokinesin-mediated PEFs along chromosome arms that would otherwise promote the premature stabilization of end-on kinetochore-microtubule attachments and lead to errors resulting in chromosome missegregation. In addition, while travelling along tyrosinated

astral microtubules, Dynein/Dynactin will be dominant over the other kinetochore motor, CENP-E, with plus-end-directed motility and a preference for more stable detyrosinated microtubules (Barisic et al., 2015). Once at the poles, phosphorylation by Aurora A will activate CENP-E, (while other centrosome kinases, such as Plk1, inactivate Dynein/Dynactin), favoring the lateral transport of chromosomes by CENP-E along detyrosinated microtubules (either k-fibers or interpolar microtubule bundles) towards the equator, where the chances for bi-orientation are maximal (Barisic et al., 2015; Kapoor et al., 2006). At the equator, Chromokinesins promote the conversion from lateral to end-on attachments, which further downregulates CENP-E and Dynein, thereby ensuring the maintenance of chromosome position at the metaphase plate (Almeida and Maiato, 2018; Cane et al., 2013; Drpic et al., 2015; Wandke et al., 2012). Once aligned and bi-oriented at the metaphase plate, the coordination between kinetochore-pulling forces and PEFs continue to determine the amplitude of chromosome oscillations, but maintenance of chromosome position near the equator will depend on additional factors that mediate the cross-linking between kinetochore and non-kinetochore microtubules.

Overall, chromosome congression in mammalian cells relies on the concerted action of motor-dependent and – independent mechanisms, which are determined by the establishment of end-on or lateral kinetochore-microtubule interactions. Therefore, any perturbation that introduces alterations of microtubules dynamics or kinetochore function will likely compromise the congression of at least some chromosomes during mitosis. To date, more than 100 proteins have been implicated in chromosome alignment (see Table 1), but their exact role in the activities necessary for either congression or maintenance of alignment remains unknown for > 90% of them.

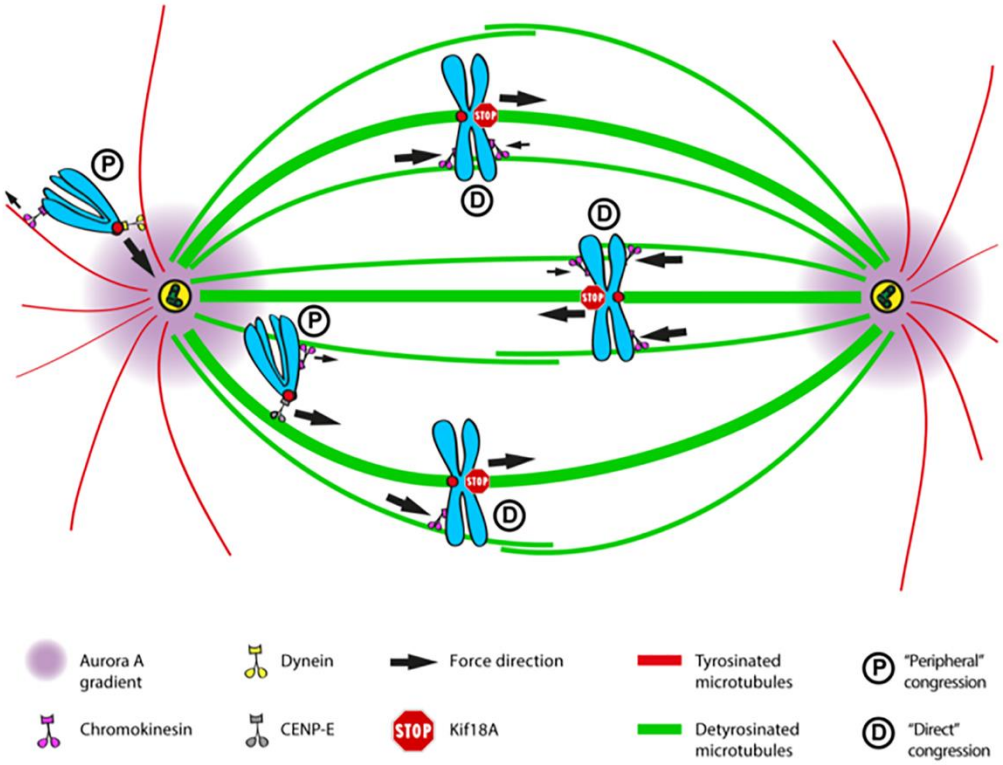

Figure 1.7: Integrated model of chromosome congression in human cells. In early prometaphase, the initial position of the chromosomes in relation to the spindle pole at NEBD dictates the mechanism by which they are translocated to the equator. Peripheral chromosomes are captured by dynein, a minus-end directed motor, which transports chromosomes along tyrosinated astral microtubules towards the spindle poles. This prevents the random ejection of the chromosome by the action of Chromokinesins on chromosome arms. Once at the pole, high Aurora A activity prevents the stabilization of end-on kinetochore-microtubule attachments. In parallel, Aurora A-mediated phosphorylation activates CENP-E at kinetochore. This initiates the lateral transport of chromosomes along detyrosinated microtubules toward the cell equator, increasing the changes of bi-orientation. In parallel, minor chromokinesin-mediated polar ejection forces assist chromosome congression by favoring the plus-end directed movement, thereby promoting the conversion from lateral to end-on attachments and kinetochore-microtubule attachment stabilization. Adapted from (Maiato et al., 2017).

1.3.4. Chromosome Congression vs. Maintenance of Alignment

One poorly understood aspect of mitosis is whether the mechanisms that mediate chromosome congression consist of the same principles that ensure the maintenance of a bi-oriented chromosome at the equator after completing congression. Clearly, motor-dependent chromosome congression does not rely on a force balance on a given kinetochore pair, as chromosome bi-orientation is not required to complete congression (Kapoor et al., 2006). Moreover, end-on kinetochore-microtubule attachments are not even required for motor-driven congression to the equator, but are essential to maintain aligned chromosomes at the metaphase plate (Cai et al., 2009). This is corroborated by

microsurgery experiments in which the kinetochore region of a once aligned chromosome is irradiated with a focused UV or laser microbeam, causing the chromosome to immediately move towards the direction of the undisturbed kinetochore (Izutsu, 1961, 1959; Takeda et al., 1960). In contrast, when k-fibers are cut on a bi-oriented chromosome positioned at the equator, chromosomes either do not shift at all or shift only slightly towards the pole of the unperturbed k-fiber (Czaban et al., 1993; Elting et al., 2014; Forer, 1965; Inoué, 1964; Izutsu, K., 1961; Kajtez et al., 2016; Maiato et al., 2004; Nicklas, 1989; Sikirzhytski et al., 2014; Spurck et al., 1990; Takeda et al., 1960). Interestingly, inter-kinetochore tension in vertebrate and insect cells is proportional to k-fiber length (Kajtez et al., 2016; Milas et al., 2016). Overall, these data indicate that while force at kinetochores is proportional to k-fiber length, maintenance of chromosome position near the equator is not.

Several theoretical and experimental studies have predicted or provided evidence for mechanical coupling between kinetochore and non-kinetochore (interpolar) microtubules (Goode, D, 1981; Kajtez et al., 2016; Margolis et al., 1978; Mastronarde et al., 1993; Matos et al., 2009; McIntosh et al., 1969; Milas et al., 2016; Nicklas et al., 1982; Pereira and Maiato, 2012; Shimamoto et al., 2011; Vladimirou et al., 2013), which might account for the maintenance of chromosome positioning at the equator independently of k-fiber length. While the molecular nature of this spindle microtubule coupling system remains unknown, it is likely to involve multiple players that possess the necessary molecular properties to serve this purpose. These include several MAPs and motors with microtubule cross-linking properties, such as PRC1, Kinesin-5, Kinesin-15, CLASPs, Clathrin/Ch-TOG/TACC3, Asp, NuMa, Kinesin-14 and Dynein (Cross and McAinsh, 2014; Maiato et al., 2004; Royle, 2012). In addition, Chromokinesins, Kif4A in particular, might also work as a coupling element between k-fibers and interpolar microtubules interacting with chromosome arms (Wandke et al., 2012).

Interestingly, many loss-of-function studies of Chromokinesins revealed only a very minor role during chromosome congression, while being critical to maintain chromosomes aligned at the equator (Barisic et al., 2014; Wandke et al., 2012). These results suggest that Chromokinesins might additionally contribute to the stabilization of kinetochore-microtubule attachments of aligned chromosomes, possibly in coordination with the activity of Kinesin-8 (Stumpff et al., 2012). Indeed, recent works in Drosophila S2 cells have shown that Chromokinesins promote kinetochore-microtubule stabilization and the conversion from lateral to end-on attachments, independently of chromosome bi-orientation (Cane et al., 2013; Drpic et al., 2015), which might be important to maintain chromosomes aligned at the equator after congression. This implies that CENP-E is no longer dominant over Chromokinesins once chromosome bi-orientation and equatorial alignment is achieved. This would be consistent with the finding that CENP-E levels at the kinetochore decrease

significantly due to Dynein-mediated stripping upon microtubule attachment and chromosome bi-orientation (Hoffman et al., 2001). However, whether CENP-E plays a role in maintaining chromosome positioning at the equator after alignment has been controversial. For instance, CENP-E has been proposed to play a role in stabilizing end-on kinetochore-microtubule attachments (Cleveland et al., 2003; McEwen et al., 2001; Putkey et al., 2002). This model is supported by electron microscopy studies after inactivation of CENP-E function, which showed a reduced microtubule number at kinetochores of aligned bi-oriented chromosomes, supporting a role for CENP-E after chromosome congression (McEwen et al., 2001; Putkey et al., 2002). Importantly, the observed differences relative to controls appear to be attenuated during a prolonged mitosis where the range of microtubule binding was similar to controls, indicating that CENP-E is not essential for binding of a full complement of microtubules at kinetochores of bi-oriented chromosomes (McEwen et al., 2001). Interestingly, original antibody micro-injection experiments in metaphase cells have indicated that CENP-E is not required for maintenance of chromosome alignment (Yen et al., 1991). In contrast, treatment of metaphase cells with a CENP-E inhibitor that forces CENP-E to bind tightly to microtubules (a “rigor” state) caused the displacement of chromosomes from the equator, supporting a role of CENP-E in maintaining chromosome alignment after bi-orientation, in addition to mediating chromosome congression (Gudimchuk et al., 2013). The availability of a second generation of CENP-E inhibitors that compromise ATPase activity without interfering with microtubule binding (Ohashi et al., 2015) will be important to clarify the role of CENP-E after chromosome alignment. Finally, many studies have reported chromosome misalignment problems after functional perturbation of several proteins (see Table 1). However, since live-cell imaging was not used in many of these studies, it remains unclear whether it truly reflects a direct role of these proteins in chromosome congression or in the maintenance of chromosome alignment. The recent discovery that apparently unrelated experimental perturbations associated with a metaphase delay often lead to “cohesion fatigue” (i.e., the uncoordinated loss of sister chromatid cohesion after chromosome congression but prior to anaphase onset, due to the action of mitotic spindle forces) (Daum et al., 2011; Gorbsky, 2013; Stevens et al., 2011) incites for a systematic re-evalution of proteins formerly associated with chromosome alignment using state-of-the-art live-cell imaging techniques.

1.4. The Spindle Assembly Checkpoint

The ultimate purpose of mitosis is to equally segregate the genetic material to the daughter cells. To achieve this, the dividing cell must commence the process of cell division only after each sister kinetochore is correctly attached to spindle microtubules emanating from opposite spindle poles. Premature anaphase onset in the presence of erroneous attachments will lead to unequal division of the genetic content and therefore the emergence of aneuploid cells (reviewed in (Musacchio and Salmon, 2007)). To avoid this fate, the cell is equipped with a surveillance mechanism, known as the spindle assembly checkpoint (SAC), which prevents cell division until all chromosomes are attached to the microtubule spindle apparatus via their kinetochores, favoring bi-orientation at the metaphase plate.

Spindle assembly checkpoint genes were originally discovered in the budding yeast *Saccharomyces cerevisiae*, after screening for mutants that failed to arrest in mitosis in the presence of microtubule poisons (Hoyt et al., 1991; Li and Murray, 1991). These studies identified the mitotic-arrest deficient genes (*MAD1*, *MAD2*, *MAD3* (*BUBR1* in humans)), and the budding uninhibited by benzimidazole genes (*BUB1, BUB2* and *BUB3*) (Hoyt et al., 1991; Li and Murray, 1991). Subsequently, other SAC components such as Mps1 were identified (Weiss and Winey, 1996). The SAC machinery is conserved from yeast to humans, despite the existence of species-specific contributions of SAC proteins to the checkpoint function (reviewed in (Vleugel et al., 2012)).

SAC signaling involves the concentration of the mitotic checkpoint complex (MCC), a heterotetramer composed by Cdc20, Mad2, BubR1/Mad3 and Bub3, at unattached kinetochores (reviewed in (Musacchio, 2015). Initial recruitment of the template composed of Mad1 and Mad2 components relies on Mps1 kinase activity that is recruited to kinetochores through Aurora B phosphorylation of the Ndc80 complex (De Antoni et al., 2005). Mps1 kinase is also responsible for kinetochore targeting of the SAC components Bub1, Bub3 and BubR1, through the phosphorylation of Knl1 (reviewed in (Lara-Gonzalez et al., 2021; Musacchio, 2015). Mad1 binding to unattached kinetochores recruits an inactive form of Mad2 (open o-Mad2), inducing a conformational change into the active closed form (c-Mad2). c-Mad2 can bind Cdc20 and the c-Mad2-Cdc20 complex interacts with BubR1 and Bub3 to form the MCC, the major inhibitor of APC/C (De Antoni et al., 2005; Mapelli et al., 2007; Sironi et al., 2002). When APC/C is inactive, Cyclin B1 and Securin are not degraded and, consequently, cell cycle progression is blocked. Once all kinetochores are stably attached to the mitotic spindle the “wait anaphase signal” is shut down and Cdc20 is free to activate the APC/C. APC/C activity then targets Cyclin B1 and Securin for proteasomal degradation. As a result of Cyclin B1 degradation, Cdk1 is inactivated, while

Securin degradation activates Separase-mediated cleavage of Scc1, a subunit of the cohesion complex. Degradation of these substrates triggers anaphase onset and mitotic exit (reviewed in (Musacchio, 2015) (Figure 1.8).

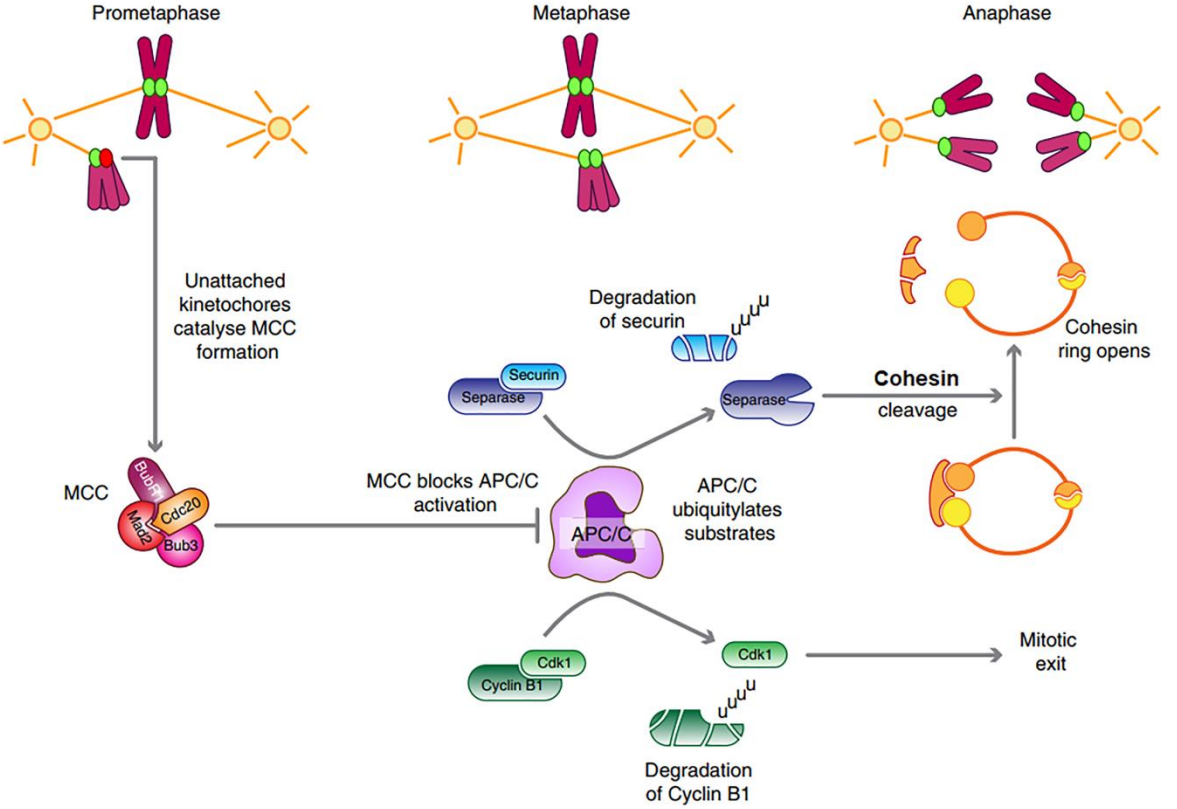

Figure 1.8: Spindle assembly checkpoint (SAC). In prometaphase, the SAC surveillance mechanism senses the unattached kinetochores and facilitates the formation of an inhibitory signal. The mitotic checkpoint complex (MCC), composed of Ccd20, Mad2, BubR1 and Bub3, inhibits the APC/C, preventing premature mitotic exit. Once all the chromosomes are aligned with their kinetochores attached to the spindle (metaphase), generation of the MCC ceases, which allows the activation of the APC/C by Cdc20, leading to the ubiquitylation and degradation of Securin and Cyclin B1. Degradation of Securin releases separase which in turn cleaves Scc1 subunit of the cohesion ring structure allowing the separation of sister chromatids (anaphase). In the meantime, degradation of Cyclin B1 inactivates Cdk1, leading to mitotic exit. Adapted from (Lara-Gonzalez et al., 2012).

The Aurora B kinase, a member of the Chromosomal Passenger Complex (CPC), enriched at the inner centromeres, plays a central role in controlling the attachment status during mitosis. Aurora B kinase destabilizes kinetochore-microtubule attachments by phosphorylating outer kinetochore proteins (Liu et al., 2009). Once all kinetochore-microtubule attachments are established, the SAC is satisfied. Until very recently, the prevailing idea was that SAC proteins are then removed from kinetochores via stripping mediated by the dynein motor protein (Gassmann et al., 2010; Howell et al., 2001; Wojcik et al., 2001). However, a recent study proposed that dynein´s role in SAC silencing is retricted to evicting checkpoint effectors (e.g. Mad1 and Mad2) from fibrous corona and not the outer kinetochore (Ide et al., 2023). Moreover, Mps1 kinetochore localization depends

on Aurora B mediated phosphorylation of its N-terminal TPR (tetratricopeptide repeat) domain. Phosphorylation of TPR domain, removes its inhibitory effect on Mps1 localization (Nijenhuis et al., 2013). Additionally, the presence of phosphatases at the outer kinetochore is essential to revert the SAC-dependent phosphorylation and promote SAC silencing (Grallert et al., 2015; Lesage et al., 2011).

The incapacity of cells to satisfy the SAC induces a prolonged mitotic delay (up to 20 hours or more in human cells). Several studies have revealed that SAC is not an all-or-nothing response, but depends on the number of unattached kinetochores that correlates with the amount of Mad2 at kinetochores (Collin et al., 2013; Dick and Gerlich, 2013). Importantly, cells cannot maintain this mitotic arrest indefinitely due to the slow degradation of Cyclin B1, independent of active SAC signaling (Brito and Rieder, 2006). Ultimately, two major outcomes have been described to follow this mitotic arrest: cells can die in mitosis or undergo mitotic slippage, returning to G1 as a tetraploid cell (Rieder and Maiato, 2004; Weaver et al., 2007). The currently accepted model proposes that mitotic cell fate during chronic arrest is determined by the balance between pro-apoptotic and pro-survival signals (the competing networks model) (Gascoigne and Taylor, 2008; Topham and Taylor, 2013) (Figure 1.9). If cyclin B1 levels drop below the threshold necessary to maintain Cdk1 activity and the mitotic state, cells slip out of mitosis. Conversely, if cells produce enough cell death signaling up to the point-of-no return from intrinsic apoptosis, cells will die in mitosis. In support of the competing networks model, delaying mitotic slippage by either Cyclin B1 overexpression, Ccd20 depletion, or APC/C pharmacologic inhibition shifts the fate profile to death in mitosis, whereas inhibiting caspase activation lays cells more predisposed to mitotic exit (Gascoigne and Taylor, 2008; Sloss et al., 2016; Zeng et al., 2010). Additionally, the duration of the mitotic arrest is determined by the presence of multiple Cdc20 proteoforms within the same cell (Tsang and Cheeseman, 2023).

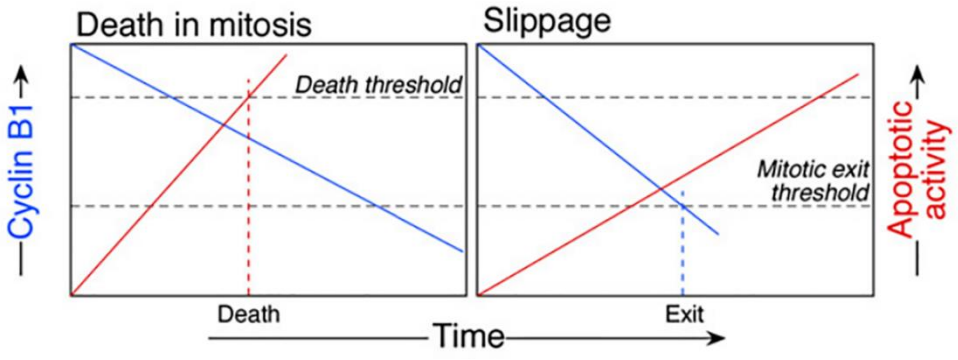

Figure 1.9: The competing networks model. After a prolonged mitotic arrest, the decision to slip out of mitosis (right) or to die in mitosis (left) is dictated by two processes during the arrest; a slow, but progressive loss of cyclin B1 and a slow, but steady rise in cell death activity. Mitotic cell fate is dictated by which threshold is reached first. Adapted from (Gascoigne and Taylor, 2008).

1.5. Kinetochore-Microtubule attachments

Faithfull segregation of chromosomes requires that all chromosomes are correctly attached to spindle microtubules before anaphase onset. The only kinetochore-microtubule attachment that ensures this principle is an amphitelic attachment, where each sister kinetochore binds in an “end-on” fashion to microtubules oriented to opposite poles. There are two models to explain kinetochore-microtubules attachments. According to the “search and capture” (S&C) model, centrosomes nucleate microtubules in all directions and the interactions between kinetochores and microtubules relies in the capacity that microtubules have to dynamically alternate between growing (polymerization) and shrinking (depolymerization) phases (Kirschner and Mitchison, 1986). Dynamic microtubules explore (“search”) different directions and once they encounter (“capture”) a kinetochore, they establish attachments that are selectively stabilized. However, theoretical models predict that, in order to achieve complete capture of all 46 chromosomes present in a human cell, the search and capture mechanism by itself is insufficient to explain the typical observed duration of prometaphase (Wollman et al., 2005). Thus, despite the unquestionable relevance of the “search and capture” model, its intrinsic limitations suggest the existence of additional mechanisms that accelerate the formation of kinetochore-microtubule interactions during prometaphase (reviewed in (Tanaka, 2013)). Furthermore, the search and capture mechanism cannot explain kinetochore-microtubule attachments in cells lacking centrosomes, such as in land plants or female oocytes (Khodjakov et al., 2000; Wadsworth and Khodjakov, 2004), or after experimental centrosome inactivation in animal somatic cells (Khodjakov et al., 2000). The acentrosomal microtubule formation model relies on at least three mechanisms: a Ran-GTP gradient and the Chromosomal Passenger Complex (CPC) promote microtubule nucleation and stabilization in the vicinity of chromosomes; the second mechanism relies on kinetochore-mediated microtubule growth; and the last involves microtubule branching from pre-existing spindle microtubules mediated by the Augmin complex (Almeida et al., 2022; Meunier and Vernos, 2016; Prosser and Pelletier, 2017; Sikirzhytski et al., 2018, 2014). Recent evidence suggest that both centrosome-dependent and –independent models contribute for kinetochore-microtubule attachments (Conway et al., 2022; Kiewisz et al., 2022).

1.6. Microtubule Binding to Kinetochores

An important feature of the kinetochore-microtubule interface is the ability to retain attachments to dynamic microtubules during chromosome congression and segregation.

Several studies have proposed the Ndc80 complex as the core of the kinetochore force-transducing microtubule binding activity (reviewed in (Wimbish and DeLuca, 2020)). The Ndc80 complex is an outer kinetochore component, conserved from yeast to vertebrates, and depletion or inactivation of this complex results in a complete failure of end-on microtubule attachments (reviewed in (Cheeseman and Desai, 2008; Ciferri et al., 2007)), leading to extensive chromosome missegregation (DeLuca et al., 2002).

In budding yeast, the Dam1 complex, which localizes along mitotic spindle microtubules, is necessary for stable kinetochore-microtubule attachments (Jones et al., 2001). The Ska complex (Ska1, Ska2 and Ska3/Rama1) has been proposed to be the functional equivalent of the yeast Dam1 complex in higher eukaryotes (reviewed in (Guimaraes and Deluca, 2009)). The Ska complex, which localizes to the outer kinetochore and along spindle microtubules, has also been pointed as an essential protein for stable kinetochore-microtubule attachments (Daum et al., 2009; Gaitanos et al., 2009; Guimaraes and Deluca, 2009; Hanisch et al., 2006; Raaijmakers et al., 2009; Welburn et al., 2009). Depending on the severity of depletion, loss of Ska results either in a metaphase-like arrest or in a more dramatic alignment defect similar in severity to that observed upon Ndc80 depletion (Daum et al., 2009; Raaijmakers et al., 2009; Sivakumar et al., 2014; Welburn et al., 2009).

1.7. Mechanisms of prometaphase error correction

Stable amphitelic microtubule attachments generate tension at kinetochores, locking the correct chromatid orientation in place. However, the initial contact between kinetochores and microtubules is stochastic and consequently erroneous attachments can be formed during early mitosis (Cimini et al., 2001; Foley and Kapoor, 2013; Thompson and Compton, 2011). These include “monotelic” attachments where only one sister kinetochore is oriented to a single spindle pole, “syntelic” attachments where both sister kinetochores are oriented to the same spindle pole, and “merotelic” attachments where one of the sister kinetochores is oriented to both spindle poles (Figure 1.10A). Monotelic or syntelic attachments are often corrected due to the loss of tension, providing a new possibility to bi-orient (reviewed in (Godek et al., 2015)). In contrast, merotelic attachments generate tension and cannot be detect by the SAC surveillance mechanism. As a result, even when cells have a functional SAC, merotelic attachments can persist into anaphase and single chromatids might missegregate (Cimini et al., 2001; Thompson and Compton, 2011). Despite the large stochasticity, chromosome segregation is remarkably accurate, which implies the presence of several surveillance mechanisms to ensure error correction before and after anaphase onset.

Tension between sister chromatids has been described as the main regulator of kinetochore-microtubule attachment stability (Biggins and Murray, 2001; Krenn and Musacchio, 2015; Liu et al., 2009). The importance of tension in mitotic progression was demonstrated by Bruce Nicklas in classic experiments in grasshopper spermatocytes, where pulling a synthelically attached bivalent towards the opposite pole, resulted in kinetochore-microtubule stabilization and meiotic progression (Nicklas and Koch, 1969). Later, it was found that the establishment of tension was correlated with an increase in the number of microtubules bound at kinetochores, suggesting that tension decreased the rate of microtubule detachment (King and Nicklas, 2000).

The regulation of kinetochore-microtubule attachment stability is closely linked to the activity of Aurora B kinase (Figure 1.10B). By phosphorylating the outer kinetochore protein Hec1, a component of the conserved Ndc80 complex, Aurora B reduces the affinity of the Ndc80 complex for microtubules, thereby destabilizing kinetochore-microtubule attachments. The phosphorylation status of Aurora B substrates depends on their distance from the kinase. In case of no attachments or erroneous attachments, there will be no tension between sister kinetochores, and Aurora B is able to phosphorylate outer kinetochore components. However, at metaphase, pulling forces at kinetochores create tension, increases interkinetochore distance and leads to physical separation of outer kinetochore components from Aurora B phosphorylation, promoting their dephosphorylation and stabilization of attachments (Liu et al., 2009; Wimbish and DeLuca, 2020). Moreover, Aurora B activity is counteracted by two phosphatases, protein phosphatase 1 (PP1) and protein phosphatase 2A (PP2A), promoting dephosphorylation of the substrates and stabilization of attachments (Egloff et al., 1997; D. Liu et al., 2010). Additionally, Aurora A kinase, localized at centrosomes, mediates the correction of aberrant attachments in the vicinity of the poles that could be stabilized due to high PEFs on chromosome arms (Barisic et al., 2014; Barisic and Maiato, 2015; Chmátal et al., 2015; Ye et al., 2015). Additionally, the dynamic nature of spindle microtubules plays an important role in error correction since hyperstabilization of microtubules increases the number of lagging chromosomes during anaphase (reviewed in (Bakhoum and Compton, 2012)). In that respect, the microtubule-depolymerizing kinesin-13s proteins, including Kif2a, Kif2b and Kif2c/MCAK, appear as central players in controlling the balance of microtubule dynamics (Manning et al., 2007; Walczak et al., 2010). During prometaphase, kinetochore localization of Kif2b facilitates the rapid turnover of kinetochore-microtubule attachments, promoting error correction. On the other hand, during metaphase, MCAK activity at kinetochore is more relevant in destabilizing erroneous attachments (Bakhoum et al., 2009b). Knock-down of MCAK or Kif2b prevents correction of erroneous attachments after monastrol washout, an experimental treatment that increases the number of aberrant attachments (Bakhoum et al.,

2009a, 2009b; Lampson et al., 2004). On the other hand, overexpression of MCAK and Kif2b prevents not only erroneous attachments, but also can significantly suppress the frequency of chromosome missegregation events (Bakhoum et al., 2009b). Recently, it was shown that MCAK has different affinity to spindle microtubules depending on certain tubulin PTMs. Specifically, detyrosinated α-tubulin accumulates on correct and more stable kinetochore-microtubule attachments impairing MCAK activity, allowing this kinesin to discriminate between correct and incorrect attachments, thereby promoting mitotic fidelity (Ferreira et al., 2020).

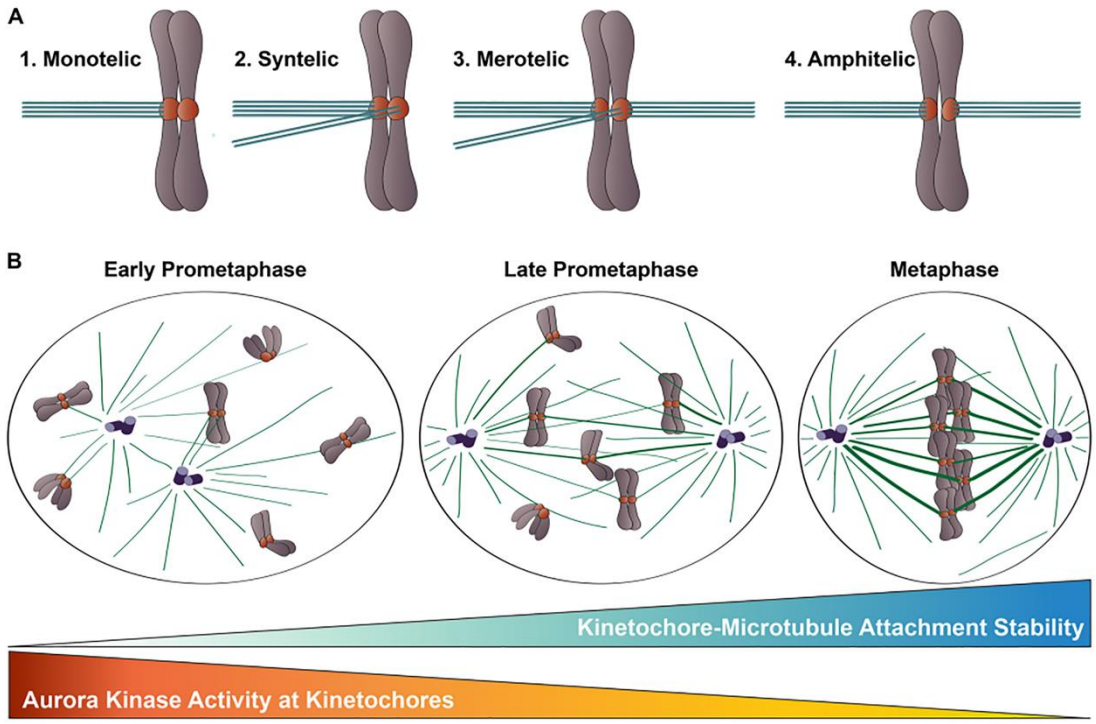

Figure 1.10: Kinetochore-microtubule attachments in mitosis. **A**. Different configurations of the kinetochore-microtubule attachments: (1) monotelic, (2) syntelic, (3) merotelic and (4) amphitelic. **B**. In early mitosis, kinetochore-microtubule attachments errors are common. As mitosis progresses, low tension and high Aurora B activity at the kinetochores allow the correction of the erroneous attachments. As kinetochores bi-orient, tension increases, Aurora B activity decreases at the kinetochores and kinetochore-microtubule stabilize. Adapted from (Wimbish and DeLuca, 2020).

1.8. Mechanism of anaphase error correction

Erroneous kinetochore-microtubule attachments are frequently observed in early mitosis, but most are corrected before anaphase onset (Cimini et al., 2004, 2003). Previous studies revealed that the frequency of lagging chromosomes was higher during early anaphase than during late anaphase, and that most lagging chromosomes were resolved by telophase, both in normal diploid cells and chromosomally unstable cancer cells (Cimini

et al., 2004; Orr et al., 2021; Sen et al., 2021). These studies suggested that merotelically attached kinetochores escape prometaphase error correction more often than originally expected. Thus, these findings would support the idea of a correction mechanism that serves as a back-up in anaphase to facilitate the incorporation of the lagging chromosome into the main nucleus, thereby protecting against micronucleus formation. When cells transit into anaphase, Aurora B leaves the centromere and is actively transported by the kinesin-6 Mklp2 towards the spindle midzone (Adriaans et al., 2020; Gruneberg et al., 2004; Orr et al., 2021), where it generated a phosphorylation gradient (Fuller et al., 2008). Inhibition of Aurora B kinase activity at anaphase onset increased the frequency of lagging chromosomes and micronuclei formation. Moreover, knock-down or inhibition of MKLP2, which disrupts midzone localization of Aurora B, also increased the frequency of lagging chromosomes that formed micronuclei, suggesting that the midzone-based Aurora B activity gradient helps to resolve lagging chromosomes during anaphase (Orr et al., 2021; Sen et al., 2021). Two possible models have been proposed to explain how a midzone-based Aurora B activity gradient mediates error correction during anaphase. One is based on the well-established microtubule destabilizing roles of Aurora B at centromeres during early mitosis (Lampson and Grishchuk, 2017) and proposes that a midzone Aurora B activity gradient promotes the phosphorylation of kinetochore substrates to destabilize merotelic kinetochore-microtubule attachments (Sen et al., 2021). The other model favors the idea that midzone Aurora B activity mediates anaphase error correction of merotelic kinetochore-microtubule attachments by assisting the mechanical transmission of spindle forces at the kinetochore-microtubule interface on lagging chromosomes (Orr et al., 2021). Indeed, reducing spindle elongation by Eg5 inhibition increased the number of cells with laggards and micronuclei (Orr et al., 2021). Therefore, in this model, midzone-localized Aurora B contributes to the resolution of lagging chromosomes by assisting spindle elongation, and by stabilizing kinetochore-microtubule attachments to allow mechanical transmission of these spindle forces. The kinetochore-microtubule stabilizing role for Aurora B during anaphase is further supported by the evidence that Aurora B can indirectly support kinetochore-microtubule attachment stability through phosphorylation of the kinetochore protein Dsn1, which prevents kinetochore disassembly during anaphase (Papini et al., 2021). Thus, most lagging chromosomes are resolved by late anaphase and incorporated into the main nucleus by telophase, but the exact mechanism underlying this anaphase surveillance mechanism is not fully understood.

A midzone-based Aurora B activity gradient on chromosomes was proposed to mediate a chromosome separation checkpoint that monitors and delays nuclear envelope reformation (NER) and chromosome decondensation until efficient separation of sister chromatids during anaphase is achieved (Afonso et al., 2014; Maiato et al., 2015).

Spatiotemporal control of NER is particularly evident on anaphase lagging chromosomes, which show a delay in NER relative to normally separating chromosomes in the same cell (Afonso et al., 2014; de Castro et al., 2018; Liu et al., 2018; Orr et al., 2021). Notably, the dependence of NER on chromosome separation during anaphase can be experimentally relieved by inhibiting Aurora B activity at anaphase onset (Afonso et al., 2014; Liu et al., 2018) or by preventing its association with the spindle midzone, causing all chromosomes to initiate NER, regardless of chromosome separation (Afonso et al., 2014; Orr et al., 2021). A chromosome separation checkpoint would provide an opportunity to correct erroneous kinetochore-microtubule attachments and allow reintegration of lagging chromosomes in the main nuclei before completion of NER. Thus, spatial control of NER appears to be important for the fidelity of chromosome segregation.

1.9. Mechanisms of mitotic chromosome missegregation

Multiple mechanisms have been so far proposed to be involved in the generation of chromosome segregation errors in human cells, such as defective SAC function, incorrect kinetochore-microtubule attachments, altered microtubule dynamics (e.g., increased stability of the attachments), mitotic spindle aberrations (e.g. multipolar spindle) and chromosome cohesion defects (Bakhoum et al., 2009a, 2009b; Barber et al., 2008; Cimini, 2008; Maiato and Logarinho, 2014) (Figure 1.11). Chromosome segregation errors occur at a very low frequency in healthy tissues (Cimini et al., 2002; Knouse et al., 2014; van den Bos et al., 2016; Worrall et al., 2018), but they are a common feature in cancer (Bakhoum et al., 2009a, 2009b).

The most obvious cause of chromosome segregation errors is a compromised SAC activity that allows chromosome segregation to occur in the presence of unattached or incorrectly attached chromosomes to the spindle (reviewed in (Lara-Gonzalez et al., 2012)) (Figure 1.11A). In mammals, complete inactivation of the SAC leads to dramatic chromosome segregation errors, thus, the SAC is necessary for organismal development and the viability of most mammalian cells (Dobles et al., 2000; Kalitsis et al., 2000; Kops et al., 2004; Michel et al., 2001). Moreover, weakening SAC function allows for premature cell-cycle progression into anaphase and dramatically increases the probability of whole chromosome missegregation leading to aneuploidy (Michel et al., 2001). Although most cells rely on SAC activity for survival, examples have emerged where the requirement for the SAC can be bypassed. For example, extending the time for chromosome alignment by lowering APC/C activity can render the SAC nonessential in cancer cells (Sansregret et al.,

2017; Wild et al., 2016). Although mutations in SAC genes are rare in human tumors, altered expression of SAC genes have been observed in a number of tumors (reviewed in (Simonetti et al., 2019)). Moreover, germline mutations in the mitotic checkpoint component BubR1 have been identified in some individuals with mosaic variegated aneuploidy (MVA), a rare disorder characterized by high levels of mosaic aneuploidy and significantly increased risk of cancer (Hanks et al., 2004; Matsuura et al., 2006; Suijkerbuijk et al., 2010). These findings indicate that impairments of the SAC may lead to chromosome missegregation.

Efficient correction of erroneous kinetochore-microtubule attachments requires the detachment of microtubules from inappropriately attached kinetochores. Consequently, diminished kinetochore-microtubule dynamics allows the persistence of erroneous attachments and increases the frequency of chromosome segregation errors. Chromosomally unstable tumors exhibit more stable kinetochore-microtubule attachments relative to normal diploid cells, which increases the frequency of merotelic attachments (Bakhoum et al., 2009a).

The separation of chromosomes at anaphase relies on the timely loss of sister cohesion. Cohesion serves to prevent premature chromosome separation during mitosis by tethering newly synthesized sister chromatids together prior to entry into anaphase. Sister chromatids are held together by ring-shaped cohesion protein complexes, which comprises four different subunits including STAG1 or STAG2, RAD21, SMC1 and SMC3, and are loaded onto the chromosomes during DNA replication. During the initial stages of mitosis (prophase to metaphase), cohesion is first lost along the length of the chromosome arms but is maintained at the centromeres through a Shugoshin-dependent mechanism (reviewed in (Gutiérrez-Caballero et al., 2012)). The remaining cohesin complexes are released by cleavage of the RAD21 subunit by Separase at the metaphase to anaphase transition. There is some evidence suggesting that aberrant sister chromatid cohesion may lead to precocious sister chromatid separation and chromosome segregation errors (Figure 1.11B). These studies suggest that altered expression and/or function of key cohesion-related genes may underlie chromosomal instability (CIN) (Barber et al., 2008; Zhang et al., 2008). Depletion of Shugoshin (Sgo1), a protein that protects centromeric cohesion from cleavage, leads to an increase in the tetraploid cells population (Iwaizumi et al., 2009). Inactivating mutations in stromal antigen 2 (STAG2), a component of the cohesion complex, result in defective sister chromatids and aneuploidy (Solomon et al., 2011).

Multipolar spindles are normally associated with supernumerary centrosomes, which in turn may arise from centriole overduplication, cytokinesis failure, or mitotic slippage (Kops et al., 2005b; Levine and Holland, 2018; Maiato and Logarinho, 2014). Interestingly, multipolar spindles with supernumerary centrosomes are normally transient due to a

centrosome clustering mechanism that circumvents potentially fatal spindle multipolarity (Cassimeris and Morabito, 2004; Quintyne et al., 2005; Silkworth et al., 2009). While clustering of centrosomes into two spindle poles provides a pathway to avoid lethal divisions, it also promotes the formation of improper kinetochore-microtubule interactions, such as merotelic attachments, which lead to chromosome segregation defects and aneuploidy (Ganem et al., 2009; Silkworth et al., 2009) (Figure 1.11C). An alternative but less understood mechanism leading to multipolar spindle formation is associated with loss of spindle pole integrity due to centriole disengagement or fragmentation of the pericentriolar material (PCM) (Cassimeris and Morabito, 2004; Logarinho et al., 2012; Maiato and Logarinho, 2014). Contrary to multipolar spindles with extra centrosomes, spindle multipolarity without centrosome amplification is normally irreversible and multipolar anaphases are common, thereby compromising the viability of the cell progeny due to massive chromosome missegregation, a phenomenon known as anaphase catastrophe (reviewed in (Galimberti et al., 2011)).

Centrosomes not only function as a primary source of microtubules that build mitotic spindles but they also determine the geometry and positioning of the spindle by regulating their own positions within the cell. In most animal cells, the centrosome pair separates to form a bipolar spindle. Numerous studies have demonstrated that defects in centrosome separation may constitute a source of erroneous kinetochore attachments, which can increase rates of lagging chromosomes and chromosome missegregation (Kaseda et al., 2012; Nam et al., 2015; Nam and van Deursen, 2014; Silkworth et al., 2012; Y. Zhang et al., 2012) (Figure 1.11D). Studies from a range of species have revealed that complete loss of centrosomes can disrupt cytokinesis (Basto et al., 2006; Hinchcliffe et al., 2001; Lambrus et al., 2015; Piel et al., 2001), which can also lead to tetraploidy.

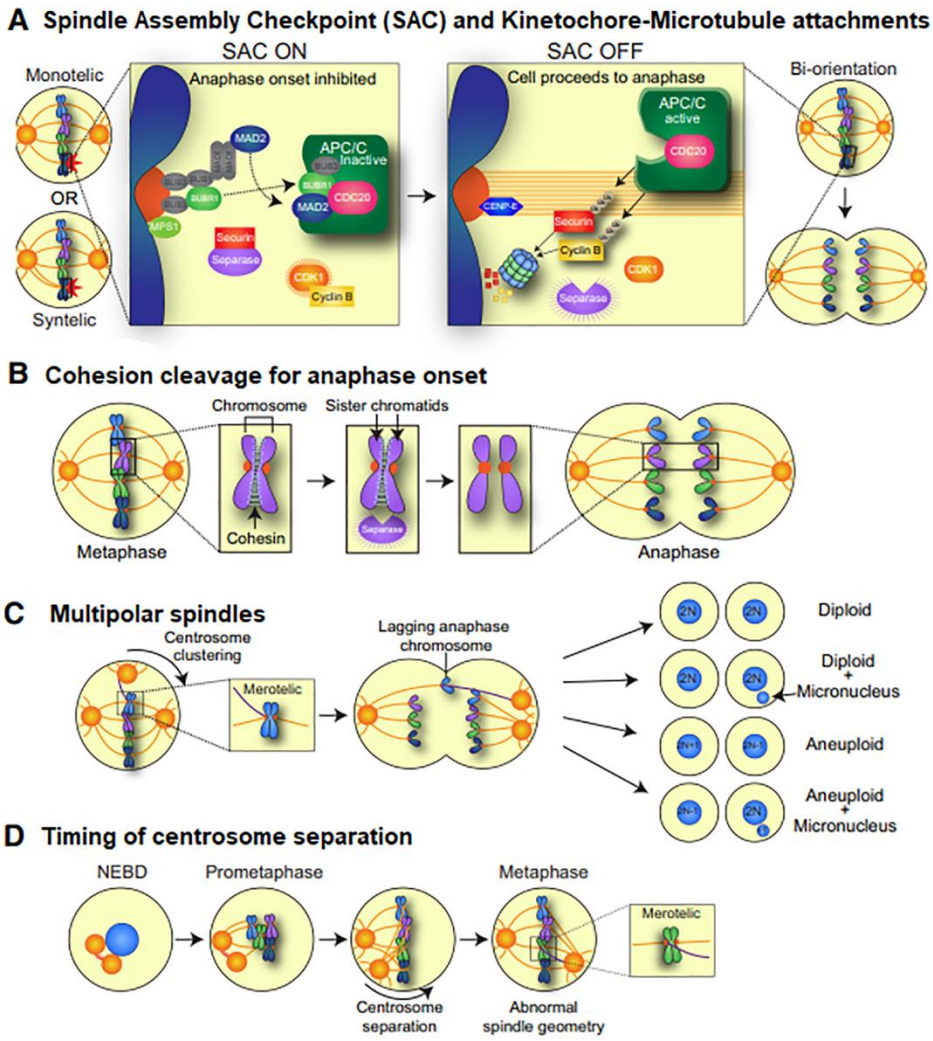

Figure 1.11: Chromosome segregation and sources of mitotic errors. A. Unattached kinetochores activate an inhibitory SAC signal, which in turn blocks progression to anaphase. **B.** Faulty sister chromatids cohesion can occur by premature loss of sister chromatid cohesion that can results in increased rates of chromosome missegregation. **C.** Multipolar spindle commonly arise in cells having more than two centrosomes. Centrosomes can cluster at the cell poles to allow bipolar anaphase, however this can lead to defective attachments. **D.** Delays in centrosome separation can lead to erroneous attachments and/or abnormal spindle geometry, resulting in chromosome missegregation. Adapted from (Levine and Holland, 2018).

1.9.1. Chromosomal abnormalities: contextualizing aneuploidy and CIN

Each day, millions of cells in human bodies undergo division to ensure tissue homeostasis and function (Sender and Milo, 2021). Numerous error correction mechanisms are at play to ensure that these divisions proceed only under ideal growth conditions and with high fidelity. Despite the presence of these surveillance mechanisms, errors in chromosomes segregation during cell division can occur which can result in imbalances of the genome (reviewed in (Potapova and Gorbsky, 2017)). Aneuploidy describes any

karyotype that differs from a normal chromosome set (euploidy) and its multiples (polyploidy). Aneuploidy can occur either by chromosome gains and losses due to chromosome segregation errors (whole chromosome aneuploidy) or due to rearrangements of chromosomal parts, often accompanied by their deletion and amplification (structural or segmental aneuploidy). This condition is distinct from the condition of polyploidy, which is defined as having a chromosome number that is a multiple greater than twice the haploid number. Polyploidy arises due to severe errors in mitosis or meiosis, leading to the formation of cells or gametes that have a complete set of duplicate chromosomes (Comai, 2005).

Acquired aneuploidy leads to huge genomic variability between somatic cells. Germline aneuploidy has been reported as the major cause of congenital birth defects, miscarriage and neurological pathologies (Hassold et al., 2007; Hassold and Hunt, 2001; Iourov et al., 2009; Martin, 2006), whereas somatic cell aneuploidy has been implicated in tumorigenesis, genomic instability, tumor evolution, metastasis, drug resistance and reduced cancer patient survival (Bakhoum et al., 2018; Cohen-Sharir et al., 2021; Crasta et al., 2012; A. J. X. Lee et al., 2011; Lukow et al., 2021; Replogle et al., 2020; Umbreit et al., 2020; van Dijk et al., 2021; Watkins et al., 2020; Weaver et al., 2007). A selective advantage of naturally occurring aneuploid cells was reported in certain cell type within the body, including hepatocytes, neural progenitor cells and neurons (Knouse et al., 2014; Yurov et al., 2007, 2005). Moreover, there is some evidence that aneuploidy can even improve cell proliferation and fitness (reviewed in (Sheltzer and Amon, 2011)).

Aneuploidy is often accompanied by high rates of chromosome missegregation, a phenomenon called chromosomal instability (CIN), in which chromosomes are permanently gained and/or lost during multiple divisions (reviewed in (Thompson et al., 2010)). Although CIN and aneuploidy are often used indistinctly, there is an important distinction: aneuploidy refers to the genomic status of a cell with an abnormal chromosome complement at a given time, while CIN refers to the behavior of cells that display a dynamic chromosomal content from one generation to the next due to persistent segregation errors. Therefore, while CIN invariably leads to aneuploidy, some cells can remain in a stable aneuploid status for multiple generations. This is the case of patients with Down syndrome (trisomy of chromosome 21), which is characterized by the presence of an extra copy of the chromosome 21, but show a stable karyotype. Besides trisomy 21, only trisomy 13 (or Patau syndrome) and trisomy 18 (or Edwards syndrome) are viable to birth in humans. Although individuals with trisomy 13 and trisomy 18 can survive to birth, they do not typically live beyond the first few years of life (Rasmussen et al., 2003).

1.9.2. Aneuploidy and cancer

Aneuploidy and CIN have been recognized as hallmarks of cancer (reviewed in (Holland and Cleveland, 2009)). Theodor Boveri was the first to propose a connection between aneuploidy and solid tumors, suggesting that aneuploidy can initiate tumor development (Boveri, 2008). Although aneuploidy and/or CIN might contribute to tumorigenesis by changing the dosage of oncogenes and tumor suppressors required for tissue homeostasis, growing evidence shows that genome imbalances might be disadvantageous for tumors in certain circumstances (Sheltzer et al., 2017; Silk et al., 2013; Weaver et al., 2007). CIN has been associated with both poor patient prognosis and resistance to some chemotherapeutic agents (Bakhoum et al., 2011; Carter et al., 2006; Choi et al., 2009; A. J. X. Lee et al., 2011; McClelland et al., 2009; Mettu et al., 2010; Ryan et al., 2012; Sato et al., 2010; Swanton et al., 2009). Paradoxically, there is also evidence that excessive CIN is a disadvantage for tumor progression and is associated with better prognosis (Bakhoum et al., 2015; Birkbak et al., 2011; Roylance et al., 2011; Zaki et al., 2014). These findings support the notion that low doses of CIN promotes tumor progression while excessive CIN beyond a critical level can be lethal to cancer cells (Godek et al., 2016; Silk et al., 2013). Whatever the case may be, and despite all controversy, direct targeting of CIN as a potential anti-cancer therapy is now the subject of active research (Burrell et al., 2010; Roschke and Kirsch, 2005).

1.9.3. Consequences of mitotic segregation errors

The consequences of mitotic segregation errors can be varied, depending on the degree and nature of the error, on the genetic background of the cell, and on the precise role of the cell in question. However, errors in chromosome segregation do not always cause aneuploidy. Many potential chromosome missegregation events are prevented by cell cycle checkpoints. However, if these checkpoints eventually fail, daughter cells will be generated with a genetic imbalance of one or more chromosomes, segments of chromosomes, or entire sets of chromosomes. Moreover, missegregating chromosomes or chromosome fragments may become isolated from the main nuclei mass during erroneous mitosis, forming micronuclei. In most normal tissue cells, aneuploidy is normally poorly tolerated and several studies demonstrated to cause a p53-dependent reduction in cell proliferation/viability (Fonseca et al., 2019; Li et al., 2010; Narkar et al., 2021; Pfau et al., 2016; Sablina et al., 1998; Santaguida et al., 2017; Thompson et al., 2010; Thompson and Compton, 2008). However, p53 activation and cell cycle arrest in response to aneuploidy

does not seem to be universal and might depend on the cell type, the nature of the segregation errors and cell culture conditions (Narkar et al., 2021; Santaguida et al., 2017; Soto et al., 2017). In this section we will discuss the direct and indirect consequences associated with chromosome segregation errors and the consequences of the exclusion of a chromosome or a part of chromosome in a micronucleus.

1.9.3.1. Consequences of imbalanced karyotypes

The fact that only few specific chromosomal abnormalities are compatible with human life suggests that karyotype variations are poorly tolerated. Indeed, several studies have demonstrated that aneuploidy is detrimental to cell physiology and fitness of eukaryotic cells (reviewed in (Gordon et al., 2012; Santaguida and Amon, 2015; Torres et al., 2008)). Even in transformed cells, extra copies of individual chromosomes result in a proliferative disadvantage and reduced capacity to form tumors *in vivo* (Sheltzer et al., 2017). The most widely accepted explanation for the observed phenotypes is the gene dosage hypothesis, which states that the observed phenotypes are a result of changes in the copy number of genes located on the aneuploid chromosomes (Stingele et al., 2012; Torres et al., 2008, 2007). Genomic and transcriptional analyses performed on aneuploid cells demonstrated that gene expression directly correlated with gene copy number. Despite transcriptome alterations, studies in yeast and human cells revealed that changes in chromosome copy number did not alter the production of a subset of proteins. The majority of proteins display extensive dosage compensation at the protein level and fail to change by the degree expected based on chromosome copy number (Brennan et al., 2019; Dephoure et al., 2014; Geiger et al., 2010; Stingele et al., 2012; Taggart et al., 2020). It has been shown that some synthesized proteins on aneuploid cells are degraded by the proteasome, which explains the enhanced proteotoxic stress observed in these cells (Ishikawa et al., 2017).

1.9.3.2. DNA damage as a consequence of segregation errors

Mitotic errors have long been recognized to be a source of whole-chromosomal aneuploidy, but recent evidence has also linked chromosome segregation errors to the induction of DNA damage that promotes structural alterations in chromosomes. Common by-products of cell division errors are lagging chromosomes, DNA bridges or misaligned chromosomes in anaphase and generation of micronuclei in the following G1, which both can be associated with DNA damage. Chromosome breakage can occur on lagging chromosomes that are trapped in the cleave furrow, where breakage can be induced by

physical forces (Janssen et al., 2011). Daughter cells that had inherited broken chromosomes activate a DNA damage response that is typical of cells dealing with double-stranded DNA breaks (DSBs), as shown by the activation of ATM/Chk2 and p53 (Janssen et al., 2011).

DNA damage can also arise from the incorrect resolution of DNA ultrafine bridges (UFBs) (K. L. Chan et al., 2009; Naim and Rosselli, 2009). UFBs are thin segments of naked DNA linking the separating sister chromatids in the anaphase of mitosis. If left unresolved, UFBs can break during anaphase and form micronuclei or lead to cytokinesis failure and tetraploidization (reviewed in (Fernández-Casañas and Chan, 2018). In addition, nuclear envelope of micronuclei is unusually fragile, thereby promoting micronuclear rupture and simultaneous DNA damage (Hatch et al., 2013) (see section 1.9.5 for in-depth characterization.

1.9.3.3. Micronuclei

Chromosome segregation errors may also lead to the exclusion of a chromosome or a fragment of a chromosome that fail to incorporate into one of the daughter nuclei during cell division. If so, the missegregated piece of DNA recruits its own nuclear envelope and forms a so-called micronucleus. Micronuclei harboring acentric chromatid/chromosome fragments usually originate after extensive DNA damage such as DSBs that, if misrepaired, result in asymmetrical chromosome rearrangements and exchanges. Micronuclei harboring whole chromosomes are primarily formed due to deficiencies in chromosome segregation during anaphase (reviewed in (Levine and Holland, 2018)).

Micronuclei have been used for decades as biomarkers for the assessment of genotoxicity of pharmaceuticals, pesticides and other chemicals. Besides the use as a biomarker in genotoxicity testing, micronuclei in human blood lymphocytes are predictive for cancer risk, which makes them a suitable tool to assess the effect of lifestyle factors or diseases on the risk of tumour formation (Bonassi et al., 2007). Increased frequency of micronuclei has been found to be associated with various diseases, such as malignancies, inflammatory and autoimmune disease, diabetes and obesity (Franzke et al., 2020; Kirsch-Volders et al., 2020; X et al., 2021).

Accumulating evidence suggest that micronuclei display reduced functionality compared to main nuclei in the same cell, with respect to DNA replication, DNA damage sensing and repairing capacity (Crasta et al., 2012; Hatch et al., 2013; Terradas et al., 2009). In addition, chromosomes within micronucleus fail to support a functional kinetochore (Vázquez-Diez et al., 2016). Consequently, micronuclei are predisposed to undergo segregation errors,

which favors the maintenance of a micronucleus over its reincorporation after mitosis (Soto et al., 2018). Moreover, recent evidence has shown that chromosomes isolated within micronuclei are prone to DNA damage, in part because the nuclear envelope of micronuclei is unusually fragile and prone to spontaneous rupture, exposing the micronuclear DNA to potentially damaging cytoplasmic components (Hatch et al., 2013; Liu et al., 2018). Additionally, there is evidence showing that following membrane rupturing, DNA in micronuclei undergoes massive rearrangements in a process called chromothripsis (Zhang et al., 2015). One of the current models for chromothripsis involves DNA shattering in micronuclei followed by reincorporation into primary nucleus, where random re-ligation of the broken DNA can take place. Chromothripsis is common in cancer and associated with poor prognosis (Rode et al., 2016; Voronina et al., 2020). Therefore, the presence of a micronucleus can eventually result in DNA damage leading to catastrophic chromosomal rearrangements that can contribute to tumorigenesis.

1.9.4. Tolerance to segregation errors

Cancer cells have evolved mechanisms to deal with the problematic consequences of aneuploidy. Considering that aneuploidy induced by chromosome missegregation results in a number of cellular stresses, it is striking how segregation errors can be tolerated in cancer cells. Numerous studies have been performed in order to understand whether errors in chromosome segregation can directly or indirectly lead to activation of the tumor suppressor protein p53 (TP53 in humans and Trp53 in mice, best known as p53) (Giam et al., 2020; Hinchcliffe et al., 2016; Janssen et al., 2011; Kurinna et al., 2013; Li et al., 2010; Santaguida et al., 2017; Soto et al., 2017; Thompson and Compton, 2010), which in turn induces a cell cycle arrest, senescence or apoptosis. p53 mutation is a common feature of highly aneuploidy tumors (Taylor et al., 2018) and is associated with poor prognosis in cancer (Donehower et al., 2019). Moreover, ablation of TP53 in certain cancer predisposed mouse models promotes CIN and overall aneuploidy (Foijer et al., 2014; Grim et al., 2012). Also, genome-editing of human derived colon organoids revealed that mutations in the tumor suppressor genes APC, SMAD4 and TP53, and in the oncogenes KRAS and/or PIK3CA *per se* were insufficient for malignant progression (Matano et al., 2015). This study proposed that chromosome instability, in addition to driver pathway mutations, is needed for invasive and metastatic transformation.

Some studies suggested that the mere presence of an imbalanced karyotype or only the presence of micronuclei would be sufficient to activate p53 followed by cell cycle arrest (Sablina et al., 1998; Thompson and Compton, 2010). Indeed, cells bearing micronuclei are

more likely to die or undergo cell cycle arrest when compared with cells without micronuclei after irradiation, and more micronuclei the cells contained more likely they will undergo arrest (Huang et al., 2011). Consistently, cancer cells under hydroxyurea treatment, showed that cells with micronuclei were more prone to undergo apoptotic cell death, compared with cells with apparently normal nuclei (Utani et al., 2010). However, the micronuclei in these studies were induced by ionizing radiation and replication stress, and there is a possibility that the increase in cell death may be due to high levels of genome-wide DNA damage and not only to the presence of micronuclei. However, a recent study also demonstrated that at least a portion of micronucleated cells resulting from chromosome alignment defects undergoes a p53-dependent cell cycle arrest (Fonseca et al., 2019). Moreover, the rate of division for micronucleated cells increases twofold to threefold after p53 depletion (Fonseca et al., 2019).

An extended mitotic duration can also trigger a p53-dependent cell-cycle arrest, irrespective of whether chromosomes have been missegregated (Fong et al., 2016; Lambrus et al., 2016; Meitinger et al., 2016; Uetake and Sluder, 2010). Another study proposed that p53-dependent cell cycle arrest can occur as a response to chromosome missegregation, and does not require other mitotic defects, such as prolonged prometaphase duration or DNA damage (Hinchcliffe et al., 2016).

However, whether aneuploidy itself directly triggers p53 activation has remained unclear. Complex aneuploidies that involve structural alterations (gain or loss of part of a chromosome) do trigger p53 activation. On the other hand, whole-chromosome aneuploidies do not always lead to p53 activation and can be propagated in a p53-proficient background (Santaguida et al., 2017; Soto et al., 2017).

1.9.5. Segregation errors and the immune response

In recent years, it has been suggested that chromosome segregation errors can lead to the activation of immune signaling pathways through the formation of micronuclei in chromosomes that lag during anaphase (Bakhoum et al., 2018; Harding et al., 2017; Mackenzie et al., 2017). In contrast to the primary nucleus, most micronuclei show aberrant nuclear envelopes (NEs) that are highly prone to spontaneous and irreparable rupture (Crasta et al., 2012; Hatch et al., 2013). One obvious explanation for nuclear envelope disruption at micronuclei is decreased recruitment of lamin proteins to micronuclei (Hatch et al., 2013; Kneissig et al., 2019; Liu et al., 2018; Vargas et al., 2012). In general, it is estimated that 30-50% of micronuclear membranes in several cell types lack correct incorporation of lamin B rendering them more vulnerable to rupture, potentially due to

physical forces generated within the cell (Hatch et al., 2013; Hatch and Hetzer, 2016). Although a large proportion of micronuclei displayed a complete lack of lamin B1, levels of lamin A/C were similar to those observed in primary nucleus (Kneissig et al., 2019). Confirming this notion, studies have revealed that reducing the lamin gaps on the micronuclei membrane by overexpression of B-type lamins mitigates micronucleus disruption (Bakhoum et al., 2018; Hatch et al., 2013). Although lamin gaps are visible at the end of mitosis (Hatch et al., 2013; Liu et al., 2018), membrane rupture frequently does not occur until many hours later (Hatch et al., 2013). In addition to defects in lamina structure, high membrane curvature and mechanical forces from the actin cytoskeleton can also contribute to micronuclear rupturing (Denais et al., 2016; Hatch and Hetzer, 2016; Raab et al., 2016; Xia et al., 2018). Therefore, lamin B1 is less likely to be present within smaller structures like micronuclei where the membrane curvature is high. In fact, lagging chromosomes always fail to recruit lamin B1 (Afonso et al., 2014) but can efficiently assemble lamin-A/C (de Castro et al., 2018), and micronuclei with high curvature display low lamin-B intensity (Xia et al., 2019). Moreover, small micronuclei have a higher tendency to rupture than larger ones (Xia et al., 2019), although it has also been reported that micronuclei rupture is not associated with micronuclei size (Hatch et al., 2013). Nuclear envelope disruption at micronuclei is frequently associated with DNA damage in micronuclei; however DNA damage in micronuclei *per se* cannot induce micronuclei rupture (Hatch et al., 2013). Nuclear envelope fragility is not specific to micronuclei, the primary nucleus, especially of cancer cells, can undergo spontaneous disruption in some circumstances (Hatch and Hetzer, 2014). Similar to micronuclei, chromatin bridges are also associated with nuclear envelope defects, which also result in exposure of DNA to the cytoplasm and leads to activation of the DNA damage response (Maciejowski et al., 2015).

A direct consequence of micronuclei membrane rupture is the release of genomic DNA into cytoplasm, which becomes accessible to the cytoplasmic enzyme cGAS (Harding et al., 2017; Mackenzie et al., 2017; Yang et al., 2017). Upon binding DNA, the enzymatic activity of cGAS is activated, resulting in the production of a small molecule second messenger, cyclic GMP-AMP (cGAMP) (Cai et al., 2014). cGAMP, in turn, binds to the central scaffold of the innate immune response called STING (stimulator of interferon genes), which then triggers a signaling cascade, thereby leading to the production of inflammatory cytokines, chemokines and type I interferons (IFNs). The discovery of cGAS activation on micronuclei provided a link between DNA damage and innate immune responses. Multiple studies have reported the recruitment of cGAS to micronuclei (Bartsch et al., 2017; Dou et al., 2017; Glück et al., 2017; Gratia et al., 2019; Harding et al., 2017; Mackenzie et al., 2017; Yang et al., 2017). However, the exact mechanism for cGAS recruitment to micronuclei remains unclear. A recent report demonstrated that cGAS

reduces the abundance of micronuclei in an autophagy-dependent manner (Zhao et al., 2021). Moreover, reduced presence of immune cells in tumors was associated with TP53 mutations (Lyu et al., 2019; Siemers et al., 2017). Recently, it was shown that mutant p53 suppresses downstream signaling from the cGAS/STING pathway by interacting with TANK-binding protein kinase 1 (TBK1), resulting in the attenuation of the type I interferon response and the promotion of tumor growth (Ghosh et al., 2021).

Evidence has emerged in recent years that tumor microenvironment can potentially be explored to eliminate aneuploid cancer cells. More specifically, activation of cGAS-STING pathway might be explored as a new therapeutic strategy to treat CIN tumors (Bakhoum et al., 2018; Hong et al., 2019; Nassour et al., 2019). Complex karyotypes induced in normally diploid RPE-1 cells are cleared more efficiently by natural killer cells in comparison to its wild type counterpart due to cGAS-STING pathway activation (Santaguida et al., 2017). However, cGAS-STING pathway can promote cytokine signaling, which maintains CIN and leads to metastasis. Metastatic breast cancer cells often display more chromosomal instability and presence of micronuclei when compared to the primary tumor (Bakhoum et al., 2018). Moreover, tumor metastasis in the mouse brain was shown to be dependent on production of cGAMP by cGAS in tumour cells (Chen et al., 2016) and inhibition of cGAS or STING expression in tumor cells prevented metastasis (Bakhoum et al., 2018; Chen et al., 2016). Furthermore, several cancers exhibit decreased cGAS-STING signaling (Xia et al., 2016a, 2016b), which has been associated with poor survival (Song et al., 2017). The role of cGAS-STING signaling in the regulation and maintenance of CIN tumors is complex and it seems contradictory. On one hand, the cGAS-STING pathway seems to have a tumor suppressive role by promoting the clearance of CIN tumors through recruitment of immune cells (Santaguida et al., 2017). On the other hand, the cGAS-STING pathway has been described to be an important regulator in the promotion of metastasis of CIN tumors (Bakhoum et al., 2018; Chen et al., 2016).

1.9.6. Exploiting mitotic errors for cancer therapy

Several studies have shown that chromosome missegregation events occur at a very low frequency in human primary or non-transformed cells, as well as with patient-derived organoids from healthy tissue, but they are a common trait in cancer cells (Bakhoum et al., 2014; Bolhaqueiro et al., 2019; Cimini et al., 2002, 2001; Crasta et al., 2012; Thompson and Compton, 2011; Worrall et al., 2018). Despite the prevalence of CIN in human cancer, its role in tumor evolution is complex and seems contradictory (Birkbak et al., 2011). CIN has become a hot topic in recent years, not only for its implications in cancer diagnosis and

prognosis, but also for its role in therapeutic responses. On one hand, CIN correlates with resistance to antineoplastic agents, such as taxol, both in tumor-derived cell lines as well as in clinical settings (Bakhoum et al., 2011; Swanton et al., 2009). It has been described that cancer cell lines with CIN display a reduced sensitivity to several cytotoxic agents compared with their diploid/near-diploid (CIN(-)) counterparts (A. J. X. Lee et al., 2011). High levels of CIN are frequently associated with poor patient outcomes, suggesting that CIN could contribute to tumor progression (Birkbak et al., 2011; van Dijk et al., 2021). Conversely, excessive levels of CIN enhanced sensitivity to cytotoxic therapies such as cisplatin and 5-fluorouracil in some cancers (Jamal-Hanjani et al., 2015; Roylance et al., 2011; Zaki et al., 2014).

Several studies demonstrated that radiotherapy induces formation of micronuclei in solid tumor samples as well as in peripheral blood lymphocytes from cancer patients (Gamulin et al., 2008; Kobayashi et al., 2020; Tichy et al., 2018; Unal et al., 2016; Werbrouck et al., 2013). Regression of tumors outside of the irradiated field was observed and is known as the abscopal effect. Recent studies suggest that immunotherapy and radiation in combination may enhance the abscopal response, a phenomenon wherein local irradiation suppresses tumors far from the site of irradiation. Likewise, successful antitumor immunity elicited by ionizing radiation (IR) is mediated by cGAS and STING pathways in the irradiated tumors (Deng et al., 2014; Harding et al., 2017; Storozynsky and Hitt, 2020). Because irradiation induces the formation of micronuclei, these findings suggested that the cGAS-STING activation during abscopal effect might be elicited due to the mere presence of micronuclei. Moreover, more recent studies are now suggesting that classic cancer therapies, such as radiotherapy and chemotherapy drugs, may have direct immunostimulatory effects through activation the cGAS-STING pathway in cancer cells (Deng et al., 2014; Hu et al., 2021; McLaughlin et al., 2020; Yum et al., 2020).

One of the most successful drugs used in cancer is paclitaxel, which has been used for decades to treat breast, ovarian, and lung cancer. Paclitaxel binds and stabilizes the MT lattice and, at high concentrations, arrests dividing cells in mitosis by preventing silencing of the SAC, leading to either cell death or senescence. However, clinically relevant doses of paclitaxel do not generate a mitotic arrest but rather lead to the formation of multipolar spindles that induce massive chromosome missegregation and micronucleation after mitotic exit (Jordan et al., 1993; Orth et al., 2011; Symmans et al., 2000; Zasadil et al., 2014). These findings support the notion that paclitaxel exerts its anticancer effects by increasing the rate of CIN above a maximally tolerated threshold. This recognition raises the question of whether this post-mitotic micronucleation might explain the therapeutic efficacy of taxanes against solid tumors (Mitchison et al., 2017) and whether this micronucleation promotes inflammatory signaling via cGAS-STING (Flynn et al., 2021; Hu

et al., 2021). Indeed, paclitaxel showed increased therapeutic efficiency in breast cancer cells that express high levels of cGAS, suggesting that high cGAS expression might be a good predictor of clinical outcome when treating with microtubule poisoning drugs. The newly discovered role of classic cancer therapies as immune stimulants provides an opportunity for the development of new therapeutic strategies.

CHAPTER 2.
EXPERIMENTAL WORK

CHAPTER 2.1.

Micronuclei from misaligned chromosomes that satisfy the spindle assembly checkpoint in cancer cells

This chapter was based on the following published paper:

Gomes AM, Orr B, Novais-Cruz M, De Sousa F, Macário-Monteiro J, Lemos C, Ferrás C, Maiato H. Micronuclei from misaligned chromosomes that satisfy the spindle assembly checkpoint in cancer cells. Curr Biol. 2022 Oct 10; 32(19):4240-4254.e5. DOI: 10.1016/j.cub.2022.08.026.

CHAPTER 2.1.

Micronuclei from misaligned chromosomes that satisfy the spindle assembly checkpoint in cancer cells

Abstract

Chromosome alignment to the spindle equator is a hallmark of mitosis thought to promote chromosome segregation fidelity in metazoans. Yet, chromosome alignment is only indirectly supervised by the spindle assembly checkpoint (SAC) as a byproduct of chromosome bi-orientation, and the consequences of defective chromosome alignment remain unclear. Here we investigated how human cells respond to chromosome alignment defects of distinct molecular nature by following the fate of live HeLa cells after RNAi-mediated depletion of 125 proteins previously implicated in chromosome alignment. We confirmed chromosome alignment defects upon depletion of 108/125 proteins. Surprisingly, in all confirmed cases, depleted cells frequently entered anaphase after a delay with misaligned chromosomes. Using depletion of prototype proteins resulting in defective chromosome alignment, we show that misaligned chromosomes often satisfy the SAC and directly missegregate without lagging behind in anaphase. In-depth analysis of specific molecular perturbations that prevent proper kinetochore-microtubule attachments revealed that misaligned chromosomes that missegregate frequently result in micronuclei. Higher-resolution live-cell imaging indicated that, contrary to most anaphase lagging chromosomes that correct and reintegrate the main nuclei, misaligned chromosomes are a strong predictor of micronuclei formation in a cancer cell model of chromosomal instability, but not in normal near-diploid cells. We provide evidence supporting that intrinsic differences in kinetochore-microtubule attachment stability on misaligned chromosomes account for this distinct outcome. Thus, misaligned chromosomes that satisfy the SAC may represent a previously overlooked mechanism driving chromosomal/genomic instability during cancer cell division, and we unveil genetic conditions predisposing for these events.

Keywords: mitosis, micronuclei, kinetochore, Mad2, Cyclin B1, chromosome congression, spindle assembly checkpoint, aneuploidy, chromosomal instability, cancer

2.1.1 Introduction

Chromosome alignment in human cells relies on the concerted action of motor-dependent and independent mechanisms, which are determined by chromosome positioning at NEB, the establishment of end-on or lateral kinetochore-microtubule interactions and specific tubulin post-translational modifications (Barisic et al., 2015, 2014; Barisic and Maiato, 2016; Kapoor et al., 2006; Maiato et al., 2017; Vorozhko et al., 2008; Wood et al., 1997; Yang et al., 2007). Despite its key role in promoting mitotic fidelity (Fonseca et al., 2019; Matos et al., 2009; Orr and Maiato, 2019), chromosome alignment is only indirectly supervised by the spindle assembly checkpoint (SAC), which monitors the establishment of end-on kinetochore-microtubule attachments required for chromosome bi-orientation and regulates the metaphase-anaphase transition (Lara-Gonzalez et al., 2021; Rieder et al., 1994). It is therefore widely assumed that, under physiological conditions, cells only enter anaphase once all chromosomes align and bi-orient (Acquaviva et al., 2004; Clute and Pines, 1999; Hein and Nilsson, 2014; Howell et al., 2000; Maresca and Salmon, 2009; Murray, 2011; Pereira and Maiato, 2012; Pesenti et al., 2016; Taylor and McKeon, 1997). However, chromosome alignment may occur independently of end-on kinetochore-microtubule attachments and chromosome bi-orientation (Cai et al., 2009a; Kapoor et al., 2006; Khodjakov et al., 1997), and conditions exist in which vertebrate cells may enter anaphase in the presence of misaligned chromosomes (Rieder et al., 1986). Additionally, misaligned chromosomes generated after functional perturbation of the kinetochore-associated CENP-E/Kinesin-7 in primary mouse fibroblasts and human HeLa cells in culture, as well as in regenerating hepatocytes in vivo, did not prevent anaphase onset in approximately 25%, 40% and 95% of cell divisions, respectively, resulting in aneuploidy (Maia et al., 2010; Tanudji et al., 2004; Weaver et al., 2003). Importantly, as opposed to massive aneuploidy that renders cells unviable and has a tumor suppressing effect (Kops et al., 2004; Silk et al., 2013), gain/loss of just one or few chromosomes that are unable to complete alignment represents a real threat to chromosomal stability and has been shown to contribute to tumorigenesis in vivo (Weaver et al., 2007). Thus, understanding how human cells respond to chromosome alignment defects and determining what happens to an enduring misaligned chromosome remain fundamental unanswered questions with strong clinical implications.

2.1.2. Results

2.1.2.1. A broad range of chromosome alignment defects directly lead to missegregation

To systematically inquire how human cells respond to chromosome alignment defects of distinct molecular nature we used siRNAs to knockdown 125 different proteins previously implicated in this process (Table 1 and 2), combined with high-content live-cell microscopy in human HeLa cells stably expressing histone H2B-GFP (to visualize chromosomes) and α-tubulin-mRFP (to visualize mitotic spindles) (Figure 2.1) (see also http://chromosomecongression.i3s.up.pt). Using this systematic approach, we were able to deplete several proteins that were previously implicated in chromosome congression (Figure 2.2, contribution of Joana Monteiro) and assess their contribution to the different mitotic processes. Control cells underwent consecutive rounds of mitosis and completed chromosome alignment in 23±8 min (mean±s.d., n=7229 cells), indicating no relevant phototoxicity. In contrast, experimental perturbation of chromosome alignment led to three main mitotic phenotypes: 1) cells that entered anaphase after a delay in completing chromosome alignment (≥2 s.d. in control-depleted cells); 2) cells that entered anaphase without completing chromosome alignment; and 3) cells that died in mitosis without completing chromosome alignment (Figure 2.3). In some cases (ILK, septin-7, Aki, HIP1r, ANKRD53, ASB7, NuMA, CENP-U, CEP164, CDCA4 and MCAK), we were unable to detect any significant defect in chromosome alignment under our experimental conditions (Table 1), while others (Shp2, GAK, CEP72, CEP90, CENP-H and Mis12) turned out to be off-targets (Figure 2.4, contribution of Joana Monteiro) and were not pursued further. Interestingly, upon depletion of several Augmin complex subunits (Uehara et al., 2009), CLASPs (Logarinho et al., 2012) or the Ska complex (Gaitanos et al., 2009), among others, a fraction of cells was also unable to maintain chromosome alignment after completing congression to the spindle equator and showed signs that resembled cohesion fatigue and/or loss of spindle pole integrity (Figure 2.5). Not surprisingly, defective chromosome alignment was often associated with a significant mitotic delay, indicating a functional SAC whose timely satisfaction was nevertheless compromised (Figure 2.3b and Figure 2.6). Moreover, the severity of the observed chromosome alignment defects varied extensively, suggesting that certain proteins, such as CENP-E, several cytoplasmic Dynein subunits, members of the KNL1, Mis12 and Ndc80 (KMN) network (Cheeseman et al., 2006), the Ska complex (Gaitanos et al., 2009), and the Augmin complex (Uehara et al., 2009), are more crucial for this process than others (Figure 2.3b). However, less penetrant phenotypes due to sub-optimal protein depletion cannot be excluded. Most relevant, and regardless of the

underlying molecular nature, cells frequently entered anaphase with misaligned chromosomes that often missegregated.

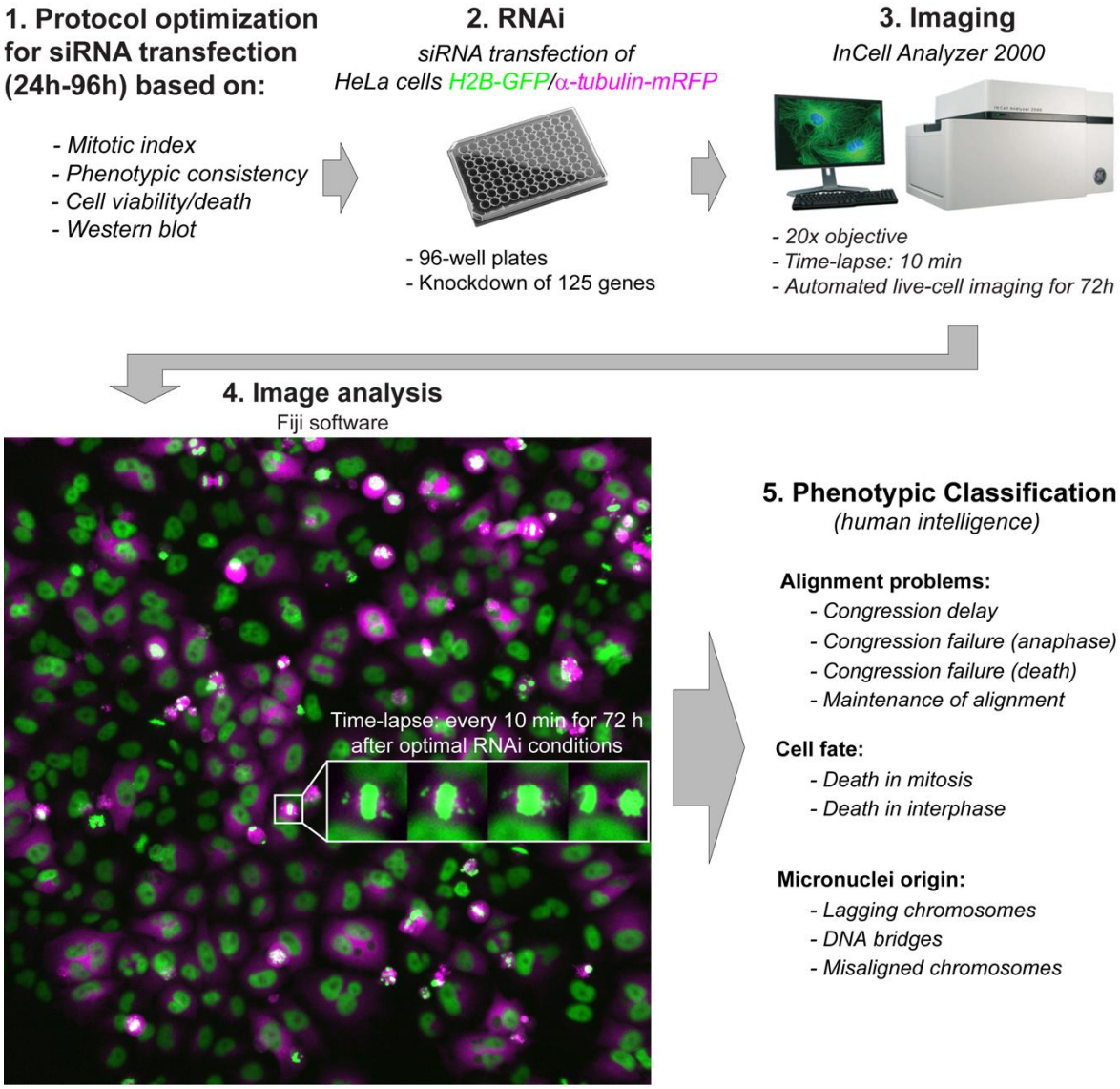

Figure 2.1. Schematic illustration of the high-content analysis of chromosome alignment defects. Different steps between protocol optimization and automated live-cell imaging of 125 different RNAi conditions against genes previously implicated in chromosome congression.

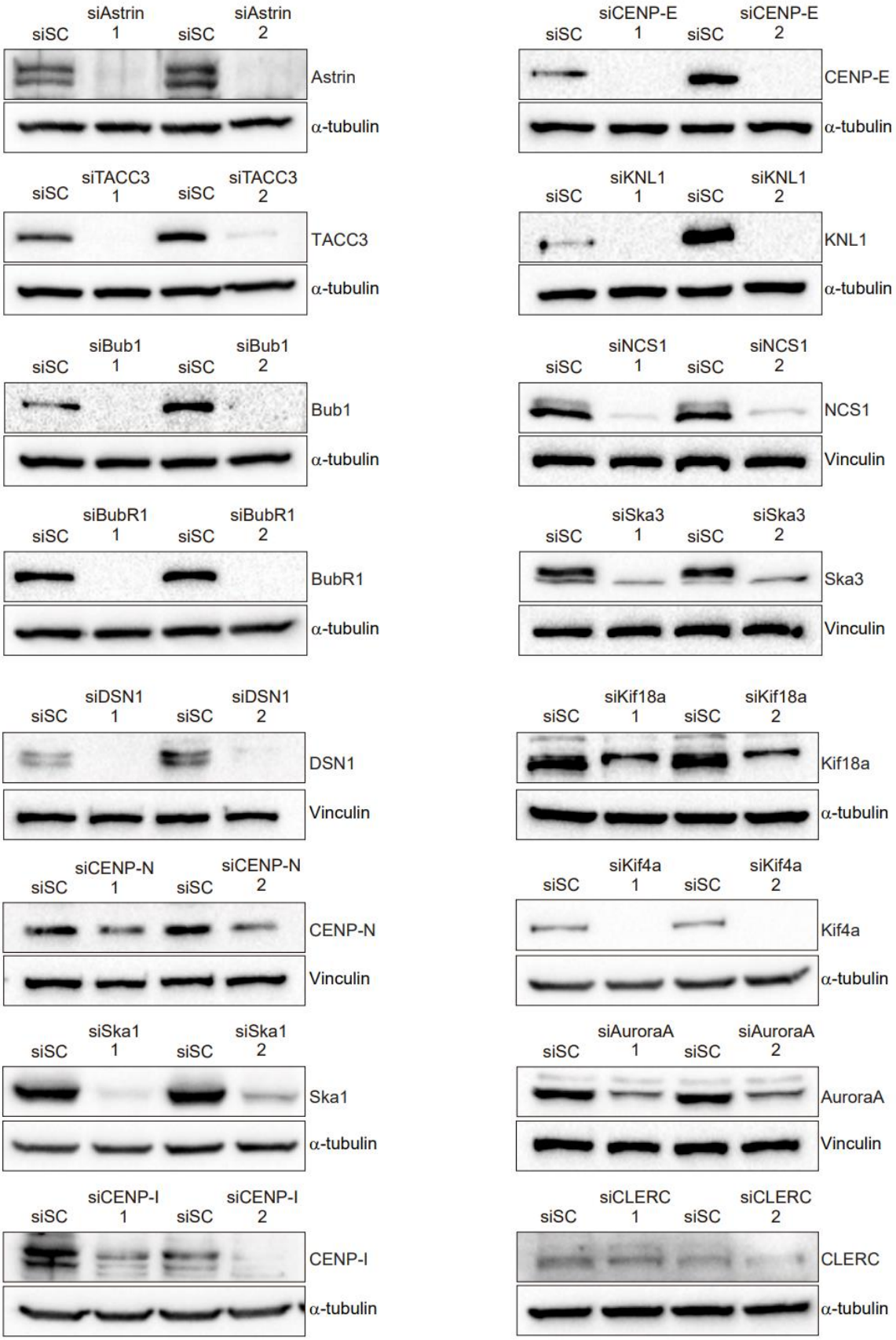
siSC
siAstrin 1
siAstrin 2
Astrin
α-tubulin
siCENP-E 1
siCENP-E 2
CENP-E
siTACC3 1
siTACC3 2
TACC3
siKNL1 1
siKNL1 2
KNL1
siBub1 1
siBub1 2
Bub1
siNCS1 1
siNCS1 2
NCS1
Vinculin
siBubR1 1
siBubR1 2
BubR1
siSka3 1
siSka3 2
Ska3
siDSN1 1
siDSN1 2
DSN1
siKif18a 1
siKif18a 2
Kif18a
siCENP-N 1
siCENP-N 2
CENP-N
siKif4a 1
siKif4a 2
Kif4a
siSka1 1
siSka1 2
Ska1
siAuroraA 1
siAuroraA 2
AuroraA
siCENP-I 1
siCENP-I 2
CENP-I
siCLERC 1
siCLERC 2
CLERC

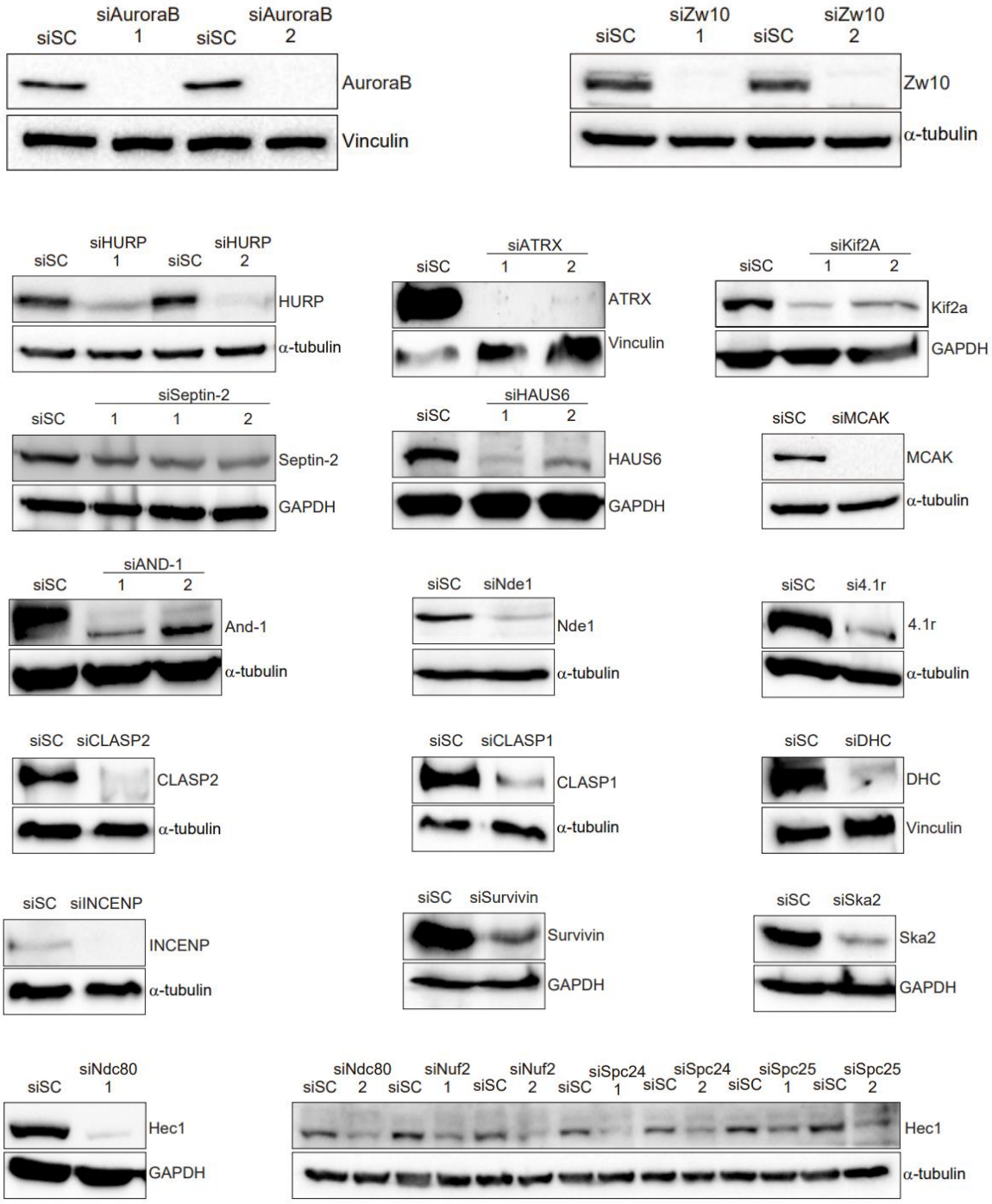

Figure 2.2. Analysis of RNAi-mediated depletion efficiency by Western blot. Validation of RNAi efficiency by immunoblotting with specific antibodies against each target protein (upper band), except for Nuf2, Spc24 and Spc25, where anti-Hec1 was used. The bottom bands corresponds to anti-α-tubulin (siAstrin, siCENP-E, siTACC3; siKNL1; siBub1; siBubR1; siKif18a; siKif4a; siSka1; siCENP-I; siCLERC; siZw10; siHURP; siMCAK; siAnd-1; siNde1; si4.1r; siCLASP2; siCLASP1; siINCENP; siNdc80; siNuf2; siSpc24; siSpc25), anti-GAPDH (siKif2a; siHAUS6; siSka2; siNdc80) and anti-Vinculin (siNsl1; siSka3; siDsn1; siCENP-N; siAurora A; siAurora B; siATRX; siDHC), which were used as loading controls. siSC= control.

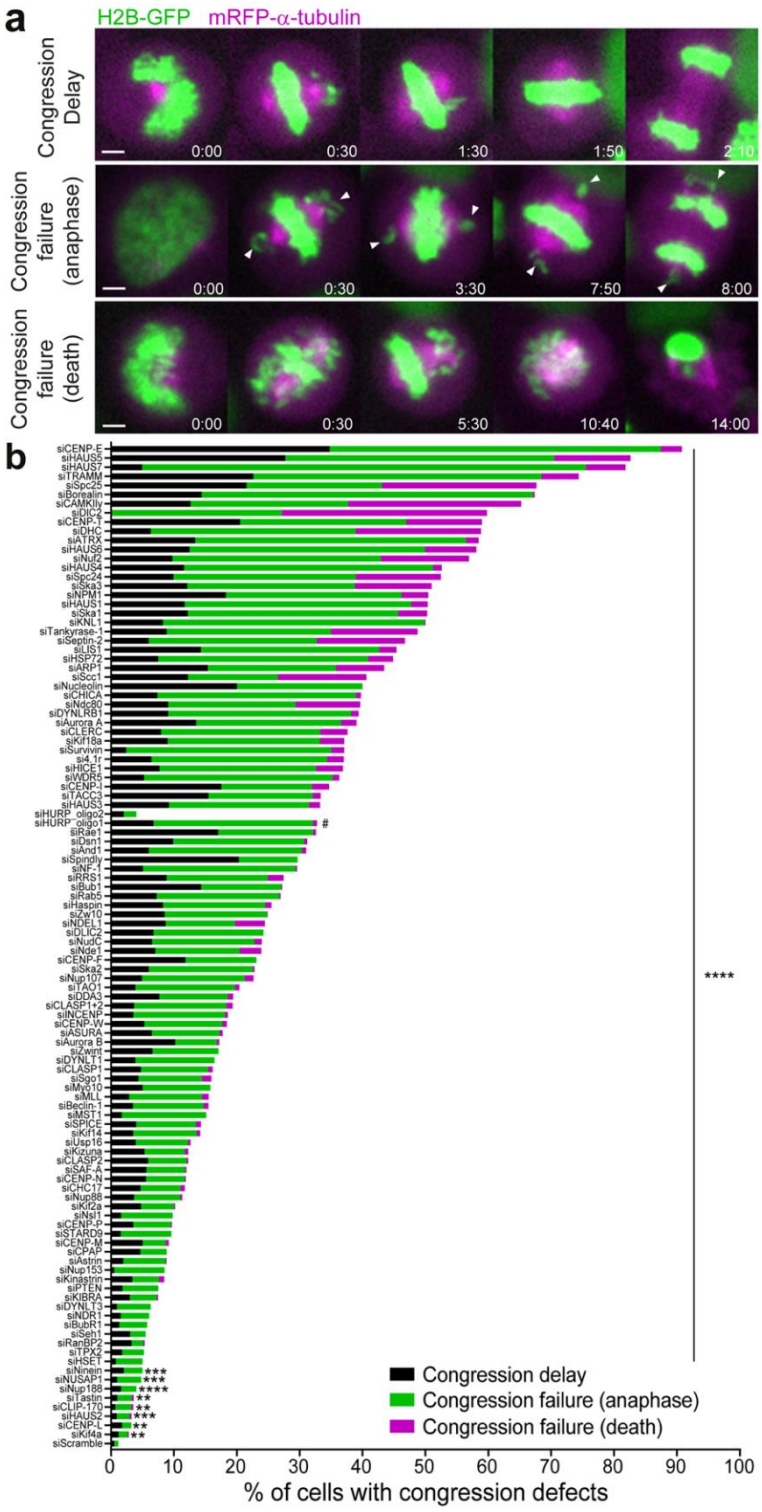

Figure 2.3. A broad range of chromosome alignment defects directly lead to missegregation. a) Examples of time-lapse sequences illustrating the three main mitotic phenotypes observed. Arrows indicate chromosomes at the poles in cells exhibiting chromosome alignment defects. Pixels were saturated for optimal visualization of misaligned chromosomes. Scale bar=5 µm. Time=h:min. **b)** Quantification of congression phenotypes in control (siScramble) and siRNA-depleted cells. At least 2 independent experiments per condition were performed. The total number of cells analyzed for each condition is indicated in Table 1. (*p≤0.05, **p≤0.01, ***p≤0.001, ****p≤0.0001, ns=not significantly different from control; Fisher´s exact two-tailed test; # highlights a possible off-target associated with siRNA oligo 1 against HURP).

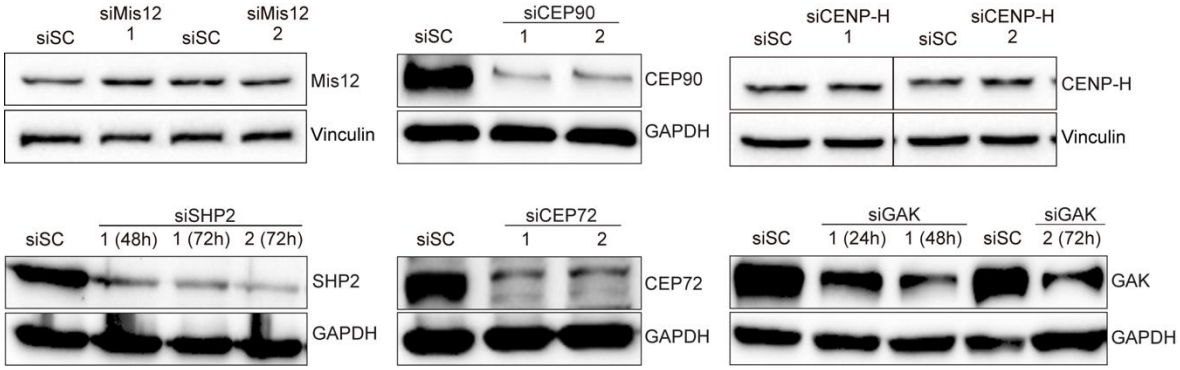

Figure 2.4. Identification of off-targets. Protein lysates obtained after RNAi treatment were immunoblotted with an antibody specific for each protein of interest (Mis12, CEP90, CENP-H, SHP2, CEP72 and GAK, upper bands). The bottom band corresponds to antibody detections of GAPDH or Vinculin, which were used as loading controls.

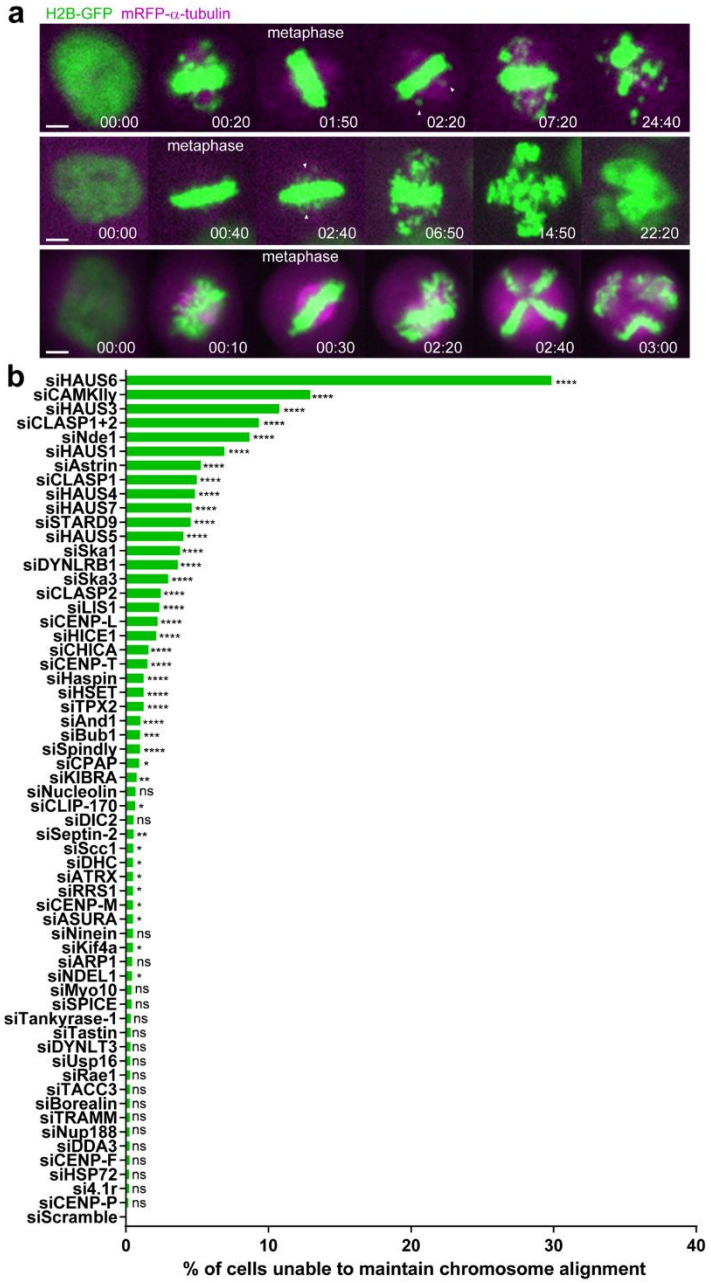

Figure 2.5. In addition to chromosome alignment defects, some defects conditions also compromise the maintenance of chromosome alignment at the metaphase plate. a) Examples of time-lapse sequences illustrating the three main mitotic phenotypes of chromosome alignment maintenance defects observed: 1) cells showed a prolonged delay in chromosome alignment but eventually completed congression, after which chromosomes/chromatids underwent gradual scattering from the metaphase plate; 2) chromosomes aligned normally at the metaphase plate, but then underwent gradual scattering; 3) chromosomes aligned normally at the metaphase plate, followed by spindle pole fragmentation and chromosome scattering. Arrows indicate scattered chromosomes/chromatids in cells that were unable to maintain chromosome alignment at the metaphase plate. Scale bar = 5 μm. Time: h:min, from nuclear envelope breakdown (NEB) to cell death or mitotic exit. **b)** Frequency of cells exhibiting problems in the maintenance of chromosome alignment at the metaphase plate. Only the conditions exhibiting problems in the maintenance of chromosome alignment were included. At least 2 independent experiments were analyzed. The total number of cells analyzed for each conditions is indicated in Table 1. (*p≤0.05, **p≤0.01, ***p≤0.001, ****p≤0.0001, ns corresponds to not significantly different from control, Fisher´s exact two-tailed test).

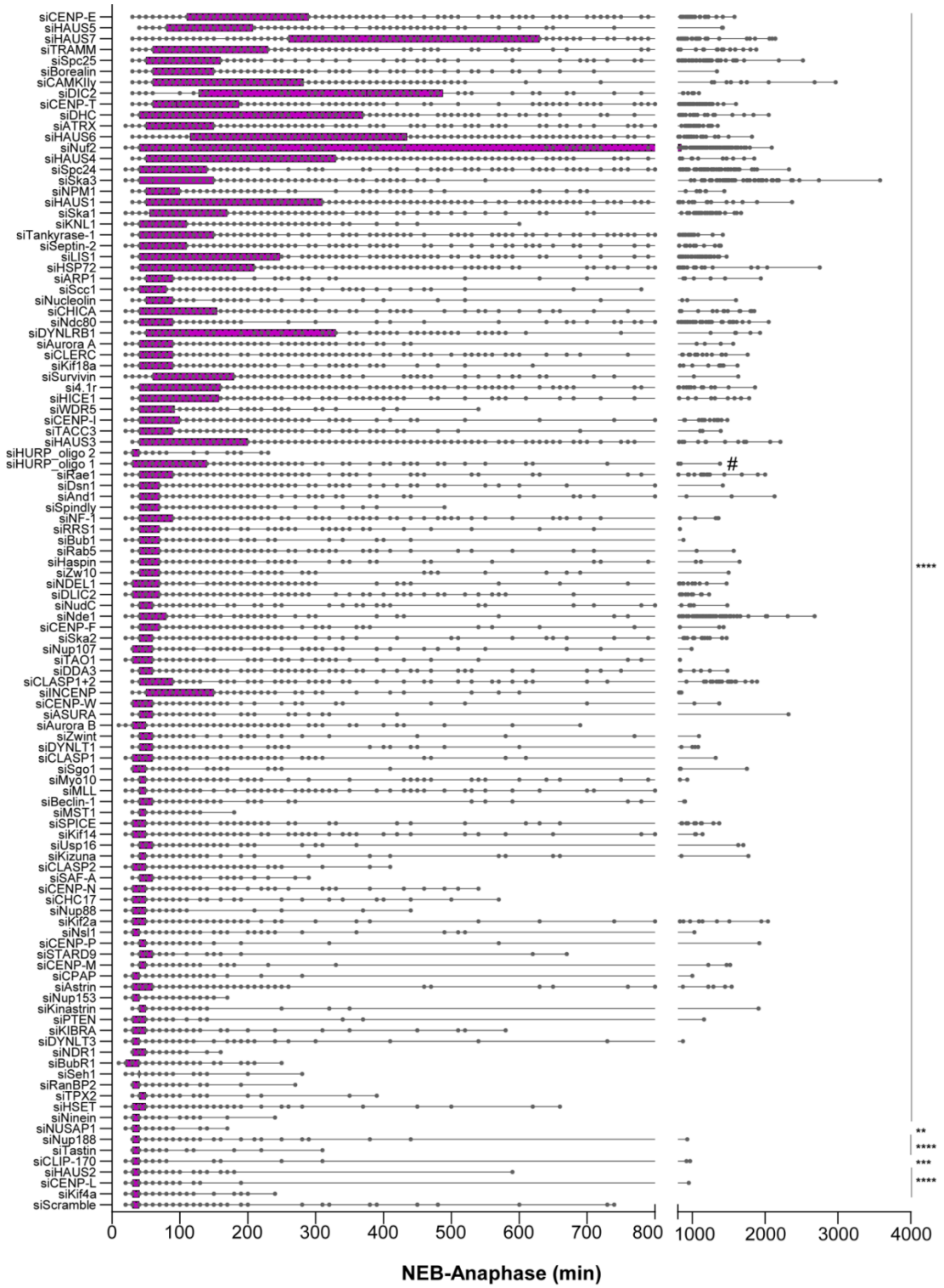

Figure 2.6. Mitotic duration upon gene-specific RNAi-mediated depletion. HeLa cells stably expressing H2B-GFP and α-tubulin-mRFP were acquired every 10 minutes. Mitotic duration was determined by measuring the time between nuclear envelope breakdown (NEB) and anaphase onset, shown in minutes. Data was presented as box-and-whiskers and each point corresponds to one cell. The difference between mean values of each RNAi condition was statistically significant from the control mean values. At least 2 independent experiments per condition were performed.

2.1.2.2. Mild, yet penetrant, chromosome alignment defects are compatible with mitotic progression and cell viability

Next, we investigated how the extent of chromosome alignment defects impacts cell viability during and after mitosis (Figure 2.7 a, b). We found a strong positive correlation between the propensity of cells to die in mitosis and the time they spent in mitosis due to chromosome alignment defects (Figure 2.7 b-d). A positive, yet weaker correlation was also observed between the likelihood of cells to die in the subsequent interphase and the time they spent in mitosis due to chromosome alignment defects (Figure 2.7b, e, f). In one particular case (NUP107 RNAi), most cells died in the subsequent interphase likely due to a well-established role in nuclear pore complex assembly and function (Beck and Hurt, 2017). Interestingly, a direct comparison between CENP-E-depleted (with mild, yet highly penetrant chromosome alignment problems) and Ndc80-depleted cells (with severe, but less penetrant chromosome alignment problems), revealed a clear link between the extent of chromosome alignment defects and cell death, either in mitosis or in the subsequent interphase (Figure 2.8). Importantly, conditions like CENP-E or Kif18a depletion, in which cells entered anaphase with only one or few misaligned chromosomes, and/or a less compact metaphase plate (Fonseca et al., 2019), were compatible with mitotic progression and cell viability (Figure 2.7.b), thereby representing a threat to chromosomal stability.

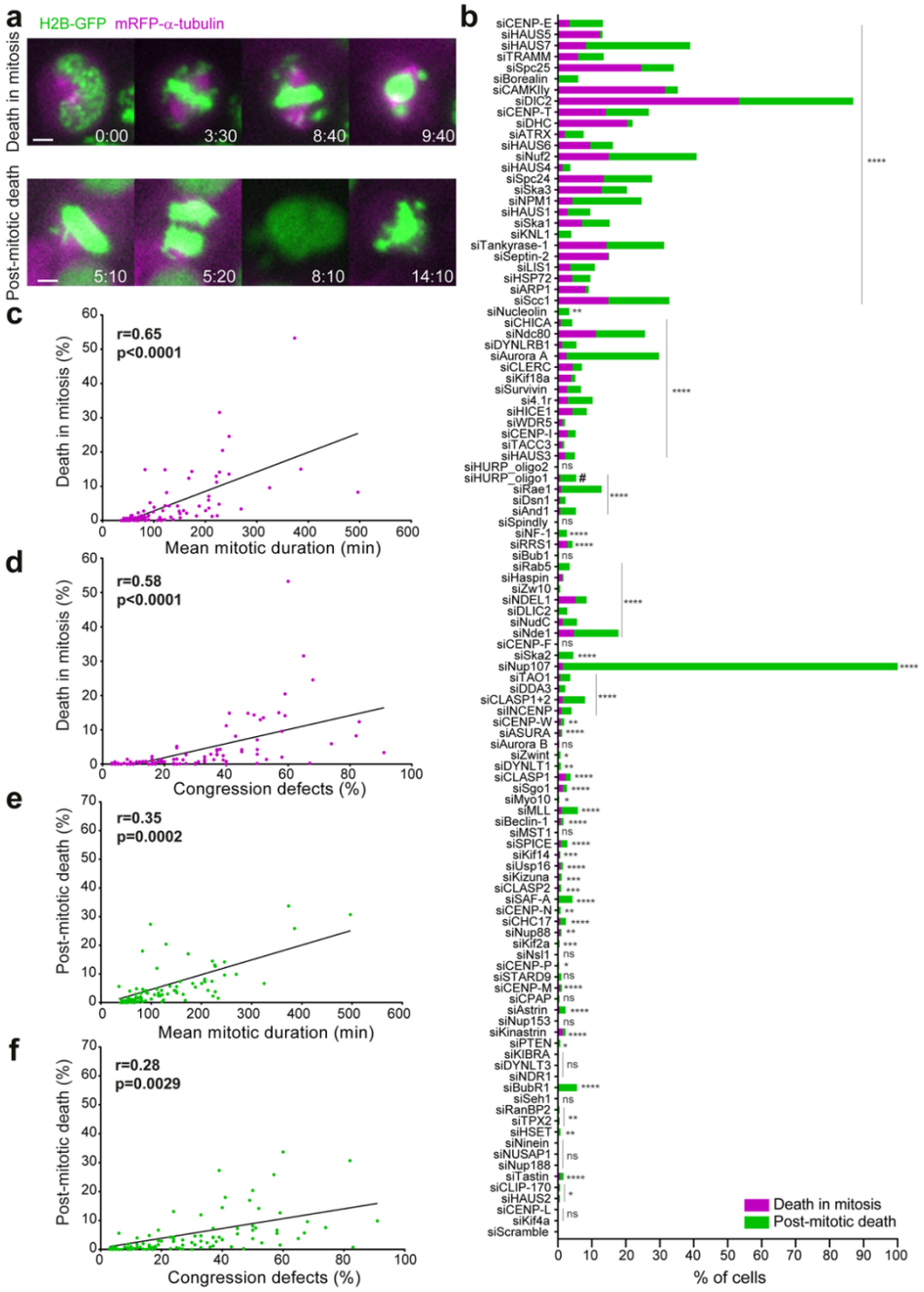

Figure 2.7. Mild, yet penetrant, chromosome alignment defects are compatible with mitotic progression and cell viability. a) Examples of time-lapse sequences illustrating the fates exhibited by HeLa cells undergoing congression defects following siRNA knockdown. Time=h:min, from nuclear envelope breakdown (NEB) to each cellular outcome. Scale bar=5 μm. **b)** Frequency of cells that either died in mitosis (magenta) or died in interphase (green) in control and siRNA-depleted cells. The total number of cells analyzed for each condition is indicated in Table 1. (*p≤0.05, **p≤0.01, ***p≤0.001, ****p≤0.0001, ns=not significantly different from control; Fisher´s exact two-tailed test; # highlights a possible off-target associated with siRNA oligo 1 against HURP). **c)** Correlation between mitotic duration and cell death in mitosis for each condition. **d)** Correlation between the severity of the congression phenotypes and the frequency of cell death in mitosis. **e)** Correlation between the mitotic duration after siRNA treatment and cell death in interphase. **f)** Correlation between congression severity and the frequency of cell death in interphase. Pearson's correlation (r) and respective P-values are indicated in the plots (two-tailed test).

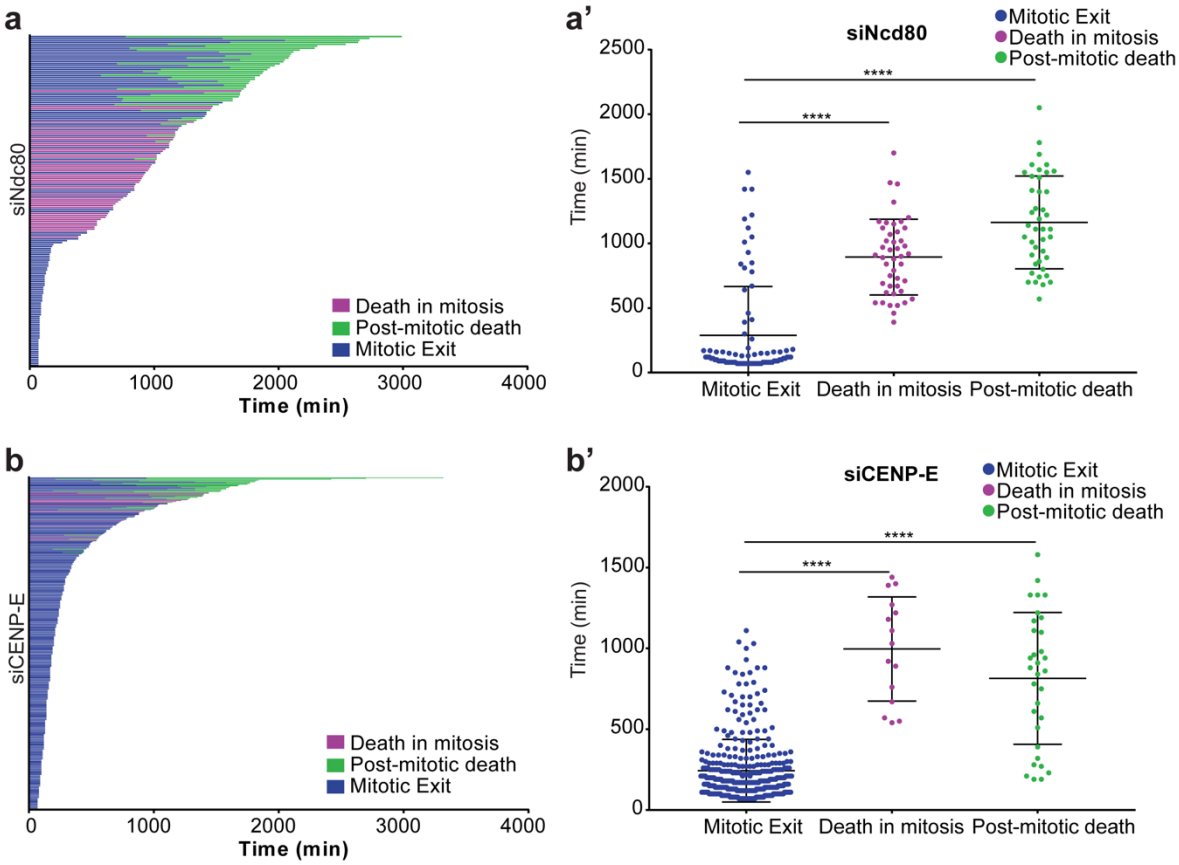

Figure 2.8. Cell fate upon induction of chromosome alignment defects of distinct molecular nature. **a)** Cell fate profiles of HeLa cells with delayed or failed chromosome alignment after Ndc80 depletion. Each line indicates a single cell and respective outcome. **a´)** Time that cells spent until mitotic exit (blue), death in mitosis (purple) or in subsequent interphase (green) after Ndc80 depletion. Each dot represents a single cell. The horizontal line indicates the mean of all quantified cells and the errors bars represent the standard deviation from a pool of four independent experiments (Mitotic exit, 289±377 min, n=83; Death in mitosis, 894±292 min, n=45; Post-mitotic death 1162±359 min, n=42; ****p≤0.0001 relative to control, analyzed using a Mann-Whitney Test). **b)** Cell fate profiles of HeLa cells with delayed or failed chromosome alignment after CENP-E depletion. **b´)** Time that cells spent until mitotic exit (blue), death in mitosis (purple) or in the subsequent interphase (green) after CENP-E depletion. Each dot represents a single cell. The horizontal line indicates the mean of all quantified cells and the errors bars represent the standard deviation from a pool of five independent experiments (Mitotic exit, 243±193 min, n=358; Death in mitosis 996±322 min, n=15; Post-mitotic death 814±408 min, n=32; ****p≤0.0001 relative to control,, analyzed using a Mann-Whitney Test).

2.1.2.3. Cells with misaligned chromosomes enter anaphase after satisfying the spindle assembly checkpoint

In contrast to cells that satisfy the SAC, human cells undergoing mitotic slippage (Rieder and Maiato, 2004) upon complete microtubule depolymerization with nocodazole retain the SAC proteins, Mad1, Mad2 and BubR1 at kinetochores and very slowly degrade Cyclin B1 due to residual APC/C activity (Brito and Rieder, 2006; Gascoigne and Taylor, 2008; Novais-Cruz et al., 2018). To distinguish between these possibilities, we used live imaging

in HeLa cells stably expressing Mad2-GFP to monitor the status of the SAC in control- or CENP-E-depleted cells that entered anaphase with one or few misaligned chromosomes at very high frequency after a mitotic delay (Figure 2.3b; see also (Maia et al., 2010; Tanudji et al., 2004)). As expected, in cells treated with a control siRNA Mad2-GFP accumulated at kinetochores during prometaphase and gradually disappeared as chromosomes bi-oriented and aligned at the metaphase plate, being undetectable at kinetochores when cells entered anaphase (Figure 2.9.a). Likewise, Mad2-GFP accumulated exclusively at the kinetochores from those few chromosomes that never completed alignment after CENP-E depletion, becoming undetectable before anaphase onset and throughout anaphase (Figure 2.9.a, contribution of Bernardo Orr). To obtain a more quantitative picture, we used immunofluorescence in fixed HeLa cells to measure the fluorescence of the SAC protein Mad1 relative to CENP-C (a constitutive kinetochore component) on misaligned chromosomes after CENP-E depletion in early anaphase (Figure 2.9.b). We found that, in striking contrast to misaligned chromosomes during prometaphase where Mad1 signal was clearly detected at kinetochores in both control- and CENP-E-depleted cells (Figure 2.9.c), virtually no Mad1 signal was detected at both kinetochores from misaligned chromosomes (an indication of syntelic attachments in which both kinetochores of a misaligned chromosome are oriented towards the same spindle pole) that persisted in early anaphase after CENP-E depletion (Figure 2.9.c). Together, these data suggest that cells with misaligned chromosomes enter anaphase after a delay by satisfying the SAC.

To further validate this conclusion, we used time-lapse fluorescence microscopy in HeLa and non-transformed near-diploid RPE-1 cells to quantify the levels and monitor the respective degradation kinetics of endogenously-tagged Cyclin B1 with the fluorescent protein Venus (Novais-Cruz et al., 2018) after depletion of CENP-E, or a second unrelated protein (TACC3) whose depletion also resulted in misaligned chromosomes (Gergely et al., 2003) (Figure 2.10 and Figure 2.11a-c; contribution of Bernardo Orr). Consistent with previous reports (Afonso et al., 2019; Clute and Pines, 1999) and in stark contrast with Cyclin B1 degradation kinetics over more than 12 hours during mitotic slippage/death upon complete microtubule depolymerization with nocodazole (Figure 2.11d, e, contribution of Marco Cruz) (see also (Brito and Rieder, 2006; Gascoigne and Taylor, 2008; Novais-Cruz et al., 2018)), Cyclin B1 starts to be steadily degraded few minutes before the onset of anaphase and continues to decline throughout anaphase in control HeLa or RPE-1 cells, becoming undetectable as chromosomes decondense in telophase (Figure 2.10a,b and Figure 2.11a,b; contribution of Bernardo Orr). Similar degradation kinetics were observed in CENP-E-depleted or TACC3-depleted cells that entered anaphase, with or without completion of chromosome alignment (Figure 2.10a,b and Figure 2.11a,b). In this particular set of experiments ~40% of the CENP-E-depleted and ~20% of the TACC3-depleted

anaphase HeLa cells formed micronuclei directly from chromosomes that never aligned at the spindle equator (Figure 2.10c). The frequency of these events was significantly lower in RPE-1 cells, likely due to higher efficiency in chromosome alignment after CENP-E depletion (Figure 2.11c). Taken together, these data indicate that cells with misaligned chromosomes may enter anaphase after satisfying the SAC and undergoing normal Cyclin B1 degradation.

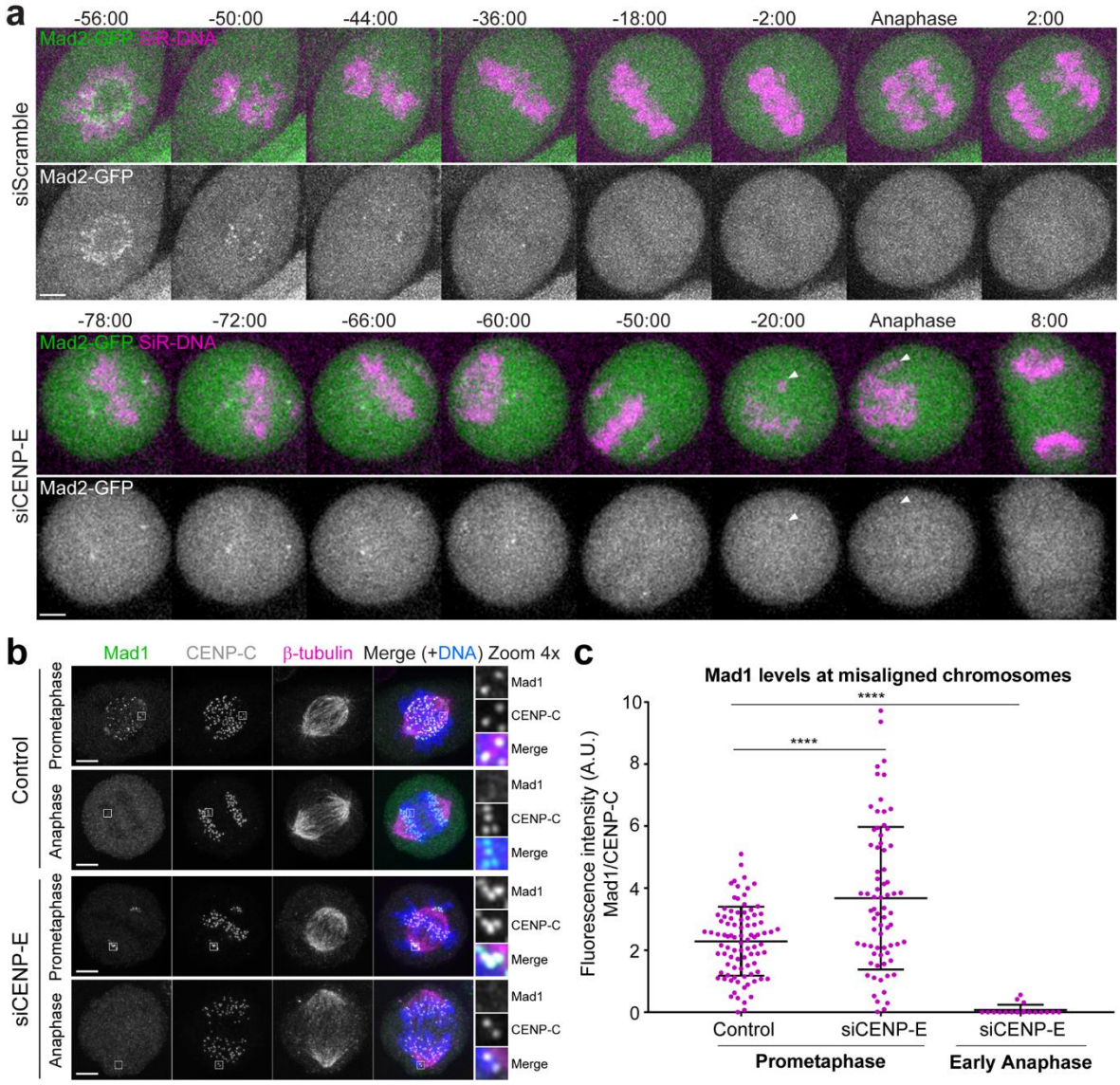

Figure 2.9. Cells with misaligned chromosomes enter anaphase after satisfying the spindle assembly checkpoint. **a)** Selected time-frames of representative HeLa cells stably expressing Mad2-GFP (green) and chromosomes labeled with SiR-DNA (magenta) in control and after CENP-E depletion. White arrowheads point to a misaligned chromosome during anaphase. Time=min:sec. Time 00:00=anaphase onset. **b)** Immunofluorescence of HeLa cells stained for DNA (blue), Mad1 (green), CENP-C (white) and β-tubulin (magenta). Insets show higher magnification of selected regions with misaligned chromosomes (grayscale for single channels of Mad1 and CENP-C). Images are maximum intensity projections of deconvolved z-stacks. Scale bar=5 µm. **c)** Quantification of the fluorescence intensity of Mad1 relative to CENP-C on misaligned chromosomes. Each dot represents an individual kinetochore. The horizontal line indicates the mean of all quantified kinetochores and the error bars represent the standard deviation from a pool of two independent experiments

(mock/prometaphase, n=90 kinetochores, 9 cells; siCENP-E/prometaphase, n=72 kinetochores, 17 cells; siCENP-E/anaphase, n=19 kinetochores, 14 cells; ****p≤0.0001 relative to control, Mann-Whitney Test).

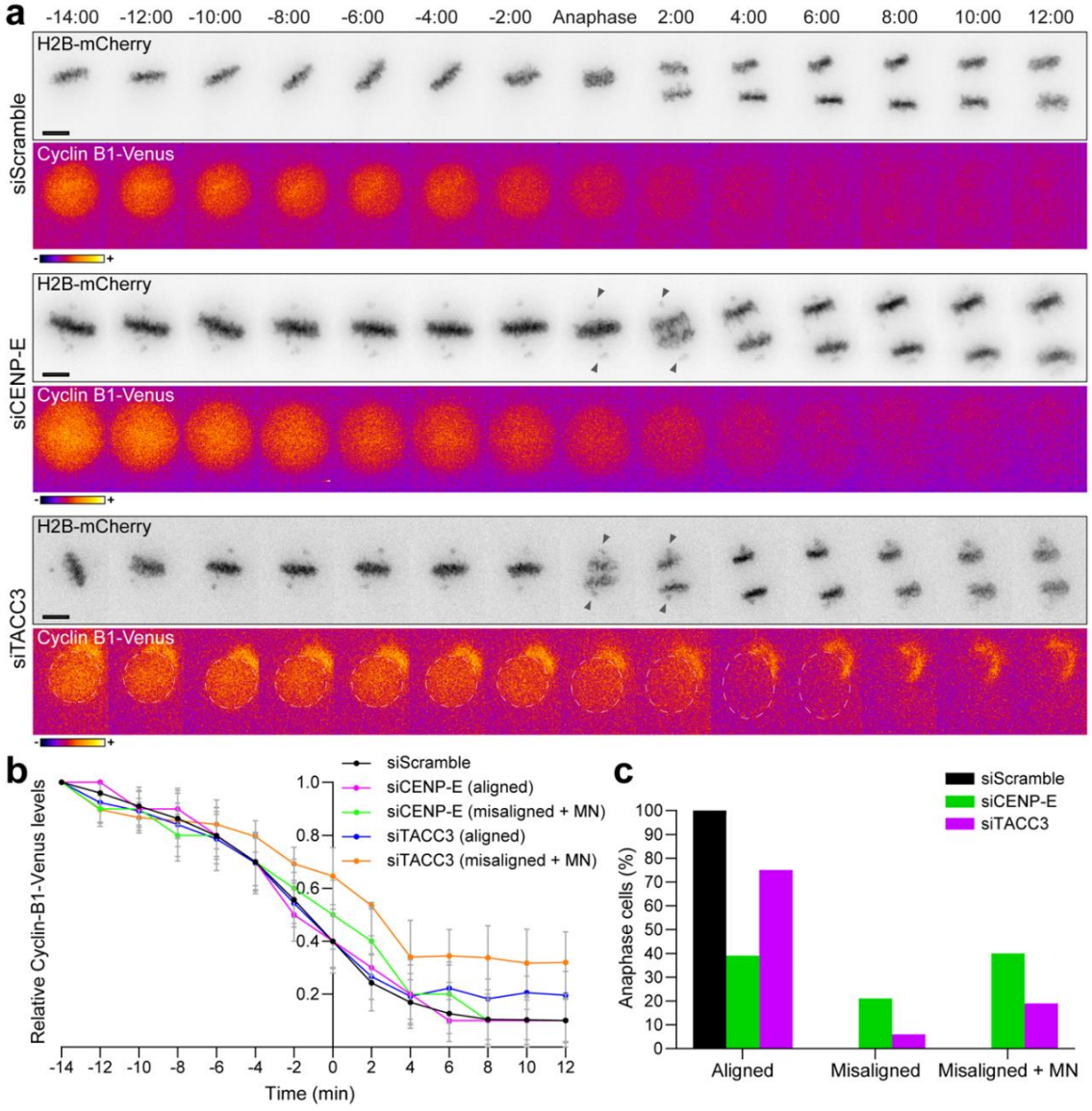

Figure 2.10. Cells with misaligned chromosomes enter anaphase after undergoing normal Cyclin B1 degradation. a) Selected time frames from live-cell microscopy of HeLa cells stably expressing H2B-mCherry and Cyclin B1-Venus in control, CENP-E and TACC3 RNAi. Time=min:sec. Time 00:00=anaphase onset. Scale bar=5 µm. Black arrowheads point to misaligned chromosomes at anaphase onset. **b)** Cyclin B1 degradation curves for control-, CENP-E- and TACC-3-depleted cells that properly align their chromosomes at the metaphase plate or exit mitosis with misaligned chromosomes and form micronuclei. The curves represent mean Cyclin B1-Venus fluorescence intensity from all analyzed cells and error bars represent the standard deviation from a pool of two independent experiments [siScramble n=20; siCENP-E (misaligned+micronuclei) n=22; siCENP-E (aligned) n=15; siTACC3 (misaligned+micronuclei) n=5; siTACC3 (aligned) n=12]. **c)** Frequency of anaphase cells with aligned chromosomes, misaligned chromosomes and misaligned chromosomes that result in micronuclei in control- (black bars), CENP-E-(green bars) and TACC3-depleted cells (magenta bars).

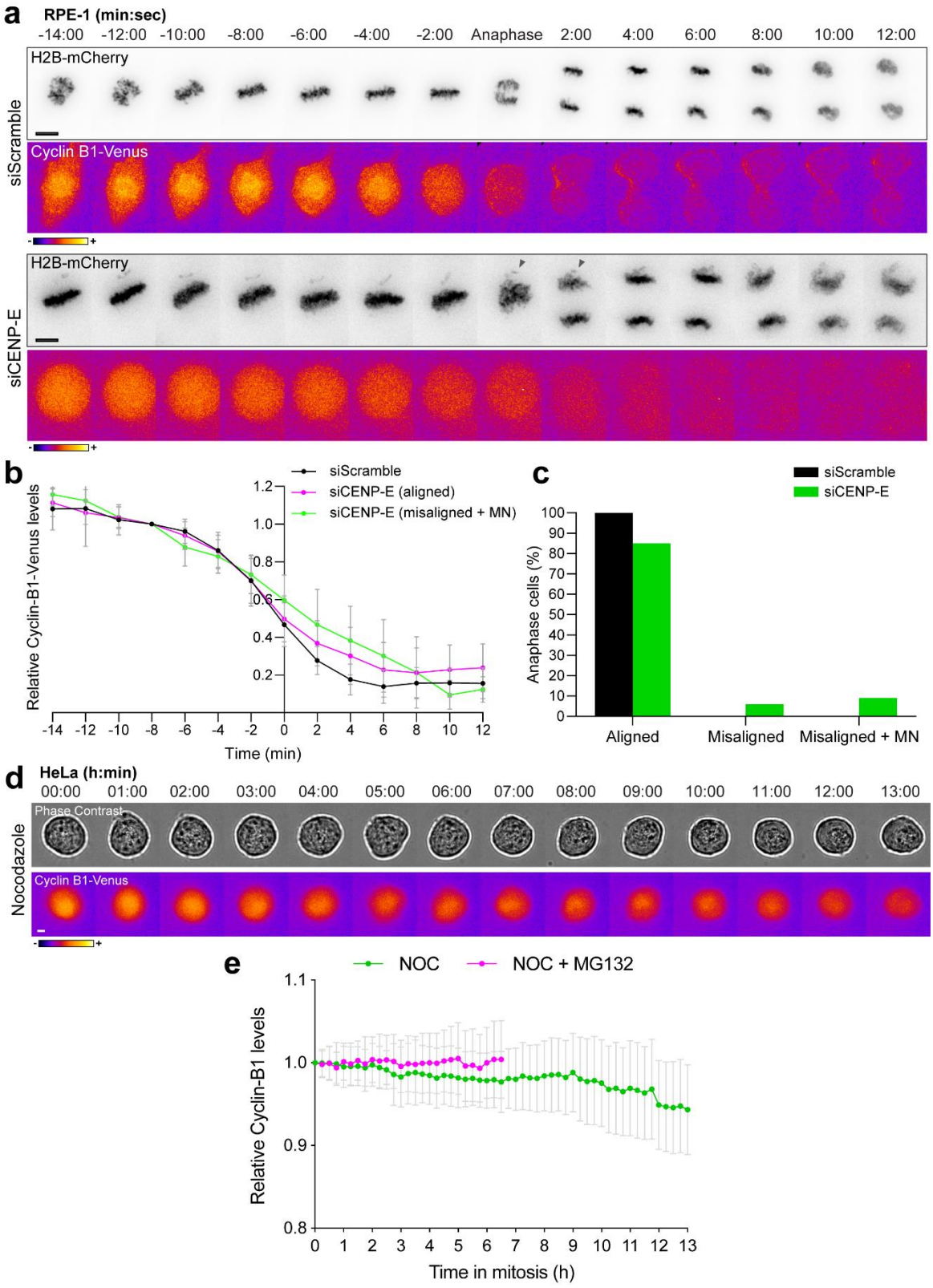

Figure 2.11. Further characterization of Cyclin B1 degradation profiles in RPE-1 and HeLa cells. **a)** Selective time frames from live-cell microscopy of RPE-1 cells stably expressing H2B-mRFP and Cyclin B1-Venus in control and siCENP-E. Images were acquired every 2 min. Time = min:sec. Time 00:00 = anaphase onset. Black arrowheads point to misaligned chromosomes that remain upon anaphase onset. **b)** Cyclin B1 degradation profile for control, CENP-E depleted cells that properly align their chromosomes at the metaphase plate and CENP-E depleted cells that exit mitosis with

misaligned chromosomes give rise to micronuclei. Fluorescence intensities were normalized to the levels at time = -8. The curves represent mean Cyclin B1-Venus fluorescence intensity from all analyzed cells and errors bars represent the standard derivation from a pool of three independent experiments (siScramble n=30; siCENP-E (aligned) n=30; siCENP-E (misaligned+micronuclei) n=5). **c)** Frequency of anaphase cells with aligned chromosomes, misaligned chromosomes and misaligned chromosomes that result in micronuclei in control (black bars) and CENP-E-depleted cells (green bars). **d)** Selected time frames from phase-contrast and fluorescence microscopy of Cyclin B1-Venus HeLa cells treated with nocodazole with or without MG132. Images were acquired every 15 min. Scale bar = 5µm. Time = h:min. **e)** Cyclin B1 degradation profiles of nocodazole-treated Cyclin B1-Venus HeLa cells in the presence or absence of MG132. Fluorescence intensities were normalized to the levels at time = 0. The curves depict mean Cyclin B1-Venus fluorescence intensity from all analyzed cells per condition (nocodazole n=12; nocodazole + MG132 n=10), and error bars represent the standard deviation. Note that acquisition in the presence of MG132 was terminated earlier relative to acquisition without MG132 due to cell death.

2.1.2.4. Although most micronuclei originate from anaphase lagging chromosomes, misaligned chromosomes are a stronger predictor of micronuclei formation

The origin of micronuclei has been linked to the presence of lagging chromosomes during anaphase that form due to incorrect merotelic kinetochore-microtubule attachments (when individual kinetochores bind to microtubules oriented to both spindle poles) (Cimini et al., 2002; Crasta et al., 2012). More recently, DNA bridges that persist during anaphase were also implicated in micronuclei formation (Umbreit et al., 2020). Here we sought to compare the relative contributions of lagging and misaligned chromosomes, as well as DNA bridges, to micronuclei formation during HeLa cell division (Figure 2.12a). To do so, we focused our analysis on a subset of experimental conditions that are recognized to prevent proper kinetochore-microtubule attachments (Figure 2.12b). As a rule, and in line with our previous findings (Orr et al., 2021), these conditions led to a substantial increase in the frequency of daughter cells with micronuclei (9.0 ± 7.3%, mean ± s.d., and up to 40% on specific conditions such as KNL1 depletion) when compared to daughter cells treated with a control siRNA (1.4%) (Figure 2.12b). As expected, most of the resulting micronuclei derived from anaphase lagging chromosomes (62 ± 19%, mean ± s.d. of all conditions) and only few (8.5 ± 6.2%, mean ± s.d. of all conditions) originated from DNA bridges (Figure 2.12b). However, we also found that a significant fraction of cells (29 ± 20%, mean ± s.d. of all conditions) formed micronuclei that derived directly from misaligned chromosomes (Figure 2.12b). Noteworthy, although occurring at much lower frequency, the relative origin of micronuclei in control HeLa cells was in line with that generally observed upon experimental perturbation of kinetochore-microtubule attachments (56%, 22% and 22%, for lagging chromosomes, DNA bridges and misaligned chromosomes, respectively; n=1700 cells) (Figure 2.12b). This scenario changed significantly both regarding frequency and origin of micronuclei upon monastrol treatment and washout, which induces the formation

of erroneous kinetochore-microtubule attachments leading to a high frequency of anaphase lagging chromosomes (Cimini et al., 2003; Lampson et al., 2004) (Figure 2.12b).

Next, we determined the respective probabilities of micronuclei formation given a specific condition, which can either be a lagging chromosome, a DNA bridge or a misaligned chromosome. Surprisingly, and despite the fact that most micronuclei derived from anaphase lagging chromosomes, we found that in unperturbed HeLa cells treated with a control siRNA the absolute and relative probability of micronuclei formation from a misaligned chromosome (0.92 and 0.70, respectively) clearly outcompeted the other two classes, including anaphase lagging chromosomes (0.28 and 0.21, for absolute and relative probabilities, respectively) (Figure 2.12c and Figure 2.13). These probabilities were significantly higher than what would be expected if all missegregation events were equally likely to cause micronuclei ($p<0.0001$; Chi-square test). Interestingly, although the experimental perturbation of kinetochore-microtubule attachment stability did not result in gross alterations of the relative origins of micronuclei, in most cases it reverted or attenuated the much higher probability of micronuclei formation from misaligned chromosomes observed in unperturbed cells (Figure 2.12c and Figure 2.13). This result is consistent with a role of stable kinetochore-microtubule attachments in anaphase error correction and micronuclei prevention from lagging chromosomes (Orr et al., 2021). One noticeable exception was HURP, which gave rise to much milder congression problems with no obvious bias for micronuclei formation from misaligned chromosomes with a second siRNA, in contrast with the original siRNA, despite equivalent depletion efficiency (Figure 2.2). We suspect that the first siRNA against HURP might by hitting the SAC component MAD2, which is highly prone to off-targeting (Sigoillot et al., 2012) and would force HURP-depleted cells with incomplete chromosome congression to enter anaphase prematurely, directly leading to micronuclei formation due to incomplete chromosome alignment. Overall, we conclude that, although the majority of micronuclei originate from anaphase lagging chromosomes, misaligned chromosomes are a stronger predictor of micronuclei formation during HeLa cell division.

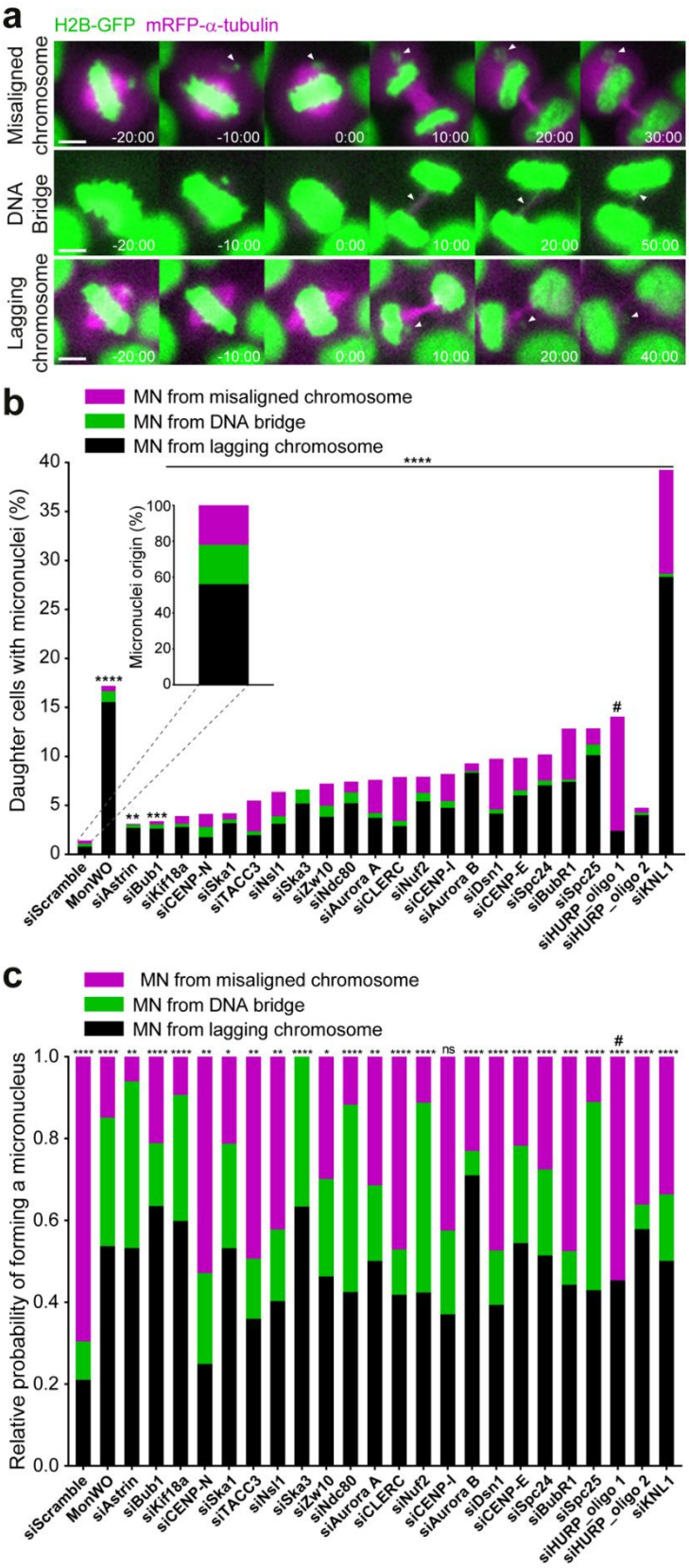

Figure 2.12. Although most micronuclei originate from anaphase lagging chromosomes, misaligned chromosomes are a stronger predictor of micronuclei formation. a) Examples of time-lapse sequences illustrating the different origins of micronuclei. Time=min:sec. Time 00:00=anaphase onset. White arrowheads track misaligned chromosomes, DNA bridges or lagging

chromosomes until they eventually form micronuclei. Pixels were saturated for optimal visualization of misaligned chromosomes, DNA bridges and lagging chromosomes. Scale bar=5 µm. **b)** Frequency of daughter cells with micronuclei that derived either from lagging chromosomes (black bars), DNA bridges (green bars) or misaligned chromosomes (magenta bars) under the specified conditions [siScramble n=1700, MonWO n=327, siAstrin n=423, siBub1 n=457, siKif18a n= 540, siCENP-N n= 422, siSka1 n=395, siTACC3 n=485, siNsl1 n=400, siSka3 n= 383, siZw10 n= 404, siNdc80 n=440, siAurora A n= 388, siCLERC n=263, siNuf2 n=428, siCENP-I n= 389, siAurora B n=499, siDsn1 n=688, siCENP-E n= 346, siSpc24 n=418, siBubR1 n=387, siSpc25 n= 425, siHURP_oligo1 n=296, siHURP_oligo2 n=200, siKNL1 n=413; pool of 2 independent experiments for each siRNAi per condition, with the exception of Aurora A and CLERC in which only 1 experiment for the second siRNAi was performed. All independent experiments were pooled]. (*p≤0.05, **p≤0.01, ***p≤0.001, ****p≤0.0001, ns=not significantly different from control; Fisher´s exact two-tailed test; # highlight a possible off-target associated with siRNA oligo 1 against HURP). **c)** Relative probability (sum of the 3 independent absolute probabilities normalized to 1) of micronuclei formation from a lagging chromosome (black bars), a DNA bridge (green bars) or a misaligned chromosome (magenta bars) under the specified conditions [*p≤0.05, **p≤0.01, ***p≤0.001, ****p≤0.0001, ns=no significant difference from what would be expected if all missegregation events were equally likely to cause micronuclei in each experimental condition (Chi-square test)].

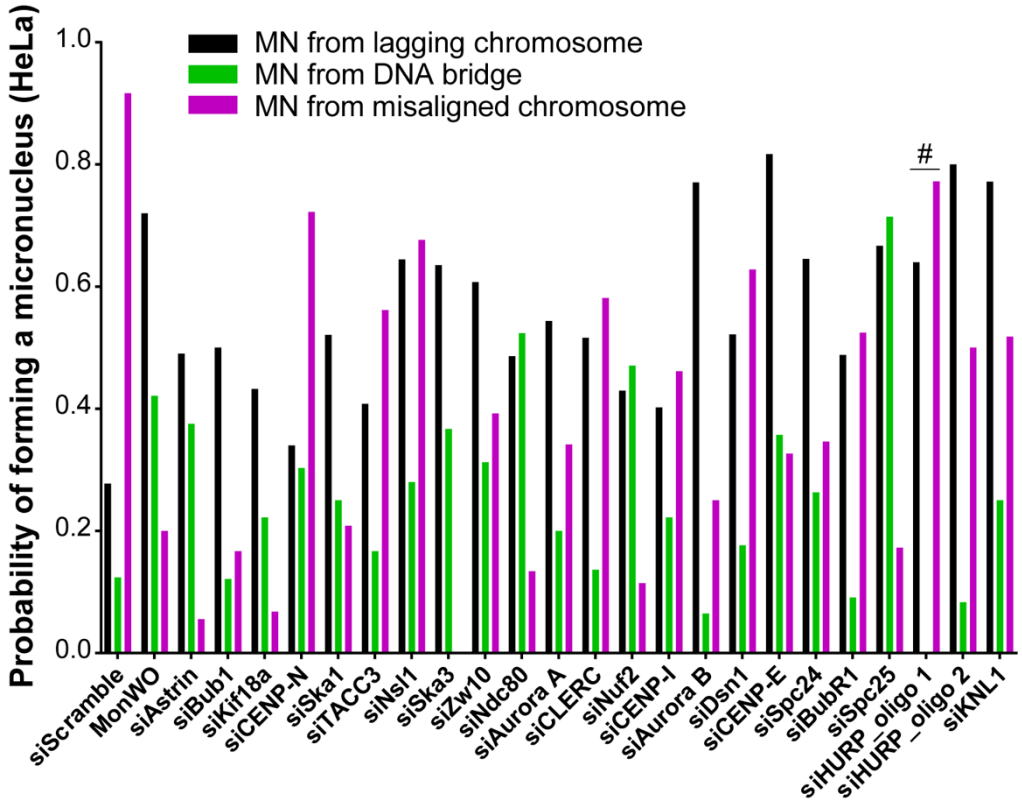

Figure 2.13. Absolute probabilities of forming a micronucleus from misaligned chromosomes, DNA bridges and lagging chromosomes in HeLa cells. Absolute probabilities of forming a micronucleus of different origins in unperturbed HeLa cells and after molecular perturbations that weaken kinetochore-microtubule attachments or promote the formation of anaphase lagging chromosomes after monastrol treatment and washout (MonWO). [siScramble n=1700, MonWO n=327, siAstrin n=423, siBub1 n=457, siKif18a n=540, siCENP-N n=422, siSka1 n=395, siTACC2 n=485, siNsl1 n=400, siSka3 n=383, siZw10 n=404, siNdc80 n=440, siAurora A n=388, siCLERC n=263, siNuf2 n=428, siCENP-I n=389, siAurora B n=499, siDsn1 n=688, siCENP-E n=346, siSpc24 n=418, siBubR1 n=387, siSpc25 n=425, siHURP_oligo1 n=296, siHURP_oligo2 n=200, siKNL1 n=413; pool of 2 independent experiments for each siRNA1 oligonucleotide per condition, with the exception of Aurora A and CLERC in which only 1 experiment for the second siRNA1 oligonucleotide was performed. All independent experiments were pooled].

2.1.2.5. Micronuclei formation from misaligned chromosomes is a frequent outcome in a cancer cell model of chromosomal instability, but not in near-diploid non-transformed cells

Next, we set out to investigate the origin of micronuclei that form spontaneously during cell division in RPE-1 and chromosomally unstable U2OS cells (Bakhoum et al., 2009a). To visualize the entire chromosome set and spindle microtubules, these cell lines were engineered to stably express Histone H2B-GFP and mRFP-α-tubulin and were inspected by 4D live-cell spinning-disk confocal microscopy, with a temporal resolution between 30 sec and 2 min (Figure 2.14a, b, contribution of Bernardo Orr). In parallel, we promoted chromosome missegregation by performing either CENP-E depletion or a monastrol treatment and washout. Unperturbed RPE-1 cells showed only a residual (1.2%) formation of micronuclei after cell division and none derived from a misaligned chromosome (Figure 2.14c). CENP-E depletion or monastrol treatment/washout in RPE-1 cells significantly increased the frequency of micronuclei formation (3.2% and 4.2%, respectively), most of which (71% and 89%, respectively) derived from anaphase lagging chromosomes, and only very few derived from a misaligned chromosome (2.1% and 0.95% of the cells, respectively) (Figure 2.14c), further demonstrating a robust chromosome alignment capacity in normal cells. This scenario was strikingly different even in unperturbed U2OS cells, which formed micronuclei in 5.8% of the cases, of which 53% derived from anaphase lagging chromosomes, 14% from DNA bridges and 33% from misaligned chromosomes (Figure 2.14c). Monastrol treatment/washout only slightly increased (without statistical significance) the percentage of dividing U2OS cells that formed micronuclei, which in this case derived mostly from anaphase lagging chromosomes (80%), likely due to an increase in merotelic attachments (Cimini et al., 2003). In contrast, CENP-E depletion in U2OS cells significantly increased the percentage of dividing U2OS cells that formed micronuclei (17.2%), of which 62% derived from anaphase lagging chromosomes, 21% from DNA bridges and 17% from misaligned chromosomes (Figure 2.14c).

We next determined the relative probabilities of micronuclei formation from lagging chromosomes, DNA bridges and misaligned chromosomes scored in both RPE-1 and U2OS cells, with and without CENP-E, as well as with and without monastrol treatment/washout (Figure 2.14d) (for absolute probabilities see Figure 2.15). In line with our previous observations in HeLa cells (Figure 2.12 and Figure 2.13), this analysis revealed that misaligned chromosomes have the highest absolute and relative probability of resulting in micronuclei in unperturbed chromosomally unstable U2OS cells (0.63 and 0.80, respectively) (Figure 2.14d and Figure 2.15). These probabilities were significantly higher than what would be expected if all missegregation events were equally likely to cause

micronuclei ($p<0.0001$; Chi-square test). In agreement with our findings in HeLa cells, both CENP-E depletion and monastrol treatment/washout reverted this tendency in U2OS cells, likely due to a significant increase in the frequency of anaphase lagging chromosomes (Figure 2.14c and Figure 2.15) (Cimini et al., 2003). Most striking, and in sharp contrast to unperturbed HeLa and U2OS cells, unperturbed RPE-1 cells always entered anaphase after completing chromosome alignment and, consequently, no micronuclei from misaligned chromosomes were ever detected in our recordings (Figure 2.14d and Figure 2.15). Likewise, human primary fibroblasts were previously shown to never enter anaphase with misaligned chromosomes even after nocodazole treatment and washout, and the resulting lagging chromosomes appear during anaphase after completing chromosome alignment during metaphase (Cimini et al., 2002). We concluded that misaligned chromosomes that form sporadically in unperturbed chromosomally unstable cancer cell models, but not in normal near-diploid cells, have a strong probability to missegregate and result in micronuclei.

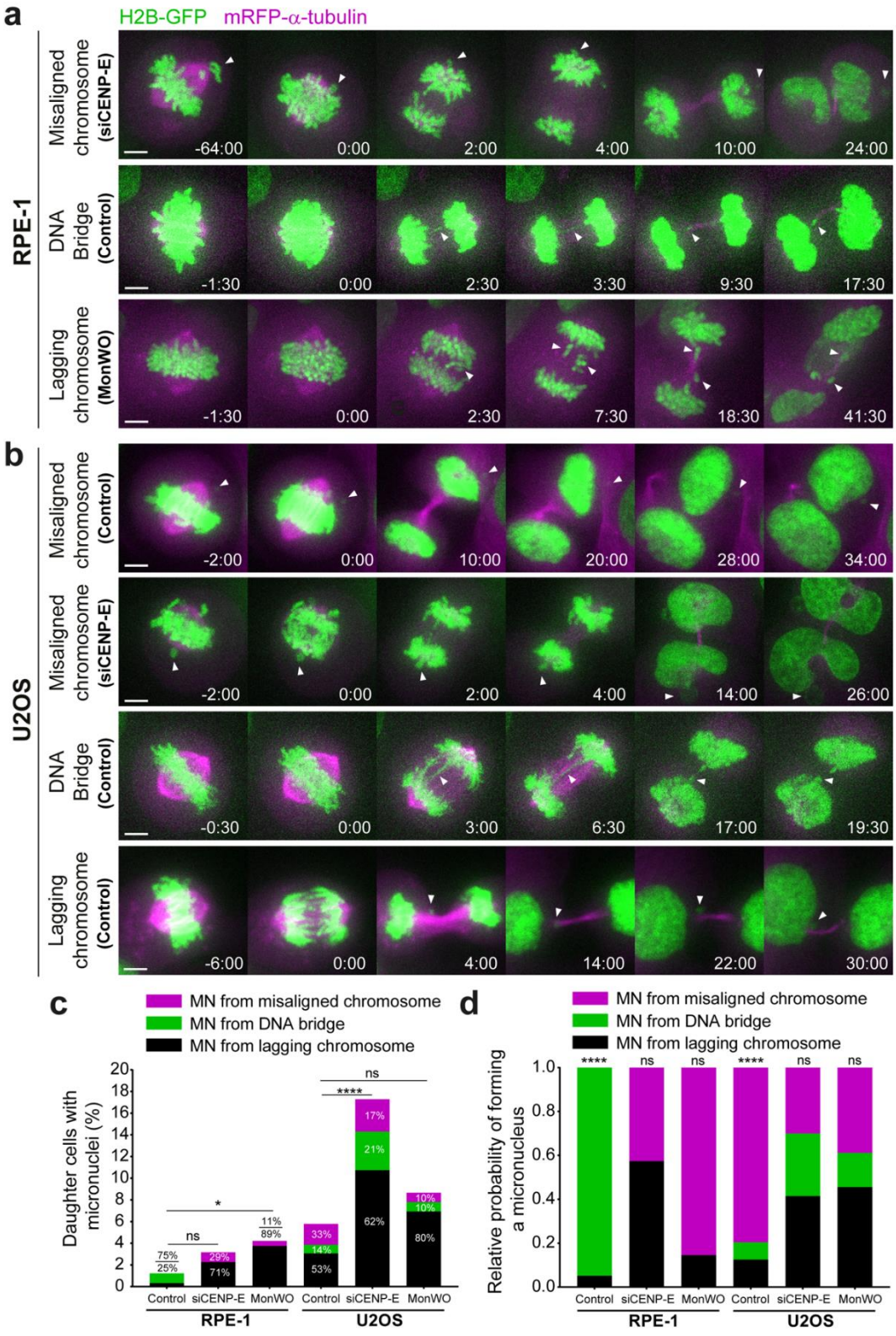

Figure 2.14. Micronuclei formation from misaligned chromosomes is a frequent outcome in a chromosomally unstable cancer cell model, but not in non-transformed cells. a, b) Examples of time-lapse sequences illustrating possible origins of micronuclei in RPE-1 and U2OS cells. Time=min:sec. Time 00:00=anaphase onset. White arrowheads track misaligned chromosomes, DNA bridges or lagging chromosomes until they eventually form micronuclei. Pixels were saturated for optimal visualization of misaligned chromosomes, DNA bridges and lagging chromosomes. Scale bar=5 µm. c) Frequency of RPE-1 and U2OS daughter cells with micronuclei that derived either from

lagging chromosomes (black bars), DNA bridges (green bars) or misaligned chromosomes (magenta bars) in control, siCENP-E and after monastrol treatment/washout (MonWO). [RPE-1 cells: control, n=163; siCENP-E, n=95; MonWO, n=105]. [U2OS cells: control, n=250; siCENP-E, n=81; MonWO, n=49] (Fisher´s exact two-tailed test). d) Relative probability (sum of the 3 independent absolute probabilities normalized to 1) of micronuclei formation from a lagging chromosome (black bars), a DNA bridge (green bars) or a misaligned chromosome (magenta bars) in RPE-1 and U2OS cells in control and after CENP-E depletion or monastrol treatment/washout. [*p≤0.05, **p≤0.01, ***p≤0.001, ****p≤0.0001, ns=no significant difference from what would be expected if all missegregation events were equally likely to cause micronuclei in each experimental condition (Chi-square test)].

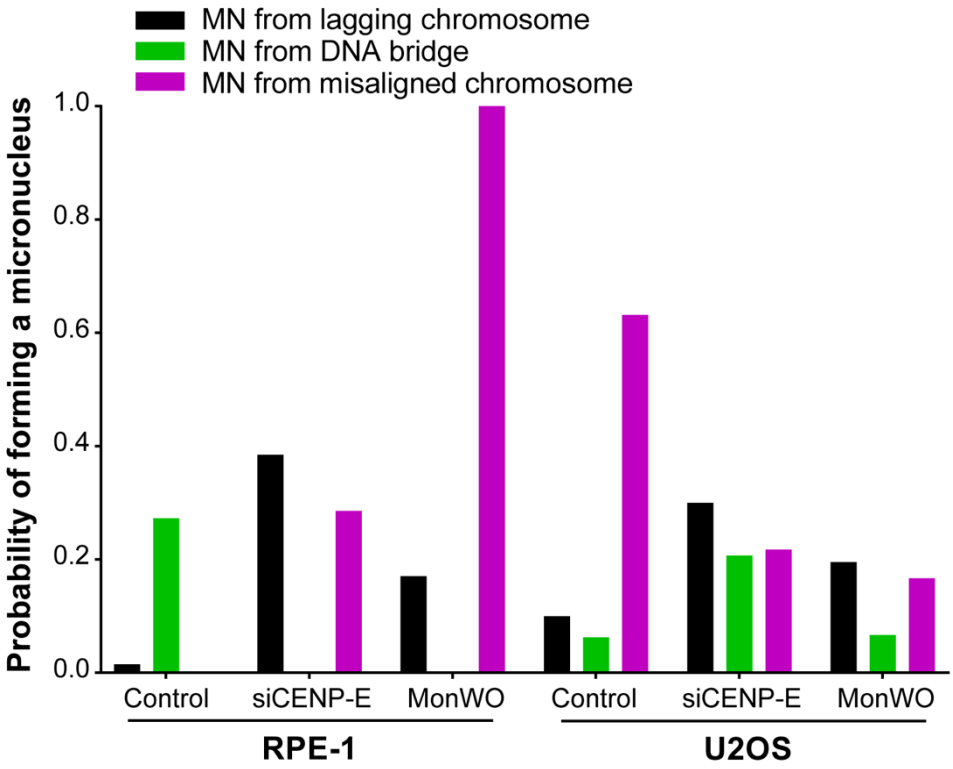

Figure 2.15. Absolute probabilities of forming a micronucleus from misaligned chromosomes, DNA bridges and lagging chromosomes in RPE-1 and U2OS cells. Absolute probabilities of forming a micronucleus of different origins in unperturbed RPE-1 and U2OS cells and after CENP-E depletion (siCENP-E) or monastrol treatment and washout. [RPE-1 cells: control, n=163; siCENP-E, n=95; MonWO, n=105]. [U2OS cells: control, n=250; siCENP-E, n=81; MonWO, n=49].

2.1.2.6. Misaligned chromosomes in chromosomally unstable cancer cells have hyper-stabilized kinetochore-microtubule attachments

Chromosomally unstable cancer cells have hyper-stabilized kinetochore-microtubule attachments and a poor error correction capacity (Bakhoum et al., 2009a; Salimian et al., 2011). To investigate whether increased kinetochore-microtubule attachment stability in chromosomally unstable cancer cells allows misaligned chromosomes to satisfy the SAC, we implemented a protocol that promotes the formation of few misaligned chromosomes after nocodazole treatment and washout (Figure 2.16a) (see Materials and Methods), followed by quantification of fluorescence intensity after a nocodazole shock to completely depolymerize microtubules in fixed cells (Figure 2.16a). Both qualitative and quantitative

analyses revealed that, under these experimental conditions, kinetochore microtubules in chromosomally unstable U2OS cells are more resistant to depolymerization when compared to normal near-diploid RPE-1 cells (Figure 2.16a and b; contribution of Marco Cruz). Measurement of the respective half-life of polymerized tubulin, confirmed ~2-fold increase in U2OS cells relative to RPE1 cells (Figure 2.16b). These results provide an explanation for the inefficient correction of few misaligned chromosomes that eventually satisfy the SAC in a chromosomally unstable cancer cell model and thus may represent major drivers of chromosomal instability and micronuclei formation in human cancers.

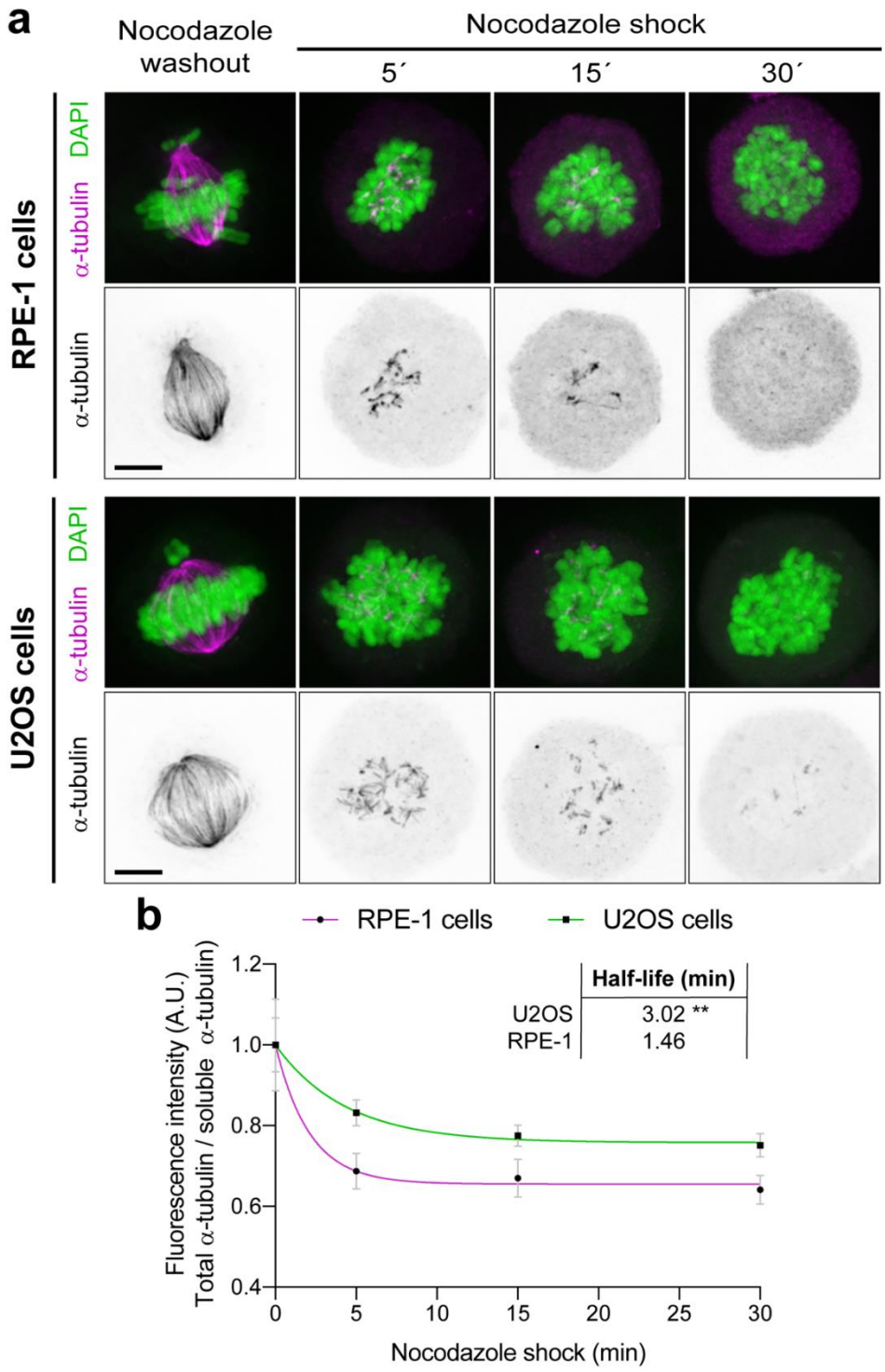

Figure 2.16. Misaligned chromosomes in chromosomally unstable cancer cells have hyper-stabilized kinetochore-microtubule attachments. a) Representative immunofluorescence images of RPE-1 and U2OS cells stained for DNA (green) and α- tubulin (magenta). RPE-1 and U2OS cells upon nocodazole treatment and washout to generate misaligned chromosomes were processed for immunofluorescence microscopy after a subsequent nocodazole shock 5, 15 and 30 min after drug addition. Representative immunofluorescence images of the mitotic spindle at each stage are shown. Images are maximum intensity projections of deconvolves z-stacks. Scale bar = 5 µm. b) Normalized α- tubulin fluorescence intensity at indicated time points in RPE-1 and U2OS cells after nocodazole shock. Fluorescence intensities were normalized to the levels at time = 0. Data represent mear ± s.d., U2OS n=22 cells, from 2 independent experiments. Whole lines show single exponential fitting curve (**p≤0.01, extra sum-of-squares F test).

2.1.3. Discussion

Mitosis is a carefully orchestrated process with the ultimate purpose of equally segregating the genetic material to the daughter cells. To ensure accurate chromosome segregation, chromosomes must align at the spindle equator. Therefore, understanding how human cells respond to chromosome alignment defects remains a fundamental unanswered question with strong clinical implications. Several proteins have been previously identified to play a role in chromosome alignment (see table 1). However, since live-cell imaging was not used in many of these studies, it remains unclear whether it truly reflects a direct role of these proteins in chromosome alignment or in maintenance of chromosome alignment. We overcame this limitation by using high-content live-cell imaging, combined with RNAi, to investigate how human cells respond to chromosome alignment defects of distinct molecular nature. Systematic analysis of 125 different genetic perturbations revealed that entering anaphase with misaligned chromosomes is a frequent outcome in cancer cells.

It is currently thought that anaphase lagging chromosomes resulting from erroneous merotelic attachments that satisfy the SAC are major drivers of genomic instability in human cancers (Bakhoum and Cantley, 2018; Soto et al., 2019). Although anaphase lagging chromosomes resulting from merotelic attachments rarely missegregate (Cimini et al., 2004; Thompson and Compton, 2011), they may fail to incorporate into the respective daughter nuclei during cell division and result in the formation of micronuclei. Micronuclei were recently implicated as key intermediates of chromothripsis, a series of massive genomic rearrangements that may drive rapid tumor evolution and account for acquired drug resistance and oncogene activation (Crasta et al., 2012; Janssen et al., 2011; Shoshani et al., 2021; Stephens et al., 2011; C.-Z. Zhang et al., 2015). We now show that although most micronuclei derive from anaphase lagging chromosomes, simply because these events occur at a very high frequency in chromosomally unstable cancer cells (Thompson and Compton, 2011), misaligned chromosomes that satisfy the SAC often directly missegregate (i.e. without lagging behind in anaphase) and have the highest probability to form micronuclei, specifically in human cancer cell models (Figure 2.17). This is consistent with recent high-resolution live-cell studies in both cancer and non-cancer human cells that showed that the vast majority of lagging chromosomes have a transient nature and are corrected during anaphase by an Aurora B-dependent mechanism that prevents micronuclei formation (Orr et al., 2021; Sen et al., 2021), and the relatively low frequency of micronuclei formation even after induction of massive chromosome segregation errors by experimental abrogation of the SAC (Cohen-Sharir et al., 2021; Klaasen et al., 2022).

Defects in chromosome alignment are normally avoided by increased Aurora B activity at centromeres of misaligned chromosomes (Maia et al., 2010). However, correction of erroneous attachments underlying some chromosome alignment defects (e.g. syntelic attachments) appears to be less robust in cancer cells that also show overly stabilized kinetochore-microtubule attachments (Bakhoum et al., 2009a; Salimian et al., 2011). Indeed, RPE-1 cells treated with microtubule-targeting drugs at concentrations that stabilize microtubules satisfy the SAC in the presence of misaligned chromosomes, and do so faster under conditions that promote the formation of syntelic attachments (Brito et al., 2008; Klaasen et al., 2022; Yang et al., 2009). In addition to direct missegregation from misaligned chromosomes, late-aligning chromosomes are also more prone to lag behind in anaphase and missegregate at higher frequencies in human cancer cells, or upon SAC inactivation or stabilization of incorrect kinetochore-microtubule attachments in normal cells (Klaasen et al., 2022; Kuniyasu et al., 2018). Together with the fact that normal human near-diploid cells rely on a robust p53-dependent mechanism that limits the proliferation of aneuploid cells (Thompson and Compton, 2010), the present work helps to explain how spontaneous misaligned chromosomes in cancer cells eventually satisfy the SAC and may constitute a direct route to chromosomal instability.

This work also unveils a wide range of genetic perturbations that predispose for these events and might account for the underlying chromosomal and genomic instability commonly observed in human cancers. A paramount case is the perturbation of CENP-E function that has been linked to tumorigenesis in vivo (Weaver et al., 2007). Previous studies have shown that ~40% of CENP-E-depleted HeLa cells enter anaphase with misaligned chromosomes (Maia et al., 2010; Tanudji et al., 2004). Fixed cell analysis revealed that these misaligned chromosomes accumulate Mad2, but micronuclei generated from CENP-E-depleted cells did not, suggesting that misaligned chromosomes satisfy the SAC (Maia et al., 2010). Although suggestive, the origin of the scored micronuclei was not determined in these fixed-cell experiments, and so it remains possible that the scored micronuclei did not derive directly from misaligned chromosomes (they may alternatively derive from anaphase lagging chromosomes, see Figure 2.12b,c), and cells with misaligned chromosomes entered anaphase without satisfying the SAC. Indeed, previous experiments in fixed CENP-E KO MEFs revealed continued localization of SAC proteins at misaligned chromosomes seen in anaphase cells, suggesting ongoing SAC signaling (Weaver et al., 2003). Our live-cell imaging of Mad2-GFP upon CENP-E depletion in HeLa cells, supported by quantitative analyses in fixed cells soon after anaphase onset, show that Mad1/Mad2 dissociate from kinetochores of misaligned chromosomes in cells that entered anaphase, suggesting SAC satisfaction. Moreover, live-cell imaging revealed a normal degradation kinetics of Cyclin B1 in CENP-E-depleted or unrelated TACC3-depleted cells that entered

anaphase with misaligned chromosomes. This contrasts with the pattern observed upon mitotic slippage, in which mitotic cells that cannot satisfy the SAC exit mitosis with high Mad1/Mad2 levels at kinetochores and after very slow and prolonged degradation of Cyclin B1 (Brito et al., 2008; Canman et al., 2002; Gascoigne and Taylor, 2008). Combined, these data provide direct evidence that, at least under certain conditions, cancer cells with misaligned chromosomes may enter anaphase after SAC satisfaction and have a high risk of forming micronuclei (Figure 2.17). In line with these findings, recent experiments in which CENP-E activity was inhibited in human RPE-1 cells suggest that endomembrane "ensheathing" of misaligned chromosomes may facilitate micronuclei formation and delay SAC satisfaction (Ferrandiz et al., 2022).

Our systematic analysis of more than 100 different molecular perturbations further indicates that entering anaphase with misaligned chromosomes might be a frequent outcome in cancer cells. In particular, perturbations such as CENP-E or Kif18a depletion were largely compatible with cell viability, despite the high incidence of cells that entered anaphase in the presence of misaligned chromosomes. This contrasts with more drastic scenarios that result from perturbation of end-on kinetochore-microtubule attachments (e.g. depletion of KMN components) that often result in massive chromosome missegregation and cell death. Noteworthy, while the loss of Kif18a, which causes asynchronous segregation of misaligned chromosomes due to loss of interchromosome compaction during anaphase, does not promote chromosomal instability and tumorigenesis (Fonseca et al., 2019; Sepaniac et al., 2021), the loss of CENP-E that typically originates one or few pole-proximal chromosomes directly leads to aneuploidy and the spontaneous formation of lymphomas and lung tumors in aged animals (Weaver et al., 2007, 2003). These data suggest that the origin and properties of the resulting micronuclei is genetically determined and might have implications for the propensity to undergo massive chromosome rearrangements, such as those commonly observed in chromothripsis.

Future research will be important to understand how is nuclear envelope reformation (NER) on enduring misaligned chromosomes is regulated relative to the main chromosomal masses. Previous studies demonstrated that delaying NER allow anaphase lagging chromosomes to reintegrate in the main nuclear mass, prevents micronuclei formation and consequently preserves genomic stability (Afonso et al., 2014; Liu et al., 2018; Orr et al., 2021). An outstanding question is whether a delay in NER also occurs in enduring misaligned chromosomes that persist during anaphase.

Moreover, further research will be required to understand the impact of micronuclei of different origins on chromosomal stability, and consequently on tumor progression. Several lines of evidence indicate that micronuclei originated from lagging chromosomes and chromosome bridges show defects in nuclear lamina assembly and are highly prone to

spontaneous rupture, leading to DNA damage (Crasta et al., 2012; Hatch et al., 2013; Liu et al., 2018). Importantly, there is a direct link between rupture of micronuclear envelope and the activation of the innate immune response through the cGAS-STING pathway (Harding et al., 2017; Mackenzie et al., 2017). Additionally, recent studies revealed that activation of the cGAS-STING pathway by cellular DNA from tumors influences the development of cancer (Bakhoum et al., 2018; Chen et al., 2016; Santaguida et al., 2017). The defective stability of nuclear envelopes and consequently its role in promoting chromosomal instability in micronuclei derived from misaligned chromosomes remain a matter of debate. Micronuclei derived from segregation errors associated with Kif18a loss of function appear to form stable nuclear envelopes (Fonseca et al., 2019; Sepaniac et al., 2021). In agreement, another study suggested that experimentally induced misaligned chromosomes recruited both core and non-core nuclear envelope proteins, unlike anaphase lagging chromosomes (Liu et al., 2018). Moreover, a recent study showed that Mps1 inhibition produced higher rates of cGAS positive cells comparative to CENP-E inhibition (Tucker et al., 2023), suggesting that lagging chromosomes can elicit a heightened cGAS response relative to misaligned chromosomes. In stark contrast, micronuclei derived from misaligned chromosomes after CENP-E perturbation were recently suggested to activate the cGAS-STING pathway in cancer cells (Hakozaki et al., 2021), thus raising the possibility that these micronuclei also have defects in nuclear envelope assembly. However, since prolonged mitotic arrest causes DNA damage (Dalton et al., 2007; Orth et al., 2012; Quignon et al., 2007), and considering that most micronuclei derived from misaligned chromosomes after CENP-E perturbation originated after a mitotic delay, it is important to demonstrate that activation of the cGAS-STING pathway in these cells is independent of DNA damage caused by a prolonged mitotic delay. Thus, cellular response to micronuclei might depend on their relative origin. Overall, our findings incite for an in-depth characterization of the properties and fate of micronuclei of different origins, while evaluating their respective potential to drive and/or sustain cell transformation.

In the future, it will be important to investigate whether micronuclei originated from misaligned chromosomes are able to properly import key proteins that are required for the integrity of the nuclear envelope. For this purpose, it is necessary to evaluate whether core and non-core nuclear envelope proteins are recruited to misaligned chromosomes at equivalent levels than to the main chromosome mass (e.g., using a high-resolution live-cell imaging microscopy assay to image cells labeled with histone and core and non-core nuclear envelope proteins). In addition, micronuclei origined from misaligned chromosomes can be photoconverted and then perform an immunofluorescence to evaluate the presence of different nuclear envelope proteins in these micronuclei in interphase. Future studies are essential to understand if micronuclei origined from misaligned chromosomes activate the

cGAS/STING pathway, and also if the levels of cGAS activation might be different in micronuclei from different origins (e.g., using high resolution live-cell imaging in cells expressing cGAS). In parallel, it will be interesting to compare the recruitment of nuclear envelope proteins, as well as cGAS activation, in spontaneously formed micronuclei from misaligned chromosomes with micronuclei origined after experimental perturbations that induce alignment defects. Finally, in the future, it will be important to further evaluate our model by examining more cell types without any experimental perturbation and preferably including primary cells.

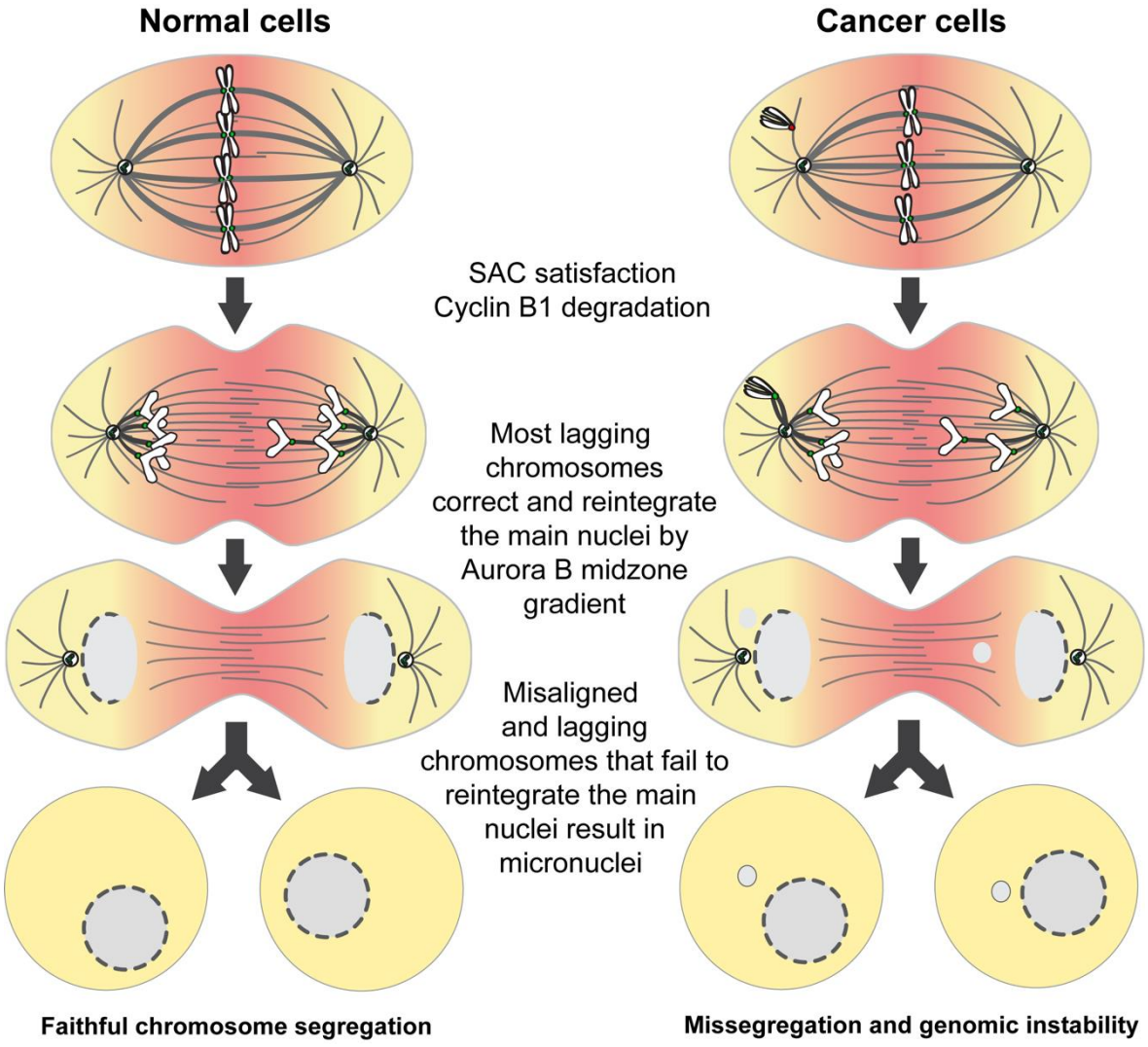

Figure 2.17. Proposed model of micronuclei formation in both cancer and non-cancer human cells. The vast majority of anaphase lagging chromosomes are corrected by a midzone-based Aurora B phosphorylation gradient (orange/yellow in the cytoplasm) both in cancer and non-cancer cells. Misaligned chromosomes that satisfy the spindle assembly checkpoint have the highest probability of resulting in micronuclei, specifically in chromosomally unstable cancer cells.

2.1.4. MATERIALS AND METHODS

2.1.4.1. Cell Lines

All cell lines were cultured at 37ºC in 5% CO_2 atmosphere in Dulbecco´s modified medium (DMEM, Gibco™, Thermofisher) containing 10% fetal bovine serum (FBS, Gibco™, Thermofisher). HeLa H2B-GFP/α-tubulin-mRFP, HeLa Cyclin B1-Venus/H2B-mRFP, RPE-1 H2B-GFP/mCherry-α-tubulin and RPE-1 Cyclin B1-Venus/H2B-mRFP cells were generated by lentiviral transduction. HeLa parental was kindly provided by Y. Mimori-Kiyosue (RIKEN, Japan). U2OS parental and H2B-GFP/mCherry-α-tubulin were kindly provided by S. Geley (Innsbruck Medical University, Innsbruck, Austria). hTERT-RPE-1 (RPE-1) parental (ATCC® CRL-400™) was kindly provided by Ben Black (U. Pennsylvania, PA, USA). HeLa Mad2-GFP cells were previously described (Schweizer et al., 2013). HeLa and RPE-1 cells expressing Cyclin B1-Venus were kindly provided by J. Pines (Cancer Research Institute, London, UK).

2.1.4.2. High-content live-cell imaging RNAi screen

All siRNA sequences used were either a commercial predesigned siRNA from Sigma-Aldrich (MISSION siRNA) or Dharmacon, many of which were previously validated by other published studies (see Table 2). For each protein, depletion efficiency was first optimized after preliminary phenotypic analysis between 24-96 h upon siRNA transfection (for specific conditions see Table 2) and confirmed by western blotting whenever antibodies against specific proteins were available (Figure 2.2). For few proteins whose role in chromosome congression remained unclear at the mechanistic level or were followed-up in subsequent experiments, a second siRNA was used to rule-out possible off-targeting effects. This led to the identification of six proteins (Shp2, GAK, CEP72, CEP90, CENP-H and Mis12), where no discernable congression phenotype was observed with the second siRNA, despite a clear reduction in protein levels with both siRNA sequences (Figure 2.4), or a clear congression phenotype was observed despite no evident reduction in protein levels with two siRNA sequences, suggesting that they are off-targets. A second siRNA was also used to validate all selected conditions that were followed-up to determine the origin of micronuclei (Table 2). Whenever the results obtained with the second siRNA oligonucleotide were consistent with those obtained with the original siRNA oligonucleotide, the data from both experiments was pooled for statistical analysis. All exceptions (Arp1, Haspin, CENP-F, HAUS4 and CENP-T) that could not be validated by western blotting due

to the poor quality of the antibodies we had access to are clearly marked in the respective figures and main text, and were not followed-up in subsequent experiments. Treatment with scramble siRNA was undistinguishable from mock transfection (Lipofectamine only) and was therefore used as a negative control throughout the manuscript. A total of 125 proteins were analyzed in this study (Table 1). For high-content live-cell imaging, Hela cells stably expressing H2B-GFP/α-tubulin-mRFP were plated onto 96-well plate in DMEM supplemented with 5% FBS and after 1 h transfected with siRNA oligonucleotides (Table 2) at a final concentration of 50 nM. Transfections were performed using Lipofectamine RNAiMAX in Opti-MEM medium (both from Thermo Fisher Scientific) according to the manufacturer's instructions. Transfection medium was replaced with complete medium after 6 h. For time-lapse microscopy acquisition, cell culture medium was changed to DMEM without phenol red supplemented with 10% FBS 6-12 h before acquisition. Cells were imaged for 72 h in an IN CELL Analyzer 2000 microscope (GE Healthcare, Chicago, IL, USA) equipped with temperature and CO_2 controller, using a Nikon 20x/0.45 NA Plan Fluor objective according to manufacturer instructions. For some validation experiments with a second siRNA oligonucleotide a Nikon ECLIPSE TI microscope (Nikon, Japan) equipped with temperature and CO_2 controller, using a Nikon 20x/0.45 NA Plan Fluor objective according to the manufacturer's instructions, using 24-well plates. Single planes were acquired every 10 min for approximately 72 h. Images were processed using ImageJ software. Long-term recordings of HeLa Cyclin B1-venus treated with nocodazole and MG132 were also performed under similar conditions using the same IN CELL Analyzer 2000 microscope system, imaged every 15 min for 13 h.

2.1.4.3. RNAi Experiments

For high-resolution live cell imaging and immunofluorescence analysis of CENP-E depletion (siCENP-E), cells were plated at 50-60% confluence onto 22 x 22 mm No. 1.5 glass coverslips in DMEM supplemented with 5% of FBS. RNAi transfection was performed using Lipofectamine™ RNAiMAX reagent (Thermofisher) with 20 nM of siRNA against human CENP-E (see siRNA sequence in Table 2), diluted in serum-free media (Opti-MEM™, Thermofisher). Depletion of CENP-E was maximal at 24 h after siRNA transfection and all of the analysis was performed at 24 h.

2.1.4.4. Drug treatments

Microtubule depolymerization was induced by nocodazole (Sigma-Aldrich) at 1 µM. To inhibit the proteasome, induce a metaphase arrest, and prevent exit due to a compromised SAC, cells were treated with 5 µM MG132 (EMD Millipore). To promote chromosome missegregation, a monastrol washout assay was performed. Briefly, cells were incubated during 8-10 h with 100 µM monastrol. After this period, monastrol was washed twice with warm PBS followed by washing with warm fresh medium and entry in anaphase was monitored under the microscope.

2.1.4.5. High-resolution time-lapse microscopy

For high-resolution time-lapse microscopy, cells were plated onto 22 x 22 mm No. 1.5 glass coverslips (Corning) and cell culture medium was changed to phenol-red-free DMEM CO_2-independent medium (Invitrogen) supplemented with 10% FBS 6-12 h before mounting. Coverslips were mounted onto 35-mm magnetic chambers (14 mm, no. 1.5, MaTek corporation) immediately before imaging. Time-lapse imaging was performed in a heated chamber (37ºC) using a 100x oil-immersion 1.40 NA Plan-Apochromatic objective mounted on an inverted microscope (Eclipse TE2000U; Nikon) equipped with a CSU-X1 spinning-disk confocal head (Yokogawa Corporation of America) controlled by NIS-Elements software and with three laser lines (488nm, 561nm, and 647 nm). Images were detected with a iXonEM+ EM-CCD camera (Andor Technology). Images of U2OS and RPE-1 expressing H2B-GFP, mCherry-α-tubulin were collected every 2 minutes or 30 seconds: 9 x 2 µm z-stacks spanning a total volume of 16 µm. For imaging of HeLa Mad2-GFP and HeLa and RPE-1 expressing Cyclin-B1-Venus/H2B-mRFP eleven 1-µm-separated z-planes covering the entire volume of the mitotic spindle were collected every 2 min. All displayed images represent maximum-intensity projections of Z-stacks, analysed with the open source image analysis software ImageJ.

2.1.4.6. Immunofluorescence microscopy

For immunofluorescence processing, cells were fixed with 4% Paraformaldehyde (Electron Microscopy Sciences) for 10 min followed by extraction with 0.3% Triton X-100 in PBS (Sigma-Aldrich) for 10 min. After blocking with 10% FBS in PBS with 0.1% Triton X-100, all primary antibodies were incubated at 4ºC overnight. Then, the cells were washed with PBS containing 0.1% Triton X-100 and incubated with the respective secondary

antibodies for 1 h at room temperature. Primary antibodies used were: mouse anti-Mad1 (1:500; Merck Millipore); mouse anti α-tubulin (1:2000; Sigma); rabbit anti-β-tubulin (1:2000; Abcam); anti-guinea pig CENP-C (1:1000; MBL International). Secondary antibodies used were Alexa Fluor 488, Alexa Fluor 568 and Alexa Fluor 647 (1:1000; Themofisher). DNA was counterstained with 1 µg/mL DAPI (4',6'-diamino-2-fenil-indol; Sigma-Aldrich) and mounted onto glass slides with 20 mM Tris pH8, 0.5 N-propyl gallate and 90% glycerol. Images were acquired using an AxioImager Z1 (63x, Plan oil differential interference contract objective lens, 1.46 NA; from Carl Zeiss), coupled with a CCD camera (ORCA-R2; Hamamatsu Photonics) and the Zen software (Carl Zeiss). Blind deconvolution of 3D image datasets was performed using Autoquant X software (Media Cybernetics).

2.1.4.7. Western Blotting

Cell extracts were collected after trypsinization and centrifuged at 1200 rpm for 5 min, washed and re-suspended in Lysis Buffer (NP-40, 20 nM HEPES/KOH pH 7.9 ; 1 mM EDTA pH 8; 1 mM EGTA; 150 mM NaCl; 0.5% NP40; 10% glycerol, 1:50 protease inhibitor; 1:100 Phenylmethylsulfonyl fluoride). The samples were then flash frozen in liquid nitrogen and kept on ice for 30 min. After centrifugation at 14000 rpm for 20 min at 4ºC the supernatant was collected and protein concentration determined by the Bradford protein assay (Bio-Rad). Fifty micrograms of total extract were then loaded in SDS-polyacrylamide gels and transferred onto nitrocellulose membranes for western blot analysis. The membranes were blocked with 5% milk in TBS with 0.1% Tween-20 (TBS-T) at room temperature during 1 h, and all primary antibodies were incubated at 4ºC overnight. After three washes in TBS-T the membranes were incubated with the secondary antibody for 1 h at room temperature. The membranes were washed in the same conditions than previously and the detection was performed with Clarity Western ECL Substrate (Bio-Rad). The following antibodies were used for western blot: mouse anti-Hec1 (9GA) (1:500; Abcam), mouse anti-Dsn1 (1:1000; a gift from Andrea Musacchio, MPI, Dortmund, Germany), rabbit anti-CENP-E (1:250; Abcam), mouse anti-Aim1 (1:1000; BD Bioscience), mouse anti-ATRX (1:1000; Santa Cruz Biotechnology), rabbit anti-CEP72 (1:1000; Novus Biologicals), mouse anti-GAK (1:500; R&D Systems), rabbit anti- WDHD1/And-1 (1:1000; Novus Biologicals), rabbit anti-Aurora-A (1:1000; Novus Biologicals), rabbit anti-HURP (1:500, a gift from Patrick Meraldi), mouse anti-INCENP (1:500; Santa Cruz Biotechnology), rabbit anti-LRRCC1/CLERC (1:1000; Abcam), mouse anti-Sgo-1 (F-8) (1:1000; Santa Cruz Biotechnology), rabbit anti-DHC (1:500; ThermoFisher Scientific), mouse anti-Nde1 (1:1000; Abnova), sheep anti-Bub1 (1:1000; a gift from Stephen Taylor); rabbit anti-Septin-

2 (1:500; Novus Biologicals), rabbit anti-CEP90/PIBF1 (1:1000; Novus Biologicals), mouse anti-Ska2 (1:1000; Santa Cruz Biotechnology), mouse anti-4.1r (B-11) (1:1000; Santa Cruz Biotechnology), rabbit anti-Astrin (N-terminal) (1:500; a gift from Duane Compton), rabbit anti-Kif4a (1:1000; ThermoFisher Scientific), rat anti-CLASP1 (1:50; Maffini et al 2009), rat anti-CLASP2 (1:50; Maffini et al 2009), rabbit anti-BubR1 (1:1000; Abcam), rabbit anti-SHP2 (1:1000; Abcam), rabbit anti-survivin (1:1000; Novus Biologicals), mouse anti-Ska3 (1:500; Santa Cruz Biotechnology), rabbit anti-Mis12 (1:1000, a gift from Claudio Sunkel), rabbit anti-Kif18a (1:1000; Bethyl Laboratories), rabbit anti-KNL1 (1:1000; Novus Biologicals), rabbit anti-Nsl1 (1:500, Novus Biologicals), rabbit anti-Ska1 (1:500; a gift from Patrick Meraldi), goat anti-TACC3 (1:1000; Novus Biologicals), rabbit anti-Zw10 (1:1500; Novus Biologicals), rabbit anti-CENP-I (1:250; a gift from Patrick Meraldi), rabbit anti-CENP-H (1:500; Novus Biologicals), rabbit anti-CENP-N (1:500; Novus Biologicals), rabbit anti-CLERC (1:500, Abcam), mouse anti-GAPDH (1:40000; Proteintech), rabbit anti-vinculin (1:1000;ThermoFisher Sientific), mouse anti-α-tubulin (clone B-512; 1:5000; Sigma-Aldrich) were used as primary antibodies, and anti-mouse-HRP, anti-rabbit-HRP, anti-sheep-HRP, anti-rat-HRP and anti-goat-HRP were used as secondary antibodies (1:5000; Jackson ImmunoResearch Laboratories, Inc.).

2.1.4.8. Quantification of mitotic errors

Mitotic errors were tracked and quantified manually through the assessment of H2B localization in single plane images. Mitotic errors were divided into 3 main classes: lagging chromosomes, DNA bridges or misaligned chromosomes and these were discriminated according to location and morphology associated with H2B localization. Lagging chromosomes retained normal DNA condensation and emerged at different stages during anaphase. Any H2B-positive material between the two chromosomes masses, but distinguishably separated from them, was counted as lagging chromosomes. DNA bridges were characterized by stretches of DNA that connected both daughter nuclei and often displayed aberrant DNA condensation as judged by H2B localization. Misaligned chromosomes were characterized by any H2B-positive material that remained near the spindle pole or clearly outside the metaphase plate. To determine micronuclei origin, fully formed micronuclei were backtracked to reveal whether these originated from lagging chromosomes, DNA bridges or misaligned chromosomes. The absolute probability of micronucleus formation from a lagging chromosome was determined by the ratio between the number of daughter cells with micronuclei derived from lagging chromosomes and the total number of cells with lagging chromosomes. The absolute probability of micronucleus

formation from a DNA bridge was determined by the ratio between the number of daughter cells with micronuclei derived from DNA bridges and the total number of cells with DNA bridges. The absolute probability of micronucleus formation from a misaligned chromosome was determined by the ratio between the number of daughter cells with micronuclei derived from misaligned chromosomes and the total number of cells that exit mitosis with a misaligned chromosome. For the relative probabilities, the sum of the 3 independent absolute probability values was normalized to 1.

2.1.4.9. Quantitative image analysis

For quantification of Mad1 fluorescence intensity, images were analysed using ImageJ. Briefly, individual kinetochores were identified by CENP-C staining and marked by a region of interest (ROI). The average fluorescence intensity of signals of Mad1 at kinetochores was measured on the focused z plan. The background signal was measured within a neighbouring region and was subtracted from the measured fluorescence intensity the region of interest. Fluorescence intensity measurements were normalized to the CENP-C signals. Mad1 negative values were considered zero, since resulted from the high background fluorescence observed in early anaphase cells. Approximately 90 kinetochore pairs from 9 cells were analysed for control prometaphase cells, 72 kinetochore pairs from 14 cells for prometaphase in CENP-E depleted cells and 19 kinetochore pairs from 14 cells for early anaphase in CENP-E depleted cells. The fluorescence levels of Cyclin B1 in HeLa cells treated with nocodazole were measured using the IN Cell Developer Toolbox software (GE Healthcare). After background subtraction, fluorescence intensities were normalized to the level at time = 0 and represented as a function of time. The levels of Cyclin B1 in siScramble, siCENP-E, siTACC3 HeLa cells and siScramble, siCENP-E RPE-1 were measured using ImageJ. A small square region of interest (ROI) was defined, and Cyclin B1 fluorescence intensity measured, throughout time in the cell. The same ROI was used to measure the background outside the region of interest. All fluorescence intensity values were then background corrected and the values were normalized at 14 or 8 minutes before anaphase onset in HeLa and RPE-1 cells, respectively. The microtubule depolymerization rate after nocodazole treatment in U2OS and RPE-1 cells was determined by the proportion of total and soluble α-tubulin levels. The total α-tubulin intensity was measured by drawing a larger oval shaped region of interest (ROI) contained the entire cell in sum-projected images (ImageJ). The soluble α-tubulin levels were determined by drawing five smaller oval shaped ROI outside the chromosome region and the average of these values were

calculated in sum-projected images. The fluorescence intensities were normalized to the level at time = 0 and represented as a function of time.

2.1.4.10. Statistical analysis

All results presented in this thesis were obtained from pooling data from at least 2 independent experiments unless otherwise stated. Sample sizes and statistical tests used for each experiment are indicated in the respective figure legends. Quantifications of mitotic errors (i.e. cell death and micronuclei) were analyzed using the Fisher's exact two-tailed test. Correlations were calculated using two-tailed Pearson´s correlation coefficients. When only two experimental groups were compared, we used either a parametric t test or a nonparametric Mann-Whitney test. Distribution normalities were assessed using the D´Agostino-Pearson omnibus test. For the comparison of the single exponential fitting curve extra sum-of square F test was used. Probabilities were calculated using Chi-squared test. For each graph, where applicable, ns= non-significant, *p≤0.05, **p≤0.01 ***p≤0.001 and ****p≤0.0001, unless stated otherwise. In all plots error bars represent standard deviation. All statistical analysis was performed using GraphPad Prism V7 (GraphPad Software, Inc).

2.1.5. Supplemental Material

Table 1. Overview of the genes associated with chromosome congression defects analyzed in the present study.

Protein name	Subcelular localization	Chromosome congression defects described previously	Number of cells analyzed	Validation of depletion by WB	References
Nuf2_oligo1	Kinetochore	Prometaphase arrest; mitotic death	310 cells from 2 independent experiments	yes	(DeLuca et al., 2005, 2002; Sundin et al., 2011)
Nuf2_oligo2			224 cells from 2 independent experiments	yes	
Beclin-1	kinetochore	Misaligned chromosomes; prometaphase arrest; mitotic death;	374 cells from 2 independent experiments	no	(Frémont et al., 2013)
CLIP-170	Kinetochore; mitotic spindle	Misaligned chromosomes; prometaphase arrest	311 cells from 2 independent experiments	no	(Amin et al., 2015; Tanenbaum et al., 2006)

ATRX_oligo1	Pericentromeric heterochromatin	Misaligned chromosomes; prometaphase arrest; abnormal nuclear morphology (lobulated nuclei and intranuclear DNA bridges); chromosome segregation defects (lagging chromosomes and chromosome bridges)	392 cells from 2 independent experiments	yes	(Ritchie et al., 2008)
ATRX_oligo2	Pericentromeric heterochromatin	Misaligned chromosomes; prometaphase arrest; abnormal nuclear morphology (lobulated nuclei and intranuclear DNA bridges); chromosome segregation defects (lagging chromosomes and chromosome bridges)	400 cells from 2 independent experiments	yes	
SPICE	Mitotic spindle; centrioles	Misaligned chromosomes; multipolar spindles	504 cells from 2 independent experiments	no	(Archinti et al., 2010; Deretic et al., 2019)
CHICA	Mitotic spindle	Misaligned chromosomes, mitotic delay	380 cells from 2 independent experiments	no	(Dunsch et al., 2012; Santamaria et al., 2008)
CDCA4		Multipolar spindle	154 cells from 2 independent experiments	no	
Kif2a_oligo1	Spindle poles	Partial knockdown of Kif2a accumulated cells with misaligned chromosomes; prometaphase delay; monopolar spindles	600 cells from 3 independent experiments	yes	(Ganem and Compton, 2004; Jang et al., 2008)
Kif2a_oligo2	Spindle poles		600 cells from 3 independent experiments	yes	(Ganem and Compton, 2004)

HIP1r	Mitotic spindle	Misaligned chromosomes; mitotic delay	200 cells from 2 independent experiments	no	(Park, 2010)
Nucleophosmin (NPM1)	Chromosome periphery	Abnormal nuclear shape, tetraploid micronuclei formation; lost proliferation ability; Misaligned chromosomes; disorganized spindles; mitotic delay	329 cells from 3 independent experiments	no	(Amin et al., 2008)
CENP-F/mitosin	kinetochore	Misaligned chromosomes; mitotic delay; aberrant spindle morphology, cell death	398 cells from 2 independent experiments	no	(Holt et al., 2005; Yang et al., 2005)
NudC	kinetochore	Misaligned chromosomes; prometaphase delay; Chromosome segregation defects (lagging chromosomes)	338 cells from 2 independent experiments	no	(Chuang et al., 2013; Nishino et al., 2006)
RRS1 (Regulator of Ribosome Synthesis 1)	Chromosome periphery	Misaligned chromosomes; prometaphase delay	397 cells from 2 independent experiments	no	(Gambe et al., 2009)
KIBRA	ND	Misaligned chromosomes; aberrant spindle morphology; Chromosome segregation defects (lagging chromosomes)	401 cells from 2 independent experiments	no	(L. Zhang et al., 2012)
Nucleolin	Nucleoli; chromosome periphery	Misaligned chromosomes; prometaphase delay; aberrant spindle morphology	150 cells from 2 independent experiments	no	(Li et al., 2009; Ma et al., 2007)
DDA3_oligo1	Spindle microtubules; kinetochores; midbody	Misaligned chromosomes; prometaphase delay	399 cells from 2 independent experiments	no	(Jang et al., 2011, 2010; Jang and Fang, 2011; Park et al., 2016)
DDA3_oligo2	Spindle microtubules;		383 cells from 2 independent experiments	no	

	kinetochores; midbody				
Bub1_oligo1	Kinetochore	Misaligned chromosomes; prometaphase delay; Chromosome segregation defects (lagging chromosomes)	400 cells from 2 independent experiments	yes	(Johnson et al., 2004; Meraldi and Sorger, 2005; Morrow et al., 2005)
Bub1_oligo2			257 cells from 2 independent experiments	yes	
BubR1_oligo1	Kinetochore	Misaligned chromosomes; Chromosome segregation defects (lagging chromosomes)	620 cells from 3 independent experiments	yes	(Ditchfield et al., 2003a; Lampson and Kapoor, 2005)
BubR1_oligo2			236 cells from 2 independent experiments	yes	
Ska3_oligo1	Kinetochore; mitotic spindle	Misaligned chromosomes, prometaphase delay, metaphase arrest, problems in maintenance of chromosome alignment, cohesion fatigue; cell death	343 cells from 2 independent experiments	yes	(Daum et al., 2009; Gaitanos et al., 2009; Raaijmakers et al., 2009; Sivakumar et al., 2014; Welburn et al., 2009)
Ska3_oligo2	Kinetochore; mitotic spindle		400 cells from 2 independent experiments	yes	
TPX2	Nucleus; spindle pole; spindle	Multipolar spindles; misaligned chromosomes	403 cells from 3 independent experiments	no	(Garrett et al., 2002; Goshima, 2011)
Nup188_oligo1	centrosomes	Misaligned chromosomes, prometaphase delay	500 cells from 3 independent experiments	no	(Itoh et al., 2013)
Nup188_oligo2	centrosomes		272 cells from 2 independent experiments	no	
Kif4a_oligo1	Chromosome arms; spindle midzone	Misaligned chromosomes; mitotic delay; spindle defects; chromosome mis-segregation (lagging chromosomes and	252 cells from 2 independent experiments	yes	(Mazumdar et al., 2004)

		chromosome bridges)			
Kif4a_oligo2	Chromosome arms; spindle midzone		348 cells from 2 independent experiments	yes	
Zw10_oligo1	kinetochore	Misaligned chromosomes; prometaphase delay	899 cells from 5 independent experiments	yes	(Y. Li et al., 2007; Yang et al., 2007)
Zw10_oligo2			217 cells from 2 independent experiments	yes	
CENP-L	kinetochore	Chromosome alignment defects; chromosome mis-segregation (lagging chromosomes)	405 cells from 3 independent experiments	no	(McHedlishvili et al., 2012)
NUSAP1	Central spindle	Aberrant mitotic spindle, chromosome alignment defects; defective chromosome segregation; cytokinesis failure	208 cells from 2 independent experiments	no	(Li et al., 2016; Raemaekers et al., 2003)
SAF-A/hnRNP-U	Spindle microtubules; spindle midzone	Aberrant mitotic spindles; Misaligned chromosomes; exit with misaligned chromosomes; prometaphase delay; cytokinesis failure	375 cells from 2 independent experiments	no	(Ma et al., 2011)
Tastin/TROAP	Mitotic spindles in mitosis; centrosomes in interphase	Mitotic delay; Chromosome alignment defects; aberrant mitotic spindles; multipolar spindles	304 cells from 2 independent experiments	no	(Yang et al., 2008)
Tankyrase-1	Centrosome	Mitotic delay; metaphase delay	566 cells from 3 independent experiments	no	(Chang et al., 2005; Dynek and Smith, 2004)
Ska1_oligo1	Kinetochore; mitotic spindle	Misaligned chromosomes, prometaphase delay, metaphase arrest, problems in maintenance of chromosome alignment, cohesion fatigue; cell death	316 cells from 2 independent experiments	yes	(Auckland et al., 2017; Gaitanos et al., 2009; Hanisch et al., 2006; Sivakumar et al., 2014; Welburn et al., 2009)

Ska1_oligo2			249 cells from 2 independent experiments	yes	
HURP	kinetochore	Misaligned chromosomes; prometaphase delay	296 cells from 2 independent experiments	yes	(Silljé et al., 2006; Wong and Fang, 2006; Ye et al., 2011; Zhang et al., 2018)
Aki1/CC2D1A	centrosome	Multipolar spindles due to spindle pole fragmentation	202 cells from 2 independent experiments	no	(Nakamura et al., 2009)
4.1r	Mature centriole	Misaligned chromosomes; Multipolar spindles; Monopolar spindles	451 cells from 3 independent experiments	yes	(Krauss et al., 2008)
HICE1/HAUS8	Centrosome; mitotic spindle, spindle midzone; midbody	Misaligned chromosomes; mitotic delay; aberrant mitotic spindles; multipolar spindles, spindle pole fragmentation	377 cells from 2 independent experiments	no	(Lawo et al., 2009; Wu et al., 2008)
Ska2	Kinetochore; mitotic spindle	Misaligned chromosomes, prometaphase delay, metaphase arrest, problems in maintenance of chromosome alignment, cohesion fatigue	399 cells from 2 independent experiments	yes	(Gaitanos et al., 2009; Hanisch et al., 2006; Sivakumar et al., 2014)
Kif18a_oligo1	Plus-ends of kMTs	Misaligned chromosomes; prometaphase delay; long mitotic spindle; chromosomes mis-segregation (lagging chromosomes); Micronuclei formation	330 cells from 2 independent experiments	yes	(Fonseca et al., 2019; Huang et al., 2009; X.-S. Liu et al., 2010; Mayr et al., 2007; Stumpff et al., 2012, 2008)
Kif18a_oligo2			236 cells from 2 independent experiments	yes	
TACC3_oligo1	centrosome	Misaligned chromosomes; mitotic delay; disorganized spindles; cell death	360 cells from 3 independent experiments	yes	(Cheeseman et al., 2013; Gergely et al., 2003; Kimura et al., 2013; Lin et al., 2010; Schneider et al., 2007)

TACC3_oligo2			285 cells from 2 independent experiments	yes	
CLERC_Oligo1	Centrosomes	Misaligned chromosomes; multipolar spindles	294 cells from 2 independent experiments	yes	(Muto et al., 2008)
CLERC_Oligo2	Centrosomes		400 cells from 2 independent experiments	yes	
Kizuna	Mature centriole; pericentriolar satellites	Misaligned chromosomes; multipolar spindles; spindle pole fragmentation	358 cells from 2 independent experiments	no	(Oshimori et al., 2006)
ILK	Plasma membrane; focal adhesion; cytosol	Aberrant mitotic spindles, Misaligned chromosomes	300 cells from 3 independent experiments	no	(Fielding et al., 2008)
Kinastrin/SKAP	Spindle pole; Kinetochore	Prometaphase delay; metaphase delay; multipolar spindles; spindle pole fragmentation	355 cells from 2 independent experiments	no	(Dunsch et al., 2011; Fang et al., 2009; Huang et al., 2012; Schmidt et al., 2010)
Ninein	Mature centriole; pericentriolar satellites	Misaligned chromosomes; multipolar spindles	200 cells from 2 independent experiments	no	(Logarinho et al., 2012)
NuMA	Nucleus; spindle pole	Aberrant mitotic spindles, Misaligned chromosomes	188 cells from 2 independent experiments	yes	(Haren et al., 2009; Iwakiri et al., 2013)
Rae1_oligo1	Nuclear pore; spindle pole	Misaligned chromosomes; multipolar spindles; lagging chromosomes;	358 cells from 2 independent experiments	no	(Blower et al., 2005; Wong et al., 2006)
Rae1_oligo2			311 cells from 2 independent experiments	no	
RanBP2_oligo1	Nuclear pore; kinetochore; spindle pole	Misaligned chromosomes; multipolar spindles	400 cells from 2 independent experiments	no	(Joseph et al., 2004)
RanBP2_oligo2			231 cells from 1 experiment	no	
Spindly	Kinetochore; spindle pole	Misaligned chromosomes; prometaphase delay	600 cells from 3 independent experiments	no	(Barisic et al., 2010; Raaijmakers et al., 2013)
STARD9	Daughter centriole	Misaligned chromosomes; mitotic delay; multipolar spindles; spindle pole	198 cells from 2 independent experiments	no	(Torres et al., 2011)

		fragmentation; mitotic death			
CAMKIIγ (CAMK2G)	Cytosol	Misaligned chromosomes; multipolar spindles	371 cells from 2 independent experiments	no	(Holmfeldt et al., 2005)
CENP-E_oligo1	Kinetochore	Misaligned chromosomes; prometaphase delay; exit with misaligned chromosomes; die in or after mitosis	259 cells from 3 independent experiments	yes	(Barisic et al., 2014; Maia et al., 2010; Stevens et al., 2011; Tanudji et al., 2004)
CENP-E_oligo2			187 cells from 2 independent experiments	yes	
CHC17 clathrin	Mitotic spindle; centrosome	Chromosome misalignment; mitotic delay; disorganized spindles; multipolar spindles; spindle pole fragmentation	299 cells from 2 independent experiments	no	(Foraker et al., 2012; Lin et al., 2010; Royle et al., 2005)
CEP72_oligo1	centrosome	Misaligned chromosomes; multipolar spindles; spindle pole fragmentation	379 cells from 2 independent experiments	yes	(Oshimori et al., 2009)
CEP72_oligo2	centrosome		170 cells from 2 independent experiments	yes	
CEP90_oligo1	Centrosome; pericentriolar satellites	Misaligned chromosomes; aberrant mitotic spindles; multipolar spindles	471 cells from 3 independent experiments	yes	(Kim and Rhee, 2011)
CEP90_oligo2	Centrosome; pericentriolar satellites		155 cells from 2 independent experiments	yes	
CLASP2b	Centrosome; kinetochore; microtubule plus ends; central spindle	Misaligned chromosomes; prometaphase delay; chromosome mis-segregation (lagging chromosomes and chromosome bridges); multipolar spindles; spindle pole fragmentation	408 cells from 2 independent experiments	yes	(Girão and Maiato, 2020; Logarinho et al., 2012; Mimori-Kiyosue et al., 2005)

CLASP1b	Centrosome; kinetochore; microtubule plus ends; central spindle	Misaligned chromosomes; chromosome mis-segregation (lagging chromosomes and chromosome bridges); multipolar spindles; spindle pole fragmentation	402 cells from 2 independent experiments	yes	(Logarinho et al., 2012; Maiato et al., 2003; Mimori-Kiyosue et al., 2005)
CLASP1+2			300 cells from 2 independent experiments	yes	
Aurora B_oligo1	Centromere; spindle, spindle midzone	Misaligned chromosomes; chromosome mis-segregation; cytokinesis defects	287 cells from 2 independent experiments	yes	(Fuller et al., 2008; Hauf et al., 2003; Hégarat et al., 2011)
Aurora B_oligo2			212 cells from 2 independent experiments	yes	
Astrin_oligo1	Spindle pole; kinetochores	Misaligned chromosomes; prometaphase delay; multipolar spindles; spindle pole fragmentation	400 cells from 2 independent experiments	yes	(Dunsch et al., 2011; Schmidt et al., 2010; Thein et al., 2007)
Astrin_oligo2			224 cells from 2 independent experiments	yes	
Aurora A_oligo1	Centrosome; central spindle	Misaligned chromosomes; mitotic delay; multipolar spindles; spindle pole fragmentation; chromosome mis-segregation (lagging chromosomes and chromosome bridges)	364 cells from 2 independent experiments	yes	(De Luca et al., 2008, 2006; Hégarat et al., 2011; Hoar et al., 2007; Sasai et al., 2008)
Aurora A_oligo2			79 cells from 1 experiment	yes	
INCENP	Centromere; spindle midzone	Prometaphase delay; Multipolar spindles; cytokinesis defects	199 cells from 2 independent experiments	yes	(Mackay et al., 1998; Xu et al., 2009)
Haspin_oligo1	Chromosome; centrosome	Misaligned chromosomes; mitotic arrest; prometaphase	399 cells from 2 independent experiments	no	(Dai et al., 2009, 2005)

		delay; multipolar spindles; spindle pole fragmentation			
Haspin_oligo2	Chromosome; centrosome		401 cells from 2 independent experiments	no	
ARP1	Kinetochore; mitotic spindle	Mitotic delay	221 cells from 2 independent experiments	no	(Raaijmakers et al., 2013)
Spc25_oligo1	Kinetochore	Misaligned chromosomes; mitotic delay; aberrant mitotic spindles; multipolar spindles; cell death	298 cells from 3 independent experiments	yes	(Bharadwaj et al., 2004; McCleland et al., 2004; P. Xu et al., 2014)
Spc25_oligo2			203 cells from 2 independent experiments	yes	
DYNLT3_oligo1	kinetochore	Increased mitotic index, particularly the number of cells in prophase/prometaphase	309 cells from 2 independent experiments	no	(Lo et al., 2007)
DYNLT3_oligo2			564 cells from 3 independent experiments	no	
DYNLRB1/ Roadblock-1	Kinetochore; mitotic spindle	Misaligned chromosomes; prometaphase delay	165 cells from 2 independent experiments	no	(Raaijmakers et al., 2013)
Spc24_oligo1	Kinetochore	Misaligned chromosomes	399 cells from 2 independent experiments	yes	(Bharadwaj et al., 2004; P. Xu et al., 2014)
Spc24_oligo2			336 cells from 2 independent experiments	yes	
NdeL1	Kinetochore; mitotic spindle	Misaligned chromosomes; prometaphase delay; chromosome mis-segregation	462 cells from 2 independent experiments	no	(Raaijmakers et al., 2013; Vergnolle and Taylor, 2007)
LIS1/PAFAH1B1	Kinetochore; mitotic spindle	Misaligned chromosomes; prometaphase delay; chromosome mis-segregation (lagging chromosomes and chromosome bridges)	469 cells from 3 independent experiments	no	(Moon et al., 2014; Raaijmakers et al., 2013)

HSET/KIF1C	Microtubules		400 cells from 2 independent experiments	no	(Auckland and McAinsh, 2015)
Nde1	Kinetochore; mitotic spindle	Misaligned chromosomes; prometaphase delay;	611 cells from 3 independent experiments	yes	(Raaijmakers et al., 2013; Vergnolle and Taylor, 2007)
DLIC2	Spindle pole	Misaligned chromosomes; prometaphase delay	400 cells from 2 independent experiments	no	(Horgan et al., 2011; Raaijmakers et al., 2013)
HAUS6_oligo1	Centrosome, spindle	Misaligned chromosomes; aberrant mitotic spindles; spindle pole fragmentation; mitotic delay	345 cells from 2 independent experiments	yes	(Lawo et al., 2009)
HAUS6_oligo2	Centrosome, spindle		168 cells from 1 experiment	yes	
HAUS1_oligo1	Centrosome, spindle	Misaligned chromosomes; aberrant mitotic spindles; spindle pole fragmentation; mitotic delay	400 cells from 2 independent experiments	no	(Einarson et al., 2004; Lawo et al., 2009)
HAUS1_oligo2	Centrosome, spindle		396 cells from 2 independent experiments	no	
DIC2/DYNC1I2	Kinetochore; mitotic spindle	Misaligned chromosomes; prometaphase delay	184 cells from 2 independent experiments	no	(Raaijmakers et al., 2013)
survivin	Centromeres; spindle midzone	Misaligned chromosomes; prometaphase delay; chromosome segregation errors; Cytokinesis failure, mitotic catastrophe	294 cells from 2 independent experiments	yes	(Carvalho et al., 2003; Lens et al., 2003; Uren et al., 2000)
CPAP/ CENP-J	centriole	Misaligned chromosomes; mitotic delay; multipolar spindles; apoptosis	215 cells from 2 independent experiments	no	(Cho et al., 2006)
Ndc80_oligo1	kinetochore	Misaligned chromosomes; mitotic arrest	191 cells from 2 independent experiments	yes	(Joseph et al., 2004; M. H. Lee et al., 2011; L. Li et al., 2007; Martin-Lluesma et al., 2002; Sundin et al., 2011)

Ndc80_oligo2			238 cells from 2 independent experiments	yes	
Borealin	Centromere; spindle midzone		368 cells from 2 independent experiments	no	(Gassmann et al., 2004)
Scc1/Rad21	Chromosome; centrosome	Misaligned chromosomes; prometaphase delay; multipolar spindles; spindle pole fragmentation	384 cells from 2 independent experiments	no	(Beauchene et al., 2010; Dai et al., 2009; Díaz-Martínez et al., 2010)
Myosin 10	Spindle pole	Misaligned chromosomes; mitotic delay; aberrant mitotic spindles; spindle pole fragmentation; cytokinesis failure	500 cells from 3 independent experiments	no	(Woolner et al., 2008)
Sgo1/Shugoshin	Centromere; Kinetochore; centrosome; spindle pole	Misaligned chromosomes; prometaphase delay; spindle pole fragmentation	414 cells from 2 independent experiments	no	(McGuinness et al., 2005; X. Wang et al., 2008)
HAUS3_oligo1	Centrosome, spindle	Misaligned chromosomes; aberrant mitotic spindles; spindle pole fragmentation;	400 cells from 2 independent experiments	no	(Lawo et al., 2009)
HAUS3_oligo2	Centrosome, spindle		400 cells from 2 independent experiments	no	
DHC/DYNC1H1	Kinetochore; mitotic spindle	Misaligned chromosomes; prometaphase delay; aberrant mitotic spindles	396 cells from 2 independent experiments	yes	(Barisic et al., 2014; Raaijmakers et al., 2013)
CENP-T	kinetochore	Misaligned chromosomes, prometaphase arrest; multipolar spindles; cell death	395 cells from 2 independent experiments	no	(McKinley et al., 2015; Prendergast et al., 2011; Wood et al., 2016)
CENP-T			229 cells from 2 independent experiments	no	
MLL	Mitotic spindle	Misaligned chromosomes; mitotic delay	560 cells from 3 independent experiments	no	(Ali et al., 2017)

CENP-W	kinetochore	Misaligned chromosomes; mitotic delay; multipolar spindles	380 cells from 2 independent experiments	no	(Chun et al., 2016; Prendergast et al., 2011)
Shp2_oligo1	Kinetochore; centrosome; spindle midzone; midbody	Misaligned chromosomes; mitotic delay; chromosome mis-segregation (lagging chromosomes)	528 cells from 3 independent experiments	yes	(Liu et al., 2012)
Shp2_oligo2			455 cells from 3 independent experiments	yes	
ASURA/PHB2	cytoplasm	Misaligned chromosomes; mitotic arrest	400 cells from 2 independent experiments	no	(Equilibrina et al., 2013, ; M. H. Lee et al., 2011; Takata et al., 2007)
CENP-H_oligo1	kinetochore	Misaligned chromosomes; aberrant mitotic spindles; multipolar spindles	324 cells from 3 independent experiments	yes	(Amaro et al., 2010; Orthaus et al., 2006)
CENP-H_oligo2			255 cells from 2 independent experiments	yes	
Kif14_oligo1	Spindle poles; mitotic spindle; midbody	Misaligned chromosomes; cytokinesis failure; binucleated cells	436 cells from 3 independent experiments	no	(Carleton et al., 2006; Zhu et al., 2005)
Kif14_oligo2	Spindle poles; mitotic spindle; midbody		277 cells from 2 independent experiments	no	
WDR5	Mitotic spindle	Misaligned chromosomes; mitotic delay	383 cells from 2 independent experiments	no	(Ali et al., 2017)
TAO1/MARKK	microtubules	Misaligned chromosomes; prometaphase delay; Muti-lobed nuclei; chromosome mis-segregation (lagging chromosomes)	416 cells from 2 independent experiments	no	(Draviam et al., 2007; Shrestha et al., 2014)
Nup88	Mitotic spindle	Misaligned chromosomes; multipolar spindles	300 cells from 2 independent experiments	no	(Hashizume et al., 2010)
ASB7	ND	Misaligned chromosomes	300 cells from 2 independent experiments	no	(Uematsu et al., 2016)

And-1_oligo1	cytoplasm	Misaligned chromosomes; prometaphase delay	415 cells from 2 independent experiments	yes	(Jaramillo-Lambert et al., 2013)
And-1_oligo2	cytoplasm		168 cells from 1 experiment	yes	
Septin-7	Spindle poles; mitotic spindle; midbody	Misaligned chromosomes; mitotic arrest	222 cells from 2 independent experiments	no	(Zhu et al., 2008)
ANKRD53	Spindle poles	Misaligned chromosomes; mitotic delay; Multinucleated cells	360 cells from 2 independent experiments	no	(Kim and Jang, 2016)
TRAMM	Perinuclear region	Misaligned chromosomes; mitotic delay	371 cells from 2 independent experiments	no	(Milev et al., 2015)
Septin-2_oligo1	plasma membrane, cleavage furrow and midbody	Misaligned chromosomes; mitotic delay; binucleated cells	411 cells from 2 independent experiments	yes	(Spiliotis et al., 2005)
Septin-2_oligo2			325 cells from 2 independent experiments	yes	
Seh1	kinetochores	Misaligned chromosomes; mitotic delay; cytokinesis defects	200 cells from 2 independent experiments	no	(Platani et al., 2009; Zuccolo et al., 2007)
CENP-Q_oligo1	kinetochore	Misaligned chromosomes; prometaphase delay	430 cells from 3 independent experiments	no	(Bancroft et al., 2015)
CENP-Q_oligo2	kinetochore		352 cells from 3 independent experiments	no	
NF-1	Astral microtubules; mitotic spindle, centrosomes; midbody	Misaligned chromosomes	375 cells from 2 independent experiments	no	(Koliou et al., 2016)
Scramble RNAi			7229 cells from 45 independent experiments		
Nup107	kinetochore	Misaligned chromosomes; mitotic delay; cytokinesis defects	428 cells from 3 independent experiments	no	(Platani et al., 2009; Zuccolo et al., 2007)
Usp16	Cytoplasmic in interphase; kinetochore	Misaligned chromosomes; prometaphase delay	663 cells from 3 independent experiments	no	(Zhuo et al., 2015)
NDR1	ND	Misaligned chromosomes	264 cells from 2 independent experiments	no	(Oh et al., 2010)

GAK_oligo1	Trans-Golgi network	Misaligned chromosomes; prometaphase arrest; multipolar spindles; spindle pole fragmentation	333 cells from 2 independent experiments	yes	(Shimizu et al., 2009)
GAK_oligo2	Trans-Golgi network		376 cells from 3 independent experiments	yes	
HAUS7	Centrosome, spindle	Misaligned chromosomes; aberrant mitotic spindles; spindle pole fragmentation;	303 cells from 2 independent experiments	no	(Lawo et al., 2009)
CENP-M	kinetochore	Misaligned chromosomes	599 cells from 3 independent experiments	no	(Basilico et al., 2014; Foltz et al., 2006)
CENP-U	kinetochore	Misaligned chromosomes; chromosome mis-segregation (lagging chromosomes)	278 cells from 3 independent experiments	no	(Hua et al., 2011)
MST1	ND	Misaligned chromosomes; prometaphase delay; cell death	300 cells from 2 independent experiments	no	(Oh et al., 2010)
PTEN	Centrosome; mitotic spindle; midbody	Misaligned chromosomes; mitotic delay; spindle pole fragmentation; mitotic catrastrophe	280 cells from 2 independent experiments	no	(He et al., 2016)
HAUS2	Centrosome, spindle	Misaligned chromosomes; aberrant mitotic spindles; spindle pole fragmentation;	339 cells from 3 independent experiments	no	(Lawo et al., 2009)
CENP-N_oligo1	kinetochore	Misaligned chromosomes, multipolar spindles	300 cells from 2 independent experiments	yes	(McKinley et al., 2015)
CENP-N_oligo2			200 cells from 2 independent experiments	yes	
Hsp72	Mitotic spindle; midbody	Misaligned chromosomes; prometaphase delay	428 cells from 3 independent experiments	no	(O'Regan et al., 2015)
HAUS5	Centrosome, spindle	Misaligned chromosomes; aberrant mitotic	397 cells from 2 independent experiments	no	(Lawo et al., 2009)

		spindles; spindle pole fragmentation;			
HAUS4_oligo1	Centrosome, spindle	Misaligned chromosomes; aberrant mitotic spindles; spindle pole fragmentation;	324 cells from 2 independent experiments	no	(Lawo et al., 2009)
HAUS4_oligo2			254 cells from 2 independent experiments	no	
DYNLT1	Kinetochore; mitotic spindle	ND	596 cells from 3 independent experiments	no	
Rab5	Early endosomes	Misaligned chromosomes; prometaphase delay	579 cells from 3 independent experiments	no	(Serio et al., 2011)
CENP-I_oligo 1	Kinetochore	Misaligned chromosomes, multipolar spindles; chromosome mis-segregation; apoptosis	305 cells from 2 independent experiments	yes	(Liu et al., 2003; McKinley et al., 2015; Nishihashi et al., 2002)
CENP-I_oligo 2			207 cells from 2 independent experiments	yes	
Dsn1_oligo1	Kinetochore	Misaligned chromosomes; prometaphase delay	582 cells from 3 independent experiments	yes	(Kline et al., 2006)
Dsn1_oligo2			229 cells from 2 independent experiments	yes	
CENP-P	kinetochore	Misaligned chromosomes; mitotic delay	567 cells from 3 independent experiments	no	(Bancroft et al., 2015)
ZwinT	Kinetochore	Misaligned chromosomes; cell death; chromosome mis-segregation (lagging chromosomes and chromosome bridges)	410 cells from 2 independent experiments	no	(Lin et al., 2006; Wang et al., 2004)
Nsl1_oligo1	Kinetochore	Misaligned chromosomes	300 cells from 2 independent experiments	yes	(Kline et al., 2006)
Nsl1_oligo2			200 cells from 2 independent experiments	yes	

Mis12_oligo1	Kinetochore	Misaligned chromosomes	200 cells from 2 independent experiments	yes	(Kline et al., 2006)
Mis12_oligo2			171 cells from 2 independent experiments	yes	
KNL1_oligo1	Kinetochore	Misaligned chromosomes	291 cells from 2 independent experiments	yes	(Caldas and DeLuca, 2014; Ghongane et al., 2014)
KNL1_oligo2			219 cells from 2 independent experiments	yes	
Nup153	ND	Multilobed nuclei; cytokinesis abnormalities	200 cells from 2 independent experiments	no	(Chatel and Fahrenkrog, 2011; Lussi et al., 2010; Mackay et al., 2009)

Table 2. List of oligonucleotide sequences and siRNA depletion conditions

Protein Name	siRNA sequence (5´-3´)	Source or reference	Identifiers	Additional information
scramble	CUUCCUCUCUUUCUCUCCCUUGUGATT	Sigma-Aldrich		
m-calpain	CCAGGACUACGAGGCGCUGTT	Sigma-Aldrich	(Honda et al., 2004)	50nM, 96h
Nuf2 Oligo1	AAGCAUGCCGUGAAACGUAUATT	Sigma-Aldrich	(DeLuca et al., 2002)	50nM, 24h
Nuf2 Oligo2	GCAUGCCGUGAAACGUAUATT	Dharmacon	(Asteriti et al., 2011)	50nM, 24h
Beclin-1	GCUCAGUAUCAGAGAGAAUTT	Sigma-Aldrich	(Frémont et al., 2013)	50nM, 48h
CLIP-170	GCACAGCUCUGAAGACACCTT	Sigma-Aldrich	(Tanenbaum et al., 2006)	50nM, 96h
ATRX Oligo1	GAGGAAACCUUCAAUUGUATT	Sigma-Aldrich	(Ritchie et al., 2008)	50nM, 72h
ATRX Oligo2	GCAGAGAAAUUCCUAAAGATT	Sigma-Aldrich	(Ritchie et al., 2008)	50nM, 72h
SPICE	GCUGAGAACAAAUGAGUCATT	Sigma-Aldrich	(Archinti et al., 2010)	50nM, 48h
CHICA	CCAGGAUAGCAAGCUCUCAAATT	Sigma-Aldrich	(Santamaria et al., 2008)	50nM, 48h
CDCA4	GCUGCAUGGAAGAGCUGUUTT	Sigma-Aldrich	(L. Wang et al., 2008)	50nM, 96h
Kif2a Oligo1	GGAAUGGCAUCCUGUGAAATT	Sigma-Aldrich	(Jang et al., 2008)	50nM, 72h

Kif2a Oligo2	GGCAAAGAGAUUGACCUGGTT	Sigma-Aldrich	(Ganem and Compton, 2004)	50nM, 72h
HIP1r	UUCUCAUGAUGCGUGCCCAGGAUGATT	Sigma-Aldrich	(Park, 2010)	50nM, 96h
Nucleophosmin	AGAUGAUGAUGAUGAUGAUUUTT	Sigma-Aldrich	(Amin et al., 2008)	50nM, 48h
CENP-F	AAGAGAAGACCCCAAGUCAUCTT	Sigma-Aldrich	(Holt et al., 2005)	50nM, 72h
NudC	AACAGACUUUUUCAUUGGAGGTT	Sigma-Aldrich	(Nishino et al., 2006)	50nM, 48h
RRS1	CUACCGGACACCAGAGUAATT	Sigma-Aldrich	(Gambe et al., 2009)	50nM, 72h
KIBRA	GGUUGGAGAUUACUUCAUATT	Sigma-Aldrich	(L. Zhang et al., 2012)	50nM,96h
Nucleolin	AGAGUUUGCUUCAUUCGAATT	Sigma-Aldrich		50nM, 96h
DDA3 Oligo1	AAGCAAGACUUCAGUAGCATT	Sigma-Aldrich	(Jang et al., 2008)	50nM, 72h
DDA3 Oligo2	CCACCGAAGTGACCCAAATTT	Sigma-Aldrich	(Jang et al., 2008)	50nM, 24h
Bub1 Oligo1	AAAUACCACAAUGACCCAAGATT	Sigma-Aldrich	(Johnson et al., 2004)	50nM, 48h
Bub1 Oligo2	GAGUGAUCACGAUUUCUAUTT	Dharmacon	(Karamysheva et al., 2009)	50nM, 48h
BubR1 Oligo1	AACGGGCAUUUGAAUAUGAAATT	Sigma-Aldrich	(Ditchfield et al., 2003b)	50nM, 48h
BubR1 Oligo2	AAAGAUCCUGGCUAACUGUUCTT	Dharmacon	(Lampson and Kapoor, 2005)	50nM, 48h
Ska3 Oligo1	AAUCCAGGCUCAAUGAUAATT	Sigma-Aldrich	(Raaijmakers et al., 2009)	50nM, 24h
Ska3 Oligo2	AGACAAACAUGAACAUUAATT	Sigma-Aldrich	(Gaitanos et al., 2009)	50nM, 48h
TPX2	AAGGAGAUACUCAAAACAUAGTT	Sigma-Aldrich	(Garrett et al., 2002)	50nM, 96h
Nup188 Oligo1	AUUUCUAGCAGCAUGGACUGUUCCCTT	Sigma-Aldrich	(Itoh et al., 2013)	50nM, 96h
Nup188 Oligo2	GGUAGUAGGCAGACCAAUATT	Sigma-Aldrich	(Labade et al., 2016)	50nM, 96h
Kif4a Oligo1	GCAAUUGAUUACCCAGUUATT	Sigma-Aldrich	(Mazumdar et al., 2004)	50nM, 96h
Kif4a Oligo2	GAAAGATCCTGGCTCAAGATT	Sigma-Aldrich	(Mazumdar et al., 2004)	50nM, 96h
Zw10 Oligo1	UGAUCAAUGUGCUGUUCAATT	Sigma-Aldrich	(Kops et al., 2005a)	50nM, 72h
Zw10 Oligo2	CCACGAAGUGAUGAAUUUATT	Dharmacon	(Y. W. Chan et al., 2009)	50nM, 48h
CENP-L	CCAUUAUGUGGCUACUACUGAAUUU	Sigma-Aldrich	(McHedlishvili et al., 2012)	50nM, 96h

NUSAP1	AAGCACCAAGAAGCUGAGAAUTT	Sigma-Aldrich	(Raemaekers et al., 2003)	50nM, 96h
SAF-A	GAACUCUCGUAUGCUAAGATT	Sigma-Aldrich	(Ma et al., 2011)	50nM, 24h
Tastin	GCCUGAUCUUCUCUUCCCATT	Sigma-Aldrich	(Yang et al., 2008)	50nM, 96h
Tankyrase-1	AACAAUUCACCGUCGUCCUCUTT	Sigma-Aldrich	(Dynek and Smith, 2004)	50nM, 72h
Ska1 Oligo1	CCCGCUUAACCUAUAAUCAAATT	Sigma-Aldrich	(Hanisch et al., 2006)	50nM, 48h
Ska1 Oligo2	GGACUUACUCGUUAUGUUATT	Dharmacon	(Thomas et al., 2016)	50nM, 24h
HURP	AAUGACUCGAUCAGCUACUCATT	Sigma-Aldrich	(Silljé et al., 2006)	50nM, 48h
Aki	CCCUGGCGAUCUGGAUGUCUUUGUU	Sigma-Aldrich	(Nakamura et al., 2009)	50nM, 96h
4.1r	GAAAGUCUGUGUAGAACAUUU	Sigma-Aldrich	(Krauss et al., 2008)	50nM, 72h
HICE1	GGGAGAACUUGAUGUUGGUGAUUCGTT	Sigma-Aldrich	(Wu et al., 2008)	50nM, 48h
Ska2	AAGAAAUCAAGACUAAUCAUCTT	Sigma-Aldrich	(Hanisch et al., 2006)	50nM, 72h
Kif18a Oligo1	ACCAACAACAGUGCCAUAAATT	Sigma-Aldrich	(Huang et al., 2009)	50nM, 24h
Kif18a Oligo2	ACAGAUUCGUGAUCUCUUATT	Dharmacon	(Mayr et al., 2007)	50nM, 24h
TACC3 Oligo1	CACGGGCGCGGAGGUGGAUUATT	Sigma-Aldrich	(Fielding et al., 2011)	50nM, 48h
TACC3 Oligo1	GUUACCGGAAGAUCGUCUGTT	Dharmacon	(Kimura et al., 2013)	50nM, 48h
CLERC Oligo1	GGAGAAAGAUGGAGACGAUTT	Sigma-Aldrich	(Muto et al., 2008)	50nM, 24h
CLERC Oligo2	CAGAUAGGCUAAAGGAAAUTT	Sigma-Aldrich	(Muto et al., 2008)	50nM, 72h
Kizuna	AAGCGAUUUGAGCGUGUCCAATT	Sigma-Aldrich	(Oshimori et al., 2006)	50nM, 72h
ILK	AAGACGCUCAGCAGACAUGUGGATT	Sigma-Aldrich	(Fielding et al., 2011)	50nM, 96h
Kinastrin	AGGCUACAAACCACUGAGUAATT	Sigma-Aldrich	(Dunsch et al., 2011)	50nM, 96h
Ninein	UAUGAGCAUUGAGGCAGAGTT	Sigma-Aldrich	(Logarinho et al., 2012)	50nM, 96h
NuMA	GGCGUGGCAGGAGAAGUUCTT	Sigma-Aldrich	(Logarinho et al., 2012)	50nM, 96h
Rae1 Oligo1	GCAGUAACCAAGCGAUACATT	Sigma-Aldrich	(Wong et al., 2006)	50nM, 72h
Rae1 Oligo2	GAGUUGCUAUUCACUAUAUTT	Sigma-Aldrich	(Blower et al., 2005)	50nM, 48h

RanBP2 Oligo1	AAGGACAGUGGGAUUGUAGUGTT	Sigma-Aldrich		50nM, 72h
RanBP2 Oligo2	AACAACACCAAAAGCAGUGGUTT	Sigma-Aldrich		50nM, 72h
Spindly	GAAAGGGUCUCAAACUGAATT	Sigma-Aldrich	(Barisic et al., 2010)	50nM, 48h
STARD9	GAGUUGCCAAAGGCUAUAATT	Sigma-Aldrich	(Srivastava and Panda, 2018)	50nM, 72h
CAMKIIγ	GCAGAUGCCAGCCACUGUATT	Sigma-Aldrich	SASI_Hs01_00118118	50nM, 24h
CENP-E Oligo1	GAACUAAGAAGAAGCGUAUTT	Sigma-Aldrich	(Maia et al., 2010)	50nM, 24h
CENP-E Oligo2	AAGGCUACAAUGGUACUAUAUTT	Dharmacon	(Johnson et al., 2004)	50nM, 24h
CHC17 clatrin	AAGCAAUGAGCUGUUUGAAGATT	Sigma-Aldrich	(Vassilopoulos et al., 2009)	50nM, 96h
CEP72 Oligo1	UUGCAGAUCGCUGGACUUCAATT	Sigma-Aldrich	(Oshimori et al., 2009)	50nM, 72h
CEP72 Oligo2	GAGUUUAACAGGUCUGAAATT	Sigma-Aldrich	SASI_Hs02_00351368	50nM, 96h
CEP90 Oligo1	GCAGCUGACAGAGACAUAUTT	Sigma-Aldrich	(Kim and Rhee, 2011)	50nM, 48h
CEP90 Oligo2	CACCUUAGAGCAAACUGUUTT	Sigma-Aldrich	SASI_HS01_00230208	50nM, 96h
CLASP1b	GGAUGAUUUACAAGACUGGTT	Sigma-Aldrich	(Mimori-Kiyosue et al., 2005)	50nM, 48h
CLASP2b	GACAUACAUGGGUCUUAGATT	Sigma-Aldrich	(Mimori-Kiyosue et al., 2005)	50nM, 48h
Aurora B Oligo1	AACGCGGCACUUCACAAUUGATT	Sigma-Aldrich	(Fuller et al., 2008)	50nM, 24h
Aurora B Oligo2	AAGGUGAUGGAGAAUAGCAGUTT	Dharmacon	(Hauf et al., 2003)	50nM, 48h
Astrin Oligo1	UCCCGACAACUCACAGAGAAATT	Sigma-Aldrich	(Thein et al., 2007)	50nM, 48h
Astrin Oligo2	CUACAGAGCCUGACUCUCUTT	Dharmacon	(Cheng et al., 2007)	50nM, 48h
Aurora A Oligo1	AUGCCCUGUCUUACUGUCATT	Sigma-Aldrich	(Kuang et al., 2017)	50nM, 24h
Aurora A Oligo2	AUGCCCUGUCUUACUGUCATT	Dharmacon	(Kesisova et al., 2013)	50nM, 24h
INCENP	CUCAGAAGAACCGACGGAATT	Sigma-Aldrich	SASI_Hs01_00219348	50nM, 24h
Haspin Oligo1	GGCUUUAUCGGGCUGAACUTT	Sigma-Aldrich	SASI_Hs02_00359157	50nM, 48h
Haspin Oligo2	GCUUUGAGCACCGAGACUUTT	Sigma-Aldrich	SASI_Hs01_00243245	50nM, 72h
ARP1	CCUUCAAUGUGCCCGCUCUTT	Sigma-Aldrich	SASI_Hs01_00015229	50nM, 48h

Spc25 Oligo1	CUGCAAAUAUCCAGGAUCUTT	Sigma-Aldrich	SASI_Hs01_00193697	50nM, 24h
Spc25 Oligo2	AAGCGAAUGCAGAGAGGUUGATT	Dharmacon	(McCleland et al., 2004)	50nM, 24h
DYNLT3 Oligo1	CAUAGUAAUUGGCAGAUUATT	Sigma-Aldrich	SASI_Hs01_00147343	50nM, 96h
DYNLT3 Oligo2	GGGAGAACCGGACCAUGAATT	Sigma-Aldrich	SASI_Hs02_00341758	50nM, 72h
DYNLRB1	GAUUCAGAAUCCAACCGAATT	Sigma-Aldrich	SASI_Hs01_00158744	50nM, 48h
Spc24 Oligo1	CUCAACUUUACCACCAAGUUATT	Sigma-Aldrich	(H. Xu et al., 2014)	50nM, 48h
Spc24 Oligo2	AAGGAGAUUGAGGCGGAUCUGTT	Dharmacon	(McCleland et al., 2004)	50nM, 48h
NdeL1	GGAUGAAGCAAGAGAUUUATT	Sigma-Aldrich	SASI_Hs01_00228104	50nM, 48h
LIS1	GAGACAAGACUAUUAAGAUTT	Sigma-Aldrich	SASI_Hs01_00019092	50nM, 48h
HSET	CAGCUAUUGCCACAGGGUUTT	Sigma-Aldrich	SASI_Hs01_00185148	50nM, 48h
Nde1	GCUUGAAUCAGGCCAUCGATT	Sigma-Aldrich	SASI_Hs01_00074363	50nM, 48h
DLIC2	GAUGCAUAUGAAGACUUUATT	Sigma-Aldrich	SASI_Hs01_00014533	50nM, 72h
HAUS6 Oligo1	CCAUUUCGCACGUAGCAGATT	Sigma-Aldrich	SASI_Hs01_00105872	50nM, 48h
HAUS6 Oligo2	CUAAUUGACUCUCUGGGUUTT	Sigma-Aldrich	SASI_Hs01_00105873	50nM, 48h
HAUS1 Oligo1	GUAUCUGAAUGCUUUGGUUTT	Sigma-Aldrich	SASI_Hs01_00107510	50nM, 48h
HAUS1 Oligo2	AAGGAUACCUCGCUAGCUAGUTT	Sigma-Aldrich	(Einarson et al., 2004)	50nM, 48h
DIC2	GAAACUCAGACUCCAGUUATT	Sigma-Aldrich	SASI_Hs01_00129736	50nM, 48h
survivin	CAGACUUGGCCCAGUGUUUTT	Sigma-Aldrich	SASI_Hs01_00052228	50nM, 24h
CPAP	GAUUUACGGGAAGAUUUGATT	Sigma-Aldrich	SASI_Hs01_00069692	50nM, 96h
Ndc80 Oligo1	GAAUUGCAGCAGACUAUUATT	Sigma-Aldrich	SASI_Hs01_00138654	50nM, 24h
Ndc80 Oligo2	AAGUUCAAAAGCUGGAUGAUCTT	Dharmacon	(Liu et al., 2007)	50nM, 24h
Borealin	CCUCUAAGGGAAUUCAGGATT	Sigma-Aldrich	SASI_Hs01_00153657	50nM, 48h
Scc1/ Rad21	CUACUACUUCUAACCUCCUTT	Sigma-Aldrich	SASI_Hs01_00195799	50nM, 48h
Myosin10	GCAAUACAGUGGGACAGUUTT	Sigma-Aldrich	SASI_Hs01_00072460	50nM, 96h

Sgo1	GCUGCACCAUGCCAAAUAATT	Sigma-Aldrich	SASI_Hs01_00168960	50nM, 24h
HAUS3 Oligo1	GAGAAUGCCCAGUUAUUGATT	Sigma-Aldrich	SASI_Hs01_00073692	50nM, 48h
HAUS3 Oligo2	GAUUAAGGCUGUUAGUCUUTT	Sigma-Aldrich	SASI_Hs01_00073693	50nM, 48h
DHC	GAACUAGACUUGGUUAAUUTT	Sigma-Aldrich	SASI_Hs01_00028998	50nM, 24h
CENP-T Oligo1	CAGUAGUGGCCAGGCUUCATT	Sigma-Aldrich	(Chun et al., 2013)	50nM, 48h
CENP-T Oligo2	AAGUAGAGCCCUUACACGATT	Dharmacon	(Kim and Yu, 2015)	50nM, 24h
MLL	GGAUGAAGUUAGAGAAAAUTT	Sigma-Aldrich	(Ali et al., 2017)	50nM, 24h
CENP-W	CAGAUAAAGCGGAAGGCUCTT	Sigma-Aldrich	(Chun et al., 2016)	50nM, 72h
Shp2 Oligo1	AAGGUGAAUAUUGUGCCUGUCTT	Sigma-Aldrich	(Liu et al., 2012)	50nM, 48h
Shp2 Oligo2	GGUUGCUACGGCUUAUCAUTT	Sigma-Aldrich	(Tsang et al., 2012)	50nM, 72h
ASURA PHB2	GAAUCGUAUCUAUCUCACATT	Sigma-Aldrich	(Takata et al., 2007)	50nM, 24h
CENP-H Oligo1	UGGUUGAUGCAAGUGAAGATT	Sigma-Aldrich	(Orthaus et al., 2006)	50nM, 48h
CENP-H Oligo2	AGAUUGAUUUGGACAGUAUTT	Dharmacon	(Kim and Yu, 2015)	50nM, 48h
Kif14 Oligo1	GUUGGCUAGAAUUGGGAAATT	Sigma-Aldrich	(Carleton et al., 2006)	50nM, 48h
Kif14 Oligo2	GGCUCAGCAAGAGCUUUCUUCUCAATT	Sigma-Aldrich	(P. Xu et al., 2014)	50nM, 48h
WDR5	UUAGCAGUCACUCUUCCACTT	Sigma-Aldrich	(Ali et al., 2017)	50nM, 48h
TAO1	CTAAGAGTTTGAAGTCTAATT	Sigma-Aldrich	(Draviam et al., 2007)	50nM, 72h
Nup88	UGCUUUGUUGAACACAUCCTT	Sigma-Aldrich	(Bernad et al., 2004)	50nM, 72h
ASB7	GAGAGAGGUCAAGCUGUGUGATT	Sigma-Aldrich	(Uematsu et al., 2016)	50nM, 96h
And-1 Oligo1	AAGATGGTCAAGAAGGCAGCATT	Sigma-Aldrich	(Zhu et al., 2007)	50nM, 72h
And-1 Oligo2	GAUGGUCAAGAAGGCAGCATT	Sigma-Aldrich	(Yoshizawa-Sugata and Masai, 2009)	50nM, 72h
Septin-7	ACGACUACAUUGAUAGUAAATT	Sigma-Aldrich	(Zhu et al., 2008)	50nM, 96h
ANKRD53	ACCUUGAUACUCAAUCAGGTT	Sigma-Aldrich	(Kim and Jang, 2016)	50nM, 96h
TRAMM	CGGACAAGCUGAACGAACATT	Sigma-Aldrich	(Milev et al., 2015)	50nM, 24h

Septin-2 Oligo1	AAGGUGAAUAUUGUGCCUGUCTT	Sigma-Aldrich	(Spiliotis et al., 2005)	50nM, 48h
Septin-2 Oligo2	GGUGAAUAUUGUGCCUGUCTT	Sigma-Aldrich	(Kremer et al., 2005)	50nM, 24h
Seh1	AAGACACAUAGUGGAUCUGUAUGTT	Sigma-Aldrich	(Zuccolo et al., 2007)	50nM, 48h
CENP-Q Oligo1	GGUCUGGCAUUACUACAGGAAGAAATT	Sigma-Aldrich	(Bancroft et al., 2015)	50nM, 72h
CENP-Q Oligo2	CAGAGUUAAUGACUGGGAAUAUUCATT	Sigma-Aldrich	(Bancroft et al., 2015)	50nM, 72h
NF-1	AACUUCGGAAUUCUGCCUCUGTT	Sigma-Aldrich	(Park et al., 2013)	50nM, 48h
Nup107	AAGAGGAAAGUGUAUUCGCAGTT	Sigma-Aldrich	(Zuccolo et al., 2007)	50nM, 48h
Usp16	UAGUGAAUGUGGAAUGGAATT	Sigma-Aldrich	(Qian et al., 2016)	50nM, 48h
NDR1	GAGCAGGTTGGCCACATTCTT	Sigma-Aldrich	(Oh et al., 2010)	50nM, 96h
GAK Oligo1	GAUGUGCGGUUGUUCCUGGTT	Sigma-Aldrich	(Shimizu et al., 2009)	50nM, 48h
GAK Oligo2	AAGCUCAAGAUGUGGGGAGUG	Sigma-Aldrich	(Lee et al., 2005)	50nM, 72h
HAUS7	GCGCUUAGAACGGAGUACUTT	Sigma-Aldrich	SASI_Hs02_00350136	50nM, 48h
CENP-M	GAAUUGACCUGAUCGUGUUTT	Sigma-Aldrich	SASI_Hs01_00144699	50nM, 72h
CENP-U	CUUUAUAAAUCAAUUGUUUTT	Sigma-Aldrich	SASI_Hs01_00175574	50nM, 96h
MST1	GACGUGUGCGGGAGAGUGATT	Sigma-Aldrich	SASI_Hs01_00161455	50nM, 48h
PTEN	GGUGUAAUGAUAUGUGCAUTT	Sigma-Aldrich	SASI_Hs01_00196478	50nM, 96h
HAUS2	CUUUAGCAAAGAUGGAUAUTT	Sigma-Aldrich	SASI_Hs01_00101146	50nM, 96h
CENP-N Oligo1	GACUGUUGCUGAGUUCAUCTT	Sigma-Aldrich	SASI_Hs02_00322304	50nM, 72h
CENP-N Oligo2	GCGUGCAAGUAUCAGUGAUTT	Dharmacon	(Wu et al., 2021)	50nM, 48h
Hsp72	CCGAGAAGGACGAGUUUGATT	Sigma-Aldrich	SASI_Hs01_00051449	50nM, 72h
HAUS5	GACAUGGAGAGGAAAGCCATT	Sigma-Aldrich	SASI_Hs02_00347509	50nM, 48h
HAUS4 Oligo1	GGAAGUUCAUCGUCUGAUUTT	Sigma-Aldrich	SASI_Hs01_00022834	50nM, 48h
HAUS4 Oligo2	GUGCUAUGAUCCUUAAGCUTT	Sigma-Aldrich	SASI_Hs01_00022835	50nM, 48h
DYNLT1	CCAUGAAUUCAGUGAACUCTT	Sigma-Aldrich	SASI_Hs01_00096434	50nM, 48h

Rab5	GUCCUAUGCAGAUGACAAUTT	Sigma-Aldrich	SASI_Hs01_00097508	50nM, 48h
CENP-I Oligo1	AAGCAACUCGAAGAACAUCUCTT	Sigma-Aldrich	(Liu et al., 2003)	50nM, 72h
CENP-I Oligo2	GAAGGUGUGUGACAUAUAUTT	Dharmacon	(Kim and Yu, 2015)	50nM, 24h
Dsn1 Oligo1	GUCUAUCAGUGUCGAUUUATT	Sigma-Aldrich	(Kim and Yu, 2015)	50nM, 48h
Dsn1 Oligo2	GGCGUUUCAGAGGAAAGAATT	Dharmacon	(Chan et al., 2012)	50nM, 24h
CENP-P	GAACCCUGGUAGGACUGCUUGGAAUTT	Sigma-Aldrich	(McHedlishvili et al., 2012)	50nM, 72h
Zwint	GGAGGACACUGCUAAGGGUTT	Sigma-Aldrich	(G. Zhang et al., 2015)	50nM, 72h
Nsl1 Oligo1	CAUGAGCUCUUUCUGUUUATT	Sigma-Aldrich	(Kim and Yu, 2015)	50nM, 48h
Nsl1 Oligo2	Nsl1_Oligo2	Dharmacon	ON-TARGETplus Human NSL1 siRNA; J-016722-05-0002	50nM, 48h
Mis12 Oligo1	GAAUCAUAAGGACUGUUCATT-	Sigma-Aldrich	SASI_Hs01_00050622	50nM, 48h
Mis12 Oligo2	GGACAUUUUGAUAACCUUUTT	Dharmacon	(Goshima and Vale, 2003)	50nM, 72h
KNL1 Oligo1	GCAUGUAUCUCUUAAGGAATT	Sigma-Aldrich	(Schleicher et al., 2017)	50nM, 24h
KNL1 Oligo2	GGAAUCCAAUGCUUUGAGATT	Dharmacon	doi.org/10.1083/jcb.201001006	50nM, 24h
Nup153	AAGGCAGACUCUACCAAAUGUTT	Sigma-Aldrich	(Hahn et al., 2004)	50nM, 48h

LIST OF REFERENCES

Acquaviva, C., Herzog, F., Kraft, C., Pines, J., 2004. The anaphase promoting complex/cyclosome is recruited to centromeres by the spindle assembly checkpoint. Nat. Cell Biol. 6, 892–898.

Adriaans, I.E., Hooikaas, P.J., Aher, A., Vromans, M.J.M., van Es, R.M., Grigoriev, I., Akhmanova, A., Lens, S.M.A., 2020. MKLP2 Is a Motile Kinesin that Transports the Chromosomal Passenger Complex during Anaphase. Curr. Biol. CB 30, 2628-2637.e9.

Afonso, O., Castellani, C.M., Cheeseman, L.P., Ferreira, J.G., Orr, B., Ferreira, L.T., Chambers, J.J., Morais-de-Sá, E., Maresca, T.J., Maiato, H., 2019. Spatiotemporal control of mitotic exit during anaphase by an aurora B-Cdk1 crosstalk. eLife 8, e47646.

Afonso, O., Matos, I., Pereira, A.J., Aguiar, P., Lampson, M.A., Maiato, H., 2014. Feedback control of chromosome separation by a midzone Aurora B gradient. Science 345, 332–336.

Akhmanova, A., Hoogenraad, C.C., Drabek, K., Stepanova, T., Dortland, B., Verkerk, T., Vermeulen, W., Burgering, B.M., De Zeeuw, C.I., Grosveld, F., Galjart, N., 2001. Clasps are CLIP-115 and -170 associating proteins involved in the regional regulation of microtubule dynamics in motile fibroblasts. Cell 104, 923–935.

Akhmanova, A., Steinmetz, M.O., 2010. Microtubule +TIPs at a glance. J. Cell Sci. 123, 3415–3419.

Akhmanova, A., Steinmetz, M.O., 2008. Tracking the ends: a dynamic protein network controls the fate of microtubule tips. Nat. Rev. Mol. Cell Biol. 9, 309–322.

Al-Bassam, J., Chang, F., 2011. Regulation of microtubule dynamics by TOG-domain proteins XMAP215/Dis1 and CLASP. Trends Cell Biol. 21, 604–614.

Al-Bassam, J., Kim, H., Brouhard, G., van Oijen, A., Harrison, S.C., Chang, F., 2010. CLASP promotes microtubule rescue by recruiting tubulin dimers to the microtubule. Dev. Cell 19, 245–258.

Ali, A., Veeranki, S.N., Chinchole, A., Tyagi, S., 2017. MLL/WDR5 Complex Regulates Kif2A Localization to Ensure Chromosome Congression and Proper Spindle Assembly during Mitosis. Dev. Cell 41, 605-622.e7.

Almeida, A.C., Maiato, H., 2018. Chromokinesins. Curr. Biol. CB 28, R1131–R1135.

Almeida, A.C., Soares-de-Oliveira, J., Drpic, D., Cheeseman, L.P., Damas, J., Lewin, H.A., Larkin, D.M., Aguiar, P., Pereira, A.J., Maiato, H., 2022. Augmin-dependent microtubule self-organization drives kinetochore fiber maturation in mammals. Cell Rep. 39, 110610.

Alvarez-Fernández, M., Malumbres, M., 2014. Preparing a cell for nuclear envelope breakdown: Spatio-temporal control of phosphorylation during mitotic entry. BioEssays News Rev. Mol. Cell. Dev. Biol. 36, 757–765.

Amaral, N., Vendrell, A., Funaya, C., Idrissi, F.-Z., Maier, M., Kumar, A., Neurohr, G., Colomina, N., Torres-Rosell, J., Geli, M.-I., Mendoza, M., 2016. The Aurora-B-dependent NoCut checkpoint prevents damage of anaphase bridges after DNA replication stress. Nat. Cell Biol. 18, 516–526.

Amaro, A.C., Samora, C.P., Holtackers, R., Wang, E., Kingston, I.J., Alonso, M., Lampson, M., McAinsh, A.D., Meraldi, P., 2010. Molecular control of kinetochore-microtubule dynamics and chromosome oscillations. Nat. Cell Biol. 12, 319–329.

Amin, M.A., Kobayashi, K., Tanaka, K., 2015. CLIP-170 tethers kinetochores to microtubule plus ends against poleward force by dynein for stable kinetochore-microtubule attachment. FEBS Lett. 589, 2739–2746.

Amin, M.A., Matsunaga, S., Uchiyama, S., Fukui, K., 2008. Nucleophosmin is required for chromosome congression, proper mitotic spindle formation, and kinetochore-microtubule attachment in HeLa cells. FEBS Lett. 582, 3839–3844.

Antonio, C., Ferby, I., Wilhelm, H., Jones, M., Karsenti, E., Nebreda, A.R., Vernos, I., 2000. Xkid, a chromokinesin required for chromosome alignment on the metaphase plate. Cell 102, 425–435.

Archinti, M., Lacasa, C., Teixidó-Travesa, N., Lüders, J., 2010. SPICE--a previously uncharacterized protein required for centriole duplication and mitotic chromosome congression. J. Cell Sci. 123, 3039–3046.

Asteriti, I.A., Giubettini, M., Lavia, P., Guarguaglini, G., 2011. Aurora-A inactivation causes mitotic spindle pole fragmentation by unbalancing microtubule-generated forces. Mol. Cancer 10, 131.

Auckland, P., Clarke, N.I., Royle, S.J., McAinsh, A.D., 2017. Congressing kinetochores progressively load Ska complexes to prevent force-dependent detachment. J. Cell Biol. 216, 1623–1639.

Auckland, P., McAinsh, A.D., 2015. Building an integrated model of chromosome congression. J. Cell Sci. 128, 3363–3374.

Bakhoum, S.F., Cantley, L.C., 2018. The Multifaceted Role of Chromosomal Instability in Cancer and Its Microenvironment. Cell 174, 1347–1360.

Bakhoum, S.F., Compton, D.A., 2012. Kinetochores and disease: keeping microtubule dynamics in check! Curr. Opin. Cell Biol. 24, 64–70.

Bakhoum, S.F., Danilova, O.V., Kaur, P., Levy, N.B., Compton, D.A., 2011. Chromosomal instability substantiates poor prognosis in patients with diffuse large B-cell lymphoma. Clin. Cancer Res. Off. J. Am. Assoc. Cancer Res. 17, 7704–7711.

Bakhoum, S.F., Genovese, G., Compton, D.A., 2009a. Deviant kinetochore microtubule dynamics underlie chromosomal instability. Curr. Biol. CB 19, 1937–1942.

Bakhoum, S.F., Kabeche, L., Wood, M.D., Laucius, C.D., Qu, D., Laughney, A.M., Reynolds, G.E., Louie, R.J., Phillips, J., Chan, D.A., Zaki, B.I., Murnane, J.P., Petritsch, C., Compton, D.A., 2015. Numerical chromosomal instability mediates susceptibility to radiation treatment. Nat. Commun. 6, 5990.

Bakhoum, S.F., Ngo, B., Laughney, A.M., Cavallo, J.-A., Murphy, C.J., Ly, P., Shah, P., Sriram, R.K., Watkins, T.B.K., Taunk, N.K., Duran, M., Pauli, C., Shaw, C., Chadalavada, K., Rajasekhar, V.K., Genovese, G., Venkatesan, S., Birkbak, N.J., McGranahan, N., Lundquist, M., LaPlant, Q., Healey, J.H., Elemento, O., Chung, C.H., Lee, N.Y., Imielenski, M., Nanjangud, G., Pe'er, D., Cleveland, D.W., Powell, S.N., Lammerding, J., Swanton, C., Cantley, L.C., 2018. Chromosomal instability drives metastasis through a cytosolic DNA response. Nature 553, 467–472.

Bakhoum, S.F., Silkworth, W.T., Nardi, I.K., Nicholson, J.M., Compton, D.A., Cimini, D., 2014. The mitotic origin of chromosomal instability. Curr. Biol. CB 24, R148-149. https://doi.org/10.1016/j.cub.2014.01.019

Bakhoum, S.F., Thompson, S.L., Manning, A.L., Compton, D.A., 2009b. Genome stability is ensured by temporal control of kinetochore-microtubule dynamics. Nat. Cell Biol. 11, 27–35.

Bancroft, J., Auckland, P., Samora, C.P., McAinsh, A.D., 2015. Chromosome congression is promoted by CENP-Q- and CENP-E-dependent pathways. J. Cell Sci. 128, 171–184.

Barber, T.D., McManus, K., Yuen, K.W.Y., Reis, M., Parmigiani, G., Shen, D., Barrett, I., Nouhi, Y., Spencer, F., Markowitz, S., Velculescu, V.E., Kinzler, K.W., Vogelstein, B., Lengauer, C., Hieter, P., 2008. Chromatid cohesion defects may underlie chromosome instability in human colorectal cancers. Proc. Natl. Acad. Sci. U. S. A. 105, 3443–3448.

Barbosa, D.J., Duro, J., Prevo, B., Cheerambathur, D.K., Carvalho, A.X., Gassmann, R., 2017. Dynactin binding to tyrosinated microtubules promotes centrosome centration in C. elegans by enhancing dynein-mediated organelle transport. PLoS Genet. 13, e1006941.

Bärenz, F., Mayilo, D., Gruss, O.J., 2011. Centriolar satellites: busy orbits around the centrosome. Eur. J. Cell Biol. 90, 983–989.

Barisic, M., Aguiar, P., Geley, S., Maiato, H., 2014. Kinetochore motors drive congression of peripheral polar chromosomes by overcoming random arm-ejection forces. Nat. Cell Biol. 16, 1249–1256.

Barisic, M., Maiato, H., 2016. The Tubulin Code: A Navigation System for Chromosomes during Mitosis. Trends Cell Biol. 26, 766–775.

Barisic, M., Maiato, H., 2015. Dynein prevents erroneous kinetochore-microtubule attachments in mitosis. Cell Cycle Georget. Tex 14, 3356–3361.

Barisic, M., Silva e Sousa, R., Tripathy, S.K., Magiera, M.M., Zaytsev, A.V., Pereira, A.L., Janke, C., Grishchuk, E.L., Maiato, H., 2015. Mitosis. Microtubule detyrosination guides chromosomes during mitosis. Science 348, 799–803.

Barisic, M., Sohm, B., Mikolcevic, P., Wandke, C., Rauch, V., Ringer, T., Hess, M., Bonn, G., Geley, S., 2010. Spindly/CCDC99 is required for efficient chromosome congression and mitotic checkpoint regulation. Mol. Biol. Cell 21, 1968–1981.

Bartsch, K., Knittler, K., Borowski, C., Rudnik, S., Damme, M., Aden, K., Spehlmann, M.E., Frey, N., Saftig, P., Chalaris, A., Rabe, B., 2017. Absence of RNase H2 triggers generation of immunogenic micronuclei removed by autophagy. Hum. Mol. Genet. 26, 3960–3972.

Basilico, F., Maffini, S., Weir, J.R., Prumbaum, D., Rojas, A.M., Zimniak, T., De Antoni, A., Jeganathan, S., Voss, B., van Gerwen, S., Krenn, V., Massimiliano, L., Valencia, A., Vetter, I.R., Herzog, F., Raunser, S., Pasqualato, S., Musacchio, A., 2014. The pseudo GTPase CENP-M drives human kinetochore assembly. eLife 3, e02978.

Basto, R., Lau, J., Vinogradova, T., Gardiol, A., Woods, C.G., Khodjakov, A., Raff, J.W., 2006. Flies without centrioles. Cell 125, 1375–1386.

Beauchene, N.A., Díaz-Martínez, L.A., Furniss, K., Hsu, W.-S., Tsai, H.-J., Chamberlain, C., Esponda, P., Giménez-Abián, J.F., Clarke, D.J., 2010. Rad21 is required for centrosome integrity in human cells independently of its role in chromosome cohesion. Cell Cycle Georget. Tex 9, 1774–1780.

Beck, M., Hurt, E., 2017. The nuclear pore complex: understanding its function through structural insight. Nat. Rev. Mol. Cell Biol. 18, 73–89.

Bernad, R., van der Velde, H., Fornerod, M., Pickersgill, H., 2004. Nup358/RanBP2 attaches to the nuclear pore complex via association with Nup88 and Nup214/CAN and plays a supporting role in CRM1-mediated nuclear protein export. Mol. Cell. Biol. 24, 2373–2384.

Bettencourt-Dias, M., Glover, D.M., 2007. Centrosome biogenesis and function: centrosomics brings new understanding. Nat. Rev. Mol. Cell Biol. 8, 451–463.

Bharadwaj, R., Qi, W., Yu, H., 2004. Identification of two novel components of the human NDC80 kinetochore complex. J. Biol. Chem. 279, 13076–13085.

Biggins, S., Murray, A.W., 2001. The budding yeast protein kinase Ipl1/Aurora allows the absence of tension to activate the spindle checkpoint. Genes Dev. 15, 3118–3129.

Birkbak, N.J., Eklund, A.C., Li, Q., McClelland, S.E., Endesfelder, D., Tan, P., Tan, I.B., Richardson, A.L., Szallasi, Z., Swanton, C., 2011. Paradoxical relationship between chromosomal instability and survival outcome in cancer. Cancer Res. 71, 3447–3452.

Blower, M.D., Nachury, M., Heald, R., Weis, K., 2005. A Rae1-containing ribonucleoprotein complex is required for mitotic spindle assembly. Cell 121, 223–234.

Bodakuntla, S., Jijumon, A.S., Villablanca, C., Gonzalez-Billault, C., Janke, C., 2019. Microtubule-Associated Proteins: Structuring the Cytoskeleton. Trends Cell Biol. 29, 804–

Bolhaqueiro, A.C.F., Ponsioen, B., Bakker, B., Klaasen, S.J., Kucukkose, E., van Jaarsveld, R.H., Vivié, J., Verlaan-Klink, I., Hami, N., Spierings, D.C.J., Sasaki, N., Dutta, D., Boj, S.F., Vries, R.G.J., Lansdorp, P.M., van de Wetering, M., van Oudenaarden, A., Clevers, H., Kranenburg, O., Foijer, F., Snippert, H.J.G., Kops, G.J.P.L., 2019. Ongoing chromosomal instability and karyotype evolution in human colorectal cancer organoids. Nat. Genet. 51, 824–834.

Bonaccorsi, S., Giansanti, M.G., Gatti, M., 1998. Spindle self-organization and cytokinesis during male meiosis in asterless mutants of Drosophila melanogaster. J. Cell Biol. 142, 751–761.

Bonassi, S., Znaor, A., Ceppi, M., Lando, C., Chang, W.P., Holland, N., Kirsch-Volders, M., Zeiger, E., Ban, S., Barale, R., Bigatti, M.P., Bolognesi, C., Cebulska-Wasilewska, A., Fabianova, E., Fucic, A., Hagmar, L., Joksic, G., Martelli, A., Migliore, L., Mirkova, E., Scarfi, M.R., Zijno, A., Norppa, H., Fenech, M., 2007. An increased micronucleus frequency in peripheral blood lymphocytes predicts the risk of cancer in humans. Carcinogenesis 28, 625–631.

Bonfils, C., Bec, N., Lacroix, B., Harricane, M.-C., Larroque, C., 2007. Kinetic analysis of tubulin assembly in the presence of the microtubule-associated protein TOGp. J. Biol. Chem. 282, 5570–5581.

Boveri, T., 2008. Concerning the origin of malignant tumours by Theodor Boveri. Translated and annotated by Henry Harris. J. Cell Sci. 121 Suppl 1, 1–84.

Brennan, C.M., Vaites, L.P., Wells, J.N., Santaguida, S., Paulo, J.A., Storchova, Z., Harper, J.W., Marsh, J.A., Amon, A., 2019. Protein aggregation mediates stoichiometry of protein complexes in aneuploid cells. Genes Dev. 33, 1031–1047.

Brito, D.A., Rieder, C.L., 2006. Mitotic checkpoint slippage in humans occurs via cyclin B destruction in the presence of an active checkpoint. Curr. Biol. CB 16, 1194–1200.

Brito, D.A., Yang, Z., Rieder, C.L., 2008. Microtubules do not promote mitotic slippage when the spindle assembly checkpoint cannot be satisfied. J. Cell Biol. 182, 623–629.

Brouhard, G.J., Stear, J.H., Noetzel, T.L., Al-Bassam, J., Kinoshita, K., Harrison, S.C., Howard, J., Hyman, A.A., 2008. XMAP215 is a processive microtubule polymerase. Cell 132, 79–88.

Burrell, R.A., Juul, N., Johnston, S.R., Reis-Filho, J.S., Szallasi, Z., Swanton, C., 2010. Targeting chromosomal instability and tumour heterogeneity in HER2-positive breast cancer. J. Cell. Biochem. 111, 782–790.

Cai, S., O'Connell, C.B., Khodjakov, A., Walczak, C.E., 2009a. Chromosome congression in the absence of kinetochore fibres. Nat. Cell Biol. 11, 832–838.

Cai, S., Weaver, L.N., Ems-McClung, S.C., Walczak, C.E., 2009b. Kinesin-14 family proteins HSET/XCTK2 control spindle length by cross-linking and sliding microtubules. Mol. Biol. Cell 20, 1348–1359.

Cai, X., Chiu, Y.-H., Chen, Z.J., 2014. The cGAS-cGAMP-STING pathway of cytosolic DNA sensing and signaling. Mol. Cell 54, 289–296.

Caldas, G.V., DeLuca, J.G., 2014. KNL1: bringing order to the kinetochore. Chromosoma 123, 169–181.

Cane, S., Ye, A.A., Luks-Morgan, S.J., Maresca, T.J., 2013. Elevated polar ejection forces stabilize kinetochore-microtubule attachments. J. Cell Biol. 200, 203–218.

Canman, J.C., Sharma, N., Straight, A., Shannon, K.B., Fang, G., Salmon, E.D., 2002. Anaphase onset does not require the microtubule-dependent depletion of kinetochore and centromere-binding proteins. J. Cell Sci. 115, 3787–3795.

Carleton, M., Mao, M., Biery, M., Warrener, P., Kim, S., Buser, C., Marshall, C.G., Fernandes, C., Annis, J., Linsley, P.S., 2006. RNA interference-mediated silencing of mitotic kinesin KIF14 disrupts cell cycle progression and induces cytokinesis failure. Mol. Cell. Biol. 26, 3853–3863.

Carter, S.L., Eklund, A.C., Kohane, I.S., Harris, L.N., Szallasi, Z., 2006. A signature of chromosomal instability inferred from gene expression profiles predicts clinical outcome in multiple human cancers. Nat. Genet. 38, 1043–1048.

Carvalho, A., Carmena, M., Sambade, C., Earnshaw, W.C., Wheatley, S.P., 2003. Survivin is required for stable checkpoint activation in taxol-treated HeLa cells. J. Cell Sci. 116, 2987–2998.

Casanova, C.M., Rybina, S., Yokoyama, H., Karsenti, E., Mattaj, I.W., 2008. Hepatoma up-regulated protein is required for chromatin-induced microtubule assembly independently of TPX2. Mol. Biol. Cell 19, 4900–4908.

Cassimeris, L., Becker, B., Carney, B., 2009. TOGp regulates microtubule assembly and density during mitosis and contributes to chromosome directional instability. Cell Motil. Cytoskeleton 66, 535–545.

Cassimeris, L., Morabito, J., 2004. TOGp, the human homolog of XMAP215/Dis1, is required for centrosome integrity, spindle pole organization, and bipolar spindle assembly. Mol. Biol. Cell 15, 1580–1590.

Chan, J.Y., 2011. A clinical overview of centrosome amplification in human cancers. Int. J. Biol. Sci. 7, 1122–1144.

Chan, K.L., Palmai-Pallag, T., Ying, S., Hickson, I.D., 2009. Replication stress induces sister-chromatid bridging at fragile site loci in mitosis. Nat. Cell Biol. 11, 753–760.

Chan, Y.W., Fava, L.L., Uldschmid, A., Schmitz, M.H.A., Gerlich, D.W., Nigg, E.A., Santamaria, A., 2009. Mitotic control of kinetochore-associated dynein and spindle orientation by human Spindly. J. Cell Biol. 185, 859–874.

Chan, Y.W., Jeyaprakash, A.A., Nigg, E.A., Santamaria, A., 2012. Aurora B controls kinetochore-microtubule attachments by inhibiting Ska complex-KMN network interaction. J. Cell Biol. 196, 563–571.

Chang, P., Coughlin, M., Mitchison, T.J., 2005. Tankyrase-1 polymerization of poly(ADP-ribose) is required for spindle structure and function. Nat. Cell Biol. 7, 1133–1139.

Chatel, G., Fahrenkrog, B., 2011. Nucleoporins: leaving the nuclear pore complex for a successful mitosis. Cell. Signal. 23, 1555–1562.

Cheeseman, I.M., 2014. The kinetochore. Cold Spring Harb. Perspect. Biol. 6, a015826. Cheeseman, I.M., Chappie, J.S., Wilson-Kubalek, E.M., Desai, A., 2006. The conserved KMN network constitutes the core microtubule-binding site of the kinetochore. Cell 127, 983–997.

Cheeseman, I.M., Desai, A., 2008. Molecular architecture of the kinetochore-microtubule interface. Nat. Rev. Mol. Cell Biol. 9, 33–46.

Cheeseman, L.P., Harry, E.F., McAinsh, A.D., Prior, I.A., Royle, S.J., 2013. Specific removal of TACC3-ch-TOG-clathrin at metaphase deregulates kinetochore fiber tension. J. Cell Sci. 126, 2102–2113.

Chen, Q., Sun, L., Chen, Z.J., 2016. Regulation and function of the cGAS-STING pathway of cytosolic DNA sensing. Nat. Immunol. 17, 1142–1149.

Cheng, T.-S., Hsiao, Y.-L., Lin, C.-C., Hsu, C.-M., Chang, M.-S., Lee, C.-I., Yu, R.C.-T., Huang, C.-Y.F., Howng, S.-L., Hong, Y.-R., 2007. hNinein is required for targeting spindle-associated protein Astrin to the centrosome during the S and G2 phases. Exp. Cell Res. 313, 1710–1721.

Chmátal, L., Yang, K., Schultz, R.M., Lampson, M.A., 2015. Spatial Regulation of Kinetochore Microtubule Attachments by Destabilization at Spindle Poles in Meiosis I. Curr. Biol. CB 25, 1835–1841.

Cho, J.-H., Chang, C.-J., Chen, C.-Y., Tang, T.K., 2006. Depletion of CPAP by RNAi disrupts centrosome integrity and induces multipolar spindles. Biochem. Biophys. Res. Commun. 339, 742–747.

Choi, C.-M., Seo, K.W., Jang, S.J., Oh, Y.-M., Shim, T.-S., Kim, W.S., Lee, D.-S., Lee, S.-D., 2009. Chromosomal instability is a risk factor for poor prognosis of adenocarcinoma of the lung: Fluorescence in situ hybridization analysis of paraffin-embedded tissue from Korean patients. Lung Cancer Amst. Neth. 64, 66–70.

Chuang, C., Pan, J., Hawke, D.H., Lin, S.-H., Yu-Lee, L., 2013. NudC deacetylation regulates mitotic progression. PloS One 8, e73841.

Chun, Y., Kim, R., Lee, S., 2016. Centromere Protein (CENP)-W Interacts with Heterogeneous Nuclear Ribonucleoprotein (hnRNP) U and May Contribute to Kinetochore-Microtubule Attachment in Mitotic Cells. PloS One 11, e0149127.

Chun, Y., Lee, M., Park, B., Lee, S., 2013. CSN5/JAB1 interacts with the centromeric components CENP-T and CENP-W and regulates their proteasome-mediated degradation. J. Biol. Chem. 288, 27208–27219.

Ciferri, C., Musacchio, A., Petrovic, A., 2007. The Ndc80 complex: hub of kinetochore activity. FEBS Lett. 581, 2862–2869.

Cimini, D., 2008. Merotelic kinetochore orientation, aneuploidy, and cancer. Biochim. Biophys. Acta 1786, 32–40.

Cimini, D., Cameron, L.A., Salmon, E.D., 2004. Anaphase spindle mechanics prevent mis-segregation of merotelically oriented chromosomes. Curr. Biol. CB 14, 2149–2155.

Cimini, D., Fioravanti, D., Salmon, E.D., Degrassi, F., 2002. Merotelic kinetochore orientation versus chromosome mono-orientation in the origin of lagging chromosomes in human primary cells. J. Cell Sci. 115, 507–515.

Cimini, D., Howell, B., Maddox, P., Khodjakov, A., Degrassi, F., Salmon, E.D., 2001. Merotelic kinetochore orientation is a major mechanism of aneuploidy in mitotic mammalian tissue cells. J. Cell Biol. 153, 517–527.

Cimini, D., Moree, B., Canman, J.C., Salmon, E.D., 2003. Merotelic kinetochore orientation occurs frequently during early mitosis in mammalian tissue cells and error correction is achieved by two different mechanisms. J. Cell Sci. 116, 4213–4225.

Cleveland, D.W., Mao, Y., Sullivan, K.F., 2003. Centromeres and kinetochores: from epigenetics to mitotic checkpoint signaling. Cell 112, 407–421.

Clute, P., Pines, J., 1999. Temporal and spatial control of cyclin B1 destruction in metaphase. Nat. Cell Biol. 1, 82–87.

Cohen-Sharir, Y., McFarland, J.M., Abdusamad, M., Marquis, C., Bernhard, S.V., Kazachkova, M., Tang, H., Ippolito, M.R., Laue, K., Zerbib, J., Malaby, H.L.H., Jones, A., Stautmeister, L.-M., Bockaj, I., Wardenaar, R., Lyons, N., Nagaraja, A., Bass, A.J., Spierings, D.C.J., Foijer, F., Beroukhim, R., Santaguida, S., Golub, T.R., Stumpff, J., Storchová, Z., Ben-David, U., 2021. Aneuploidy renders cancer cells vulnerable to mitotic checkpoint inhibition. Nature 590, 486–491.

Collin, P., Nashchekina, O., Walker, R., Pines, J., 2013. The spindle assembly checkpoint works like a rheostat rather than a toggle switch. Nat. Cell Biol. 15, 1378–1385.

Comai, L., 2005. The advantages and disadvantages of being polyploid. Nat. Rev. Genet. 6, 836–846.

Conduit, P.T., Wainman, A., Raff, J.W., 2015. Centrosome function and assembly in animal cells. Nat. Rev. Mol. Cell Biol. 16, 611–624.

Conway, W., Kiewisz, R., Fabig, G., Kelleher, C.P., Wu, H.-Y., Anjur-Dietrich, M., Müller-Reichert, T., Needleman, D.J., 2022. Self-organization of kinetochore-fibers in human mitotic spindles. eLife 11, e75458.

Crasta, K., Ganem, N.J., Dagher, R., Lantermann, A.B., Ivanova, E.V., Pan, Y., Nezi, L., Protopopov, A., Chowdhury, D., Pellman, D., 2012. DNA breaks and chromosome pulverization from errors in mitosis. Nature 482, 53–58.

Cross, R.A., McAinsh, A., 2014. Prime movers: the mechanochemistry of mitotic kinesins. Nat. Rev. Mol. Cell Biol. 15, 257–271.

Czaban, B.B., Forer, A., Bajer, A.S., 1993. Ultraviolet microbeam irradiation of chromosomal spindle fibres in Haemanthus katherinae endosperm. I. Behaviour of the irradiated region. J. Cell Sci. 105 (Pt 2), 571–578.

Dai, J., Kateneva, A.V., Higgins, J.M.G., 2009. Studies of haspin-depleted cells reveal that spindle-pole integrity in mitosis requires chromosome cohesion. J. Cell Sci. 122, 4168–4176.

Dai, J., Sultan, S., Taylor, S.S., Higgins, J.M.G., 2005. The kinase haspin is required for mitotic histone H3 Thr 3 phosphorylation and normal metaphase chromosome alignment. Genes Dev. 19, 472–488.

Dalton, W.B., Nandan, M.O., Moore, R.T., Yang, V.W., 2007. Human cancer cells commonly acquire DNA damage during mitotic arrest. Cancer Res. 67, 11487–11492.

Darlington, C.D., 1937. Recent Advances in Cytology, 2nd ed. ed. ; The Blakiston Company: Philadelphia, PA, USA.

Darzynkiewicz, Z., Gong, J., Juan, G., Ardelt, B., Traganos, F., 1996. Cytometry of cyclin proteins. Cytometry 25, 1–13.

Daum, J.R., Potapova, T.A., Sivakumar, S., Daniel, J.J., Flynn, J.N., Rankin, S., Gorbsky, G.J., 2011. Cohesion fatigue induces chromatid separation in cells delayed at metaphase. Curr. Biol. CB 21, 1018–1024.

Daum, J.R., Wren, J.D., Daniel, J.J., Sivakumar, S., McAvoy, J.N., Potapova, T.A., Gorbsky, G.J., 2009. Ska3 is required for spindle checkpoint silencing and the maintenance of chromosome cohesion in mitosis. Curr. Biol. CB 19, 1467–1472.

De Antoni, A., Pearson, C.G., Cimini, D., Canman, J.C., Sala, V., Nezi, L., Mapelli, M., Sironi, L., Faretta, M., Salmon, E.D., Musacchio, A., 2005. The Mad1/Mad2 complex as a template for Mad2 activation in the spindle assembly checkpoint. Curr. Biol. CB 15, 214–225.

De Brabander, M., Geuens, G., De Mey, J., Joniau, M., 1981. Nucleated assembly of mitotic microtubules in living PTK2 cells after release from nocodazole treatment. Cell Motil. 1, 469–483.

de Castro, I.J., Gil, R.S., Ligammari, L., Di Giacinto, M.L., Vagnarelli, P., 2018. CDK1 and PLK1 coordinate the disassembly and reassembly of the nuclear envelope in vertebrate mitosis. Oncotarget 9, 7763–7773.

De Luca, M., Brunetto, L., Asteriti, I.A., Giubettini, M., Lavia, P., Guarguaglini, G., 2008. Aurora-A and ch-TOG act in a common pathway in control of spindle pole integrity. Oncogene 27, 6539–6549.

De Luca, M., Lavia, P., Guarguaglini, G., 2006. A functional interplay between Aurora-A, Plk1 and TPX2 at spindle poles: Plk1 controls centrosomal localization of Aurora-A and TPX2 spindle association. Cell Cycle Georget. Tex 5, 296–303.

DeLuca, J.G., Dong, Y., Hergert, P., Strauss, J., Hickey, J.M., Salmon, E.D., McEwen, B.F., 2005. Hec1 and nuf2 are core components of the kinetochore outer plate essential for organizing microtubule attachment sites. Mol. Biol. Cell 16, 519–531.

DeLuca, J.G., Moree, B., Hickey, J.M., Kilmartin, J.V., Salmon, E.D., 2002. hNuf2 inhibition blocks stable kinetochore-microtubule attachment and induces mitotic cell death in HeLa cells. J. Cell Biol. 159, 549–555.

den Elzen, N., Pines, J., 2001. Cyclin A is destroyed in prometaphase and can delay chromosome alignment and anaphase. J. Cell Biol. 153, 121–136.

Denais, C.M., Gilbert, R.M., Isermann, P., McGregor, A.L., te Lindert, M., Weigelin, B., Davidson, P.M., Friedl, P., Wolf, K., Lammerding, J., 2016. Nuclear envelope rupture and repair during cancer cell migration. Science 352, 353–358.

Deng, L., Liang, H., Xu, M., Yang, X., Burnette, B., Arina, A., Li, X.-D., Mauceri, H., Beckett, M., Darga, T., Huang, X., Gajewski, T.F., Chen, Z.J., Fu, Y.-X., Weichselbaum, R.R., 2014. STING-Dependent Cytosolic DNA Sensing Promotes Radiation-Induced Type I Interferon-Dependent Antitumor Immunity in Immunogenic Tumors. Immunity 41, 843–852.

Dephoure, N., Hwang, S., O'Sullivan, C., Dodgson, S.E., Gygi, S.P., Amon, A., Torres, E.M., 2014. Quantitative proteomic analysis reveals posttranslational responses to aneuploidy in yeast. eLife 3, e03023.

Deretic, J., Kerr, A., Welburn, J.P.I., 2019. A rapid computational approach identifies SPICE1 as an Aurora kinase substrate. Mol. Biol. Cell 30, 312–323.

Desai, A., Mitchison, T.J., 1997. Microtubule polymerization dynamics. Annu. Rev. Cell Dev. Biol. 13, 83–117.

Desai, A., Verma, S., Mitchison, T.J., Walczak, C.E., 1999. Kin I kinesins are microtubule-destabilizing enzymes. Cell 96, 69–78.

Díaz-Martínez, L.A., Beauchene, N.A., Furniss, K., Esponda, P., Giménez-Abián, J.F., Clarke, D.J., 2010. Cohesin is needed for bipolar mitosis in human cells. Cell Cycle Georget. Tex 9, 1764–1773.

Dick, A.E., Gerlich, D.W., 2013. Kinetic framework of spindle assembly checkpoint signalling. Nat. Cell Biol. 15, 1370–1377.

Ditchfield, C., Johnson, V.L., Tighe, A., Ellston, R., Haworth, C., Johnson, T., Mortlock, A., Keen, N., Taylor, S.S., 2003a. Aurora B couples chromosome alignment with anaphase by targeting BubR1, Mad2, and Cenp-E to kinetochores. J. Cell Biol. 161, 267–280.

Ditchfield, C., Johnson, V.L., Tighe, A., Ellston, R., Haworth, C., Johnson, T., Mortlock, A., Keen, N., Taylor, S.S., 2003b. Aurora B couples chromosome alignment with anaphase by targeting BubR1, Mad2, and Cenp-E to kinetochores. J. Cell Biol. 161, 267–280.

Dobles, M., Liberal, V., Scott, M.L., Benezra, R., Sorger, P.K., 2000. Chromosome missegregation and apoptosis in mice lacking the mitotic checkpoint protein Mad2. Cell 101, 635–645.

Donehower, L.A., Soussi, T., Korkut, A., Liu, Y., Schultz, A., Cardenas, M., Li, X., Babur, O., Hsu, T.-K., Lichtarge, O., Weinstein, J.N., Akbani, R., Wheeler, D.A., 2019. Integrated Analysis of TP53 Gene and Pathway Alterations in The Cancer Genome Atlas. Cell Rep. 28, 3010.

Dou, Z., Ghosh, K., Vizioli, M.G., Zhu, J., Sen, P., Wangensteen, K.J., Simithy, J., Lan, Y., Lin, Y., Zhou, Z., Capell, B.C., Xu, C., Xu, M., Kieckhaefer, J.E., Jiang, T., Shoshkes-Carmel, M., Tanim, K.M.A.A., Barber, G.N., Seykora, J.T., Millar, S.E., Kaestner, K.H., Garcia, B.A., Adams, P.D., Berger, S.L., 2017. Cytoplasmic chromatin triggers inflammation in senescence and cancer. Nature 550, 402–406.

Draviam, V.M., Stegmeier, F., Nalepa, G., Sowa, M.E., Chen, J., Liang, A., Hannon, G.J., Sorger, P.K., Harper, J.W., Elledge, S.J., 2007. A functional genomic screen identifies a role for TAO1 kinase in spindle-checkpoint signalling. Nat. Cell Biol. 9, 556–564.

Drechsel, D.N., Kirschner, M.W., 1994. The minimum GTP cap required to stabilize microtubules. Curr. Biol. CB 4, 1053–1061.

Drpic, D., Pereira, A.J., Barisic, M., Maresca, T.J., Maiato, H., 2015. Polar Ejection Forces Promote the Conversion from Lateral to End-on Kinetochore-Microtubule Attachments on Mono-oriented Chromosomes. Cell Rep. 13, 460–468.

Du, Y., English, C.A., Ohi, R., 2010. The kinesin-8 Kif18A dampens microtubule plus-end dynamics. Curr. Biol. CB 20, 374–380.

Dujardin, D., Wacker, U.I., Moreau, A., Schroer, T.A., Rickard, J.E., De Mey, J.R., 1998. Evidence for a role of CLIP-170 in the establishment of metaphase chromosome alignment. J. Cell Biol. 141, 849–862.

Dumont, S., Mitchison, T.J., 2009. Force and length in the mitotic spindle. Curr. Biol. CB 19, R749-761.

Dunsch, A.K., Hammond, D., Lloyd, J., Schermelleh, L., Gruneberg, U., Barr, F.A., 2012. Dynein light chain 1 and a spindle-associated adaptor promote dynein asymmetry and spindle orientation. J. Cell Biol. 198, 1039–1054.

Dunsch, A.K., Linnane, E., Barr, F.A., Gruneberg, U., 2011. The astrin-kinastrin/SKAP complex localizes to microtubule plus ends and facilitates chromosome alignment. J. Cell Biol. 192, 959–968.

Dynek, J.N., Smith, S., 2004. Resolution of sister telomere association is required for progression through mitosis. Science 304, 97–100.

Egloff, M.P., Johnson, D.F., Moorhead, G., Cohen, P.T., Cohen, P., Barford, D., 1997. Structural basis for the recognition of regulatory subunits by the catalytic subunit of protein phosphatase 1. EMBO J. 16, 1876–1887.

Einarson, M.B., Cukierman, E., Compton, D.A., Golemis, E.A., 2004. Human enhancer of invasion-cluster, a coiled-coil protein required for passage through mitosis. Mol. Cell. Biol. 24, 3957–3971.

Elting, M.W., Hueschen, C.L., Udy, D.B., Dumont, S., 2014. Force on spindle microtubule minus ends moves chromosomes. J. Cell Biol. 206, 245–256.

Equilibrina, I., Matsunaga, S., Morimoto, A., Hashimoto, T., Uchiyama, S., Fukui, K., 2013. ASURA (PHB2) interacts with Scc1 through chromatin. Cytogenet. Genome Res. 139, 225–233.

Fang, L., Seki, A., Fang, G., 2009. SKAP associates with kinetochores and promotes the metaphase-to-anaphase transition. Cell Cycle Georget. Tex 8, 2819–2827.

Ferenz, N.P., Paul, R., Fagerstrom, C., Mogilner, A., Wadsworth, P., 2009. Dynein antagonizes eg5 by crosslinking and sliding antiparallel microtubules. Curr. Biol. CB 19, 1833–1838.

Fernández-Casañas, M., Chan, K.-L., 2018. The Unresolved Problem of DNA Bridging. Genes 9, 623.

Ferrandiz, N., Downie, L., Starling, G.P., Royle, S.J., 2022. Endomembranes promote chromosome missegregation by ensheathing misaligned chromosomes. J. Cell Biol. 221, e202203021.

Ferreira, L.T., Orr, B., Rajendraprasad, G., Pereira, A.J., Lemos, C., Lima, J.T., Guasch Boldú, C., Ferreira, J.G., Barisic, M., Maiato, H., 2020. α-Tubulin detyrosination impairs mitotic error correction by suppressing MCAK centromeric activity. J. Cell Biol. 219, e201910064.

Fielding, A.B., Dobreva, I., McDonald, P.C., Foster, L.J., Dedhar, S., 2008. Integrin-linked kinase localizes to the centrosome and regulates mitotic spindle organization. J. Cell Biol. 180, 681–689.

Fielding, A.B., Lim, S., Montgomery, K., Dobreva, I., Dedhar, S., 2011. A critical role of integrin-linked kinase, ch-TOG and TACC3 in centrosome clustering in cancer cells. Oncogene 30, 521–534.

Fink, G., Schuchardt, I., Colombelli, J., Stelzer, E., Steinberg, G., 2006. Dynein-mediated pulling forces drive rapid mitotic spindle elongation in Ustilago maydis. EMBO J. 25, 4897–4908.

Flynn, P.J., Koch, P.D., Mitchison, T.J., 2021. Chromatin bridges, not micronuclei, activate cGAS after drug-induced mitotic errors in human cells. Proc. Natl. Acad. Sci. U. S. A. 118, e2103585118.

Foijer, F., Xie, S.Z., Simon, J.E., Bakker, P.L., Conte, N., Davis, S.H., Kregel, E., Jonkers, J., Bradley, A., Sorger, P.K., 2014. Chromosome instability induced by Mps1 and p53

mutation generates aggressive lymphomas exhibiting aneuploidy-induced stress. Proc. Natl. Acad. Sci. U. S. A. 111, 13427–13432.

Foley, E.A., Kapoor, T.M., 2013. Microtubule attachment and spindle assembly checkpoint signalling at the kinetochore. Nat. Rev. Mol. Cell Biol. 14, 25–37.

Foltz, D.R., Jansen, L.E.T., Black, B.E., Bailey, A.O., Yates, J.R., Cleveland, D.W., 2006. The human CENP-A centromeric nucleosome-associated complex. Nat. Cell Biol. 8, 458–469.

Fong, C.S., Mazo, G., Das, T., Goodman, J., Kim, M., O'Rourke, B.P., Izquierdo, D., Tsou, M.-F.B., 2016. 53BP1 and USP28 mediate p53-dependent cell cycle arrest in response to centrosome loss and prolonged mitosis. eLife 5, e16270.

Fonseca, C.L., Malaby, H.L.H., Sepaniac, L.A., Martin, W., Byers, C., Czechanski, A., Messinger, D., Tang, M., Ohi, R., Reinholdt, L.G., Stumpff, J., 2019. Mitotic chromosome alignment ensures mitotic fidelity by promoting interchromosomal compaction during anaphase. J. Cell Biol. 218, 1148–1163.

Foraker, A.B., Camus, S.M., Evans, T.M., Majeed, S.R., Chen, C.-Y., Taner, S.B., Corrêa, I.R., Doxsey, S.J., Brodsky, F.M., 2012. Clathrin promotes centrosome integrity in early mitosis through stabilization of centrosomal ch-TOG. J. Cell Biol. 198, 591–605.

Forer, A., 1965. LOCAL REDUCTION OF SPINDLE FIBER BIREFRINGENCE IN LIVING NEPHROTOMA SUTURALIS (LOEW) SPERMATOCYTES INDUCED BY ULTRAVIOLET MICROBEAM IRRADIATION. J. Cell Biol. 25, SUPPL:95-117.

Franzke, B., Schwingshackl, L., Wagner, K.-H., 2020. Chromosomal damage measured by the cytokinesis block micronucleus cytome assay in diabetes and obesity - A systematic review and meta-analysis. Mutat. Res. Rev. Mutat. Res. 786, 108343.

Frémont, S., Gérard, A., Galloux, M., Janvier, K., Karess, R.E., Berlioz-Torrent, C., 2013. Beclin-1 is required for chromosome congression and proper outer kinetochore assembly. EMBO Rep. 14, 364–372.

Fukagawa, T., Earnshaw, W.C., 2014. The centromere: chromatin foundation for the kinetochore machinery. Dev. Cell 30, 496–508.

Fuller, B.G., Lampson, M.A., Foley, E.A., Rosasco-Nitcher, S., Le, K.V., Tobelmann, P., Brautigan, D.L., Stukenberg, P.T., Kapoor, T.M., 2008. Midzone activation of aurora B in anaphase produces an intracellular phosphorylation gradient. Nature 453, 1132–1136.

Funabiki, H., Murray, A.W., 2000. The Xenopus chromokinesin Xkid is essential for metaphase chromosome alignment and must be degraded to allow anaphase chromosome movement. Cell 102, 411–424.

Gaetz, J., Kapoor, T.M., 2004. Dynein/dynactin regulate metaphase spindle length by targeting depolymerizing activities to spindle poles. J. Cell Biol. 166, 465–471.

Gaitanos, T.N., Santamaria, A., Jeyaprakash, A.A., Wang, B., Conti, E., Nigg, E.A., 2009. Stable kinetochore-microtubule interactions depend on the Ska complex and its new component Ska3/C13Orf3. EMBO J. 28, 1442–1452.

Galimberti, F., Thompson, S.L., Ravi, S., Compton, D.A., Dmitrovsky, E., 2011. Anaphase catastrophe is a target for cancer therapy. Clin. Cancer Res. Off. J. Am. Assoc. Cancer Res. 17, 1218–1222.

Gambe, A.E., Matsunaga, S., Takata, H., Ono-Maniwa, R., Baba, A., Uchiyama, S., Fukui, K., 2009. A nucleolar protein RRS1 contributes to chromosome congression. FEBS Lett. 583, 1951–1956.

Gamulin, M., Kopjar, N., Grgić, M., Ramić, S., Bisof, V., Garaj-Vrhovac, V., 2008. Genome damage in oropharyngeal cancer patients treated by radiotherapy. Croat. Med. J. 49, 515–527.

Gandhi, R., Bonaccorsi, S., Wentworth, D., Doxsey, S., Gatti, M., Pereira, A., 2004. The Drosophila kinesin-like protein KLP67A is essential for mitotic and male meiotic spindle assembly. Mol. Biol. Cell 15, 121–131.

Gandhi, S.R., Gierliński, M., Mino, A., Tanaka, K., Kitamura, E., Clayton, L., Tanaka, T.U., 2011. Kinetochore-dependent microtubule rescue ensures their efficient and sustained interactions in early mitosis. Dev. Cell 21, 920–933.

Ganem, N.J., Compton, D.A., 2004. The KinI kinesin Kif2a is required for bipolar spindle assembly through a functional relationship with MCAK. J. Cell Biol. 166, 473–478.

Ganem, N.J., Godinho, S.A., Pellman, D., 2009. A mechanism linking extra centrosomes to chromosomal instability. Nature 460, 278–282.

Ganem, N.J., Upton, K., Compton, D.A., 2005. Efficient mitosis in human cells lacking poleward microtubule flux. Curr. Biol. CB 15, 1827–1832.

Gard, D.L., Kirschner, M.W., 1987. A microtubule-associated protein from Xenopus eggs that specifically promotes assembly at the plus-end. J. Cell Biol. 105, 2203–2215.

Garrett, S., Auer, K., Compton, D.A., Kapoor, T.M., 2002. hTPX2 is required for normal spindle morphology and centrosome integrity during vertebrate cell division. Curr. Biol. CB 12, 2055–2059.

Gascoigne, K.E., Taylor, S.S., 2008. Cancer cells display profound intra- and interline variation following prolonged exposure to antimitotic drugs. Cancer Cell 14, 111–122.

Gassmann, R., Carvalho, A., Henzing, A.J., Ruchaud, S., Hudson, D.F., Honda, R., Nigg, E.A., Gerloff, D.L., Earnshaw, W.C., 2004. Borealin: a novel chromosomal passenger required for stability of the bipolar mitotic spindle. J. Cell Biol. 166, 179–191.

Gassmann, R., Holland, A.J., Varma, D., Wan, X., Civril, F., Cleveland, D.W., Oegema, K., Salmon, E.D., Desai, A., 2010. Removal of Spindly from microtubule-attached kinetochores controls spindle checkpoint silencing in human cells. Genes Dev. 24, 957–971.

Gatlin, J.C., Bloom, K., 2010. Microtubule motors in eukaryotic spindle assembly and maintenance. Semin. Cell Dev. Biol. 21, 248–254.

Geiger, T., Cox, J., Mann, M., 2010. Proteomic changes resulting from gene copy number variations in cancer cells. PLoS Genet. 6, e1001090.

Gergely, F., Draviam, V.M., Raff, J.W., 2003. The ch-TOG/XMAP215 protein is essential for spindle pole organization in human somatic cells. Genes Dev. 17, 336–341.

Ghongane, P., Kapanidou, M., Asghar, A., Elowe, S., Bolanos-Garcia, V.M., 2014. The dynamic protein Knl1 - a kinetochore rendezvous. J. Cell Sci. 127, 3415–3423.

Ghosh, M., Saha, S., Bettke, J., Nagar, R., Parrales, A., Iwakuma, T., van der Velden, A.W.M., Martinez, L.A., 2021. Mutant p53 suppresses innate immune signaling to promote tumorigenesis. Cancer Cell 39, 494-508.e5.

Giam, M., Wong, C.K., Low, J.S., Sinelli, M., Dreesen, O., Rancati, G., 2020. P53 induces senescence in the unstable progeny of aneuploid cells. Cell Cycle Georget. Tex 19, 3508–3520.

Girão, H., Maiato, H., 2020. Measurement of Microtubule Half-Life and Poleward Flux in the Mitotic Spindle by Photoactivation of Fluorescent Tubulin. Methods Mol. Biol. Clifton NJ 2101, 235–246.

Glotzer, M., 2009. The 3Ms of central spindle assembly: microtubules, motors and MAPs. Nat. Rev. Mol. Cell Biol. 10, 9–20.

Glück, S., Guey, B., Gulen, M.F., Wolter, K., Kang, T.-W., Schmacke, N.A., Bridgeman, A., Rehwinkel, J., Zender, L., Ablasser, A., 2017. Innate immune sensing of cytosolic chromatin fragments through cGAS promotes senescence. Nat. Cell Biol. 19, 1061–1070.

Godek, K.M., Kabeche, L., Compton, D.A., 2015. Regulation of kinetochore-microtubule attachments through homeostatic control during mitosis. Nat. Rev. Mol. Cell Biol. 16, 57–64.

Godek, K.M., Venere, M., Wu, Q., Mills, K.D., Hickey, W.F., Rich, J.N., Compton, D.A., 2016. Chromosomal Instability Affects the Tumorigenicity of Glioblastoma Tumor-Initiating Cells. Cancer Discov. 6, 532–545.

Gönczy, P., Hatzopoulos, G.N., 2019. Centriole assembly at a glance. J. Cell Sci. 132, jcs228833.

Goode, D, 1981. Microtubule turnover as a mechanism of mitosis and its possible evolution. Biosystems 271–287.

Gorbsky, G.J., 2013. Cohesion fatigue. Curr. Biol. CB 23, R986–R988.

Gordon, D.J., Resio, B., Pellman, D., 2012. Causes and consequences of aneuploidy in cancer. Nat. Rev. Genet. 13, 189–203.

Goshima, G., 2011. Identification of a TPX2-like microtubule-associated protein in Drosophila. PloS One 6, e28120.

Goshima, G., Scholey, J.M., 2010. Control of mitotic spindle length. Annu. Rev. Cell Dev. Biol. 26, 21–57.

Goshima, G., Vale, R.D., 2003. The roles of microtubule-based motor proteins in mitosis: comprehensive RNAi analysis in the Drosophila S2 cell line. J. Cell Biol. 162, 1003–1016.

Goshima, G., Wollman, R., Stuurman, N., Scholey, J.M., Vale, R.D., 2005. Length control of the metaphase spindle. Curr. Biol. CB 15, 1979–1988.

Grallert, A., Boke, E., Hagting, A., Hodgson, B., Connolly, Y., Griffiths, J.R., Smith, D.L., Pines, J., Hagan, I.M., 2015. A PP1-PP2A phosphatase relay controls mitotic progression. Nature 517, 94–98.

Gratia, M., Rodero, M.P., Conrad, C., Bou Samra, E., Maurin, M., Rice, G.I., Duffy, D., Revy, P., Petit, F., Dale, R.C., Crow, Y.J., Amor-Gueret, M., Manel, N., 2019. Bloom syndrome protein restrains innate immune sensing of micronuclei by cGAS. J. Exp. Med. 216, 1199–1213.

Grim, J.E., Knoblaugh, S.E., Guthrie, K.A., Hagar, A., Swanger, J., Hespelt, J., Delrow, J.J., Small, T., Grady, W.M., Nakayama, K.I., Clurman, B.E., 2012. Fbw7 and p53 cooperatively suppress advanced and chromosomally unstable intestinal cancer. Mol. Cell. Biol. 32, 2160–2167.

Gruneberg, U., Neef, R., Honda, R., Nigg, E.A., Barr, F.A., 2004. Relocation of Aurora B from centromeres to the central spindle at the metaphase to anaphase transition requires MKlp2. J. Cell Biol. 166, 167–172.

Gudimchuk, N., Vitre, B., Kim, Y., Kiyatkin, A., Cleveland, D.W., Ataullakhanov, F.I., Grishchuk, E.L., 2013. Kinetochore kinesin CENP-E is a processive bi-directional tracker of dynamic microtubule tips. Nat. Cell Biol. 15, 1079–1088.

Guimaraes, G.J., Deluca, J.G., 2009. Connecting with Ska, a key complex at the kinetochore-microtubule interface. EMBO J. 28, 1375–1377.

Gupta, M.L., Carvalho, P., Roof, D.M., Pellman, D., 2006. Plus end-specific depolymerase activity of Kip3, a kinesin-8 protein, explains its role in positioning the yeast mitotic spindle. Nat. Cell Biol. 8, 913–923.

Gutiérrez-Caballero, C., Cebollero, L.R., Pendás, A.M., 2012. Shugoshins: from protectors of cohesion to versatile adaptors at the centromere. Trends Genet. TIG 28, 351–360.

Hahn, P., Schmidt, C., Weber, M., Kang, J., Bielke, W., 2004. RNA interference: PCR strategies for the quantification of stable degradation-fragments derived from siRNA-targeted mRNAs. Biomol. Eng. 21, 113–117.

Hakozaki, Y., Kashima, Y., Morita, T.Y., Tanaka, K., Kobayashi, S.S., Ohashi, A., 2021. Abstract 1030: CENP-E inhibition generates micronucleus formation activating the cGAS-STING pathway in cancer cells. Cancer Res. 81, 1030.

Hanisch, A., Silljé, H.H.W., Nigg, E.A., 2006. Timely anaphase onset requires a novel spindle and kinetochore complex comprising Ska1 and Ska2. EMBO J. 25, 5504–5515.

Hanks, S., Coleman, K., Reid, S., Plaja, A., Firth, H., Fitzpatrick, D., Kidd, A., Méhes, K., Nash, R., Robin, N., Shannon, N., Tolmie, J., Swansbury, J., Irrthum, A., Douglas, J., Rahman, N., 2004. Constitutional aneuploidy and cancer predisposition caused by biallelic mutations in BUB1B. Nat. Genet. 36, 1159–1161.

Hara, M., Fukagawa, T., 2018. Kinetochore assembly and disassembly during mitotic entry and exit. Curr. Opin. Cell Biol. 52, 73–81. https://doi.org/10.1016/j.ceb.2018.02.005

Harding, S.M., Benci, J.L., Irianto, J., Discher, D.E., Minn, A.J., Greenberg, R.A., 2017. Mitotic progression following DNA damage enables pattern recognition within micronuclei. Nature 548, 466–470.

Haren, L., Gnadt, N., Wright, M., Merdes, A., 2009. NuMA is required for proper spindle assembly and chromosome alignment in prometaphase. BMC Res. Notes 2, 64.

Hartwell, L.H., Weinert, T.A., 1989. Checkpoints: controls that ensure the order of cell cycle events. Science 246, 629–634.

Hashizume, C., Nakano, H., Yoshida, K., Wong, R.W., 2010. Characterization of the role of the tumor marker Nup88 in mitosis. Mol. Cancer 9, 119.

Hassold, T., Hall, H., Hunt, P., 2007. The origin of human aneuploidy: where we have been, where we are going. Hum. Mol. Genet. 16 Spec No. 2, R203-208.

Hassold, T., Hunt, P., 2001. To err (meiotically) is human: the genesis of human aneuploidy. Nat. Rev. Genet. 2, 280–291.

Hatch, E., Hetzer, M., 2014. Breaching the nuclear envelope in development and disease. J. Cell Biol. 205, 133–141.

Hatch, E.M., Fischer, A.H., Deerinck, T.J., Hetzer, M.W., 2013. Catastrophic nuclear envelope collapse in cancer cell micronuclei. Cell 154, 47–60.

Hatch, E.M., Hetzer, M.W., 2016. Nuclear envelope rupture is induced by actin-based nucleus confinement. J. Cell Biol. 215, 27–36.

Hauf, S., Cole, R.W., LaTerra, S., Zimmer, C., Schnapp, G., Walter, R., Heckel, A., van Meel, J., Rieder, C.L., Peters, J.-M., 2003. The small molecule Hesperadin reveals a role for Aurora B in correcting kinetochore-microtubule attachment and in maintaining the spindle assembly checkpoint. J. Cell Biol. 161, 281–294.

He, J., Zhang, Z., Ouyang, M., Yang, F., Hao, H., Lamb, K.L., Yang, J., Yin, Y., Shen, W.H., 2016. PTEN regulates EG5 to control spindle architecture and chromosome congression during mitosis. Nat. Commun. 7, 12355.

Hégarat, N., Smith, E., Nayak, G., Takeda, S., Eyers, P.A., Hochegger, H., 2011. Aurora A and Aurora B jointly coordinate chromosome segregation and anaphase microtubule dynamics. J. Cell Biol. 195, 1103–1113.

Hein, J.B., Nilsson, J., 2014. Stable MCC binding to the APC/C is required for a functional spindle assembly checkpoint. EMBO Rep. 15, 264–272.

Hepperla, A.J., Willey, P.T., Coombes, C.E., Schuster, B.M., Gerami-Nejad, M., McClellan, M., Mukherjee, S., Fox, J., Winey, M., Odde, D.J., O'Toole, E., Gardner, M.K., 2014. Minus-end-directed Kinesin-14 motors align antiparallel microtubules to control metaphase spindle length. Dev. Cell 31, 61–72.

Hinchcliffe, E.H., 2011. The centrosome and bipolar spindle assembly: does one have anything to do with the other? Cell Cycle Georget. Tex 10, 3841–3848.

Hinchcliffe, E.H., Day, C.A., Karanjeet, K.B., Fadness, S., Langfald, A., Vaughan, K.T., Dong, Z., 2016. Chromosome missegregation during anaphase triggers p53 cell cycle arrest through histone H3.3 Ser31 phosphorylation. Nat. Cell Biol. 18, 668–675.

Hinchcliffe, E.H., Miller, F.J., Cham, M., Khodjakov, A., Sluder, G., 2001. Requirement of a centrosomal activity for cell cycle progression through G1 into S phase. Science 291, 1547–1550.

Hoar, K., Chakravarty, A., Rabino, C., Wysong, D., Bowman, D., Roy, N., Ecsedy, J.A., 2007. MLN8054, a small-molecule inhibitor of Aurora A, causes spindle pole and chromosome congression defects leading to aneuploidy. Mol. Cell. Biol. 27, 4513–4525.

Hochegger, H., Takeda, S., Hunt, T., 2008. Cyclin-dependent kinases and cell-cycle transitions: does one fit all? Nat. Rev. Mol. Cell Biol. 9, 910–916.

Hoffman, D.B., Pearson, C.G., Yen, T.J., Howell, B.J., Salmon, E.D., 2001. Microtubule-dependent changes in assembly of microtubule motor proteins and mitotic spindle checkpoint proteins at PtK1 kinetochores. Mol. Biol. Cell 12, 1995–2009.

Holder, J., Poser, E., Barr, F.A., 2019. Getting out of mitosis: spatial and temporal control of mitotic exit and cytokinesis by PP1 and PP2A. FEBS Lett. 593, 2908–2924.

Holland, A.J., Cleveland, D.W., 2009. Boveri revisited: chromosomal instability, aneuploidy and tumorigenesis. Nat. Rev. Mol. Cell Biol. 10, 478–487.

Holmfeldt, P., Zhang, X., Stenmark, S., Walczak, C.E., Gullberg, M., 2005. CaMKIIgamma-mediated inactivation of the Kin I kinesin MCAK is essential for bipolar spindle formation. EMBO J. 24, 1256–1266.

Holt, S.V., Vergnolle, M.A.S., Hussein, D., Wozniak, M.J., Allan, V.J., Taylor, S.S., 2005. Silencing Cenp-F weakens centromeric cohesion, prevents chromosome alignment and activates the spindle checkpoint. J. Cell Sci. 118, 4889–4900.

Honda, S., Marumoto, T., Hirota, T., Nitta, M., Arima, Y., Ogawa, M., Saya, H., 2004. Activation of m-calpain is required for chromosome alignment on the metaphase plate during mitosis. J. Biol. Chem. 279, 10615–10623.

Hong, C., Tijhuis, A.E., Foijer, F., 2019. The cGAS Paradox: Contrasting Roles for cGAS-STING Pathway in Chromosomal Instability. Cells 8, E1228.

Horgan, C.P., Hanscom, S.R., McCaffrey, M.W., 2011. Dynein LIC1 localizes to the mitotic spindle and midbody and LIC2 localizes to spindle poles during cell division. Cell Biol. Int. 35, 171–178.

Howell, B.J., Hoffman, D.B., Fang, G., Murray, A.W., Salmon, E.D., 2000. Visualization of Mad2 dynamics at kinetochores, along spindle fibers, and at spindle poles in living cells. J. Cell Biol. 150, 1233–1250.

Howell, B.J., McEwen, B.F., Canman, J.C., Hoffman, D.B., Farrar, E.M., Rieder, C.L., Salmon, E.D., 2001. Cytoplasmic dynein/dynactin drives kinetochore protein transport to the spindle poles and has a role in mitotic spindle checkpoint inactivation. J. Cell Biol. 155, 1159–1172.

Hoyt, M.A., Totis, L., Roberts, B.T., 1991. S. cerevisiae genes required for cell cycle arrest in response to loss of microtubule function. Cell 66, 507–517.

Hu, Y., Manasrah, B.K., McGregor, S.M., Lera, R.F., Norman, R.X., Tucker, J.B., Scribano, C.M., Yan, R.E., Humayun, M., Wisinski, K.B., Tevaarwerk, A.J., O'Regan, R.M., Wilke, L.G., Weaver, B.A., Beebe, D.J., Jin, N., Burkard, M.E., 2021. Paclitaxel Induces Micronucleation and Activates Pro-Inflammatory cGAS-STING Signaling in Triple-Negative Breast Cancer. Mol. Cancer Ther. 20, 2553–2567.

Hua, S., Wang, Z., Jiang, K., Huang, Y., Ward, T., Zhao, L., Dou, Z., Yao, X., 2011. CENP-U cooperates with Hec1 to orchestrate kinetochore-microtubule attachment. J. Biol. Chem. 286, 1627–1638.

Huang, Y., Hou, H., Yi, Q., Zhang, Y., Chen, D., Jiang, E., Xia, Y., Fenech, M., Shi, Q., 2011. The fate of micronucleated cells post X-irradiation detected by live cell imaging. DNA Repair 10, 629–638.

Huang, Y., Wang, W., Yao, P., Wang, X., Liu, X., Zhuang, X., Yan, F., Zhou, J., Du, J., Ward, T., Zou, H., Zhang, J., Fang, G., Ding, X., Dou, Z., Yao, X., 2012. CENP-E kinesin interacts with SKAP protein to orchestrate accurate chromosome segregation in mitosis. J. Biol. Chem. 287, 1500–1509.

Huang, Y., Yao, Y., Xu, H.-Z., Wang, Z.-G., Lu, L., Dai, W., 2009. Defects in chromosome congression and mitotic progression in KIF18A-deficient cells are partly mediated through impaired functions of CENP-E. Cell Cycle Georget. Tex 8, 2643–2649.

Ide, A.H., DeLuca, K.F., Wiggan, O., Markus, S.M., DeLuca, J.G., 2023. The role of kinetochore dynein in checkpoint silencing is restricted to disassembly of the corona. Mol. Biol. Cell mbcE23040130.

Inoué, S., 1964. Organization and Function of the Mitotic Spindle. Elsevier, pp. 549–598.

Iourov, I.Y., Vorsanova, S.G., Liehr, T., Yurov, Y.B., 2009. Aneuploidy in the normal, Alzheimer's disease and ataxia-telangiectasia brain: differential expression and pathological meaning. Neurobiol. Dis. 34, 212–220.

Ishikawa, K., Makanae, K., Iwasaki, S., Ingolia, N.T., Moriya, H., 2017. Post-Translational Dosage Compensation Buffers Genetic Perturbations to Stoichiometry of Protein Complexes. PLoS Genet. 13, e1006554.

Itoh, G., Sugino, S., Ikeda, M., Mizuguchi, M., Kanno, S., Amin, M.A., Iemura, K., Yasui, A., Hirota, T., Tanaka, K., 2013. Nucleoporin Nup188 is required for chromosome alignment in mitosis. Cancer Sci. 104, 871–879.

Iwaizumi, M., Shinmura, K., Mori, H., Yamada, H., Suzuki, M., Kitayama, Y., Igarashi, H., Nakamura, T., Suzuki, H., Watanabe, Y., Hishida, A., Ikuma, M., Sugimura, H., 2009. Human Sgo1 downregulation leads to chromosomal instability in colorectal cancer. Gut 58, 249–260.

Iwakiri, Y., Kamakura, S., Hayase, J., Sumimoto, H., 2013. Interaction of NuMA protein with the kinesin Eg5: its possible role in bipolar spindle assembly and chromosome alignment. Biochem. J. 451, 195–204.

Izutsu, K., 1961. Effects of ultraviolet microbeam irradiation upon division in grasshoper spermatocytes. II. Results of irradiation during metaphase and anaphase I. Mie Med J 213–232.

Izutsu, K., 1959. Irradiation of parts of single mitotic apparatus in grasshopper spermatocytes with an ultraviolet-microbeam. Mie Med J 15–29.

Jamal-Hanjani, M., A'Hern, R., Birkbak, N.J., Gorman, P., Grönroos, E., Ngang, S., Nicola, P., Rahman, L., Thanopoulou, E., Kelly, G., Ellis, P., Barrett-Lee, P., Johnston, S.R.D., Bliss, J., Roylance, R., Swanton, C., 2015. Extreme chromosomal instability forecasts improved outcome in ER-negative breast cancer: a prospective validation cohort study from the TACT trial. Ann. Oncol. Off. J. Eur. Soc. Med. Oncol. 26, 1340–1346. Jang, C.-Y., Coppinger, J.A., Yates, J.R., Fang, G., 2011. Mitotic kinases regulate MT-polymerizing/MT-bundling activity of DDA3. Biochem. Biophys. Res. Commun. 408, 174–179.

Jang, C.-Y., Coppinger, J.A., Yates, J.R., Fang, G., 2010. Phospho-regulation of DDA3 function in mitosis. Biochem. Biophys. Res. Commun. 393, 259–263.

Jang, C.-Y., Fang, G., 2011. DDA3 associates with MCAK and controls chromosome congression. Biochem. Biophys. Res. Commun. 407, 610–614.

Jang, C.-Y., Wong, J., Coppinger, J.A., Seki, A., Yates, J.R., Fang, G., 2008. DDA3 recruits microtubule depolymerase Kif2a to spindle poles and controls spindle dynamics and mitotic chromosome movement. J. Cell Biol. 181, 255–267.

Janke, C., 2014. The tubulin code: molecular components, readout mechanisms, and functions. J. Cell Biol. 206, 461–472.

Janke, C., Bulinski, J.C., 2011. Post-translational regulation of the microtubule cytoskeleton: mechanisms and functions. Nat. Rev. Mol. Cell Biol. 12, 773–786.

Janke, C., Magiera, M.M., 2020. The tubulin code and its role in controlling microtubule properties and functions. Nat. Rev. Mol. Cell Biol. 21, 307–326.

Janssen, A., van der Burg, M., Szuhai, K., Kops, G.J.P.L., Medema, R.H., 2011. Chromosome segregation errors as a cause of DNA damage and structural chromosome aberrations. Science 333, 1895–1898.

Jaqaman, K., King, E.M., Amaro, A.C., Winter, J.R., Dorn, J.F., Elliott, H.L., McHedlishvili, N., McClelland, S.E., Porter, I.M., Posch, M., Toso, A., Danuser, G., McAinsh, A.D., Meraldi, P., Swedlow, J.R., 2010. Kinetochore alignment within the metaphase plate is regulated by centromere stiffness and microtubule depolymerases. J. Cell Biol. 188, 665–679.

Jaramillo-Lambert, A., Hao, J., Xiao, H., Li, Y., Han, Z., Zhu, W., 2013. Acidic nucleoplasmic DNA-binding protein (And-1) controls chromosome congression by regulating the assembly of centromere protein A (CENP-A) at centromeres. J. Biol. Chem. 288, 1480–1488.

Joglekar, A.P., 2016. A Cell Biological Perspective on Past, Present and Future Investigations of the Spindle Assembly Checkpoint. Biology 5, E44.

Johnson, V.L., Scott, M.I.F., Holt, S.V., Hussein, D., Taylor, S.S., 2004. Bub1 is required for kinetochore localization of BubR1, Cenp-E, Cenp-F and Mad2, and chromosome congression. J. Cell Sci. 117, 1577–1589.

Jones, M.H., He, X., Giddings, T.H., Winey, M., 2001. Yeast Dam1p has a role at the kinetochore in assembly of the mitotic spindle. Proc. Natl. Acad. Sci. U. S. A. 98, 13675–13680.

Jordan, M.A., Toso, R.J., Thrower, D., Wilson, L., 1993. Mechanism of mitotic block and inhibition of cell proliferation by taxol at low concentrations. Proc. Natl. Acad. Sci. U. S. A. 90, 9552–9556.

Joseph, J., Liu, S.-T., Jablonski, S.A., Yen, T.J., Dasso, M., 2004. The RanGAP1-RanBP2 complex is essential for microtubule-kinetochore interactions in vivo. Curr. Biol. CB 14, 611–617.

Jusino, S., Fernández-Padín, F.M., Saavedra, H.I., 2018. Centrosome aberrations and chromosome instability contribute to tumorigenesis and intra-tumor heterogeneity. J. Cancer Metastasis Treat. 4, 43.

Kabeche, L., Compton, D.A., 2013. Cyclin A regulates kinetochore microtubules to promote faithful chromosome segregation. Nature 502, 110–113.

Kajtez, J., Solomatina, A., Novak, M., Polak, B., Vukušić, K., Rüdiger, J., Cojoc, G., Milas, A., Šumanovac Šestak, I., Risteski, P., Tavano, F., Klemm, A.H., Roscioli, E., Welburn, J., Cimini, D., Glunčić, M., Pavin, N., Tolić, I.M., 2016. Overlap microtubules link sister k-fibres and balance the forces on bi-oriented kinetochores. Nat. Commun. 7, 10298.

Kakeno, M., Matsuzawa, K., Matsui, T., Akita, H., Sugiyama, I., Ishidate, F., Nakano, A., Takashima, S., Goto, H., Inagaki, M., Kaibuchi, K., Watanabe, T., 2014. Plk1 phosphorylates CLIP-170 and regulates its binding to microtubules for chromosome alignment. Cell Struct. Funct. 39, 45–59.

Kalitsis, P., Earle, E., Fowler, K.J., Choo, K.H., 2000. Bub3 gene disruption in mice reveals essential mitotic spindle checkpoint function during early embryogenesis. Genes Dev. 14, 2277–2282.

Kapoor, T.M., Lampson, M.A., Hergert, P., Cameron, L., Cimini, D., Salmon, E.D., McEwen, B.F., Khodjakov, A., 2006. Chromosomes can congress to the metaphase plate before biorientation. Science 311, 388–391.

Karamysheva, Z., Diaz-Martinez, L.A., Crow, S.E., Li, B., Yu, H., 2009. Multiple Anaphase-promoting Complex/Cyclosome Degrons Mediate the Degradation of Human Sgo1*. J. Biol. Chem. 284, 1772–1780.

Kaseda, K., McAinsh, A.D., Cross, R.A., 2012. Dual pathway spindle assembly increases both the speed and the fidelity of mitosis. Biol. Open 1, 12–18.

Kesisova, I.A., Nakos, K.C., Tsolou, A., Angelis, D., Lewis, J., Chatzaki, A., Agianian, B., Giannis, A., Koffa, M.D., 2013. Tripolin A, a novel small-molecule inhibitor of aurora A kinase, reveals new regulation of HURP's distribution on microtubules. PloS One 8, e58485.

Khodjakov, A., Cole, R.W., McEwen, B.F., Buttle, K.F., Rieder, C.L., 1997. Chromosome fragments possessing only one kinetochore can congress to the spindle equator. J. Cell Biol. 136, 229–240.

Khodjakov, A., Cole, R.W., Oakley, B.R., Rieder, C.L., 2000. Centrosome-independent mitotic spindle formation in vertebrates. Curr. Biol. CB 10, 59–67.

Kiewisz, R., Fabig, G., Conway, W., Baum, D., Needleman, D., Müller-Reichert, T., 2022. Three-dimensional structure of kinetochore-fibers in human mitotic spindles. eLife 11, e75459.

Kim, K., Rhee, K., 2011. The pericentriolar satellite protein CEP90 is crucial for integrity of the mitotic spindle pole. J. Cell Sci. 124, 338–347.

Kim, S., Jang, C.-Y., 2016. ANKRD53 interacts with DDA3 and regulates chromosome integrity during mitosis. Biochem. Biophys. Res. Commun. 470, 484–491.

Kim, S., Yu, H., 2015. Multiple assembly mechanisms anchor the KMN spindle checkpoint platform at human mitotic kinetochores. J. Cell Biol. 208, 181–196.

Kimura, M., Yoshioka, T., Saio, M., Banno, Y., Nagaoka, H., Okano, Y., 2013. Mitotic catastrophe and cell death induced by depletion of centrosomal proteins. Cell Death Dis. 4, e603.

King, J.M., Nicklas, R.B., 2000. Tension on chromosomes increases the number of kinetochore microtubules but only within limits. J. Cell Sci. 113 Pt 21, 3815–3823.

Kirschner, M.W., Mitchison, T., 1986. Microtubule dynamics. Nature 324, 621.

Kirsch-Volders, M., Bolognesi, C., Ceppi, M., Bruzzone, M., Fenech, M., 2020. Micronuclei, inflammation and auto-immune disease. Mutat. Res. Rev. Mutat. Res. 786, 108335.

Kitamura, E., Tanaka, K., Komoto, S., Kitamura, Y., Antony, C., Tanaka, T.U., 2010. Kinetochores generate microtubules with distal plus ends: their roles and limited lifetime in mitosis. Dev. Cell 18, 248–259.

Klaasen, S.J., Truong, M.A., van Jaarsveld, R.H., Koprivec, I., Štimac, V., de Vries, S.G., Risteski, P., Kodba, S., Vukušić, K., de Luca, K.L., Marques, J.F., Gerrits, E.M., Bakker, B., Foijer, F., Kind, J., Tolić, I.M., Lens, S.M.A., Kops, G.J.P.L., 2022. Nuclear chromosome locations dictate segregation error frequencies. Nature 607, 604–609.

Kline, S.L., Cheeseman, I.M., Hori, T., Fukagawa, T., Desai, A., 2006. The human Mis12 complex is required for kinetochore assembly and proper chromosome segregation. J. Cell Biol. 173, 9–17.

Kline-Smith, S.L., Walczak, C.E., 2002. The microtubule-destabilizing kinesin XKCM1 regulates microtubule dynamic instability in cells. Mol. Biol. Cell 13, 2718–2731.

Kneissig, M., Keuper, K., de Pagter, M.S., van Roosmalen, M.J., Martin, J., Otto, H., Passerini, V., Campos Sparr, A., Renkens, I., Kropveld, F., Vasudevan, A., Sheltzer, J.M., Kloosterman, W.P., Storchova, Z., 2019. Micronuclei-based model system reveals functional consequences of chromothripsis in human cells. eLife 8, e50292.

Knouse, K.A., Wu, J., Whittaker, C.A., Amon, A., 2014. Single cell sequencing reveals low levels of aneuploidy across mammalian tissues. Proc. Natl. Acad. Sci. U. S. A. 111, 13409–13414.

Kobayashi, D., Oike, T., Murata, K., Irie, D., Hirota, Y., Sato, H., Shibata, A., Ohno, T., 2020. Induction of Micronuclei in Cervical Cancer Treated with Radiotherapy. J. Pers. Med. 10, E110.

Koliou, X., Fedonidis, C., Kalpachidou, T., Mangoura, D., 2016. Nuclear import mechanism of neurofibromin for localization on the spindle and function in chromosome congression. J. Neurochem. 136, 78–91.

Komarova, Y.A., Akhmanova, A.S., Kojima, S.-I., Galjart, N., Borisy, G.G., 2002. Cytoplasmic linker proteins promote microtubule rescue in vivo. J. Cell Biol. 159, 589–599.

Konishi, Y., Setou, M., 2009. Tubulin tyrosination navigates the kinesin-1 motor domain to axons. Nat. Neurosci. 12, 559–567.

Kops, G.J.P.L., Foltz, D.R., Cleveland, D.W., 2004. Lethality to human cancer cells through massive chromosome loss by inhibition of the mitotic checkpoint. Proc. Natl. Acad. Sci. U. S. A. 101, 8699–8704.

Kops, G.J.P.L., Gassmann, R., 2020. Crowning the Kinetochore: The Fibrous Corona in Chromosome Segregation. Trends Cell Biol. 30, 653–667.

Kops, G.J.P.L., Kim, Y., Weaver, B.A.A., Mao, Y., McLeod, I., Yates, J.R., Tagaya, M., Cleveland, D.W., 2005a. ZW10 links mitotic checkpoint signaling to the structural kinetochore. J. Cell Biol. 169, 49–60.

Kops, G.J.P.L., Weaver, B.A.A., Cleveland, D.W., 2005b. On the road to cancer: aneuploidy and the mitotic checkpoint. Nat. Rev. Cancer 5, 773–785.

Kotak, S., Busso, C., Gönczy, P., 2012. Cortical dynein is critical for proper spindle positioning in human cells. J. Cell Biol. 199, 97–110.

Krauss, S.W., Spence, J.R., Bahmanyar, S., Barth, A.I.M., Go, M.M., Czerwinski, D., Meyer, A.J., 2008. Downregulation of protein 4.1R, a mature centriole protein, disrupts centrosomes, alters cell cycle progression, and perturbs mitotic spindles and anaphase. Mol. Cell. Biol. 28, 2283–2294.

Kremer, B.E., Haystead, T., Macara, I.G., 2005. Mammalian septins regulate microtubule stability through interaction with the microtubule-binding protein MAP4. Mol. Biol. Cell 16, 4648–4659.

Krenn, V., Musacchio, A., 2015. The Aurora B Kinase in Chromosome Bi-Orientation and Spindle Checkpoint Signaling. Front. Oncol. 5, 225.

Kuang, P., Chen, Z., Wang, JiaYuan, Liu, Z., Wang, Jingyuan, Gao, J., Shen, L., 2017. Characterization of Aurora A and Its Impact on the Effect of Cisplatin-Based Chemotherapy in Patients with Non-Small Cell Lung Cancer. Transl. Oncol. 10, 367–377.

Kuniyasu, K., Iemura, K., Tanaka, K., 2018. Delayed Chromosome Alignment to the Spindle Equator Increases the Rate of Chromosome Missegregation in Cancer Cell Lines. Biomolecules 9, 10.

Kurinna, S., Stratton, S.A., Coban, Z., Schumacher, J.M., Grompe, M., Duncan, A.W., Barton, M.C., 2013. p53 regulates a mitotic transcription program and determines ploidy in normal mouse liver. Hepatol. Baltim. Md 57, 2004–2013.

Labade, A.S., Karmodiya, K., Sengupta, K., 2016. HOXA repression is mediated by nucleoporin Nup93 assisted by its interactors Nup188 and Nup205. Epigenetics Chromatin 9, 54.

Lambrus, B.G., Daggubati, V., Uetake, Y., Scott, P.M., Clutario, K.M., Sluder, G., Holland, A.J., 2016. A USP28-53BP1-p53-p21 signaling axis arrests growth after centrosome loss or prolonged mitosis. J. Cell Biol. 214, 143–153.

Lambrus, B.G., Uetake, Y., Clutario, K.M., Daggubati, V., Snyder, M., Sluder, G., Holland, A.J., 2015. p53 protects against genome instability following centriole duplication failure. J. Cell Biol. 210, 63–77.

Lampson, M.A., Grishchuk, E.L., 2017. Mechanisms to Avoid and Correct Erroneous Kinetochore-Microtubule Attachments. Biology 6, E1.

Lampson, M.A., Kapoor, T.M., 2005. The human mitotic checkpoint protein BubR1 regulates chromosome-spindle attachments. Nat. Cell Biol. 7, 93–98.

Lampson, M.A., Renduchitala, K., Khodjakov, A., Kapoor, T.M., 2004. Correcting improper chromosome-spindle attachments during cell division. Nat. Cell Biol. 6, 232–237.

Landskron, L., Bak, J., Adamopoulos, A., Kaplani, K., Moraiti, M., van den Hengel, L.G., Song, J.-Y., Bleijerveld, O.B., Nieuwenhuis, J., Heidebrecht, T., Henneman, L., Moutin, M.-J., Barisic, M., Taraviras, S., Perrakis, A., Brummelkamp, T.R., 2022. Posttranslational modification of microtubules by the MATCAP detyrosinase. Science 376, eabn6020.

Lara-Gonzalez, P., Pines, J., Desai, A., 2021. Spindle assembly checkpoint activation and silencing at kinetochores. Semin. Cell Dev. Biol. 117, 86–98.

Lara-Gonzalez, P., Westhorpe, F.G., Taylor, S.S., 2012. The spindle assembly checkpoint. Curr. Biol. CB 22, R966-980.

Lawo, S., Bashkurov, M., Mullin, M., Ferreria, M.G., Kittler, R., Habermann, B., Tagliaferro, A., Poser, I., Hutchins, J.R.A., Hegemann, B., Pinchev, D., Buchholz, F., Peters, J.-M., Hyman, A.A., Gingras, A.-C., Pelletier, L., 2009. HAUS, the 8-subunit human Augmin complex, regulates centrosome and spindle integrity. Curr. Biol. CB 19, 816–826.

Lee, A.J.X., Endesfelder, D., Rowan, A.J., Walther, A., Birkbak, N.J., Futreal, P.A., Downward, J., Szallasi, Z., Tomlinson, I.P.M., Howell, M., Kschischo, M., Swanton, C., 2011. Chromosomal instability confers intrinsic multidrug resistance. Cancer Res. 71, 1858–1870.

Lee, D., Zhao, X., Zhang, F., Eisenberg, E., Greene, L.E., 2005. Depletion of GAK/auxilin 2 inhibits receptor-mediated endocytosis and recruitment of both clathrin and clathrin adaptors. J. Cell Sci. 118, 4311–4321.

Lee, M.H., Lin, L., Equilibrina, I., Uchiyama, S., Matsunaga, S., Fukui, K., 2011. ASURA (PHB2) Is Required for Kinetochore Assembly and Subsequent Chromosome Congression. Acta Histochem. Cytochem. 44, 247–258.

Lens, S.M.A., Wolthuis, R.M.F., Klompmaker, R., Kauw, J., Agami, R., Brummelkamp, T., Kops, G., Medema, R.H., 2003. Survivin is required for a sustained spindle checkpoint arrest in response to lack of tension. EMBO J. 22, 2934–2947.

Lesage, B., Qian, J., Bollen, M., 2011. Spindle checkpoint silencing: PP1 tips the balance. Curr. Biol. CB 21, R898-903.

Levesque, A.A., Compton, D.A., 2001. The chromokinesin Kid is necessary for chromosome arm orientation and oscillation, but not congression, on mitotic spindles. J. Cell Biol. 154, 1135–1146.

Levine, M.S., Holland, A.J., 2018. The impact of mitotic errors on cell proliferation and tumorigenesis. Genes Dev. 32, 620–638.

Li, C., Xue, C., Yang, Q., Low, B.C., Liou, Y.-C., 2016. NuSAP governs chromosome oscillation by facilitating the Kid-generated polar ejection force. Nat. Commun. 7, 10597.

Li, L., Yang, L., Scudiero, D.A., Miller, S.A., Yu, Z.-X., Stukenberg, P.T., Shoemaker, R.H., Kotin, R.M., 2007. Development of recombinant adeno-associated virus vectors carrying small interfering RNA (shHec1)-mediated depletion of kinetochore Hec1 protein in tumor cells. Gene Ther. 14, 814–827.

Li, M., Fang, X., Baker, D.J., Guo, L., Gao, X., Wei, Z., Han, S., van Deursen, J.M., Zhang, P., 2010. The ATM-p53 pathway suppresses aneuploidy-induced tumorigenesis. Proc. Natl. Acad. Sci. U. S. A. 107, 14188–14193.

Li, N., Yuan, K., Yan, F., Huo, Y., Zhu, T., Liu, X., Guo, Z., Yao, X., 2009. PinX1 is recruited to the mitotic chromosome periphery by Nucleolin and facilitates chromosome congression. Biochem. Biophys. Res. Commun. 384, 76–81.

Li, R., Murray, A.W., 1991. Feedback control of mitosis in budding yeast. Cell 66, 519–531.

Li, Y., Yu, W., Liang, Y., Zhu, X., 2007. Kinetochore dynein generates a poleward pulling force to facilitate congression and full chromosome alignment. Cell Res. 17, 701–712.

Liao, S., Rajendraprasad, G., Wang, N., Eibes, S., Gao, J., Yu, H., Wu, G., Tu, X., Huang, H., Barisic, M., Xu, C., 2019. Molecular basis of vasohibins-mediated detyrosination and its impact on spindle function and mitosis. Cell Res. 29, 533–547.

Lin, C.-H., Hu, C.-K., Shih, H.-M., 2010. Clathrin heavy chain mediates TACC3 targeting to mitotic spindles to ensure spindle stability. J. Cell Biol. 189, 1097–1105.

Lin, Y.-T., Chen, Y., Wu, G., Lee, W.-H., 2006. Hec1 sequentially recruits Zwint-1 and ZW10 to kinetochores for faithful chromosome segregation and spindle checkpoint control. Oncogene 25, 6901–6914.

Liu, D., Ding, X., Du, J., Cai, X., Huang, Y., Ward, T., Shaw, A., Yang, Y., Hu, R., Jin, C., Yao, X., 2007. Human NUF2 Interacts with Centromere-associated Protein E and Is Essential for a Stable Spindle Microtubule-Kinetochore Attachment*. J. Biol. Chem. 282, 21415–21424.

Liu, D., Vader, G., Vromans, M.J.M., Lampson, M.A., Lens, S.M.A., 2009. Sensing chromosome bi-orientation by spatial separation of aurora B kinase from kinetochore substrates. Science 323, 1350–1353.

Liu, D., Vleugel, M., Backer, C.B., Hori, T., Fukagawa, T., Cheeseman, I.M., Lampson, M.A., 2010. Regulated targeting of protein phosphatase 1 to the outer kinetochore by KNL1 opposes Aurora B kinase. J. Cell Biol. 188, 809–820.

Liu, S., Kwon, M., Mannino, M., Yang, N., Renda, F., Khodjakov, A., Pellman, D., 2018. Nuclear envelope assembly defects link mitotic errors to chromothripsis. Nature 561, 551–555.

Liu, S.-T., Hittle, J.C., Jablonski, S.A., Campbell, M.S., Yoda, K., Yen, T.J., 2003. Human CENP-I specifies localization of CENP-F, MAD1 and MAD2 to kinetochores and is essential for mitosis. Nat. Cell Biol. 5, 341–345.

Liu, X., Zheng, H., Qu, C.-K., 2012. Protein tyrosine phosphatase Shp2 (Ptpn11) plays an important role in maintenance of chromosome stability. Cancer Res. 72, 5296–5306.

Liu, X.-S., Zhao, X.-D., Wang, X., Yao, Y.-X., Zhang, L.-L., Shu, R.-Z., Ren, W.-H., Huang, Y., Huang, L., Gu, M.-M., Kuang, Y., Wang, L., Lu, S.-Y., Chi, J., Fen, J.-S., Wang, Y.-F., Fei, J., Dai, W., Wang, Z.-G., 2010. Germinal Cell Aplasia in Kif18a Mutant Male Mice Due to Impaired Chromosome Congression and Dysregulated BubR1 and CENP-E. Genes Cancer 1, 26–39.

Lo, K.W.-H., Kogoy, J.M., Pfister, K.K., 2007. The DYNLT3 light chain directly links cytoplasmic dynein to a spindle checkpoint protein, Bub3. J. Biol. Chem. 282, 11205–11212.

Logarinho, E., Maffini, S., Barisic, M., Marques, A., Toso, A., Meraldi, P., Maiato, H., 2012. CLASPs prevent irreversible multipolarity by ensuring spindle-pole resistance to traction forces during chromosome alignment. Nat. Cell Biol. 14, 295–303. 3

Lopes, D., Maiato, H., 2020. The Tubulin Code in Mitosis and Cancer. Cells 9, 2356.

Ludueña, R.F., 2013. A hypothesis on the origin and evolution of tubulin. Int. Rev. Cell Mol. Biol. 302, 41–185.

Lukow, D.A., Sausville, E.L., Suri, P., Chunduri, N.K., Wieland, A., Leu, J., Smith, J.C., Girish, V., Kumar, A.A., Kendall, J., Wang, Z., Storchova, Z., Sheltzer, J.M., 2021. Chromosomal instability accelerates the evolution of resistance to anti-cancer therapies. Dev. Cell 56, 2427-2439.e4.

Lussi, Y.C., Shumaker, D.K., Shimi, T., Fahrenkrog, B., 2010. The nucleoporin Nup153 affects spindle checkpoint activity due to an association with Mad1. Nucl. Austin Tex 1, 71–84.

Lyu, H., Li, M., Jiang, Z., Liu, Z., Wang, X., 2019. Correlate the TP53 Mutation and the HRAS Mutation with Immune Signatures in Head and Neck Squamous Cell Cancer. Comput. Struct. Biotechnol. J. 17, 1020–1030.

Winey M., Cl, M., Et, O., Dn, M., Th, G., Kl, M., Jr, M., 1995. Three-dimensional ultrastructural analysis of the Saccharomyces cerevisiae mitotic spindle. J. Cell Biol. 129.

Ma, N., Matsunaga, S., Morimoto, A., Sakashita, G., Urano, T., Uchiyama, S., Fukui, K., 2011. The nuclear scaffold protein SAF-A is required for kinetochore-microtubule attachment and contributes to the targeting of Aurora-A to mitotic spindles. J. Cell Sci. 124, 394–404.

Ma, N., Matsunaga, S., Takata, H., Ono-Maniwa, R., Uchiyama, S., Fukui, K., 2007. Nucleolin functions in nucleolus formation and chromosome congression. J. Cell Sci. 120, 2091–2105.

Maciejowski, J., Li, Y., Bosco, N., Campbell, P.J., de Lange, T., 2015. Chromothripsis and Kataegis Induced by Telomere Crisis. Cell 163, 1641–1654.

Mackay, A.M., Ainsztein, A.M., Eckley, D.M., Earnshaw, W.C., 1998. A dominant mutant of inner centromere protein (INCENP), a chromosomal protein, disrupts prometaphase congression and cytokinesis. J. Cell Biol. 140, 991–1002.

Mackay, D.R., Elgort, S.W., Ullman, K.S., 2009. The nucleoporin Nup153 has separable roles in both early mitotic progression and the resolution of mitosis. Mol. Biol. Cell 20, 1652–1660.

Mackenzie, K.J., Carroll, P., Martin, C.-A., Murina, O., Fluteau, A., Simpson, D.J., Olova, N., Sutcliffe, H., Rainger, J.K., Leitch, A., Osborn, R.T., Wheeler, A.P., Nowotny, M., Gilbert, N., Chandra, T., Reijns, M.A.M., Jackson, A.P., 2017. cGAS surveillance of micronuclei links genome instability to innate immunity. Nature 548, 461–465.

Maffini, S., Maia, A.R.R., Manning, A.L., Maliga, Z., Pereira, A.L., Junqueira, M., Shevchenko, A., Hyman, A., Yates, J.R., Galjart, N., Compton, D.A., Maiato, H., 2009. Motor-independent targeting of CLASPs to kinetochores by CENP-E promotes microtubule turnover and poleward flux. Curr. Biol. CB 19, 1566–1572.

Magidson, V., O'Connell, C.B., Lončarek, J., Paul, R., Mogilner, A., Khodjakov, A., 2011. The spatial arrangement of chromosomes during prometaphase facilitates spindle assembly. Cell 146, 555–567.

Maia, A.F., Feijão, T., Vromans, M.J.M., Sunkel, C.E., Lens, S.M.A., 2010. Aurora B kinase cooperates with CENP-E to promote timely anaphase onset. Chromosoma 119, 405–413.

Maia, A.R.R., Garcia, Z., Kabeche, L., Barisic, M., Maffini, S., Macedo-Ribeiro, S., Cheeseman, I.M., Compton, D.A., Kaverina, I., Maiato, H., 2012. Cdk1 and Plk1 mediate a CLASP2 phospho-switch that stabilizes kinetochore-microtubule attachments. J. Cell Biol. 199, 285–301.

Maiato, H., Afonso, O., Matos, I., 2015. A chromosome separation checkpoint: A midzone Aurora B gradient mediates a chromosome separation checkpoint that regulates the anaphase-telophase transition. BioEssays News Rev. Mol. Cell. Dev. Biol. 37, 257–266.

Maiato, H., Fairley, E.A.L., Rieder, C.L., Swedlow, J.R., Sunkel, C.E., Earnshaw, W.C., 2003. Human CLASP1 is an outer kinetochore component that regulates spindle microtubule dynamics. Cell 113, 891–904.

Maiato, H., Gomes, A.M., Sousa, F., Barisic, M., 2017. Mechanisms of Chromosome Congression during Mitosis. Biology 6, E13.

Maiato, H., Khodjakov, A., Rieder, C.L., 2005. Drosophila CLASP is required for the incorporation of microtubule subunits into fluxing kinetochore fibres. Nat. Cell Biol. 7, 42–47.

Maiato, H., Logarinho, E., 2014. Mitotic spindle multipolarity without centrosome amplification. Nat. Cell Biol. 16, 386–394.

Maiato, Helder, Rieder, C.L., Khodjakov, A., 2004. Kinetochore-driven formation of kinetochore fibers contributes to spindle assembly during animal mitosis. J. Cell Biol. 167, 831–840.

Maiato, Hélder, Sampaio, P., Sunkel, C.E., 2004. Microtubule-associated proteins and their essential roles during mitosis. Int. Rev. Cytol. 241, 53–153.

Manning, A.L., Bakhoum, S.F., Maffini, S., Correia-Melo, C., Maiato, H., Compton, D.A., 2010. CLASP1, astrin and Kif2b form a molecular switch that regulates kinetochore-microtubule dynamics to promote mitotic progression and fidelity. EMBO J. 29, 3531–3543.

Manning, A.L., Ganem, N.J., Bakhoum, S.F., Wagenbach, M., Wordeman, L., Compton, D.A., 2007. The kinesin-13 proteins Kif2a, Kif2b, and Kif2c/MCAK have distinct roles during mitosis in human cells. Mol. Biol. Cell 18, 2970–2979.

Mapelli, M., Massimiliano, L., Santaguida, S., Musacchio, A., 2007. The Mad2 conformational dimer: structure and implications for the spindle assembly checkpoint. Cell 131, 730–743.

Maresca, T.J., Salmon, E.D., 2009. Intrakinetochore stretch is associated with changes in kinetochore phosphorylation and spindle assembly checkpoint activity. J. Cell Biol. 184, 373–381.

Margolis, R.L.; Wilson, L.; Keifer, B.I., 1978. Mitotic mechanism based on intrinsic microtubule behaviour. Nature.

Martin, R.H., 2006. Meiotic chromosome abnormalities in human spermatogenesis. Reprod. Toxicol. Elmsford N 22, 142–147.

Martínez-Alonso, D., Malumbres, M., 2020. Mammalian cell cycle cyclins. Semin. Cell Dev. Biol. 107, 28–35.

Martin-Lluesma, S., Stucke, V.M., Nigg, E.A., 2002. Role of Hec1 in spindle checkpoint signaling and kinetochore recruitment of Mad1/Mad2. Science 297, 2267–2270.

Mastronarde, D.N., McDonald, K.L., Ding, R., McIntosh, J.R., 1993. Interpolar spindle microtubules in PTK cells. J. Cell Biol. 123, 1475–1489.

Matano, M., Date, S., Shimokawa, M., Takano, A., Fujii, M., Ohta, Y., Watanabe, T., Kanai, T., Sato, T., 2015. Modeling colorectal cancer using CRISPR-Cas9-mediated engineering of human intestinal organoids. Nat. Med. 21, 256–262.

Matos, I., Pereira, A.J., Lince-Faria, M., Cameron, L.A., Salmon, E.D., Maiato, H., 2009. Synchronizing chromosome segregation by flux-dependent force equalization at kinetochores. J. Cell Biol. 186, 11–26.

Matsuura, S., Matsumoto, Y., Morishima, K., Izumi, H., Matsumoto, H., Ito, E., Tsutsui, K., Kobayashi, J., Tauchi, H., Kajiwara, Y., Hama, S., Kurisu, K., Tahara, H., Oshimura, M., Komatsu, K., Ikeuchi, T., Kajii, T., 2006. Monoallelic BUB1B mutations and defective mitotic-spindle checkpoint in seven families with premature chromatid separation (PCS) syndrome. Am. J. Med. Genet. A. 140, 358–367.

Matthews, H.K., Bertoli, C., de Bruin, R.A.M., 2022. Cell cycle control in cancer. Nat. Rev. Mol. Cell Biol. 23, 74–88.

Mayr, M.I., Hümmer, S., Bormann, J., Grüner, T., Adio, S., Woehlke, G., Mayer, T.U., 2007. The human kinesin Kif18A is a motile microtubule depolymerase essential for chromosome congression. Curr. Biol. CB 17, 488–498.

Mazumdar, M., Sundareshan, S., Misteli, T., 2004. Human chromokinesin KIF4A functions in chromosome condensation and segregation. J. Cell Biol. 166, 613–620.

McCleland, M.L., Kallio, M.J., Barrett-Wilt, G.A., Kestner, C.A., Shabanowitz, J., Hunt, D.F., Gorbsky, G.J., Stukenberg, P.T., 2004. The vertebrate Ndc80 complex contains Spc24 and Spc25 homologs, which are required to establish and maintain kinetochore-microtubule attachment. Curr. Biol. CB 14, 131–137.

McClelland, S.E., Burrell, R.A., Swanton, C., 2009. Chromosomal instability: a composite phenotype that influences sensitivity to chemotherapy. Cell Cycle Georget. Tex 8, 3262–3266.

McEwen, B.F., Chan, G.K., Zubrowski, B., Savoian, M.S., Sauer, M.T., Yen, T.J., 2001. CENP-E is essential for reliable bioriented spindle attachment, but chromosome alignment can be achieved via redundant mechanisms in mammalian cells. Mol. Biol. Cell 12, 2776–2789.

McGuinness, B.E., Hirota, T., Kudo, N.R., Peters, J.-M., Nasmyth, K., 2005. Shugoshin prevents dissociation of cohesin from centromeres during mitosis in vertebrate cells. PLoS Biol. 3, e86.

McHedlishvili, N., Wieser, S., Holtackers, R., Mouysset, J., Belwal, M., Amaro, A.C., Meraldi, P., 2012. Kinetochores accelerate centrosome separation to ensure faithful chromosome segregation. J. Cell Sci. 125, 906–918.

McIntosh, J.R.; Hepler, P.K.; Van Wie, D.G, 1969. Model for mitosis. Nature 659–663.

McKinley, K.L., Sekulic, N., Guo, L.Y., Tsinman, T., Black, B.E., Cheeseman, I.M., 2015. The CENP-L-N Complex Forms a Critical Node in an Integrated Meshwork of Interactions at the Centromere-Kinetochore Interface. Mol. Cell 60, 886–898.

McLaughlin, M., Patin, E.C., Pedersen, M., Wilkins, A., Dillon, M.T., Melcher, A.A., Harrington, K.J., 2020. Inflammatory microenvironment remodelling by tumour cells after radiotherapy. Nat. Rev. Cancer 20, 203–217.

Megraw, T.L., Kao, L.R., Kaufman, T.C., 2001. Zygotic development without functional mitotic centrosomes. Curr. Biol. CB 11, 116–120.

Meitinger, F., Anzola, J.V., Kaulich, M., Richardson, A., Stender, J.D., Benner, C., Glass, C.K., Dowdy, S.F., Desai, A., Shiau, A.K., Oegema, K., 2016. 53BP1 and USP28 mediate p53 activation and G1 arrest after centrosome loss or extended mitotic duration. J. Cell Biol. 214, 155–166.

Meraldi, P., Sorger, P.K., 2005. A dual role for Bub1 in the spindle checkpoint and chromosome congression. EMBO J. 24, 1621–1633.

Mettu, R.K.R., Wan, Y.-W., Habermann, J.K., Ried, T., Guo, N.L., 2010. A 12-gene genomic instability signature predicts clinical outcomes in multiple cancer types. Int. J. Biol. Markers 25, 219–228.

Meunier, S., Vernos, I., 2016. Acentrosomal Microtubule Assembly in Mitosis: The Where, When, and How. Trends Cell Biol. 26, 80–87.

Michel, L.S., Liberal, V., Chatterjee, A., Kirchwegger, R., Pasche, B., Gerald, W., Dobles, M., Sorger, P.K., Murty, V.V., Benezra, R., 2001. MAD2 haplo-insufficiency causes premature anaphase and chromosome instability in mammalian cells. Nature 409, 355–359.

Milas, A.; Tolic, I.M.; Zür, M., 2016. Relaxation of interkinetochore tension after severing of a k-fiber depends on the length of the k-fiber stub. Matters.

Milev, M.P., Hasaj, B., Saint-Dic, D., Snounou, S., Zhao, Q., Sacher, M., 2015. TRAMM/TrappC12 plays a role in chromosome congression, kinetochore stability, and CENP-E recruitment. J. Cell Biol. 209, 221–234.

Miller, M.P., Asbury, C.L., Biggins, S., 2016. A TOG Protein Confers Tension Sensitivity to Kinetochore-Microtubule Attachments. Cell 165, 1428–1439.

Mimori-Kiyosue, Y., Grigoriev, I., Lansbergen, G., Sasaki, H., Matsui, C., Severin, F., Galjart, N., Grosveld, F., Vorobjev, I., Tsukita, S., Akhmanova, A., 2005. CLASP1 and CLASP2 bind to EB1 and regulate microtubule plus-end dynamics at the cell cortex. J. Cell Biol. 168, 141–153.

Mitchison, T., Kirschner, M., 1984. Dynamic instability of microtubule growth. Nature 312, 237–242.

Mitchison, T.J., 1989. Polewards microtubule flux in the mitotic spindle: evidence from photoactivation of fluorescence. J. Cell Biol. 109, 637–652.

Mitchison, T.J., Pineda, J., Shi, J., Florian, S., 2017. Is inflammatory micronucleation the key to a successful anti-mitotic cancer drug? Open Biol. 7, 170182.

Moon, H.M., Youn, Y.H., Pemble, H., Yingling, J., Wittmann, T., Wynshaw-Boris, A., 2014. LIS1 controls mitosis and mitotic spindle organization via the LIS1-NDEL1-dynein complex. Hum. Mol. Genet. 23, 449–466.

Morgan, D. O., 2007. The Cell Cycle: Principles of control. New Science Press.

Moritz, M., Agard, D.A., 2001. Gamma-tubulin complexes and microtubule nucleation. Curr. Opin. Struct. Biol. 11, 174–181.

Moritz, M., Braunfeld, M.B., Guénebaut, V., Heuser, J., Agard, D.A., 2000. Structure of the gamma-tubulin ring complex: a template for microtubule nucleation. Nat. Cell Biol. 2, 365–370.

Moritz, M., Braunfeld, M.B., Sedat, J.W., Alberts, B., Agard, D.A., 1995. Microtubule nucleation by gamma-tubulin-containing rings in the centrosome. Nature 378, 638–640.

Morrow, C.J., Tighe, A., Johnson, V.L., Scott, M.I.F., Ditchfield, C., Taylor, S.S., 2005. Bub1 and aurora B cooperate to maintain BubR1-mediated inhibition of APC/CCdc20. J. Cell Sci. 118, 3639–3652.

Mountain, V., Compton, D.A., 2000. Dissecting the role of molecular motors in the mitotic spindle. Anat. Rec. 261, 14–24.

Murata, T., Sonobe, S., Baskin, T.I., Hyodo, S., Hasezawa, S., Nagata, T., Horio, T., Hasebe, M., 2005. Microtubule-dependent microtubule nucleation based on recruitment of gamma-tubulin in higher plants. Nat. Cell Biol. 7, 961–968.

Murray, A., 1994. Cell cycle checkpoints. Curr. Opin. Cell Biol. 6, 872–876.

Murray, A.W., 2011. A brief history of error. Nat. Cell Biol. 13, 1178–1182.

Musacchio, A., 2015. The Molecular Biology of Spindle Assembly Checkpoint Signaling Dynamics. Curr. Biol. CB 25, R1002-1018.

Musacchio, A., Desai, A., 2017. A Molecular View of Kinetochore Assembly and Function. Biology 6, E5.

Musacchio, A., Salmon, E.D., 2007. The spindle-assembly checkpoint in space and time. Nat. Rev. Mol. Cell Biol. 8, 379–393.

Muto, Y., Yoshioka, T., Kimura, M., Matsunami, M., Saya, H., Okano, Y., 2008. An evolutionarily conserved leucine-rich repeat protein CLERC is a centrosomal protein required for spindle pole integrity. Cell Cycle Georget. Tex 7, 2738–2748.

Nähse, V., Christ, L., Stenmark, H., Campsteijn, C., 2017. The Abscission Checkpoint: Making It to the Final Cut. Trends Cell Biol. 27, 1–11.

Naim, V., Rosselli, F., 2009. The FANC pathway and BLM collaborate during mitosis to prevent micro-nucleation and chromosome abnormalities. Nat. Cell Biol. 11, 761–768.

Nakamura, A., Arai, H., Fujita, N., 2009. Centrosomal Aki1 and cohesin function in separase-regulated centriole disengagement. J. Cell Biol. 187, 607–614.

Nam, H.-J., Naylor, R.M., van Deursen, J.M., 2015. Centrosome dynamics as a source of chromosomal instability. Trends Cell Biol. 25, 65–73.

Nam, H.-J., van Deursen, J.M., 2014. Cyclin B2 and p53 control proper timing of centrosome separation. Nat. Cell Biol. 16, 538–549.

Narkar, A., Johnson, B.A., Bharne, P., Zhu, J., Padmanaban, V., Biswas, D., Fraser, A., Iglesias, P.A., Ewald, A.J., Li, R., 2021. On the role of p53 in the cellular response to aneuploidy. Cell Rep. 34, 108892.

Nassour, J., Radford, R., Correia, A., Fusté, J.M., Schoell, B., Jauch, A., Shaw, R.J., Karlseder, J., 2019. Autophagic cell death restricts chromosomal instability during replicative crisis. Nature 565, 659–663.

Nicklas, R.B., 1989. The motor for poleward chromosome movement in anaphase is in or near the kinetochore. J. Cell Biol. 109, 2245–2255.

Nicklas, R.B., Gordon, G.W., 1985. The total length of spindle microtubules depends on the number of chromosomes present. J. Cell Biol. 100, 1–7.

Nicklas, R.B., Koch, C.A., 1969. Chromosome micromanipulation. 3. Spindle fiber tension and the reorientation of mal-oriented chromosomes. J. Cell Biol. 43, 40–50.

Nicklas, R.B.; Kubai, D.F.; Hays, T.S., 1982. Spindle microtubules and their mechanical associations after micromanipulation in anaphase. J Cell Biol 91–104.

Nigg, E.A., 2007. Centrosome duplication: of rules and licenses. Trends Cell Biol. 17, 215–221.

Nigg, E.A., Raff, J.W., 2009. Centrioles, centrosomes, and cilia in health and disease. Cell 139, 663–678.

Nijenhuis, W., von Castelmur, E., Littler, D., De Marco, V., Tromer, E., Vleugel, M., van Osch, M.H.J., Snel, B., Perrakis, A., Kops, G.J.P.L., 2013. A TPR domain-containing N-terminal module of MPS1 is required for its kinetochore localization by Aurora B. J. Cell Biol. 201, 217–231.

Nishihashi, A., Haraguchi, T., Hiraoka, Y., Ikemura, T., Regnier, V., Dodson, H., Earnshaw, W.C., Fukagawa, T., 2002. CENP-I is essential for centromere function in vertebrate cells. Dev. Cell 2, 463–476.

Nishino, M., Kurasawa, Y., Evans, R., Lin, S.-H., Brinkley, B.R., Yu-Lee, L.-Y., 2006. NudC is required for Plk1 targeting to the kinetochore and chromosome congression. Curr. Biol. CB 16, 1414–1421

Nogales, E., Whittaker, M., Milligan, R.A., Downing, K.H., 1999. High-resolution model of the microtubule. Cell 96, 79–88.

Novais-Cruz, M., Alba Abad, M., van IJcken, W.F., Galjart, N., Jeyaprakash, A.A., Maiato, H., Ferrás, C., 2018. Mitotic progression, arrest, exit or death relies on centromere structural integrity, rather than de novo transcription. eLife 7, e36898.

Oh, H.J., Kim, M.J., Song, S.J., Kim, T., Lee, D., Kwon, S.-H., Choi, E.-J., Lim, D.-S., 2010. MST1 limits the kinase activity of aurora B to promote stable kinetochore-microtubule attachment. Curr. Biol. CB 20, 416–422.

Ohashi, A., Ohori, M., Iwai, K., Nambu, T., Miyamoto, M., Kawamoto, T., Okaniwa, M., 2015. A Novel Time-Dependent CENP-E Inhibitor with Potent Antitumor Activity. PloS One 10, e0144675.

Ohtsubo, M., Theodoras, A.M., Schumacher, J., Roberts, J.M., Pagano, M., 1995. Human cyclin E, a nuclear protein essential for the G1-to-S phase transition. Mol. Cell. Biol. 15, 2612–2624.

O'Regan, L., Sampson, J., Richards, M.W., Knebel, A., Roth, D., Hood, F.E., Straube, A., Royle, S.J., Bayliss, R., Fry, A.M., 2015. Hsp72 is targeted to the mitotic spindle by Nek6 to promote K-fiber assembly and mitotic progression. J. Cell Biol. 209, 349–358.

Orr, B., De Sousa, F., Gomes, A.M., Afonso, O., Ferreira, L.T., Figueiredo, A.C., Maiato, H., 2021. An anaphase surveillance mechanism prevents micronuclei formation from frequent chromosome segregation errors. Cell Rep. 37, 109783.

Orr, B., Maiato, H., 2019. No chromosome left behind: The importance of metaphase alignment for mitotic fidelity. J. Cell Biol. 218, 1086–1088.

Orth, J.D., Kohler, R.H., Foijer, F., Sorger, P.K., Weissleder, R., Mitchison, T.J., 2011. Analysis of mitosis and antimitotic drug responses in tumors by in vivo microscopy and single-cell pharmacodynamics. Cancer Res. 71, 4608–4616.

Orth, J.D., Loewer, A., Lahav, G., Mitchison, T.J., 2012. Prolonged mitotic arrest triggers partial activation of apoptosis, resulting in DNA damage and p53 induction. Mol. Biol. Cell 23, 567–576.

Orthaus, S., Ohndorf, S., Diekmann, S., 2006. RNAi knockdown of human kinetochore protein CENP-H. Biochem. Biophys. Res. Commun. 348, 36–46.

Oshimori, N., Li, X., Ohsugi, M., Yamamoto, T., 2009. Cep72 regulates the localization of key centrosomal proteins and proper bipolar spindle formation. EMBO J. 28, 2066–2076.

Oshimori, N., Ohsugi, M., Yamamoto, T., 2006. The Plk1 target Kizuna stabilizes mitotic centrosomes to ensure spindle bipolarity. Nat. Cell Biol. 8, 1095–1101.

Pagano, M., Pepperkok, R., Verde, F., Ansorge, W., Draetta, G., 1992. Cyclin A is required at two points in the human cell cycle. EMBO J. 11, 961–971.

Papini, D., Levasseur, M.D., Higgins, J.M.G., 2021. The Aurora B gradient sustains kinetochore stability in anaphase. Cell Rep. 37, 109818.

Park, H.-J., Lee, S.-J., Sohn, Y.B., Jin, H.-S., Han, J.-H., Kim, Y.-B., Yim, H., Jeong, S.-Y., 2013. NF1 deficiency causes Bcl-xL upregulation in Schwann cells derived from neurofibromatosis type 1-associated malignant peripheral nerve sheath tumors. Int. J. Oncol. 42, 657–666.

Park, J.E., Song, H., Kwon, H.J., Jang, C.-Y., 2016. Ska1 cooperates with DDA3 for spindle dynamics and spindle attachment to kinetochore. Biochem. Biophys. Res. Commun. 470, 586–592.

Park, S.J., 2010. Huntingtin-interacting protein 1-related is required for accurate congression and segregation of chromosomes. BMB Rep. 43, 795–800.

Peeper, D.S., van der Eb, A.J., Zantema, A., 1994. The G1/S cell-cycle checkpoint in eukaryotic cells. Biochim. Biophys. Acta 1198, 215–230.

Pereira, A.J., Maiato, H., 2012. Maturation of the kinetochore-microtubule interface and the meaning of metaphase. Chromosome Res. Int. J. Mol. Supramol. Evol. Asp. Chromosome Biol. 20, 563–577.

Pereira, A.L., Pereira, A.J., Maia, A.R.R., Drabek, K., Sayas, C.L., Hergert, P.J., Lince-Faria, M., Matos, I., Duque, C., Stepanova, T., Rieder, C.L., Earnshaw, W.C., Galjart, N., Maiato, H., 2006. Mammalian CLASP1 and CLASP2 cooperate to ensure mitotic fidelity by regulating spindle and kinetochore function. Mol. Biol. Cell 17, 4526–4542.

Perez, F., Diamantopoulos, G.S., Stalder, R., Kreis, T.E., 1999. CLIP-170 highlights growing microtubule ends in vivo. Cell 96, 517–527.

Perpelescu, M., Fukagawa, T., 2011. The ABCs of CENPs. Chromosoma 120, 425–446.

Pesenti, M.E., Weir, J.R., Musacchio, A., 2016. Progress in the structural and functional characterization of kinetochores. Curr. Opin. Struct. Biol. 37, 152–163.

Petrovic, A., Keller, J., Liu, Y., Overlack, K., John, J., Dimitrova, Y.N., Jenni, S., van Gerwen, S., Stege, P., Wohlgemuth, S., Rombaut, P., Herzog, F., Harrison, S.C., Vetter, I.R., Musacchio, A., 2016. Structure of the MIS12 Complex and Molecular Basis of Its Interaction with CENP-C at Human Kinetochores. Cell 167, 1028-1040.e15.

Pfarr, C.M., Coue, M., Grissom, P.M., Hays, T.S., Porter, M.E., McIntosh, J.R., 1990. Cytoplasmic dynein is localized to kinetochores during mitosis. Nature 345, 263–265.

Pfau, S.J., Silberman, R.E., Knouse, K.A., Amon, A., 2016. Aneuploidy impairs hematopoietic stem cell fitness and is selected against in regenerating tissues in vivo. Genes Dev. 30, 1395–1408.

Piel, M., Nordberg, J., Euteneuer, U., Bornens, M., 2001. Centrosome-dependent exit of cytokinesis in animal cells. Science 291, 1550–1553.

Platani, M., Santarella-Mellwig, R., Posch, M., Walczak, R., Swedlow, J.R., Mattaj, I.W., 2009. The Nup107-160 nucleoporin complex promotes mitotic events via control of the localization state of the chromosome passenger complex. Mol. Biol. Cell 20, 5260–5275. 7

Potapova, T., Gorbsky, G.J., 2017. The Consequences of Chromosome Segregation Errors in Mitosis and Meiosis. Biology 6, 12.

Prendergast, L., van Vuuren, C., Kaczmarczyk, A., Doering, V., Hellwig, D., Quinn, N., Hoischen, C., Diekmann, S., Sullivan, K.F., 2011. Premitotic assembly of human CENPs -T and -W switches centromeric chromatin to a mitotic state. PLoS Biol. 9, e1001082.

Prosser, S.L., Pelletier, L., 2017. Mitotic spindle assembly in animal cells: a fine balancing act. Nat. Rev. Mol. Cell Biol. 18, 187–201.

Putkey, F.R., Cramer, T., Morphew, M.K., Silk, A.D., Johnson, R.S., McIntosh, J.R., Cleveland, D.W., 2002. Unstable kinetochore-microtubule capture and chromosomal instability following deletion of CENP-E. Dev. Cell 3, 351–365.

Qian, Y., Wang, B., Ma, A., Zhang, L., Xu, G., Ding, Q., Jing, T., Wu, L., Liu, Yun, Yang, Z., Liu, Yongzhong, 2016. USP16 Downregulation by Carboxyl-terminal Truncated HBx Promotes the Growth of Hepatocellular Carcinoma Cells. Sci. Rep. 6, 33039.

Quignon, F., Rozier, L., Lachages, A.-M., Bieth, A., Simili, M., Debatisse, M., 2007. Sustained mitotic block elicits DNA breaks: one-step alteration of ploidy and chromosome integrity in mammalian cells. Oncogene 26, 165–172.

Quintyne, N.J., Reing, J.E., Hoffelder, D.R., Gollin, S.M., Saunders, W.S., 2005. Spindle multipolarity is prevented by centrosomal clustering. Science 307, 127–129.

Raab, M., Gentili, M., de Belly, H., Thiam, H.R., Vargas, P., Jimenez, A.J., Lautenschlaeger, F., Voituriez, R., Lennon-Duménil, A.M., Manel, N., Piel, M., 2016. ESCRT III repairs nuclear envelope ruptures during cell migration to limit DNA damage and cell death. Science 352, 359–362.

Raaijmakers, J.A., Tanenbaum, M.E., Maia, A.F., Medema, R.H., 2009. RAMA1 is a novel kinetochore protein involved in kinetochore-microtubule attachment. J. Cell Sci. 122, 2436–2445.

Raaijmakers, J.A., Tanenbaum, M.E., Medema, R.H., 2013. Systematic dissection of dynein regulators in mitosis. J. Cell Biol. 201, 201–215.

Raemaekers, T., Ribbeck, K., Beaudouin, J., Annaert, W., Van Camp, M., Stockmans, I., Smets, N., Bouillon, R., Ellenberg, J., Carmeliet, G., 2003. NuSAP, a novel microtubule-associated protein involved in mitotic spindle organization. J. Cell Biol. 162, 1017–1029.

Rasmussen, S.A., Wong, L.-Y.C., Yang, Q., May, K.M., Friedman, J.M., 2003. Population-based analyses of mortality in trisomy 13 and trisomy 18. Pediatrics 111, 777–784.

Reed, N.A., Cai, D., Blasius, T.L., Jih, G.T., Meyhofer, E., Gaertig, J., Verhey, K.J., 2006. Microtubule acetylation promotes kinesin-1 binding and transport. Curr. Biol. CB 16, 2166–2172.

Replogle, J.M., Zhou, W., Amaro, A.E., McFarland, J.M., Villalobos-Ortiz, M., Ryan, J., Letai, A., Yilmaz, O., Sheltzer, J., Lippard, S.J., Ben-David, U., Amon, A., 2020. Aneuploidy increases resistance to chemotherapeutics by antagonizing cell division. Proc. Natl. Acad. Sci. U. S. A. 117, 30566–30576.

Rieder, C.L., Davison, E.A., Jensen, L.C., Cassimeris, L., Salmon, E.D., 1986. Oscillatory movements of monooriented chromosomes and their position relative to the spindle pole result from the ejection properties of the aster and half-spindle. J. Cell Biol. 103, 581–591.

Rieder, C.L., Maiato, H., 2004. Stuck in division or passing through: what happens when cells cannot satisfy the spindle assembly checkpoint. Dev. Cell 7, 637–651.

Rieder, C.L., Schultz, A., Cole, R., Sluder, G., 1994. Anaphase onset in vertebrate somatic cells is controlled by a checkpoint that monitors sister kinetochore attachment to the spindle. J. Cell Biol. 127, 1301–1310.

Rischitor, P.E., Konzack, S., Fischer, R., 2004. The Kip3-like kinesin KipB moves along microtubules and determines spindle position during synchronized mitoses in Aspergillus nidulans hyphae. Eukaryot. Cell 3, 632–645.

Ritchie, K., Seah, C., Moulin, J., Isaac, C., Dick, F., Bérubé, N.G., 2008. Loss of ATRX leads to chromosome cohesion and congression defects. J. Cell Biol. 180, 315–324.

Rivera-Rivera, Y., Saavedra, H.I., 2016. Centrosome - a promising anti-cancer target. Biol. Targets Ther. 10, 167–176.

Rode, A., Maass, K.K., Willmund, K.V., Lichter, P., Ernst, A., 2016. Chromothripsis in cancer cells: An update. Int. J. Cancer 138, 2322–2333.

Roll-Mecak, A., 2020. The Tubulin Code in Microtubule Dynamics and Information Encoding. Dev. Cell 54, 7–20.

Roschke, A.V., Kirsch, I.R., 2005. Targeting cancer cells by exploiting karyotypic complexity and chromosomal instability. Cell Cycle Georget. Tex 4, 679–682.

Rosenblatt, J., 2005. Spindle assembly: asters part their separate ways. Nat. Cell Biol. 7, 219–222.

Roylance, R., Endesfelder, D., Gorman, P., Burrell, R.A., Sander, J., Tomlinson, I., Hanby, A.M., Speirs, V., Richardson, A.L., Birkbak, N.J., Eklund, A.C., Downward, J., Kschischo, M., Szallasi, Z., Swanton, C., 2011. Relationship of extreme chromosomal instability with long-term survival in a retrospective analysis of primary breast cancer. Cancer Epidemiol. Biomark. Prev. Publ. Am. Assoc. Cancer Res. Cosponsored Am. Soc. Prev. Oncol. 20, 2183–2194.

Royle, S.J., 2012. The role of clathrin in mitotic spindle organisation. J. Cell Sci. 125, 19–28.

Royle, S.J., Bright, N.A., Lagnado, L., 2005. Clathrin is required for the function of the mitotic spindle. Nature 434, 1152–1157.

Ryan, S.D., Britigan, E.M.C., Zasadil, L.M., Witte, K., Audhya, A., Roopra, A., Weaver, B.A., 2012. Up-regulation of the mitotic checkpoint component Mad1 causes chromosomal instability and resistance to microtubule poisons. Proc. Natl. Acad. Sci. U. S. A. 109, E2205-2214.

Sablina, A.A., Ilyinskaya, G.V., Rubtsova, S.N., Agapova, L.S., Chumakov, P.M., Kopnin, B.P., 1998. Activation of p53-mediated cell cycle checkpoint in response to micronuclei formation. J. Cell Sci. 111 (Pt 7), 977–984.

Salimian, K.J., Ballister, E.R., Smoak, E.M., Wood, S., Panchenko, T., Lampson, M.A., Black, B.E., 2011. Feedback control in sensing chromosome biorientation by the Aurora B kinase. Curr. Biol. CB 21, 1158–1165.

Sansregret, L., Patterson, J.O., Dewhurst, S., López-García, C., Koch, A., McGranahan, N., Chao, W.C.H., Barry, D.J., Rowan, A., Instrell, R., Horswell, S., Way, M., Howell, M., Singleton, M.R., Medema, R.H., Nurse, P., Petronczki, M., Swanton, C., 2017. APC/C Dysfunction Limits Excessive Cancer Chromosomal Instability. Cancer Discov. 7, 218–233.

Santaguida, S., Amon, A., 2015. Short- and long-term effects of chromosome mis-segregation and aneuploidy. Nat. Rev. Mol. Cell Biol. 16, 473–485.

Santaguida, S., Richardson, A., Iyer, D.R., M'Saad, O., Zasadil, L., Knouse, K.A., Wong, Y.L., Rhind, N., Desai, A., Amon, A., 2017. Chromosome Mis-segregation Generates Cell-Cycle-Arrested Cells with Complex Karyotypes that Are Eliminated by the Immune System. Dev. Cell 41, 638-651.e5.

Santamaria, A., Nagel, S., Sillje, H.H.W., Nigg, E.A., 2008. The spindle protein CHICA mediates localization of the chromokinesin Kid to the mitotic spindle. Curr. Biol. CB 18, 723–729.

Sasai, K., Parant, J.M., Brandt, M.E., Carter, J., Adams, H.P., Stass, S.A., Killary, A.M., Katayama, H., Sen, S., 2008. Targeted disruption of Aurora A causes abnormal mitotic spindle assembly, chromosome misalignment and embryonic lethality. Oncogene 27, 4122–4127.

Sato, H., Uzawa, N., Takahashi, K.-I., Myo, K., Ohyama, Y., Amagasa, T., 2010. Prognostic utility of chromosomal instability detected by fluorescence in situ hybridization in fine-needle aspirates from oral squamous cell carcinomas. BMC Cancer 10, 182.

Schek, H.T., Gardner, M.K., Cheng, J., Odde, D.J., Hunt, A.J., 2007. Microtubule assembly dynamics at the nanoscale. Curr. Biol. CB 17, 1445–1455.

Schleicher, K., Porter, M., Ten Have, S., Sundaramoorthy, R., Porter, I.M., Swedlow, J.R., 2017. The Ndc80 complex targets Bod1 to human mitotic kinetochores. Open Biol. 7, 170099.

Schmidt, J.C., Kiyomitsu, T., Hori, T., Backer, C.B., Fukagawa, T., Cheeseman, I.M., 2010. Aurora B kinase controls the targeting of the Astrin-SKAP complex to bioriented kinetochores. J. Cell Biol. 191, 269–280.

Schneider, L., Essmann, F., Kletke, A., Rio, P., Hanenberg, H., Wetzel, W., Schulze-Osthoff, K., Nürnberg, B., Piekorz, R.P., 2007. The transforming acidic coiled coil 3 protein is essential for spindle-dependent chromosome alignment and mitotic survival. J. Biol. Chem. 282, 29273–29283.

Schuh, M., Ellenberg, J., 2007. Self-organization of MTOCs replaces centrosome function during acentrosomal spindle assembly in live mouse oocytes. Cell 130, 484–498.

Schuyler, S.C., Pellman, D., 2001. Microtubule “plus-end-tracking proteins”: The end is just the beginning. Cell 105, 421–424.

Schweizer, N., Ferrás, C., Kern, D.M., Logarinho, E., Cheeseman, I.M., Maiato, H., 2013. Spindle assembly checkpoint robustness requires Tpr-mediated regulation of Mad1/Mad2 proteostasis. J. Cell Biol. 203, 883–893.

Sen, O., Harrison, J.U., Burroughs, N.J., McAinsh, A.D., 2021. Kinetochore life histories reveal an Aurora-B-dependent error correction mechanism in anaphase. Dev. Cell 56, 3082-3099.e5

Sender, R., Milo, R., 2021. The distribution of cellular turnover in the human body. Nat. Med. 27, 45–48.

Sepaniac, L.A., Martin, W., Dionne, L.A., Stearns, T.M., Reinholdt, L.G., Stumpff, J., 2021. Micronuclei in Kif18a mutant mice form stable micronuclear envelopes and do not promote tumorigenesis. J. Cell Biol. 220, e202101165.

Serio, G., Margaria, V., Jensen, S., Oldani, A., Bartek, J., Bussolino, F., Lanzetti, L., 2011. Small GTPase Rab5 participates in chromosome congression and regulates localization of the centromere-associated protein CENP-F to kinetochores. Proc. Natl. Acad. Sci. U. S. A. 108, 17337–17342.

Sheltzer, J.M., Amon, A., 2011. The aneuploidy paradox: costs and benefits of an incorrect karyotype. Trends Genet. TIG 27, 446–453.

Sheltzer, J.M., Ko, J.H., Replogle, J.M., Habibe Burgos, N.C., Chung, E.S., Meehl, C.M., Sayles, N.M., Passerini, V., Storchova, Z., Amon, A., 2017. Single-chromosome Gains Commonly Function as Tumor Suppressors. Cancer Cell 31, 240–255.

Sherr, C.J., 1994. G1 phase progression: cycling on cue. Cell 79, 551–555.

Shimamoto, Y., Maeda, Y.T., Ishiwata, S., Libchaber, A.J., Kapoor, T.M., 2011. Insights into the micromechanical properties of the metaphase spindle. Cell 145, 1062–1074.

Shimizu, H., Nagamori, I., Yabuta, N., Nojima, H., 2009. GAK, a regulator of clathrin-mediated membrane traffic, also controls centrosome integrity and chromosome congression. J. Cell Sci. 122, 3145–3152.

Shoshani, O., Brunner, S.F., Yaeger, R., Ly, P., Nechemia-Arbely, Y., Kim, D.H., Fang, R., Castillon, G.A., Yu, M., Li, J.S.Z., Sun, Y., Ellisman, M.H., Ren, B., Campbell, P.J., Cleveland, D.W., 2021. Chromothripsis drives the evolution of gene amplification in cancer. Nature 591, 137–141.

Shrestha, R.L., Tamura, N., Fries, A., Levin, N., Clark, J., Draviam, V.M., 2014. TAO1 kinase maintains chromosomal stability by facilitating proper congression of chromosomes. Open Biol. 4, 130108.

Siemers, N.O., Holloway, J.L., Chang, H., Chasalow, S.D., Ross-MacDonald, P.B., Voliva, C.F., Szustakowski, J.D., 2017. Genome-wide association analysis identifies genetic correlates of immune infiltrates in solid tumors. PloS One 12, e0179726.

Sigoillot, F.D., Lyman, S., Huckins, J.F., Adamson, B., Chung, E., Quattrochi, B., King, R.W., 2012. A bioinformatics method identifies prominent off-targeted transcripts in RNAi screens. Nat. Methods 9, 363–366.

Sikirzhytski, V., Magidson, V., Steinman, J.B., He, J., Le Berre, M., Tikhonenko, I., Ault, J.G., McEwen, B.F., Chen, J.K., Sui, H., Piel, M., Kapoor, T.M., Khodjakov, A., 2014. Direct kinetochore-spindle pole connections are not required for chromosome segregation. J. Cell Biol. 206, 231–243.

Sikirzhytski, V., Renda, F., Tikhonenko, I., Magidson, V., McEwen, B.F., Khodjakov, A., 2018. Microtubules assemble near most kinetochores during early prometaphase in human cells. J. Cell Biol. 217, 2647–2659.

Silk, A.D., Zasadil, L.M., Holland, A.J., Vitre, B., Cleveland, D.W., Weaver, B.A., 2013. Chromosome missegregation rate predicts whether aneuploidy will promote or suppress tumors. Proc. Natl. Acad. Sci. U. S. A. 110, E4134-4141.

Silkworth, W.T., Nardi, I.K., Paul, R., Mogilner, A., Cimini, D., 2012. Timing of centrosome separation is important for accurate chromosome segregation. Mol. Biol. Cell 23, 401–411.

Silkworth, W.T., Nardi, I.K., Scholl, L.M., Cimini, D., 2009. Multipolar spindle pole coalescence is a major source of kinetochore mis-attachment and chromosome mis-segregation in cancer cells. PloS One 4, e6564.

Silljé, H.H.W., Nagel, S., Körner, R., Nigg, E.A., 2006. HURP is a Ran-importin beta-regulated protein that stabilizes kinetochore microtubules in the vicinity of chromosomes. Curr. Biol. CB 16, 731–742.

Simonetti, G., Bruno, S., Padella, A., Tenti, E., Martinelli, G., 2019. Aneuploidy: Cancer strength or vulnerability? Int. J. Cancer 144, 8–25.

Sironi, L., Mapelli, M., Knapp, S., De Antoni, A., Jeang, K.-T., Musacchio, A., 2002. Crystal structure of the tetrameric Mad1-Mad2 core complex: implications of a “safety belt” binding mechanism for the spindle checkpoint. EMBO J. 21, 2496–2506.

Sivakumar, S., Daum, J.R., Tipton, A.R., Rankin, S., Gorbsky, G.J., 2014. The spindle and kinetochore-associated (Ska) complex enhances binding of the anaphase-promoting complex/cyclosome (APC/C) to chromosomes and promotes mitotic exit. Mol. Biol. Cell 25, 594–605.

Sloss, O., Topham, C., Diez, M., Taylor, S., 2016. Mcl-1 dynamics influence mitotic slippage and death in mitosis. Oncotarget 7, 5176–5192.

Solomon, D.A., Kim, T., Diaz-Martinez, L.A., Fair, J., Elkahloun, A.G., Harris, B.T., Toretsky, J.A., Rosenberg, S.A., Shukla, N., Ladanyi, M., Samuels, Y., James, C.D., Yu, H., Kim, J.-S., Waldman, T., 2011. Mutational inactivation of STAG2 causes aneuploidy in human cancer. Science 333, 1039–1043.

Song, S., Peng, P., Tang, Z., Zhao, J., Wu, W., Li, H., Shao, M., Li, L., Yang, C., Duan, F., Zhang, M., Zhang, J., Wu, H., Li, C., Wang, X., Wang, H., Ruan, Y., Gu, J., 2017. Decreased expression of STING predicts poor prognosis in patients with gastric cancer. Sci. Rep. 7, 39858.

Soto, M., García-Santisteban, I., Krenning, L., Medema, R.H., Raaijmakers, J.A., 2018. Chromosomes trapped in micronuclei are liable to segregation errors. J. Cell Sci. 131, jcs214742.

Soto, M., Raaijmakers, J.A., Bakker, B., Spierings, D.C.J., Lansdorp, P.M., Foijer, F., Medema, R.H., 2017. p53 Prohibits Propagation of Chromosome Segregation Errors that Produce Structural Aneuploidies. Cell Rep. 19, 2423–2431.

Soto, M., Raaijmakers, J.A., Medema, R.H., 2019. Consequences of Genomic Diversification Induced by Segregation Errors. Trends Genet. TIG 35, 279–291.

Spiliotis, E.T., Kinoshita, M., Nelson, W.J., 2005. A mitotic septin scaffold required for Mammalian chromosome congression and segregation. Science 307, 1781–1785.

Spurck, T.P., Stonington, O.G., Snyder, J.A., Pickett-Heaps, J.D., Bajer, A., Mole-Bajer, J., 1990. UV microbeam irradiations of the mitotic spindle. II. Spindle fiber dynamics and force production. J. Cell Biol. 111, 1505–1518.

Srivastava, S., Panda, D., 2018. A centrosomal protein STARD9 promotes microtubule stability and regulates spindle microtubule dynamics. Cell Cycle Georget. Tex 17, 2052–2068.

Steigemann, P., Wurzenberger, C., Schmitz, M.H.A., Held, M., Guizetti, J., Maar, S., Gerlich, D.W., 2009. Aurora B-mediated abscission checkpoint protects against tetraploidization. Cell 136, 473–484.

Stephens, P.J., Greenman, C.D., Fu, B., Yang, F., Bignell, G.R., Mudie, L.J., Pleasance, E.D., Lau, K.W., Beare, D., Stebbings, L.A., McLaren, S., Lin, M.-L., McBride, D.J., Varela, I., Nik-Zainal, S., Leroy, C., Jia, M., Menzies, A., Butler, A.P., Teague, J.W., Quail, M.A., Burton, J., Swerdlow, H., Carter, N.P., Morsberger, L.A., Iacobuzio-Donahue, C., Follows, G.A., Green, A.R., Flanagan, A.M., Stratton, M.R., Futreal, P.A., Campbell, P.J., 2011. Massive genomic rearrangement acquired in a single catastrophic event during cancer development. Cell 144, 27–40.

Stevens, D., Gassmann, R., Oegema, K., Desai, A., 2011. Uncoordinated loss of chromatid cohesion is a common outcome of extended metaphase arrest. PloS One 6, e22969.

Stingele, S., Stoehr, G., Peplowska, K., Cox, J., Mann, M., Storchova, Z., 2012. Global analysis of genome, transcriptome and proteome reveals the response to aneuploidy in human cells. Mol. Syst. Biol. 8, 608.

Storozynsky, Q., Hitt, M.M., 2020. The Impact of Radiation-Induced DNA Damage on cGAS-STING-Mediated Immune Responses to Cancer. Int. J. Mol. Sci. 21, 8877.

Straight, A.F., Marshall, W.F., Sedat, J.W., Murray, A.W., 1997. Mitosis in living budding yeast: anaphase A but no metaphase plate. Science 277, 574–578.

Straight, A.F., Sedat, J.W., Murray, A.W., 1998. Time-lapse microscopy reveals unique roles for kinesins during anaphase in budding yeast. J. Cell Biol. 143, 687–694.

Stumpff, J., Du, Y., English, C.A., Maliga, Z., Wagenbach, M., Asbury, C.L., Wordeman, L., Ohi, R., 2011. A tethering mechanism controls the processivity and kinetochore-microtubule plus-end enrichment of the kinesin-8 Kif18A. Mol. Cell 43, 764–775.

Stumpff, J., von Dassow, G., Wagenbach, M., Asbury, C., Wordeman, L., 2008. The kinesin-8 motor Kif18A suppresses kinetochore movements to control mitotic chromosome alignment. Dev. Cell 14, 252–262.

Stumpff, J., Wagenbach, M., Franck, A., Asbury, C.L., Wordeman, L., 2012. Kif18A and chromokinesins confine centromere movements via microtubule growth suppression and spatial control of kinetochore tension. Dev. Cell 22, 1017–1029.

Suijkerbuijk, S.J.E., van Osch, M.H.J., Bos, F.L., Hanks, S., Rahman, N., Kops, G.J.P.L., 2010. Molecular causes for BUBR1 dysfunction in the human cancer predisposition syndrome mosaic variegated aneuploidy. Cancer Res. 70, 4891–4900.

Sundin, L.J.R., Guimaraes, G.J., Deluca, J.G., 2011. The NDC80 complex proteins Nuf2 and Hec1 make distinct contributions to kinetochore-microtubule attachment in mitosis. Mol. Biol. Cell 22, 759–768.

Swanton, C., Nicke, B., Schuett, M., Eklund, A.C., Ng, C., Li, Q., Hardcastle, T., Lee, A., Roy, R., East, P., Kschischo, M., Endesfelder, D., Wylie, P., Kim, S.N., Chen, J.-G., Howell, M., Ried, T., Habermann, J.K., Auer, G., Brenton, J.D., Szallasi, Z., Downward, J., 2009. Chromosomal instability determines taxane response. Proc. Natl. Acad. Sci. U. S. A. 106, 8671–8676.

Symmans, W.F., Volm, M.D., Shapiro, R.L., Perkins, A.B., Kim, A.Y., Demaria, S., Yee, H.T., McMullen, H., Oratz, R., Klein, P., Formenti, S.C., Muggia, F., 2000. Paclitaxel-induced apoptosis and mitotic arrest assessed by serial fine-needle aspiration: implications for early prediction of breast cancer response to neoadjuvant treatment. Clin. Cancer Res. Off. J. Am. Assoc. Cancer Res. 6, 4610–4617.

Taggart, J.C., Zauber, H., Selbach, M., Li, G.-W., McShane, E., 2020. Keeping the Proportions of Protein Complex Components in Check. Cell Syst. 10, 125–132.

Takata, H., Matsunaga, S., Morimoto, A., Ma, N., Kurihara, D., Ono-Maniwa, R., Nakagawa, M., Azuma, T., Uchiyama, S., Fukui, K., 2007. PHB2 protects sister-chromatid cohesion in mitosis. Curr. Biol. CB 17, 1356–1361.

Takeda, S.; Izutsu, K., 1960. Partial irradiation of individual mitotic cells with ultraviolet microbeam. Symp. Cell Chem 245–259.

Tanaka, K., 2013. Regulatory mechanisms of kinetochore-microtubule interaction in mitosis. Cell. Mol. Life Sci. CMLS 70, 559–579.

Tanenbaum, M.E., Galjart, N., van Vugt, M.A.T.M., Medema, R.H., 2006. CLIP-170 facilitates the formation of kinetochore-microtubule attachments. EMBO J. 25, 45–57.

Tanenbaum, M.E., Vale, R.D., McKenney, R.J., 2013. Cytoplasmic dynein crosslinks and slides anti-parallel microtubules using its two motor domains. eLife 2, e00943.

Tanudji, M., Shoemaker, J., L'Italien, L., Russell, L., Chin, G., Schebye, X.M., 2004. Gene silencing of CENP-E by small interfering RNA in HeLa cells leads to missegregation of chromosomes after a mitotic delay. Mol. Biol. Cell 15, 3771–3781.

Taylor, A.M., Shih, J., Ha, G., Gao, G.F., Zhang, X., Berger, A.C., Schumacher, S.E., Wang, C., Hu, H., Liu, J., Lazar, A.J., Cancer Genome Atlas Research Network, Cherniack, A.D., Beroukhim, R., Meyerson, M., 2018. Genomic and Functional Approaches to Understanding Cancer Aneuploidy. Cancer Cell 33, 676-689.e3.

Taylor, S.S., McKeon, F., 1997. Kinetochore localization of murine Bub1 is required for normal mitotic timing and checkpoint response to spindle damage. Cell 89, 727–735.

Terradas, M., Martín, M., Tusell, L., Genescà, A., 2009. DNA lesions sequestered in micronuclei induce a local defective-damage response. DNA Repair 8, 1225–1234.

Thein, K.H., Kleylein-Sohn, J., Nigg, E.A., Gruneberg, U., 2007. Astrin is required for the maintenance of sister chromatid cohesion and centrosome integrity. J. Cell Biol. 178, 345–354.

Theurkauf, W.E., Hawley, R.S., 1992. Meiotic spindle assembly in Drosophila females: behavior of nonexchange chromosomes and the effects of mutations in the nod kinesin-like protein. J. Cell Biol. 116, 1167–1180.

Thomas, G.E., Bandopadhyay, K., Sutradhar, S., Renjith, M.R., Singh, P., Gireesh, K.K., Simon, S., Badarudeen, B., Gupta, H., Banerjee, M., Paul, R., Mitra, J., Manna, T.K., 2016. EB1 regulates attachment of Ska1 with microtubules by forming extended structures on the microtubule lattice. Nat. Commun. 7, 11665.

Thompson, S.L., Bakhoum, S.F., Compton, D.A., 2010. Mechanisms of chromosomal instability. Curr. Biol. CB 20, R285-295.

Thompson, S.L., Compton, D.A., 2011. Chromosome missegregation in human cells arises through specific types of kinetochore-microtubule attachment errors. Proc. Natl. Acad. Sci. U. S. A. 108, 17974–17978.

Thompson, S.L., Compton, D.A., 2010. Proliferation of aneuploid human cells is limited by a p53-dependent mechanism. J. Cell Biol. 188, 369–381.

Thompson, S.L., Compton, D.A., 2008. Examining the link between chromosomal instability and aneuploidy in human cells. J. Cell Biol. 180, 665–672.

Tichy, A., Kabacik, S., O'Brien, G., Pejchal, J., Sinkorova, Z., Kmochova, A., Sirak, I., Malkova, A., Beltran, C.G., Gonzalez, J.R., Grepl, J., Majewski, M., Ainsbury, E., Zarybnicka, L., Vachelova, J., Zavrelova, A., Davidkova, M., Markova Stastna, M., Abend, M., Pernot, E., Cardis, E., Badie, C., 2018. The first in vivo multiparametric comparison of different radiation exposure biomarkers in human blood. PloS One 13, e0193412.

Topham, C.H., Taylor, S.S., 2013. Mitosis and apoptosis: how is the balance set? Curr. Opin. Cell Biol. 25, 780–785.

Torres, E.M., Sokolsky, T., Tucker, C.M., Chan, L.Y., Boselli, M., Dunham, M.J., Amon, A., 2007. Effects of aneuploidy on cellular physiology and cell division in haploid yeast. Science 317, 916–924.

Torres, E.M., Williams, B.R., Amon, A., 2008. Aneuploidy: cells losing their balance. Genetics 179, 737–746.

Torres, J.Z., Summers, M.K., Peterson, D., Brauer, M.J., Lee, J., Senese, S., Gholkar, A.A., Lo, Y.-C., Lei, X., Jung, K., Anderson, D.C., Davis, D.P., Belmont, L., Jackson, P.K., 2011.

The STARD9/Kif16a kinesin associates with mitotic microtubules and regulates spindle pole assembly. Cell 147, 1309–1323.

Tsang, M.-J., Cheeseman, I.M., 2023. Alternative CDC20 translational isoforms tune mitotic arrest duration. Nature 617, 154–161.

Tsang, Y.H., Han, X., Man, W.Y., Lee, N., Poon, R.Y.C., 2012. Novel functions of the phosphatase SHP2 in the DNA replication and damage checkpoints. PloS One 7, e49943.

Tucker, J.B., Bonema, S.C., García-Varela, R., Denu, R.A., Hu, Y., McGregor, S.M., Burkard, M.E., Weaver, B.A., 2023. Misaligned Chromosomes are a Major Source of Chromosomal Instability in Breast Cancer. Cancer Res. Commun. 3, 54–65.

Uehara, R., Nozawa, R., Tomioka, A., Petry, S., Vale, R.D., Obuse, C., Goshima, G., 2009. The augmin complex plays a critical role in spindle microtubule generation for mitotic progression and cytokinesis in human cells. Proc. Natl. Acad. Sci. U. S. A. 106, 6998–7003.

Uematsu, K., Okumura, F., Tonogai, S., Joo-Okumura, A., Alemayehu, D.H., Nishikimi, A., Fukui, Y., Nakatsukasa, K., Kamura, T., 2016. ASB7 regulates spindle dynamics and genome integrity by targeting DDA3 for proteasomal degradation. J. Cell Biol. 215, 95–106.

Uetake, Y., Sluder, G., 2010. Prolonged prometaphase blocks daughter cell proliferation despite normal completion of mitosis. Curr. Biol. CB 20, 1666–1671.

Umbreit, N.T., Zhang, C.-Z., Lynch, L.D., Blaine, L.J., Cheng, A.M., Tourdot, R., Sun, L., Almubarak, H.F., Judge, K., Mitchell, T.J., Spektor, A., Pellman, D., 2020. Mechanisms generating cancer genome complexity from a single cell division error. Science 368, eaba0712.

Unal, D., Kiraz, A., Avci, D., Tasdemir, A., Unal, T.D., Cagli, S., Eroglu, C., Yuce, I., Ozcan, I., Kaplan, B., 2016. Cytogenetic damage of radiotherapy in long-term head and neck cancer survivors. Int. J. Radiat. Biol. 92, 364–370.

Uren, A.G., Wong, L., Pakusch, M., Fowler, K.J., Burrows, F.J., Vaux, D.L., Choo, K.H., 2000. Survivin and the inner centromere protein INCENP show similar cell-cycle localization and gene knockout phenotype. Curr. Biol. CB 10, 1319–1328.

Utani, K., Kohno, Y., Okamoto, A., Shimizu, N., 2010. Emergence of micronuclei and their effects on the fate of cells under replication stress. PloS One 5, e10089.

van den Bos, H., Spierings, D.C.J., Taudt, A.S., Bakker, B., Porubský, D., Falconer, E., Novoa, C., Halsema, N., Kazemier, H.G., Hoekstra-Wakker, K., Guryev, V., den Dunnen, W.F.A., Foijer, F., Tatché, M.C., Boddeke, H.W.G.M., Lansdorp, P.M., 2016. Single-cell whole genome sequencing reveals no evidence for common aneuploidy in normal and Alzheimer's disease neurons. Genome Biol. 17, 116.

van Dijk, E., van den Bosch, T., Lenos, K.J., El Makrini, K., Nijman, L.E., van Essen, H.F.B., Lansu, N., Boekhout, M., Hageman, J.H., Fitzgerald, R.C., Punt, C.J.A., Tuynman, J.B., Snippert, H.J.G., Kops, G.J.P.L., Medema, J.P., Ylstra, B., Vermeulen, L., Miedema, D.M., 2021. Chromosomal copy number heterogeneity predicts survival rates across cancers. Nat. Commun. 12, 3188. Vanneste, D., Ferreira, V., Vernos, I., 2011. Chromokinesins: localization-dependent functions and regulation during cell division. Biochem. Soc. Trans. 39, 1154–1160.

Varga, V., Helenius, J., Tanaka, K., Hyman, A.A., Tanaka, T.U., Howard, J., 2006. Yeast kinesin-8 depolymerizes microtubules in a length-dependent manner. Nat. Cell Biol. 8, 957–962.

Varga, V., Leduc, C., Bormuth, V., Diez, S., Howard, J., 2009. Kinesin-8 motors act cooperatively to mediate length-dependent microtubule depolymerization. Cell 138, 1174–1183.

Vargas, J.D., Hatch, E.M., Anderson, D.J., Hetzer, M.W., 2012. Transient nuclear envelope rupturing during interphase in human cancer cells. Nucl. Austin Tex 3, 88–100.

Varma, D., P, M., Sa, S., Rb, V., 2008. Direct role of dynein motor in stable kinetochore-microtubule attachment, orientation, and alignment. J. Cell Biol. 182.

Vassilopoulos, S., Esk, C., Hoshino, S., Funke, B.H., Chen, C.-Y., Plocik, A.M., Wright, W.E., Kucherlapati, R., Brodsky, F.M., 2009. A role for the CHC22 clathrin heavy-chain isoform in human glucose metabolism. Science 324, 1192–1196.

Vázquez-Diez, C., Yamagata, K., Trivedi, S., Haverfield, J., FitzHarris, G., 2016. Micronucleus formation causes perpetual unilateral chromosome inheritance in mouse embryos. Proc. Natl. Acad. Sci. U. S. A. 113, 626–631.

Vergnolle, M.A.S., Taylor, S.S., 2007. Cenp-F links kinetochores to Ndel1/Nde1/Lis1/dynein microtubule motor complexes. Curr. Biol. CB 17, 1173–1179.

Vernos, I., Raats, J., Hirano, T., Heasman, J., Karsenti, E., Wylie, C., 1995. Xklp1, a chromosomal Xenopus kinesin-like protein essential for spindle organization and chromosome positioning. Cell 81, 117–127.

Vladimirou, E., Mchedlishvili, N., Gasic, I., Armond, J.W., Samora, C.P., Meraldi, P., McAinsh, A.D., 2013. Nonautonomous movement of chromosomes in mitosis. Dev. Cell 27, 60–71.

Vleugel, M., Hoogendoorn, E., Snel, B., Kops, G.J.P.L., 2012. Evolution and function of the mitotic checkpoint. Dev. Cell 23, 239–250.

Voronina, N., Wong, J.K.L., Hübschmann, D., Hlevnjak, M., Uhrig, S., Heilig, C.E., Horak, P., Kreutzfeldt, S., Mock, A., Stenzinger, A., Hutter, B., Fröhlich, M., Brors, B., Jahn, A., Klink, B., Gieldon, L., Sieverling, L., Feuerbach, L., Chudasama, P., Beck, K., Kroiss, M., Heining, C., Möhrmann, L., Fischer, A., Schröck, E., Glimm, H., Zapatka, M., Lichter, P., Fröhling, S., Ernst, A., 2020. The landscape of chromothripsis across adult cancer types. Nat. Commun. 11, 2320.

Vorozhko, V.V., Emanuele, M.J., Kallio, M.J., Stukenberg, P.T., Gorbsky, G.J., 2008. Multiple mechanisms of chromosome movement in vertebrate cells mediated through the Ndc80 complex and dynein/dynactin. Chromosoma 117, 169–179.

Wadsworth, P., Khodjakov, A., 2004. E pluribus unum: towards a universal mechanism for spindle assembly. Trends Cell Biol. 14, 413–419.

Walczak, C.E., 2003. The Kin I kinesins are microtubule end-stimulated ATPases. Mol. Cell 11, 286–288.

Walczak, C.E., Cai, S., Khodjakov, A., 2010. Mechanisms of chromosome behaviour during mitosis. Nat. Rev. Mol. Cell Biol. 11, 91–102.

Walczak, C.E., Gayek, S., Ohi, R., 2013. Microtubule-depolymerizing kinesins. Annu. Rev. Cell Dev. Biol. 29, 417–441.

Walczak, C.E., Mitchison, T.J., Desai, A., 1996. XKCM1: a Xenopus kinesin-related protein that regulates microtubule dynamics during mitotic spindle assembly. Cell 84, 37–47.

Wandke, C., Barisic, M., Sigl, R., Rauch, V., Wolf, F., Amaro, A.C., Tan, C.H., Pereira, A.J., Kutay, U., Maiato, H., Meraldi, P., Geley, S., 2012. Human chromokinesins promote

chromosome congression and spindle microtubule dynamics during mitosis. J. Cell Biol. 198, 847–863.

Wang, H., Hu, X., Ding, X., Dou, Z., Yang, Z., Shaw, A.W., Teng, M., Cleveland, D.W., Goldberg, M.L., Niu, L., Yao, X., 2004. Human Zwint-1 specifies localization of Zeste White 10 to kinetochores and is essential for mitotic checkpoint signaling. J. Biol. Chem. 279, 54590–54598.

Wang, L., Zhu, G., Yang, D., Li, Q., Li, Y., Xu, X., He, D., Zeng, C., 2008. The spindle function of CDCA4. Cell Motil. Cytoskeleton 65, 581–593.

Wang, S.Z., Adler, R., 1995. Chromokinesin: a DNA-binding, kinesin-like nuclear protein. J. Cell Biol. 128, 761–768.

Wang, X., Yang, Y., Duan, Q., Jiang, N., Huang, Y., Darzynkiewicz, Z., Dai, W., 2008. sSgo1, a major splice variant of Sgo1, functions in centriole cohesion where it is regulated by Plk1. Dev. Cell 14, 331–341.

Waterman-Storer, C., Desai, A., Salmon, E.D., 1999. Fluorescent speckle microscopy of spindle microtubule assembly and motility in living cells. Methods Cell Biol. 61, 155–173.

Waterman-Storer, C.M., 1998. Microtubules and microscopes: how the development of light microscopic imaging technologies has contributed to discoveries about microtubule dynamics in living cells. Mol. Biol. Cell 9, 3263–3271.

Watkins, T.B.K., Lim, E.L., Petkovic, M., Elizalde, S., Birkbak, N.J., Wilson, G.A., Moore, D.A., Grönroos, E., Rowan, A., Dewhurst, S.M., Demeulemeester, J., Dentro, S.C., Horswell, S., Au, L., Haase, K., Escudero, M., Rosenthal, R., Bakir, M.A., Xu, H., Litchfield, K., Lu, W.T., Mourikis, T.P., Dietzen, M., Spain, L., Cresswell, G.D., Biswas, D., Lamy, P., Nordentoft, I., Harbst, K., Castro-Giner, F., Yates, L.R., Caramia, F., Jaulin, F., Vicier, C., Tomlinson, I.P.M., Brastianos, P.K., Cho, R.J., Bastian, B.C., Dyrskjøt, L., Jönsson, G.B., Savas, P., Loi, S., Campbell, P.J., Andre, F., Luscombe, N.M., Steeghs, N., Tjan-Heijnen, V.C.G., Szallasi, Z., Turajlic, S., Jamal-Hanjani, M., Van Loo, P., Bakhoum, S.F., Schwarz, R.F., McGranahan, N., Swanton, C., 2020. Pervasive chromosomal instability and karyotype order in tumour evolution. Nature 587, 126–132.

Weaver, B.A.A., Bonday, Z.Q., Putkey, F.R., Kops, G.J.P.L., Silk, A.D., Cleveland, D.W., 2003. Centromere-associated protein-E is essential for the mammalian mitotic checkpoint to prevent aneuploidy due to single chromosome loss. J. Cell Biol. 162, 551–563.

Weaver, B.A.A., Silk, A.D., Montagna, C., Verdier-Pinard, P., Cleveland, D.W., 2007. Aneuploidy acts both oncogenically and as a tumor suppressor. Cancer Cell 11, 25–36.

Weir, J.R., Faesen, A.C., Klare, K., Petrovic, A., Basilico, F., Fischböck, J., Pentakota, S., Keller, J., Pesenti, M.E., Pan, D., Vogt, D., Wohlgemuth, S., Herzog, F., Musacchio, A., 2016. Insights from biochemical reconstitution into the architecture of human kinetochores. Nature 537, 249–253.

Weiss, E., Winey, M., 1996. The Saccharomyces cerevisiae spindle pole body duplication gene MPS1 is part of a mitotic checkpoint. J. Cell Biol. 132, 111–123.

Welburn, J.P.I., Grishchuk, E.L., Backer, C.B., Wilson-Kubalek, E.M., Yates, J.R., Cheeseman, I.M., 2009. The human kinetochore Ska1 complex facilitates microtubule depolymerization-coupled motility. Dev. Cell 16, 374–385.

Werbrouck, J., Ost, P., Fonteyne, V., De Meerleer, G., De Neve, W., Bogaert, E., Beels, L., Bacher, K., Vral, A., Thierens, H., 2013. Early biomarkers related to secondary primary cancer risk in radiotherapy treated prostate cancer patients: IMRT versus IMAT. Radiother. Oncol. J. Eur. Soc. Ther. Radiol. Oncol. 107, 377–381.

West, R.R., Malmstrom, T., McIntosh, J.R., 2002. Kinesins klp5(+) and klp6(+) are required for normal chromosome movement in mitosis. J. Cell Sci. 115, 931–940.

Wild, T., Larsen, M.S.Y., Narita, T., Schou, J., Nilsson, J., Choudhary, C., 2016. The Spindle Assembly Checkpoint Is Not Essential for Viability of Human Cells with Genetically Lowered APC/C Activity. Cell Rep. 14, 1829–1840.

Wimbish, R.T., DeLuca, J.G., 2020. Hec1/Ndc80 Tail Domain Function at the Kinetochore-Microtubule Interface. Front. Cell Dev. Biol. 8, 43.

Witt, P.L., Ris, H., Borisy, G.G., 1980. Origin of kinetochore microtubules in Chinese hamster ovary cells. Chromosoma 81, 483–505.

Wojcik, E., Basto, R., Serr, M., Scaërou, F., Karess, R., Hays, T., 2001. Kinetochore dynein: its dynamics and role in the transport of the Rough deal checkpoint protein. Nat. Cell Biol. 3, 1001–1007.

Wollman, R., Cytrynbaum, E.N., Jones, J.T., Meyer, T., Scholey, J.M., Mogilner, A., 2005. Efficient chromosome capture requires a bias in the “search-and-capture” process during mitotic-spindle assembly. Curr. Biol. CB 15, 828–832.

Wong, J., Fang, G., 2006. HURP controls spindle dynamics to promote proper interkinetochore tension and efficient kinetochore capture. J. Cell Biol. 173, 879–891.

Wong, R.W., Blobel, G., Coutavas, E., 2006. Rae1 interaction with NuMA is required for bipolar spindle formation. Proc. Natl. Acad. Sci. U. S. A. 103, 19783–19787.

Wood, K.W., Sakowicz, R., Goldstein, L.S., Cleveland, D.W., 1997. CENP-E is a plus end-directed kinetochore motor required for metaphase chromosome alignment. Cell 91, 357–366.

Wood, L., Booth, D.G., Vargiu, G., Ohta, S., deLima Alves, F., Samejima, K., Fukagawa, T., Rappsilber, J., Earnshaw, W.C., 2016. Auxin/AID versus conventional knockouts: distinguishing the roles of CENP-T/W in mitotic kinetochore assembly and stability. Open Biol. 6, 150230.

Woolner, S., O’Brien, L.L., Wiese, C., Bement, W.M., 2008. Myosin-10 and actin filaments are essential for mitotic spindle function. J. Cell Biol. 182, 77–88.

Wordeman, L., Wagenbach, M., von Dassow, G., 2007. MCAK facilitates chromosome movement by promoting kinetochore microtubule turnover. J. Cell Biol. 179, 869–879.

Worrall, J.T., Tamura, N., Mazzagatti, A., Shaikh, N., van Lingen, T., Bakker, B., Spierings, D.C.J., Vladimirou, E., Foijer, F., McClelland, S.E., 2018. Non-random Mis-segregation of Human Chromosomes. Cell Rep. 23, 3366–3380.

Wu, G., Lin, Y.-T., Wei, R., Chen, Y., Shan, Z., Lee, W.-H., 2008. Hice1, a novel microtubule-associated protein required for maintenance of spindle integrity and chromosomal stability in human cells. Mol. Cell. Biol. 28, 3652–3662.

Wu, Hailong, Zhou, Y., Wu, Haiyang, Xu, L., Yan, Y., Tong, X., Yan, H., 2021. CENPN Acts as a Novel Biomarker that Correlates With the Malignant Phenotypes of Glioma Cells. Front. Genet. 12, 732376.

X, G., X, D., X, Wu, N, C., X, Wang, 2021. Small but strong: Mutational and functional landscapes of micronuclei in cancer genomes. Int. J. Cancer 148.

Xia, T., Konno, H., Ahn, J., Barber, G.N., 2016a. Deregulation of STING Signaling in Colorectal Carcinoma Constrains DNA Damage Responses and Correlates With Tumorigenesis. Cell Rep. 14, 282–297.

Xia, T., Konno, H., Barber, G.N., 2016b. Recurrent Loss of STING Signaling in Melanoma Correlates with Susceptibility to Viral Oncolysis. Cancer Res. 76, 6747–6759.

Xia, Y., Ivanovska, I.L., Zhu, K., Smith, L., Irianto, J., Pfeifer, C.R., Alvey, C.M., Ji, J., Liu, D., Cho, S., Bennett, R.R., Liu, A.J., Greenberg, R.A., Discher, D.E., 2018. Nuclear rupture at sites of high curvature compromises retention of DNA repair factors. J. Cell Biol. 217, 3796–3808.

Xu, H., Choe, C., Shin, S.-H., Park, S.-W., Kim, H.-S., Jung, S.-H., Yim, S.-H., Kim, T.-M., Chung, Y.-J., 2014. Silencing of KIF14 interferes with cell cycle progression and cytokinesis by blocking the p27(Kip1) ubiquitination pathway in hepatocellular carcinoma. Exp. Mol. Med. 46, e97.

Xu, P., Virshup, D.M., Lee, S.H., 2014. B56-PP2A regulates motor dynamics for mitotic chromosome alignment. J. Cell Sci. 127, 4567–4573.

Xu, Z., Ogawa, H., Vagnarelli, P., Bergmann, J.H., Hudson, D.F., Ruchaud, S., Fukagawa, T., Earnshaw, W.C., Samejima, K., 2009. INCENP-aurora B interactions modulate kinase activity and chromosome passenger complex localization. J. Cell Biol. 187, 637–653.

Xia, Y., Pfeifer C.R, Zhu K., Irianto, J., Liu D., Pannel, K., Chen, E.J., Dooling, L.J., Tobin, M.P., Wang, M., Ivanovska I.L., Smith, L.R., Greenberg R. A., Discher, D.E., 2019. Rescue of DNA damage after constricted migration reveals a mechano-regulated threshold for cell cycle. J. Cell Biol. 218.

Yang, H., Wang, H., Ren, J., Chen, Q., Chen, Z.J., 2017. cGAS is essential for cellular senescence. Proc. Natl. Acad. Sci. U. S. A. 114, E4612–E4620.

Yang, S., Liu, X., Yin, Y., Fukuda, M.N., Zhou, J., 2008. Tastin is required for bipolar spindle assembly and centrosome integrity during mitosis. FASEB J. Off. Publ. Fed. Am. Soc. Exp. Biol. 22, 1960–1972.

Yang, Z., Guo, J., Chen, Q., Ding, C., Du, J., Zhu, X., 2005. Silencing mitosin induces misaligned chromosomes, premature chromosome decondensation before anaphase onset, and mitotic cell death. Mol. Cell. Biol. 25, 4062–4074.

Yang, Z., Kenny, A.E., Brito, D.A., Rieder, C.L., 2009. Cells satisfy the mitotic checkpoint in Taxol, and do so faster in concentrations that stabilize syntelic attachments. J. Cell Biol. 186, 675–684.

Yang, Z., Tulu, U.S., Wadsworth, P., Rieder, C.L., 2007. Kinetochore dynein is required for chromosome motion and congression independent of the spindle checkpoint. Curr. Biol. CB 17, 973–980.

Ye, A.A., Deretic, J., Hoel, C.M., Hinman, A.W., Cimini, D., Welburn, J.P., Maresca, T.J., 2015. Aurora A Kinase Contributes to a Pole-Based Error Correction Pathway. Curr. Biol. CB 25, 1842–1851.

Ye, F., Tan, L., Yang, Q., Xia, Y., Deng, L.-W., Murata-Hori, M., Liou, Y.-C., 2011. HURP regulates chromosome congression by modulating kinesin Kif18A function. Curr. Biol. CB 21, 1584–1591.

Yen, T.J., Compton, D.A., Wise, D., Zinkowski, R.P., Brinkley, B.R., Earnshaw, W.C., Cleveland, D.W., 1991. CENP-E, a novel human centromere-associated protein required for progression from metaphase to anaphase. EMBO J. 10, 1245–1254.

Yoshizawa-Sugata, N., Masai, H., 2009. Roles of human AND-1 in chromosome transactions in S phase. J. Biol. Chem. 284, 20718–20728.

Yu, I., Garnham, C.P., Roll-Mecak, A., 2015. Writing and Reading the Tubulin Code. J. Biol. Chem. 290, 17163–17172.

Yum, S., Li, M., Chen, Z.J., 2020. Old dogs, new trick: classic cancer therapies activate cGAS. Cell Res. 30, 639–648.

Yurov, Y.B., Iourov, I.Y., Monakhov, V.V., Soloviev, I.V., Vostrikov, V.M., Vorsanova, S.G., 2005. The variation of aneuploidy frequency in the developing and adult human brain revealed by an interphase FISH study. J. Histochem. Cytochem. Off. J. Histochem. Soc. 53, 385–390.

Yurov, Y.B., Iourov, I.Y., Vorsanova, S.G., Liehr, T., Kolotii, A.D., Kutsev, S.I., Pellestor, F., Beresheva, A.K., Demidova, I.A., Kravets, V.S., Monakhov, V.V., Soloviev, I.V., 2007. Aneuploidy and confined chromosomal mosaicism in the developing human brain. PloS One 2, e558.

Zaki, B.I., Suriawinata, A.A., Eastman, A.R., Garner, K.M., Bakhoum, S.F., 2014. Chromosomal instability portends superior response of rectal adenocarcinoma to chemoradiation therapy. Cancer 120, 1733–1742.

Zasadil, L.M., Andersen, K.A., Yeum, D., Rocque, G.B., Wilke, L.G., Tevaarwerk, A.J., Raines, R.T., Burkard, M.E., Weaver, B.A., 2014. Cytotoxicity of paclitaxel in breast cancer is due to chromosome missegregation on multipolar spindles. Sci. Transl. Med. 6, 229ra43.

Zeng, X., Sigoillot, F., Gaur, S., Choi, S., Pfaff, K.L., Oh, D.-C., Hathaway, N., Dimova, N., Cuny, G.D., King, R.W., 2010. Pharmacologic inhibition of the anaphase-promoting complex induces a spindle checkpoint-dependent mitotic arrest in the absence of spindle damage. Cancer Cell 18, 382–395.

Zhang, C.-Z., Spektor, A., Cornils, H., Francis, J.M., Jackson, E.K., Liu, S., Meyerson, M., Pellman, D., 2015. Chromothripsis from DNA damage in micronuclei. Nature 522, 179–184.

Zhang, G., Lischetti, T., Hayward, D.G., Nilsson, J., 2015. Distinct domains in Bub1 localize RZZ and BubR1 to kinetochores to regulate the checkpoint. Nat. Commun. 6, 7162.

Zhang, L., Iyer, J., Chowdhury, A., Ji, M., Xiao, L., Yang, S., Chen, Y., Tsai, M.-Y., Dong, J., 2012. KIBRA regulates aurora kinase activity and is required for precise chromosome alignment during mitosis. J. Biol. Chem. 287, 34069–34077.

Zhang, N., Ge, G., Meyer, R., Sethi, S., Basu, D., Pradhan, S., Zhao, Y.-J., Li, X.-N., Cai, W.-W., El-Naggar, A.K., Baladandayuthapani, V., Kittrell, F.S., Rao, P.H., Medina, D., Pati, D., 2008. Overexpression of Separase induces aneuploidy and mammary tumorigenesis. Proc. Natl. Acad. Sci. U. S. A. 105, 13033–13038.

Zhang, Y., Foreman, O., Wigle, D.A., Kosari, F., Vasmatzis, G., Salisbury, J.L., van Deursen, J., Galardy, P.J., 2012. USP44 regulates centrosome positioning to prevent aneuploidy and suppress tumorigenesis. J. Clin. Invest. 122, 4362–4374.

Zhang, Y., Tan, L., Yang, Q., Li, C., Liou, Y.-C., 2018. The microtubule-associated protein HURP recruits the centrosomal protein TACC3 to regulate K-fiber formation and support chromosome congression. J. Biol. Chem. 293, 15733–15747.

Zhao, M., Wang, F., Wu, J., Cheng, Y., Cao, Y., Wu, X., Ma, M., Tang, F., Liu, Z., Liu, H., Ge, B., 2021. CGAS is a micronucleophagy receptor for the clearance of micronuclei. Autophagy 17, 3976–3991.

Zhu, C., Zhao, J., Bibikova, M., Leverson, J.D., Bossy-Wetzel, E., Fan, J.-B., Abraham, R.T., Jiang, W., 2005. Functional analysis of human microtubule-based motor proteins, the kinesins and dyneins, in mitosis/cytokinesis using RNA interference. Mol. Biol. Cell 16, 3187–3199.

Zhu, M., Wang, F., Yan, F., Yao, P.Y., Du, J., Gao, X., Wang, X., Wu, Q., Ward, T., Li, J., Kioko, S., Hu, R., Xie, W., Ding, X., Yao, X., 2008. Septin 7 interacts with centromere-associated protein E and is required for its kinetochore localization. J. Biol. Chem. 283, 18916–18925.

Zhu, W., Ukomadu, C., Jha, S., Senga, T., Dhar, S.K., Wohlschlegel, J.A., Nutt, L.K., Kornbluth, S., Dutta, A., 2007. Mcm10 and And-1/CTF4 recruit DNA polymerase alpha to chromatin for initiation of DNA replication. Genes Dev. 21, 2288–2299.

Zhuo, X., Guo, X., Zhang, X., Jing, G., Wang, Y., Chen, Q., Jiang, Q., Liu, J., Zhang, C., 2015. Usp16 regulates kinetochore localization of Plk1 to promote proper chromosome alignment in mitosis. J. Cell Biol. 210, 727–735.

Zuccolo, M., Alves, A., Galy, V., Bolhy, S., Formstecher, E., Racine, V., Sibarita, J.-B., Fukagawa, T., Shiekhattar, R., Yen, T., Doye, V., 2007. The human Nup107-160 nuclear pore subcomplex contributes to proper kinetochore functions. EMBO J. 26, 1853–1864.